# Exploration of the potential effect of some selected Indian medicinal plants against Alzheimer's disease

Thesis submitted for the degree of Doctor of Philosophy

By

**Suparna Ghosh, M.Pharm**
**(Registration No.: D-7/ISLM/66/21 of 21-22)**

**School of Natural Product Studies**
**Faculty of Interdisciplinary Science, Law & Management (FISLM)**
**Jadavpur University**
**Kolkata 700032, India**

**2025**

# DEDICATED TO
# MY PARENTS

## Certificates from Supervisors

This is to certify that the thesis entitled "Exploration of the potential effect of some selected Indian medicinal plants against Alzheimer's disease" submitted by Ms. Suparna Ghosh, who got registered (registration no D-7/ISLM/66/21 of 21-22, dated 06.01.2022) her name under the Faculty of Interdisciplinary Studies, Law & Management for the award PhD (Pharmacy) degree of Jadavpur University is absolutely based upon her own work under the supervision of Prof. Pulok Kumar Mukherjee and Prof. Pallab Kanti Haldar and that neither her thesis nor any part of the thesis has been submitted for any degree / diploma or any other academic award anywhere before.


**Prof. Pulok Kumar Mukherjee**
PhD, FAScT, FNAAS, FRSC, FNASc

Professor
Dept. of Pharmaceutical Technology
School of Natural Product Studies
Jadavpur University
Kolkata 700032, India

**Prof. Pulok Kumar Mukherjee**
**प्रो. पुलोक कुमार मुखर्जी**
FAScT, FNAAS, FRSC, FNASc
प्रोफ़ेसर / Professor
यादवपुर विश्वविद्यालय / Jadavpur University
Department of Pharmaceutical Technology
कोलकाता / Kolkata - 700032, भारत / India

**Prof. Pallab Kanti Haldar**
PhD, FIC, FNESA

Director
School of Natural Product Studies
Professor & Head
Dept. of Pharmaceutical Technology
Jadavpur University
Kolkata 700032, India

*Prof. Pallab Kanti Haldar*
Ph.D., FIC, FNESA
Director
School of Natural Product Studies
Jadavpur University, Kolkata-700032

## Statement of Originality

I, Suparna Ghosh (D-7/ISLM/66/21 of 21-22) registered on 06.01.2022 do hereby declare that this thesis entitled "Exploration of the potential effect of some selected Indian medicinal plants against Alzheimer's disease" contains literature survey and original research work done by the undersigned candidates as part of Doctoral studies.

All information in this thesis has been obtained and presented in accordance with existing academic rules and ethical conduct. I declare that, as required by thesis rules and conduct, I have fully cited and referred all materials and results that are not original to this work.

I also declare that I have checked this thesis as per the "Policy on Anti Plagiarism, Jadavpur University, 2019", and the level of similarity as checked by iThenticate software is 7%.

Signature of the candidate with date:

Signature of the Supervisors with date and seal:


**Prof. Pulok Kumar Mukherjee**
PhD, FAScT, FNAAS, FRSC, FNASc
Professor
Dept. of Pharmaceutical Technology
School of Natural Product Studies
Jadavpur University
Kolkata - 700032, India

**Prof. Pallab Kanti Haldar** 8-9-22
PhD, FIC, FNESA
Director
School of Natural Product Studies
Professor & Head
Dept. of Pharmaceutical Technology
Jadavpur University
Kolkata - 700032, India

**Prof. Pulok Kumar Mukherjee**
**प्रो. पुलोक कुमार मुखर्जी**
FAScT, FNAAS, FRSC, FNASc
प्रोफ़ेसर / Professor
यादवपुर विश्वविद्यालय / Jadavpur University
Department of Pharmaceutical Technology
कोलकाता / Kolkata - 700032, भारत / India

*Prof. Pallab Kanti Haldar*
Ph.D., FIC, FNESA
Director
School of Natural Product Studies
Jadavpur University, Kolkata-700032

## Thesis details

1. **Registration Number and the Date of Registration:** D-7/ISLM/66/21 of 21-22, dated 06.01.2022.

2. **Title of the Thesis:** Exploration of the potential effect of some selected Indian medicinal plants against Alzheimer's disease.

3. **Name and Designation of the Supervisor(s):**
   Prof. Pulok Kumar Mukherjee, Professor, Department of Pharmaceutical Technology, Jadavpur University
   Prof. Pallab Kanti Haldar, Director, School of Natural Product Studies, Department of Pharmaceutical Technology, Jadavpur University.

4. **E-mail ID of the Supervisor(s):** pulok.mukherjee@jadavpuruniversity.in; pallab.haldar@jadavpuruniversity.in

5. **List of Publications:**

   **5a) Publications related to Doctoral work:**

   i. **Ghosh S**, Das B, Jana S, Singh KO, Sharma N, Mukherjee PK, Haldar PK (2025) Mechanistic insight into neuroprotective effect of standardized ginger chemo varieties from Manipur, India in scopolamine induced learning and memory impaired mice. *Metabolic Brain Disease* 40, 101, 1-17. https://doi.org/10.1007/s11011-025-01535-8.

   ii. **Ghosh S**, Das B, Haldar PK, Kar A, Chaudhary SK, Singh KO, Bhardwaj PK, Sharma N, Mukherjee PK (2023) 6-Gingerol contents of several ginger varieties of Northeast India and correlation of their antioxidant activity in respect to phenolics and flavonoids contents. *Phytochemical Analysis* 34, 259-268. https://doi.org/10.1002/pca.3201.

   **5b) Other Publications during the period of Doctoral Research (if any):**

   i. Chowdhury S, Gupta BD, **Ghosh S**, Gayen S, Kar A, Mukherjee PK, Haldar PK (2025) Metabolite profiling and neuroprotective potential of *Clitoria ternatea* L. through in-vitro and in-vivo

experimental models. *Fitoterapia* 185, 106772, 1-10. https://doi.org/10.1016/j.fitote.2025.106772.

ii. Kshetrimayum V, Chanu KD, **Ghosh S**, Haldar PK, Mukherjee PK, Sharma N, 2023. Paris polyphylla Sm. extract enriched with diosgenin as an antidiabetic agent: In vitro and in vivo study. *Phytomedicine Plus* 3, 100497, 1-9. https://doi.org/10.1016/j.phyplu.2023.100497.

iii. Jana S, Gayen S, Gupta BD, Singha S, Mondal J, Kar A, Nepal A, **Ghosh S**, Rajabalaya R, David SR, Balaraman AK, Bala A, Mukerjee PK, Haldar PK (2024) Investigation on anti-diabetic efficacy of a Cucurbitaceae food plant from the North-East region of India: Exploring the molecular mechanism through modulation of oxidative stress and glycosylated hemoglobin (HbA1c). *Endocrine Metabolic & Immune Disorders - Drug Targets* 24, 220-234. http://dx.doi.org/10.2174/1871530323666230907115818.

iv. Chanu KD, Sharma N, Kshetrimayum V, Chaudhary SK, **Ghosh S**, Haldar PK, Mukherjee PK (2023) Ageratina adenophora (Spreng.) King & H. Rob. standardized leaf extract as an antidiabetic agent for type 2 diabetes: An in vitro and in vivo evaluation. *Frontiers in Pharmacology* 14, 1178904, 1-17. https://doi.org/10.3389/fphar.2 023.1178904.

v. Mukherjee PK, Efferth T, Das B, Kar A, **Ghosh S**, Singha S, Debnath P, Sharma N, Bhardwaj PK, Haldar PK (2022) Role of medicinal plants in inhibiting SARS-CoV-2 and in the management of post- COVID-19 complications. *Phytomedicine* 98, 153930, 1-33. https://doi.org/10.1016/j.phymed.2022.153930.

**6. List of Patents:** NIL

**7. List of Presentations in National/International Conferences:**

i. Presented a paper in Oral presentation session in the National Seminar on “Role of Medicinal Plants to Ameliorate Diabetes and Related Disorders” organized by School of Natural Product Studies, Jadavpur University, Kolkata held on 08-09 March, 2024.

**Ghosh S**, Das B, Haldar PK, Ameliorative effects of ginger varieties from Northeast India on scopolamine induced memory impairment in mice: The role of cholinesterase and oxidative stress.

ii. Presented a paper in the Poster session in the International Bioresources Conclave & Ethnopharmacology Congress (ISESFEC-2023) on the theme “Reimagine Ethnopharmacology: Globalization of Traditional Medicine” at City Convention Centre, Imphal, Manipur, India during February 24-26, 2023.

**Ghosh S**, Das B, Haldar PK, Kar A, Chaudhary SK, Singh KO, Bhardwaj PK, Sharma N, Mukherjee PK, C Comparative antioxidant and anti-cholinesterase potential of ginger varieties of North-East India in respect to variation of 6-Gingerol content.

iii. Presented a paper in Oral presentation session in the 9th Convention of SFE-INDIA and National Seminar on “Translational Research on Indian Medicinal Plants” at Jadavpur University, Kolkata during September 23-24, 2022.

**Ghosh S**, Das B, Haldar PK, Kar A, Chaudhary SK, Bhardwaj PK, Sharma N, Mukherjee PK, Quality evaluation of several ginger varieties of North-East India.

**8. Participation in Workshops, Seminars and Symposiums:**

i. Participated in the National workshop on “Basic Techniques in Animal Handling and Pre-clinical Applications” sponsored by the Committee for Control and Supervision of Experiments on Animals (CCSEA), Govt. of India at the School of Natural Product Studies, Jadavpur University during July 03-04, 2025.

ii. Participated in the International Conference on the theme “Indian Medicinal Plants in Drug Discovery: Tradition, Science & Innovation” organized by School of Natural Product Studies, Jadavpur University at Jadavpur University, Kolkata during January 21-22, 2025.

iii. Participated in the “Training & Capacity Building Program on Extraction and Downstream Processing” at Jadavpur University, Kolkata during September 24-26, 2024.

iv. Participated in the “Hands-on Training on Basic Techniques in Animal Handling and Research” at Jadavpur University, Kolkata and Centre for Translational Animal Research (Centralized Animal Facility), Bose Institute, Madhyamgram, Kolkata during August 29-30, 2024.

## Abstract

Alzheimer's disease (AD) is a progressive and irreversible neurodegenerative disorder that manifests as memory deficits, cognitive deterioration, behavioral abnormalities, language impairments, and a gradual decline in the ability to perform routine activities. *Zingiber officinale* Roscoe (ginger), a valued medicinal plant in Ayurveda, has long been utilized for the treatment of neurological ailments. The present work focuses on an in-depth phytochemical and pharmacological assessment of nine ginger chemo-varieties sourced from different agro-climatic zones of Northeast India, with special emphasis on Manipur, a region renowned for its biodiversity.

Following collection and taxonomic authentication, the rhizomes were processed for extract preparation and subjected to detailed analytical and biological investigations. Among the tested varieties, ginger variety 6 (GV6) was distinguished by its markedly higher 6-gingerol concentration and total phenolic content (TPC), which were closely associated with its superior antioxidant activities. Statistical analysis confirmed a strong positive correlation between 6-gingerol content and TPC, while total flavonoid content (TFC) showed weaker associations. High-Performance Thin Layer Chromatography (HPTLC) profiling substantiated GV6 as the richest source of 6-gingerol. In vitro bioassays further demonstrated notable acetylcholinesterase (AChE, $IC_{50}$ = 336.10 µg/mL) and butyrylcholinesterase (BChE, $IC_{50}$ = 411.73 µg/mL) inhibitory effects of GV6. The neuroprotective efficacy of GV6 was subsequently validated in a scopolamine-induced mouse model of cognitive impairment at doses of 200 and 400 mg/kg. Behavioral assessments revealed significant enhancement of spatial recognition, as well as improvements in both short- and long-term memory. Treatment with GV6 also modulated cholinergic activity by reducing AChE and BChE activity, elevating acetylcholine (ACh) levels, mitigating oxidative stress, and suppressing neuroinflammation. Histopathological examination confirmed restoration of neuronal density, improved organization of nerve fibers, and reversal of nuclear shrinkage. Furthermore, molecular docking simulations indicated stable interactions of 6-gingerol and galantamine with both AChE (−7.5 and −7.3 kcal/mol) and BChE (−7.3 and −8.5 kcal/mol), corroborating their inhibitory potential.

In conclusion, this investigation underscores the therapeutic relevance of ginger chemo-varieties from Northeast India, with GV6 emerging as the most promising candidate. Its administration demonstrated significant cognitive benefits by restoring neurotransmitter balance, reinforcing antioxidant defenses, and modulating inflammatory pathways, thereby offering potential as a natural adjunct in AD management.

## Table of contents

## List of tables

## List of figures

## Abbreviations

Alzheimer's disease: AD

Amyloid-β: Aβ

Late-Onset AD: LOAD

Early-Onset AD: EOAD

Apolipoprotein E ε4: APOE ε4

Complement Receptor 1: CR1

CD2-Associated Protein: CD2AP

Bridging Integrator 1: BIN1

Triggering Receptor Expressed on Myeloid Cells 2: TREM2

Phospholipase D3: PLD3

Phosphatidylinositol Binding Clathrin Assembly Protein: PICALM

Presenilin 2: PSEN2

Amyloid Precursor Protein: APP

ATP-Binding Cassette Sub-Family A Member 7: ABCA7

Sortilin-Related Receptor 1: SORLA

Phospholipase D Family Member 3: PLD3

T-Cell Immune Regulator 1: TCIRG1

RUN and FYVE Domain-Containing Protein 1: RUFY1

Ras and Rab Interactor 3: RIN3

Chromosome 9 Open Reading Frame 72: C9ORF72

Granulin: GRN

Microtubule-Associated Protein Tau: MAPT

Presenilin-1: PSEN1

Food and Drug Administration: FDA

Acetylcholinesterase Inhibitors: AChEIs

Acetylcholinesterase: AChE

Acetylcholine: ACh

Butyrylcholinesterase: BChE

Total Phenolic Content: TPC

Total Flavonoid Content: TFC

High Performance Liquid Chromatography: HPLC

High Performance Thin Layer Chromatography: HPTLC

High-Resolution Liquid Chromatography-Mass Spectrometry-Quadrupole Time-of-Flight: HR-LCMS-QTOF

Novel Object Recognition: NOR

Aluminium Chloride: $AlCl_3$

2,2-Diphenyl-1-Picrylhydrazyl: DPPH

Ferric Chloride: $FeCl_3$

Ethylenediaminetetraacetic Acid: EDTA

Hydrogen Peroxide: $H_2O_2$

Trichloro Acetic Acid: TCA

Thiobarbituric Acid: TBA

Sodium Hydroxide: NaOH

2,2′-Azinobis(3-Ethylbenzothiazoline-6-Sulfonic Acid): ABTS

Acetylthiocholine Iodide: ATCI

Butyrylthiocholine Iodide: BTCI

Reverse-Phase-High-Performance-Liquid-Chromatography: RP-HPLC

Limit of Detection: LOD

Limit of Quantification: LOQ

Relative Standard Deviation: RSD

Absorbance Unit: AU

Retention Time: RT

5,5′-Dithiobis(2-Nitrobenzoic Acid): DTNB

Tumor Necrosis Factor- α: TNF-α

Enzyme-Linked Immunosorbent Assay: ELISA

Institutional Animal Ethics Committee: IAEC

Committee for the Purpose of Control and Supervision of Experiments on Animals: CPCSEA

Organization for Economic Co-operation and Development: OECD

body weight: b.w.

per os: p.o.

Intraperitoneal: i.p.

Phosphate Buffer Saline: PBS

Bovine Serum Albumin: BSA

5-Thio-2-Nitrobenzoic Acid: TNB

Thiobarbituric Acid Reactive Substances: TBARS

Trichloroacetic Acid: TCA

Thiobarbituric Acid: TBA

2,4-Iodophenyl-3,4-Nitrophenyl-5-Phenyltetrazolium Chloride: INT

Potassium Cyanide: KCN

Malondialdehyde: MDA

Superoxide Dismutase: SOD

Glutathione: GSH

Glutathione Disulfide: GSSG

Catalase: CAT

Hydrogen Peroxide: $H_2O_2$

Nitrate/nitrite: NOx

Hematoxylin and Eosin: H&E

## Acknowledgement

First and foremost, I express my deepest gratitude to my supervisor(s), Prof. Pulok Kumar Mukherjee and Prof. Pallab Kanti Haldar, for their invaluable guidance, encouragement, and continuous support throughout the course of my doctoral research. Their insightful advice and inspiring mentorship have been instrumental in shaping both my research and my academic growth.

I am also sincerely thankful to my doctoral research committee members, teachers, and faculty of the School of Natural Product Studies, Jadavpur University, for their academic support, constructive feedback, and encouragement at every stage of my work.

I wish to acknowledge the Savitribai Jyotirao Phule Fellowship for Single Girl Child scheme of 2022-23, University Grants Commission, Govt. of India, for supporting my research project, which significantly contributed to the successful execution of this work.

On a personal note, I extend my immense gratitude to the fellow research scholar Dr. Bhaskar Das, and heartfelt thanks to the senior research scholar Dr. Amit Kar, Dr. Subhadip Banerjee, Dr. Akansha Sharma Pandey, Dr. Seha Singha Gayen, Dr. Sandipan Jana, and other research scholar Mr. Barun Dasgupta, Mr. Srijon Gayen, Mrs. Soma Chowdhury, Mr. Agnipravo Naskar, Ms. Manihar Parvin, Ms. Anirbita Ghosh, Mr. Soham Dey, Mr. Lalchand Seikh, Mr. Suman Tudu, Ms. Sukla Dhara and all the lab members for their constant motivation, discussions, and for creating a pleasant working environment.

I am deeply indebted to my parents and family members, whose unconditional love, sacrifices, and encouragement have been my strongest source of strength. Without their constant support and patience, this work would not have been possible.

Finally, I offer my humble thanks to the Almighty for giving me courage, perseverance, and blessings to accomplish this thesis.

# Chapter 1

## Alzheimer's Disease – Pathways and phytochemical therapeutics

1.1 Alzheimer's Disease – An overview

1.2 Epidemiology of Alzheimer's Disease – Global and regional trends

1.3 Pathophysiological mechanisms underlying Alzheimer's Disease

1.4 Medicinal herbs in the management of Alzheimer's Disease

1.5 Herbal bioactive compounds in the management of Alzheimer's Disease

1.6 Challenges and future prospects

1.7 Conclusion

## 1.1. Alzheimer's Disease – An overview

Alzheimer's Disease (AD) is a chronic and progressive neurodegenerative condition characterized by declined cognitive abilities, memory loss, behavioral changes, speech impairments, and a progressive loss of capacity to manage everyday tasks. AD is the leading cause of dementia, contributing to around 70% of all cases. It is broadly divided into two categories: (i) sporadic AD and (ii) familial AD. Sporadic AD, which represents nearly 95% of total cases, is complex in origin and is usually classified as Late-Onset AD (LOAD). This type typically happens in individuals aged 65 years and older. In contrast, familial AD accounts for only about 5% of cases and is usually inherited. It typically develops before the age of 65 and is referred to as Early-Onset AD (EOAD). EOAD is known to exhibit unique clinical symptoms and neurobiological characteristics, often necessitating tailored therapeutic strategies that differ from those used for LOAD (Long and Holtzman, 2019; Andrade-Guerrero et al., 2023). LOAD is not attributed to a single dominant genetic mutation and is relatively widespread in the general population, though it typically presents a modest individual risk. Among the genetic contributors, the Apolipoprotein E ε4 (APOE ε4) allele is recognized as the most significant risk factor for LOAD. However, its presence is not determinative. Individuals carrying one copy of the APOE ε4 allele have an elevated risk of developing the disease, and the risk increases further in those with two copies. Interestingly, many people diagnosed with LOAD do not possess the APOE ε4 allele, indicating the involvement of other genetic elements. LOAD is considered polygenic, meaning it is influenced by multiple genetic variations. Till now, researchers have identified more than 600 genes potentially linked to increased susceptibility to AD. Among these, notable genes are Complement Receptor 1 (CR1), CD2-Associated Protein (CD2AP), Clusterin, Bridging Integrator 1 (BIN1), Triggering Receptor Expressed on Myeloid Cells 2 (TREM2), Phospholipase D3 (PLD3), and Phosphatidylinositol Binding Clathrin Assembly Protein (PICALM). Together, these genetic factors contribute to the complex hereditary basis of LOAD (Raman et al., 2020; Andrews et al., 2020; Van Acker et al., 2019; DeTure and Dickson, 2019). EOAD is primarily driven by specific

genetic mutations. Among the most prominent genes linked to EOAD are Presenilin 2 (PSEN2) and Amyloid Precursor Protein (APP). Mutations in either of these genes can significantly elevate the risk of EOAD, with symptoms often emerging between the ages of 30 and 50. Recent advancements in whole-genome and whole-exome sequencing have explored the understanding of genetic underpinnings of EOAD. These approaches have identified more than 20 genetic loci associated with EOAD, implicating a variety of metabolic and cellular pathways in the disease process. Among these genes the ATP-Binding Cassette Sub-Family A Member 7 (ABCA7), Sortilin-Related Receptor 1 (SORLA), and TREM2, plays an important role in lipid metabolism and amyloid processing. Additional genes such as Phospholipase D Family Member 3 (PLD3), T-Cell Immune Regulator 1 (TCIRG1), RUN and FYVE Domain-Containing Protein 1 (RUFY1), and Ras and Rab Interactor 3 (RIN3) are involved in pathways including endocytosis, immune response, and vesicular transport. Furthermore, other genes such as Chromosome 9 Open Reading Frame 72 (C9ORF72), Granulin (GRN), and Microtubule-Associated Protein Tau (MAPT) are also being explored for their potential roles in increasing EOAD susceptibility (Lanoiselee et al., 2017; Goldman and Hou, 2004; Nudelman et al., 2023; Bellenguez et al., 2017). While genetic mutations are central to the development of EOAD, environmental and lifestyle factors may also contribute to disease risk. One notable example is head trauma, which has been identified as a significant risk factor for EOAD. Individuals carrying pathogenic genetic variants may be especially susceptible to the harmful effects of traumatic brain injuries, as these mutations can increase vulnerability to neurodegenerative processes triggered by such events (Rao et al., 2015; Guo et al., 2000). Conversely, a variety of environmental and lifestyle factors have been linked to LOAD, including hypertension, type 2 diabetes, smoking, elevated cholesterol, physical inactivity, and poor dietary habits. Persistent high blood pressure can disrupt cerebrovascular function and raise LOAD risk. In type 2 diabetes, insulin resistance and impaired glucose regulation contribute to cognitive decline. Tobacco use exacerbates oxidative stress and neuroinflammation, hastening

disease progression. Meanwhile, high cholesterol levels may promote Amyloid-β (Aβ) fibril formation in the brain, further driving LOAD pathology (Yaffe et al., 2021; Diniz et al., 2021; Durazzo et al., 2014; Xu et al., 2020; Di Liegro et al., 2019). The below section provides an overview of the current scenery of AD, including its epidemiology, underlying pathophysiological mechanisms, existing therapeutic options, and potential future directions.

## 1.2. Epidemiology of Alzheimer's Disease - Global and regional trends

An estimated 44 million people are living with dementia globally, and this number is expected to rise to over 152 million by the middle of this century. A significant proportion of these cases will occur in low and middle income countries, where the burden of the disease is growing rapidly (Zhang et al., 2021). Research indicates that in 1994, approximately 24.3 million individuals were living with AD, with an estimated 4.6 million new cases emerging annually, roughly equating to one new diagnosis every seven seconds. Projections suggest that by the year 2040, the global AD population may exceed 80 million. However, this rise is not evenly distributed worldwide. While developed Nations are expected to see a doubling in AD cases, developing countries may experience a threefold increase, reflecting significant differences in disease prevalence and growth rates (Ernst and Hay, 1994; Cornutiu, 2015). A study conducted in 2016 identified dementia as the fifth leading cause of death globally, responsible for approximately 4.4% of all fatalities. The growing number of dementia related deaths can be partially attributed to the rising global population and increasing life expectancy, which have led to a higher prevalence of age related conditions (Monfared et al., 2022). Moreover, deaths associated with AD have shown a rising trend. Data from 2010 in the United States revealed that the prevalence of AD increased with age, affecting around 12% of individuals aged over 65, approximately 23% of those over 75, and nearly 47% of people aged over 85 (Cornutiu, 2015). The incidence of AD related dementia increases sharply with age, rising from 7 cases per 1,000 individuals at age 65 to 118 cases per 1,000 among those over 85, a nearly 17 fold escalation. In Australia, data from the McCusker Alzheimer's Research

Foundation indicated a considerable rise in AD diagnoses, with 245,000 reported cases in 2009 compared to just 52,000 in 2005. This represents more than a fourfold increase within a span of four years, underscoring the growing impact of the disease (Bachman et al., 1993; Adair et al., 2022). In India, a study by Chandra and colleagues, observed an incidence rate of AD of 1.74 per 1,000 individuals aged 55 and above, which increased to 4.7 per 1,000 among those over 65 years of age. In countries such as India and various regions of Africa, where birth rates remain comparatively high and a significant proportion of the population consists of children and youths, the overall incidence of AD tends to be lower. This reflects an inverse association between population aging and birth rates, which in turn influences the prevalence of age related disorders like AD. However, with the gradual reduction in birth rates and a consequent demographic shift toward an aging population, these regions are likely to experience a rising incidence of AD in the future (Chandra et al., 2001). Research conducted in Denmark reported an AD incidence rate of 20.9 per 1,000 individuals, with no notable gender difference observed. In contrast, data from the Alzheimer Society of Canada indicated that approximately 72% of individuals diagnosed with AD are women. While men tend to be more frequently affected by other forms of dementia, the higher occurrence of AD among women is largely accredited to their greater average life expectancy, which increases the likelihood of developing age related neurodegenerative conditions (Andersen et al., 1999). In 2010, estimates indicated that approximately 754,000 individuals in France were living with dementia, accounting for around 1.2% of the National population. Projections suggest that this figure will increase to about 1.81 million by the year 2050, representing roughly 2.6% of the population. Across Europe, the number of dementia cases was estimated at 7.21 million in 2006, with expectations that it will rise to 16.51 million by 2050. Focusing specifically on AD in France, the estimated prevalence in 2010 was 504 cases per 1,000 inhabitants, with a reported range between 360 and 626 per 1,000. In the broader European context, there were around 6 million individuals diagnosed with AD in 2010, of whom approximately 74.3% were women. Forecasts indicate that by 2050, the

total number of AD cases in Europe will reach 14.5 million. This trend suggests a significant increase in prevalence, from an estimated 754 per 1,000 individuals in 2010, to a projected 1,813 per 1,000 by 2050 (Mura et al., 2010; de Pedro-Cuesta et al., 2009).

### 1.3. Pathophysiological mechanisms underlying Alzheimer's Disease

AD is a progressive neurodegenerative condition with a complex and multifactorial origin, primarily characterized by the buildup of Aβ plaques and the formation of neurofibrillary tangles within the brain (Slot et al., 2019). These hallmark neuropathological changes have been closely associated with mutations in certain genes, including the APP gene on the chromosome 21, Presenilin-1 (PSEN1) located on chromosome 14, and PSEN2 (Cacace et al., 2016; Agarwal et al., 2020). Mutations in these genes disrupt the normal processing of APP, leading to increased production and extracellular accumulation of Aβ aggregates. Simultaneously, tau proteins become abnormally hyperphosphorylated, resulting in the intracellular formation of neurofibrillary tangles. These molecular disturbances contribute to the degeneration of cholinergic pathways and progressive neuronal loss, particularly affecting regions of the brain responsible for cognitive function, such as the hippocampus and cerebral cortex (Li et al., 2019; Moore et al., 2023). In light of these complex pathological processes, various hypotheses have been proposed to elucidate the mechanisms underlying disease progression. Among them the major hypotheses are the Aβ hypothesis, Tau hypothesis, cholinergic hypothesis, inflammatory hypothesis and the oxidative stress hypothesis (Nasb et al., 2024). The key pathophysiological mechanisms are illustrated in the following schematic diagram:

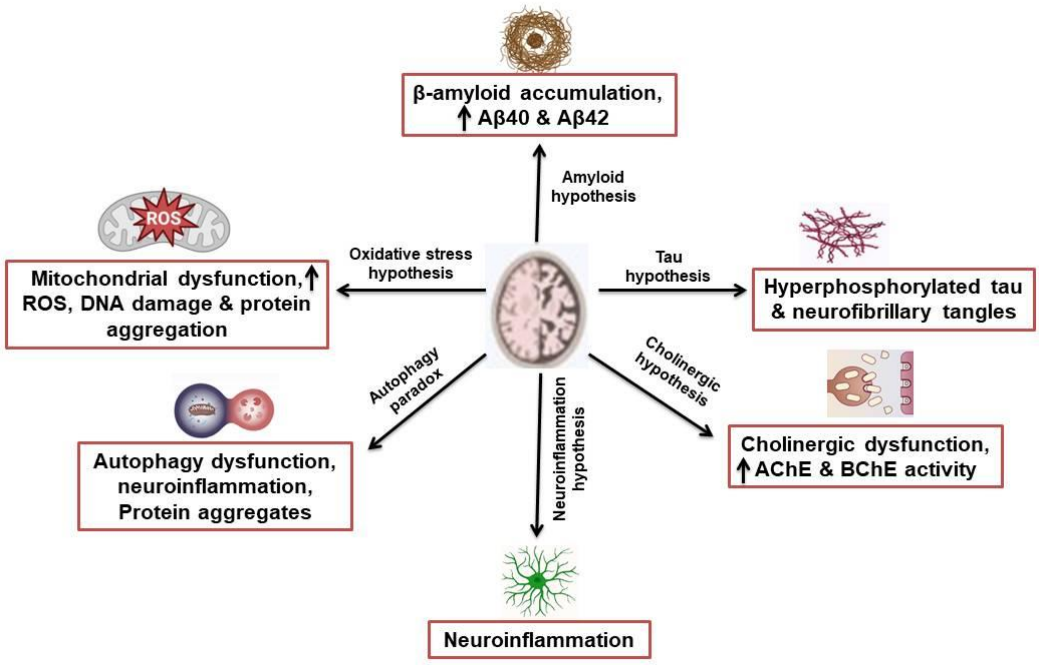


**Figure 1.1: Key pathphysiological mechanisms underlying AD**

Although the number of AD related deaths has risen significantly over the past two decades, no curative treatment is currently available. The U.S. Food and Drug Administration (FDA) have approved Acetylcholinesterase Inhibitors (AChEIs) such as galantamine, rivastigmine, and donepezil, along with the NMDA receptor antagonist memantine. All the approved drugs offer only the symptomatic improvement rather than halting or reversing the disease progression (Martins et al., 2023; Xing et al., 2025).

## 1.4. Medicinal herbs in the management of Alzheimer's Disease

Medicinal plants have been utilized for centuries in the management of AD and other cognitive impairments. Traditional healthcare systems such as Ayurveda, Unani, Siddha, and Homeopathy provide valuable knowledge regarding the use of natural remedies for neurological health (Kushwah et al., 2023). Among these, Unani medicine is particularly recognized for its well-structured and holistic

therapeutic principles. These indigenous practices prioritize both prevention and treatment while generally presenting fewer adverse effects compared to conventional pharmaceuticals, thereby positioning herbal-based interventions as a potentially safer alternative to synthetic drug therapies (Khan et al., 2022; Jansen et al., 2021).

Plant-based therapies have their origins in ancient civilizations, including those of Egypt, India, and China, and continue to receive worldwide recognition in modern healthcare (Elendu, 2024). A significant number of present-day pharmaceuticals are derived from bioactive plant constituents, underscoring the importance of botanicals in drug discovery. The rising global demand for herbal products is driven by both public interest and an expanding body of scientific evidence supporting their efficacy (Ahmad et al., 2025; Najmi et al., 2022). Neurodegenerative disorders such as AD affect the central and autonomic nervous systems, impairing voluntary and involuntary functions. Certain phytochemicals possess the ability to influence brain activity, exerting sedative, stimulant, anticonvulsant, and neuroprotective effects. Given that conventional therapies often cause adverse effects or offer only modest benefits, there is increasing interest in natural alternatives (Singh et al., 2025; Kumar and Khanum, 2012). Many medicinal plants are recognized for their cognitive-enhancing potential, with recent research highlighting their capacity to inhibit Aβ aggregation, tau aggregation, cholinesterase enzyme inhibition, neuroinflammation and oxidative stress inhibition (ALNasser et al., 2025). Plant families such as Amaryllidaceae, Valerianaceae, Rutaceae, and Polygonaceae contain alkaloids, flavonoids, terpenoids, and phenolic compounds that display notable neuroprotective activity against AD (Taqui et al., 2022). These discoveries have positioned herbal medicines as a promising avenue in AD management. The table below (Table 1.1) showed the medicinal plants investigated between 2000 and 2025, outlining their possible mechanisms of action relevant to AD therapy.

**Table 1.1. Plant species with neuroprotective potential in AD**

| Plant name | Family | Parts | Fraction | MOA | References |
|---|---|---|---|---|---|
| *Abutilon indicum* (L.) Sweet | Malvaceae | Whole plant | Methanol | Cholinesterase enzyme inhibition | Ingkaninan et al., 2003 |
| *Acacia nilotica* (L.) Delile | Mimosaceae | Leaves | Ethyl acetate | Cholinesterase enzyme inhibition | Eldeen et al., 2005 |
| *Acacia sieberiana* D C. | Mimosaceae | Roots | Ethyl acetate | Cholinesterase enzyme inhibition | Eldeen et al., 2005 |
| *Acanthus ebracteatus* Vahl | Acanthaceae | Aerial parts | Methanol | Cholinesterase enzyme inhibition | Ingkaninan et al., 2003 |
| *Achillea millefolium* L. | Asteraceae | Aerial parts | Aqueous | Cholinesterase enzyme inhibition | Verma et al., 2018 |
| *Acorus calamus* L. | Acoraceae | Rhizomes | Methanol | Cholinesterase enzyme inhibition | Oh et al., 2004 |
| *Acorus gramineus* Sol. | Araceae | Rhizomes | Methanol | Cholinesterase enzyme inhibition | Orhan et al., 2008 |
| *Aegle marmelos* (L.) Corrêa | Rutaceae | Fruit pulps | Methanol | Cholinesterase enzyme inhibition | Ingkaninan et al., 2003 |
| *Albizia adianthifolia* (Schumach.) W.F.Wight | Fabaceae | Leaves | Methanol | Cholinesterase enzyme inhibition | Sonibare et al., 2017 |
| *Albizia procera* (Roxb.) Benth. | Leguminosae | Bark | Methanol | Cholinesterase enzyme | Ingkaninan et al., 2003 |

| | | | | | |
|---|---|---|---|---|---|
| | | | | inhibition | |
| *Allium roseum* L. | Amaryllidaceae | Whole plant | Ethanol | Aβ aggregation inhibition | Boubakri et al., 2020 |
| *Allium sativum* L. | Amaryllidaceae | Bulbs | Aqueous | Aβ aggregation inhibition | Gupta et al., 2009 |
| | | | Ethanol | Aβ induced neuroinflammation inhibition | Nillert et al., 2017 |
| *Aloe vera* (L.) Burm.f. | Liliaceae | Leaves | Ethanol | Cholinesterase enzyme inhibition | Khattak et al., 2005 |
| *Ammodaucus leucotrichus* Coss. | Apiaceae | Aerial parts | Aqueous | Cholinesterase enzyme inhibition | Sadaoui et al., 2018 |
| *Anagallis arvensis* L. | Primulaceae | Aerial and root parts | Methanol | Cholinesterase enzyme inhibition | Saleem et al., 2020 |
| *Anethum graveolens* L. | Apiaceae | Leaves | Aqueous | Cholinesterase enzyme inhibition | Orhan et al., 2008 |
| *Angelica decursiva* (Miq.) Franch. & Sav. | Apiaceae | Whole plant | Methanol | Cholinesterase enzyme inhibition | Ali et al., 2015 |
| *Angelica sinensis* (Oliv.) Diels | Apiaceae | Rhizomes | Ethanol | Aβ associated oxidative stress | Huang et al., 2008 |

| | | | | | |
|---|---|---|---|---|---|
| | | | | inhibition | |
| *Anthriscus nemorosa* (M.Bieb.) Spreng. | Apiaceae | Aerial parts | Aqueous | Cholinesterase enzyme inhibition | Karakaya et al., 2019 |
| *Arnica chamissonis* Less. | Asteraceae | Flowers | Hexane: methanol | Cholinesterase enzyme inhibition | Wszelaki et al., 2010 |
| *Artemisia dracunculus* L. | Asteraceae | Leaves | Aqueous | Cholinesterase enzyme inhibition | Dohi et al., 2009 |
| *Aquilaria subintegra* Ding Hou | Thymelaeaceae | Leaves and stems | Chloroform | Cholinesterase enzyme inhibition | Bahrani et al., 2014 |
| *Avicennia officinalis* L. | Verbenaceae | Leaves | Methanol | Cholinesterase enzyme inhibition | Suganthy et al., 2009 |
| *Bacopa monnieri* (L.) Pennell | Scrophulariaceae | Whole plant | Ethanol | Cholinesterase enzyme inhibition | Das et al., 2002 |
| *Berberis darwinii* Hook. | Berberidaceae | Stem-bark | Methanol | Cholinesterase enzyme inhibition | Habtemariam, 2011 |
| *Betula platyphylla* Sukaczev | Betulaceae | Bark | Ethanol | Aβ aggregation inhibition | Cho et al., 2014 |
| *Borago officinalis* L. | Boraginaceae | Leaves | Ethanol | Aβ aggregation inhibition | Ghahremani tamadon et al., 2014 |
| *Boswellia dalzielii* Hutch. | Burseraceae | Leaves | Aqueous | Cholinesterase enzyme inhibition | Kohoude et al., 2017 |

| | | | | | |
|---|---|---|---|---|---|
| *Boswellia socotranao* Balf.f. | Burseraceae | Resins | Chloroform and methanol | Cholinesterase enzyme inhibition | Bakthir et al., 2011 |
| *Brassica oleracea* L. | Brassicaceae | Flower heads | Aqueous | Cholinesterase enzyme inhibition | Orhan et al., 2008 |
| *Buchanania axillaris* (Desr.) Ramamoorthy | Anacardiaceae | Whole plant | Methanol | Cholinesterase enzyme inhibition | Penumala et al., 2018 |
| *Bupleurum falcatum* L. | Umbelliferae | Roots | Methanol | Cholinesterase enzyme inhibition | Orhan et al. 2008 |
| *Butea superba* Roxb. | Leguminosae | Root barks | Methanol | Cholinesterase enzyme inhibition | Ingkaninan et al., 2003 |
| *Buxus sempervirens* L. | Buxaceae | Whole plant | Chloroform: methanol | Cholinesterase enzyme inhibition | Orhan et al., 2004 |
| *Caesalpinia crista* L. | Fabaceae | Leaves | Methanol | Aβ aggregation and cholinesterase enzyme inhibition | Chethana et al., 2018 |
| *Capparis spinosa* Linnaeus | Capparaceae | Leaves and fruits | Methanol | Down regulation of APP, BACE-1, PSEN-1 and PSEN-2 gene | Mohebali et al., 2016 |

| | | | | | |
|---|---|---|---|---|---|
| *Capsella bursa-pastoris* (L.) Medik. | Brassicaceae | Whole plant | Methanol | Cholinesterase enzyme inhibition | Sancheti et al., 2010 |
| *Carpobrotus edulis* (L.) N.E.Br. | Aizoaceae | Leaves | Methanol | Cholinesterase enzyme inhibition | Rocha et al., 2017 |
| *Carum carvi* L. | Apiaceae | Roots | Methanol | Cholinesterase enzyme inhibition | Adsersen et al., 2006 |
| *Carum copticum* (L.) Benth. & Hook. f. | Apiaceae | Seeds | Aqueous | Cholinesterase enzyme inhibition | Piri et al., 2020 |
| *Cassia fistula* L. | Leguminosae | Roots | Methanol | Cholinesterase enzyme inhibition | Ingkaninan et al., 2003 |
| *Cassia obtusifolia* L. | Leguminosae | Seeds | Methanol | Cholinesterase enzyme inhibition | Jung et al., 2016 |
| *Cassia tora* L. | Leguminosae | Leaves | Methanol | Cholinesterase enzyme inhibition | Chethana et al., 2017 |
| *Centella asiatica* (L.) Urb. | Umbelliferae | Whole plant | Methanol | Cholinesterase enzyme inhibition | Mukherjee et al., 2007 |
| *Chaerophyllum aromaticum* L. | Apiaceae | Roots | Essential oil and methanol | Cholinesterase enzyme inhibition | Petrovi´ et al., 2017 |
| *Chamaemelum nobile* (L.) All. | Asteraceae | Flowers | Aqueous | Cholinesterase enzyme inhibition | Seo et al., 2014 |
| *Cinnamomum* | Lauraceae | Leaves | Methanol | Cholinester | Dalai et al., |

| | | | | | |
|---|---|---|---|---|---|
| *tamala* (Buch.-Ham.) T.Nees & Eberm. | | | | ase enzyme inhibition | 2014 |
| *Cinnamomum verum* J.S. Presl. | Lauraceae | Bark | Aqueous | Aβ aggregation inhibition | Ramshini et al., 2015 |
| *Cinnamomum zeylanicum* J.Presl | Lauraceae | Bark | Aqueous | Tau aggregation inhibition | Peterson et al., 2009 |
| *Citrus limon* (L.) Osbeck | Lamiaceae | Fruit peel | Essential oil | Cholinesterase enzyme inhibition | Menichini et al., 2011 |
| *Citrus medica* L. | Rutaceae | Fruits | Hydroalcohol | Cholinesterase enzyme inhibition | Menichini et al., 2011 |
| *Citrus reticulata* Blanco | Rutaceae | Leaves | Aqueous | Cholinesterase enzyme inhibition | Chaiyana and Okonogi, 2012 |
| *Cistus libanotis* L. | Cistaceae | Leaves | Aqueous | Cholinesterase enzyme inhibition | Loizzo et al., 2013a |
| *Cistus monspeliensis* L. | Cistaceae | Leaves | Aqueous | Cholinesterase enzyme inhibition | Loizzo et al., 2013a |
| *Clitoria ternatea* L. | Fabaceae | Leaves, roots & the combination of leaves & roots | Methanol | Cholinesterase enzyme inhibition | Chowdhury et al., 2025 |

| | | | | | |
|---|---|---|---|---|---|
| *Cistus salvifolius* L. | Cistaceae | Leaves | Aqueous | Cholinesterase enzyme inhibition | Loizzo et al., 2013a |
| *Cistus villosus* L. | Cistaceae | Leaves | Aqueous | Cholinesterase enzyme inhibition | Loizzo et al., 2013a |
| *Cleome rutidosperma* DC. | Capparaceae | Whole plant | Aqueous | Cholinesterase enzyme inhibition | McNeil et al., 2018 |
| *Combretum kraussii* Hochst. | Combretaceae | Leaves | Ethyl acetate | Cholinesterase enzyme inhibition | Eldeen et al., 2005 |
| *Corydalis solida* (L.) Clairv. | Papaveraceae | Whole plant | Chloroform: methanol | Cholinesterase enzyme inhibition | Orhan et al., 2004 |
| *Crinum jagus* (J.Thomps.) Dandy | Amaryllidaceae | Bulbs and leaves | Alkaloid | Cholinesterase enzyme inhibition | Cortes et al., 2018 |
| *Crithmum maritimum* L. | Apiaceae | Aerial parts | Hydroalcohol | Cholinesterase enzyme inhibition | Mekinić et al., 2018 |
| *Croton socotranus* Balf.f. | Euphorbiaceae | Bark | Chloroform and methanol | Cholinesterase enzyme inhibition | Bakthir et al., 2011 |
| *Cymbopogon citratus* (DC.) Stapf | Poaceae | Stems | Aqueous | Cholinesterase enzyme inhibition | Chaiyana and Okonogi, 2012 |
| *Cyphostemma adenocaule* (Steud. ex A.Rich.) Desc. ex | Vitaceae | Leaves and fruits | Hydroalcohol | Cholinesterase enzyme inhibition | Bello et al., 2019 |

| | | | | | |
|---|---|---|---|---|---|
| Wild & R.B.Drumm. | | | | | |
| *Derris scandens* (Roxb.) Benth. | Leguminosae | Stems | Methanol | Cholinesterase enzyme inhibition | Ingkaninan et al., 2003 |
| *Diospyros kaki* Thunb. | Ebenaceae | Leaves | Ethanol | Aβ aggregation inhibition | Ma et al., 2018 |
| *Dorstenia gigas* Schweinf. ex Balf.f. | Moraceae | Leaves | Chloroform and methanol | Cholinesterase enzyme inhibition | Bakthir et al., 2011 |
| *Echinacea pallida* (Nutt.) Nutt. | Asteraceae | Root and aerial parts | Pet. ether and chloroform | Cholinesterase enzyme inhibition | Orhan et al., 2009 |
| *Echinacea purpurea* (L.) Moench | Asteraceae | Root and aerial parts | Pet. ether and chloroform | Cholinesterase enzyme inhibition | Orhan et al., 2009 |
| *Epimedium koreanum* Nakai | Berberidaceae | Whole plant | Methanol | Cholinesterase enzyme inhibition | Orhan et al., 2004 |
| *Eucharis bonplandii* (Kunth) Traub | Amaryllidaceae | Bulbs | Alkaloid | Cholinesterase enzyme inhibition | Cortes et al., 2018 |
| *Eucommia ulmoides* Oliv. | Eucommiaceae | Bark | Aqeuous | Aβ aggregation inhibition | Kwon et al., 2011 |
| *Eugenia brasiliensis* Lam. | Myrtaceae | Leaves | Essential oil | Cholinesterase enzyme inhibition | Siebert et al., 2015 |
| *Euonymus* | Celastracea | Leaves | Methanol | Cholinester | Sancheti et |

| | | | | | |
|---|---|---|---|---|---|
| *sachalinensis* (F.Schmidt) Maxim. | e | | | ase enzyme inhibition | al., 2010 |
| *Euphorbia characias* L. | Euphorbiaceae | Flowers and leaves | Ethanol | Cholinesterase enzyme inhibition | Pisano et al., 2016 |
| *Eupatorium odoratum* L. | Asteraceae | Whole plant | Aqueous | Cholinesterase enzyme inhibition | Chaiyana and Okonogi, 2012 |
| *Eureiandra balfourii* Cogn. & Balf.f. | Cucurbitaceae | Tubers | Chloroform and methanol | Cholinesterase enzyme inhibition | Bakthir et al., 2011 |
| *Fagopyrum tataricum* (L.) Gaertn. | Polygonaceae | Seeds | Methanol | Aβ aggregation inhibition | Choi et al., 2013 |
| *Ferula lutea* (Poir.) Grande | Apiaceae | Flowers | Volatile oil | Cholinesterase enzyme inhibition | Loizzo et al., 2013b |
| *Foeniculum vulgare* Mill. | Apiaceae | Aerial parts | Hydroalcohol | Cholinesterase enzyme inhibition | Menichini et al., 2011 |
| *Fragaria ananassa* ( Duchesne ex Weston) Duchesne ex Rozier | Rosaceae | Fruits | Aqueous | Cholinesterase enzyme inhibition | Orhan et al., 2008 |
| *Fragaria vesca* L. | Rosaceae | Fruits | Aqueous | Cholinesterase enzyme inhibition | Orhan et al., 2008 |
| *Glaucium corniculatum* (L.) Curtis | Papaveraceae | Whole plant | Chloroform: methanol | Cholinesterase enzyme inhibition | Orhan et al., 2004 |

| | | | | | |
|---|---|---|---|---|---|
| *Hemidesmus indicus* (L.) R. Br. ex Schult. | Apocynaceae | Whole plant | Methanol | Cholinesterase enzyme inhibition | Penumala et al., 2018 |
| *Huperzia reflexa* (Lam.) Trevis. | Lycopodiaceae | Aerial parts | Alkaloid | Cholinesterase enzyme inhibition | Konrath et al., 2012 |
| *Inula graveolens* (L.) Desf. | Asteraceae | Leaves | Aqueous | Cholinesterase enzyme inhibition | Dohi et al., 2009 |
| *Laurus nobilis* L. | Lauraceae | Leaves | Essential oil and ethanol | Cholinesterase enzyme inhibition | Ferreira et al., 2006 |
| *Lycopodium clavatum* L. | Lycopodiaceae | Aerial parts | Chloroform and methanol | Cholinesterase enzyme inhibition | Orhan et al., 2016 |
| *Lycopersicon esculentum* Mill. | Solanaceae | Fruits | Aqueous | Cholinesterase enzyme inhibition | Orhan et al., 2008 |
| *Lycium barbarum* L. | Solanaceae | Fruits | Ethanol | Aβ induced neurotoxicity inhibition | Ho et al., 2007 |
| *Maesilea quadrifolia* Linn. | Marsileaceae | Whole plant | Methanol | Cholinesterase enzyme inhibition | Bhadra et al., 2011 |
| *Malus domestica* Baumg. | Rosaceae | Fruits | Juice | Cholinesterase enzyme inhibition | Orhan et al., 2008 |
| *Malva sylvestris* L. | Malvaceae | Flowers | Essential oil and ethanol | Cholinesterase enzyme inhibition | Ferreira et al., 2006 |
| *Meliosma oldhamii* | Sabiaceae | Whole | Methanol | Cholinester | Sancheti et |

| | | | | | |
|---|---|---|---|---|---|
| Miq. | | plant | | ase enzyme inhibition | al., 2010 |
| *Mentha longifolia* (L.) Huds. | Lamiaceae | Aerial parts | Ethanol | Cholinesterase enzyme inhibition | Vladimir-Knežević et al., 2014 |
| *Mentha piperita* L. | Lamiaceae | Leaves, aerial parts, and Flowers | Ethanol | Cholinesterase enzyme inhibition | Vladimir-Knežević et al., 2014 |
| *Mentha spicata* L. | Lamiaceae | Whole plant | Methanol | Cholinesterase enzyme inhibition | Adsersen et al., 2006 |
| *Michelia champaca* L. | Magnoliaceae | Leaves | Methanol | Cholinesterase enzyme inhibition | Ingkaninan et al., 2003 |
| *Mimusops elengi* L. | Sapotaceae | Flowers | Methanol | Cholinesterase enzyme inhibition | Ingkaninan et al., 2003 |
| Mollugo oppositifolia Linn. | Molluginaceae | Aerial parts | Methanol | Cholinesterase enzyme, β secretase inhibition | Das et al., 2020 |
| *Morina persica* L. | Caprifoliaceae | Aerial parts | Acetone, methanol, and aqueous | Cholinesterase enzyme inhibition | Mocan et al., 2016 |
| *Morus alba* L. | Moraceae | Rhizomes | Ethanol | Aβ aggregation | Liu and Du, 2020 |

| | | | | | |
|---|---|---|---|---|---|
| | | | | inhibition | |
| *Musa paradisiaca* L. | Musaceae | Immature fruits | Aqueous | Cholinesterase enzyme inhibition | Orhan et al., 2008 |
| *Musa sapientum* L. | Musaceae | Fruits | Methanol | Cholinesterase enzyme inhibition | Ingkaninan et al., 2003 |
| *Myricaria elegans* Royle | Tamaricaceae | Aerial parts | Methanol | Cholinesterase enzyme inhibition | Ahmad et al. 2003 |
| *Myrciaria floribunda* (H.West ex Willd.) O.Berg | Myrtaceae | Fruit peels | Aqueous | Cholinesterase enzyme inhibition | Barbosa et al., 2020 |
| *Narcissus abscissus* (Haw.) Schult. & Schult.f. | Amaryllidaceae | Bulbs | Methanol | Cholinesterase enzyme inhibition | Lopez et al., 2002 |
| *Narcissus assoanus* Dufour ex Schult. & Schult.f. | Amaryllidaceae | Bulbs | Methanol | Cholinesterase enzyme inhibition | Lopez et al., 2002 |
| *Narcissus baeticus* Fern.Casas | Amaryllidaceae | Bulbs | Methanol | Cholinesterase enzyme inhibition | Lopez et al., 2002 |
| *Nardostachys jatamansi* (D.Don) DC. | Valerianaceae | Rhizomes | Methanol | Cholinesterase enzyme inhibition | Mukherjee et al., 2007 |
| *Nelumbo nucifera* Gaertn. | Nymphaeaceae | Rhizomes | Methanol | Cholinesterase enzyme inhibition | Mukherjee et al., 2007 |
| *Paederia linearis* Hook.f. | Rubiaceae | Whole plant | Methanol | Cholinesterase enzyme inhibition | Ingkaninan et al., 2003 |

| | | | | | |
|---|---|---|---|---|---|
| *Paronychia argentea* Lam. | Caryophyllaceae | Aerial parts | Essential oil and ethanol | Cholinesterase enzyme inhibition | Ferreira et al., 2006 |
| *Peganum harmala* L. | Zygophyllaceae | Seeds | Methanol | Cholinesterase enzyme inhibition | Ali et al., 2013 |
| *Piper divaricatum* G. Mey. | Piperaceae | Aerial parts | Essential oil | Cholinesterase enzyme inhibition | de Oliveira et al., 2019 |
| *Piper interruptum* Opiz | Piperaceae | Stems | Methanol | Cholinesterase enzyme inhibition | Ingkaninan et al., 2003 |
| *Piper nigrum* L. | Piperaceae | Fruits | Methanol | Rduction of oxidative stress induced by Aβ | Hritcu et al., 2014 |
| *Piper sarmentosum* Roxb. | Piperaceae | Leaves | Aqueous | Cholinesterase enzyme inhibition | Chaiyana and Okonogi, 2012 |
| *Pistacia lentiscus* L. | Anacardiaceae | Aerial parts | Aqueous | Cholinesterase enzyme inhibition | Aissi et al., 2016 |
| *Plumbago indica* L. | Plumbaginaceae | Roots | Methanol | Cholinesterase enzyme inhibition | Ingkaninan et al., 2003 |
| *Polianthes tuberosa* L. | Asparagaceae | Aerial parts | Hydroalcohol | Cholinesterase enzyme inhibition | Das et al., 2020 |
| *Polygonatum* | Polygonace | Whole | Aquous | Cholinester | Chaiyana |

| | | | | | |
|---|---|---|---|---|---|
| *odoratum* (Mill.) Druce | ae | plant | | ase enzyme inhibition | and Okonogi, 2012 |
| *Polygonum multifloru m* Thunb. | Polygonace ae | Roots | Ethanol | Cholinester ase enzyme inhibition | Li et al., 2017 |
| *Polyscias fruticosa* (L.) Harms | Araliaceae | Leaves | Aqueous | Cholinester ase enzyme inhibition | Chaiyana and Okonogi, 2012 |
| *Prunus domestica* L. | Rosaceae | Fruits | Aqueous | Cholinester ase enzyme inhibition | Orhan et al., 2008 |
| *Pulicaria stephanocarpa* Balf.f. | Compositae | Leaves | Chlorofor m and methanol | Cholinester ase enzyme inhibition | Bakthir et al., 2011 |
| *Punica granatum* L. | Lythraceae | Fruit peels | Hydroalco hol | Aβ aggregation inhibition, acetylcholin esterase (AChE) inhibition | Morzelle et al., 2016 |
| | | Fruits | Aqueous | Cholinester ase enzyme inhibition | Orhan et al., 2008 |
| *Pyrola japonica* Klen ze ex Alef. | Pyrolaceae | Whole plant | Methanol | Cholinester ase enzyme inhibition | Sancheti et al., 2010 |
| *Rotheca myricoides* (Hochst.) Steane & | Lamiaceae | Aerial parts | Hydroalco hol | Cholinester ase enzyme | Das et al., 2020 |

| | | | | | |
|---|---|---|---|---|---|
| Mabb. | | | | inhibition | |
| *Rhizophora lamarckii* Montrouz. | Rhizophoraceae | Leaves | Methanol | Cholinesterase enzyme inhibition | Suganthy et al., 2009 |
| *Rhizophora mucronata* Lam | Rhizophoraceae | Leaves | Methanol | Cholinesterase enzyme inhibition | Suganthy and Devi, 2016 |
| *Rhodiola crenulata* (Hook.f. & Thomson) H.Ohba | Crassulaceae | Roots | Freeze drying extract | Aβ aggregation inhibition | Zhang et al., 2019 |
| *Rhus mysorensis* G.Don | Anacardiaceae | Whole plant | Methanol | Cholinesterase enzyme inhibition | Penumala et al., 2018 |
| *Rosa damascene* Mill | Rosaceae | Flowers | Methanol | Improvement of the Aβ induced memory abnormalities | Esfandiary et al., 2015 |
| *Rumex hastatus* Baldw. | Polygonaceae | Whole plant | Methanol | Cholinesterase enzyme inhibition | Ahmad et al., 2015 |
| *Ruta graveolens* L. | Rutaceae | Whole plant | Hexane | Cholinesterase enzyme inhibition | Wszelaki et al., 2010 |
| *Salix mucronata* Thunb. | Salicaceae | Bark | Ethyl acetate | Cholinesterase enzyme inhibition | Eldeen et al., 2005 |
| *Salvia officinalis* L. | Lamiaceae | Leaves | Ethanol | Cholinesterase enzyme inhibition | Vladimir-Knežević et al., 2014 |

| | | | | | |
|---|---|---|---|---|---|
| *Salvia trichoclada* Benth. | Lamiaceae | Aerial parts | Methanol | Cholinesterase enzyme inhibition | Demirezer et al., 2015 |
| *Salvia triloba* L.f. | Lamiaceae | Seeds | Alcohol | Cholinesterase enzyme inhibition | Ahmed et al., 2013 |
| *Sanguisorba minor* Bertol. | Rosaceae | Aerial parts | Essential oil, ethanol | Cholinesterase enzyme inhibition | Ferreira et al., 2006 |
| *Satureja bachtiarica* Bunge | Lamiaceae | Aerial parts | Methanol | Cholinesterase enzyme inhibition | Soodi et al., 2016 |
| *Satureja montana* L. | Lamiaceae | Leaves, aerial parts, and flowers | Ethanol | Cholinesterase enzyme inhibition | Vladimir-Knežević et al., 2014 |
| *Securidaca longipedunculata* Fresen. | Polygalaceae | Roots | Aqueous | Cholinesterase enzyme inhibition | Saliu et al., 2017 |
| *Senna occidentalis* (L.) Link | Leguminosae | Aerial parts | Hydroalcohol | Cholinesterase enzyme inhibition | Das et al., 2020 |
| *Senna tora* (L.) Roxb. | Leguminosae | Leaves | Methanol | Cholinesterase enzyme inhibition | Chethana et al. 2017 |
| *Sesuvium portulacastrum* (L.) L. | Aizoaceae | Leaves | Methanol | Cholinesterase enzyme inhibition | Suganthy et al., 2009 |
| *Sonchus asper* (L.) Hill | Asteraceae | Aerial parts | Methanol | Cholinesterase enzyme | Khan et al., 2012 |

| | | | | | |
|---|---|---|---|---|---|
| | | | | inhibition | |
| *Spinacia oleracea* L. | Chenopodiaceae | Aerial parts | Dichloromethane, ethanol and water | Cholinesterase enzyme inhibition | Boga et al., 2011 |
| *Stephania suberosa* Forman | Menispermaceae | Roots | Methanol | Cholinesterase enzyme inhibition | Ingkaninan et al., 2003 |
| *Streblus asper* Lour. | Moraceae | Seeds | Methanol | Cholinesterase enzyme inhibition | Ingkaninan et al., 2003 |
| *Sterculia tragacantha* Lindl. | Malvaceae | leaves | Methanol | Cholinesterase enzyme inhibition | Sadeer et al., 2019 |
| *Suaeda monica* Forssk. ex J.F.Gmel. | Amaranthaceae | Leaves | Methanol | Cholinesterase enzyme inhibition | Suganthy et al., 2009 |
| *Symplocos chinensis* (Lour.) Druce | Symplocaceae | Whole plant | Methanol | Cholinesterase enzyme inhibition | Sancheti et al., 2010 |
| *Tabernaemontana divaricata* (Lour.) G. Don | Apocynaceae | Roots | Methanol | Cholinesterase enzyme inhibition | Ingkaninan et al., 2003 |
| *Tanacetum abrotanifolium* (L.) Druce | Asteraceae | Flowers | Aqueous | Cholinesterase enzyme inhibition | Polatoğlu et al., 2015 |
| *Terminalia bellirica* (Gaertn.) Roxb. | *Combretaceae* | Fruits | Methanol | Cholinesterase enzyme inhibition | Ingkaninan et al., 2003 |
| *Teucrium arduini* L. | Lamiaceae | Aerial parts | Ethanol | Cholinesterase enzyme | Vladimir-Knežević et |

| | | | | | |
|---|---|---|---|---|---|
| | | | | inhibition | al., 2014 |
| *Teucrium chamaedrys* L. | Lamiaceae | Aerial parts | Ethanol | Cholinesterase enzyme inhibition | Vladimir-Knežević et al., 2014 |
| *Teucrium montanum* L. | Lamiaceae | Aerial parts | Ethanol | Cholinesterase enzyme inhibition | Vladimir-Knežević et al., 2014 |
| *Teucrium polium* L. | Lamiaceae | Aerial parts | Ethanol | Cholinesterase enzyme inhibition | Vladimir-Knežević et al., 2014 |
| *Thymus lotocephalus* G.López & R.Morales | Lamiaceae | Aerial parts | Aqueous | Cholinesterase enzyme inhibition | Costa et al., 2012 |
| *Thymus vulgaris* L. | Lamiaceae | Aerial parts | Ethanol | Cholinesterase enzyme inhibition | Vladimir-Knežević et al., 2014 |
| *Tiliacora triandra* (Colebr.) Diels | Menispermaceae | Roots | Methanol | Cholinesterase enzyme inhibition | Ingkaninan et al., 2003 |
| *Tinospora crispa* (L.) Hook. f. & Thomson | Menispermaceae | Stems | Methanol | Cholinesterase enzyme inhibition | Ingkaninan et al., 2003 |
| *Vanda roxburghii* R.Br. | Orchidaceae | Roots | Chloroform | Cholinesterase enzyme inhibition | Uddin et al., 2015 |
| *Viola odorata* L. | Violaceae | Aerial parts | Ethanol | Cholinesterase enzyme inhibition | Khattak et al., 2005 |
| *Vitex trifolia* L. | Lamiaceae | Roots | Methanol | Cholinesterase enzyme inhibition | Ingkaninan et al., 2003 |

| | | | | | |
|---|---|---|---|---|---|
| *Vitis vinifera* L. | Vitaceae | Fruits | Aqueous | Cholinesterase enzyme inhibition | Orhan et al., 2008 |
| *Vitis vinifera* L. | Vitaceae | Leaves | Methanol | Cholinesterase enzyme inhibition | Pintać et al., 2019 |
| *Withania somnifera* (L.) Dunal | Solanaceae | Roots | Ethanol | Cholinesterase enzyme inhibition | Khattak et al., 2005 |
| *Wolfiporia extensa* (Peck) Ginns | Polyporaceae | Whole plant | Methanol | Cholinesterase enzyme inhibition | Orhan et al., 2008 |
| *Xeranthemum annuum* L. | Asteraceae | Flowers | Chloroform | Cholinesterase enzyme inhibition | Orhan et al., 2016 |
| *Zanthoxylum gilletii* (De Wild.) P.G.Waterman | Rutaceae | Leaves | Methanol | Cholinesterase enzyme inhibition | Sadeer et al., 2019 |
| *Ziziphus jujuba* Mill. | Rhamnaceae | Fruits | Methanol | Cholinesterase enzyme inhibition | Orhan et al., 2008 |

## 1.5. Herbal bioactive compounds in the management of Alzheimer's Disease

Diet is now recognized as an essential component to maintain health and safety against oxidative stress, inflammation and related degenerative diseases. Plants, animals, marine organisms, and microorganisms are the rich sources of naural bioactive compounds, which possess diverse chemical structures and broad pharmacological activities. Many bioactive food-derived compounds have the potential to modulate the pathological process involved in AD. Notably, phenolic compounds such as fat-soluble vitamins, omega-3 fatty acids, carotenoids and

isothiocyanates showed significant results. These compounds acts not only as an antioxidants and anti-inflammatory agents, but also as modulators of major molecular pathways involved in AD such as Aβ plaque aggregation, tau aggregation, cholinergic imbalance etc (Grodzicki and Dziendzikowska, 2020). Experimental studies on rats of 3 months old were used to model AD which revealed that resveratrol, a natural compound of plant origin, provided neuroprotection (Rao et al., 2021). Similarly, cellular studies indicate that barberine, isolated from *Coptis salisb*, can inhibit the activation of GSK-3β and decrease tau hyperphosphorylation (Wang et al., 2025). Moreover, compounds such as nicotine (*Nicotiana tabacum*, Solanaceae), huperzine A (*Huperzia serrata*, Lycopodiaceae), curcumin (*Curcuma longa*, Zingiberaceae) and melatonin have been identified as effective candidates against AD and are currently in various stages of clinical trials (Ayaz et al., 2019). Some other classes of natural compounds, including alkaloids, flavonoids, terpenoids, phenylpropanoids, anthraquinones, glycosides, saponins, sesquiterpenes, and xanthones, have exhibited neuroprotective potential by targeting key cellular pathways implicated in AD (Sharifi-Rad et al., 2017).

The development of galantamine from European ethnopharmacological knowledge represents one of the most significant innovations among cholinesterase inhibitors. It was licensed for clinical use in the symptomatic management of AD. Initially, galantamine was isolated from *Galanthus woronowii* Losinsk., but it has since been identified in other plants such as daffodil and snowflake. The anticholinergic activity of galantamine was first reported in 1951 by Mashkovsky and Kruglikova-Lvova using a rat model (Heinrich, 2010).

Cholinesterase inhibitors became the first class of drugs approved by the U.S. FDA in 1990 for the treatment of AD and other cholinergic disorders, and they continue to represent the most effective therapeutic option currently in clinical practice. By reversibly inhibiting AChE, these agents enhance both the levels and duration of acetylcholine (ACh) activity, which helps alleviate disease symptoms while improving cognitive performance, behavioral outcomes, and overall

functional abilities (de Oliveira et al., 2024; Yiannopoulou and Papageorgiou, 2020).

Several isolated secondary metabolites of different chemical classes from the natural source reported to possess neuroprotective activity against AD are listed below.

**Table 1.2. Secondary metabolites isolated from plant species involved in management of AD**

| Plant name | Family | Parts used | Compound | Chemical class | References |
|---|---|---|---|---|---|
| *Acanthopanax henryi* (Oliv.) Harms | Araliaceae | Leaves | Quercetin, 4-caffeoyl-quinic acid and 4,5-caffeoyl quinic acid | Flavonoid, and phenylpropanoids | Zhang et al., 2014 |
| *Aconitum leave* Royle | Ranunculaceae | Roots | Swatinine-c and hohenackerine | Alkaloids | Ahmad et al., 2018 |
| *Aquilaria crassna* Pierre | Thymelaeaceae | Agarwood | 2-(2-hydroxy-2-phenylethyl)chromones | Phenolic | Wang et al., 2018 |
| *Artocarpus lacucha* Buch.-Ham. | Moraceae | Root barks | Lakoochin b | Polyphenol | Namdaung et al., 2018 |
| *Berberis aetnensis* C.Presl | Berberidaceae | Roots | Berberine and palmatine | Alkaloids | Bonesi et al., 2013 |
| *Buxus hyrcana* Pojark | Buxaceae | Leaves | Buxamine-C | Alkaloid | Khalid et al., 2005 |
| *Buxus papillosa* C.K. | Buxaceae | Leave | Buxahejramine | Alkaloids | Rahman et al., |

| | | | | | |
|---|---|---|---|---|---|
| Schneid. | | s | | | 2001 |
| | | | Buxakarachiamine | | Rahman et al., 2001 |
| | | | Buxamine-B | | Khalid et al., 2005 |
| *Cleistocalyx operculatus* (Roxb.) Merr. & L.M.Perry | Myrtaceae | Buds | Quercetin | Flavonoid | Min et al., 2010 |
| *Cocculus pendulus* (J. R.Forst. & G.Forst.) Diels | Menispermaceae | Whole plant | Cocsuline | Alkaloid | Rahman et al., 2004 |
| *Cortinarius infractus* (Pers.) Fr. | Cortinariaceae | Fruits | Infractopicrin and 10-hydroxy-infractopicrin | Alkaloids | Geissler et al., 2010 |
| *Corydalis incisa* (Thunb.) Pers | Papaveraceae | Aerial parts | Corynoline | Alkaloid | Kim, 2002 |
| *Crinum moorei* Hook.f. | Amaryllidaceae | Non-flowering whole plant | 1-O-acetyllycorine | Alkaloid | Elgorashi et al., 2004 |
| *Cryptocarya densiflora* Blume | Lauraceae | Leaves | (+)-nornantenine, (-)-desmethylsecoantofine, (+)-oridine, and (+)-laurotetanine | Alkaloids | Othman et al., 2016 |

| | | | | | |
|---|---|---|---|---|---|
| *Cryptocarya griffithiana* Wight | Lauraceae | Bark | 2-methoxy atherospermine, and (+)-reticuline | Alkaloids | Othman et al., 2016 |
| *Cryptocarya infectoria* (Blume) Miq. | Lauraceae | Bark | Atherospermine, (+)-n-methylisococlaurine, and (+)-n-methyllaurotetanine | Alkaloids | Othman et al., 2016 |
| *Delphinium denudatum* Wall. ex Hook.f. & Thomson | Ranunculaceae | Aerial parts | Isotalatazidine | Alkaloid | Ahmad et al., 2017 |
| *Hemidesmus indicus* (L.) R.Br. | Apocynaceae | Roots | Vanillin | Phenolic | Kundu and Mitra, 2013 |
| *Holarrhena pubescens* Wall. ex G.Don | Apocynaceae | Bark | Mokluangins a-c | Alkaloids | Cheenpracha et al., 2016 |
| *Melissa officinalis* L. | Lamiaceae | Leaves | Rosmarinic acid and its derivative | Phenolic acids | Dastmalchi et al., 2009 |
| *Momordica charantia* L. | Cucurbitaceae | Green fruits | Ligballinol | Lignan | Kuanhuta et al., 2014 |
| *Morus alba* L. | Moraceae | Root bark | Mulberrofurang, and albanol b | Flavonoids | Kuk et al., 2017 |
| *Mutellina purpurea* (Poir.) Reduron, | Apiaceae | Fruits | Pteryxin | Phenolic | Orhan et al., 2016 |

| | | | | | |
|---|---|---|---|---|---|
| Charpin & Pimenov | | | | | |
| *Narcissus assoanus* Dufour ex Schult. & Schult.f. | Amaryllidaceae | Dormant bulbs | Assoanine | Alkaloid | Lo´pez et al., 2002 |
| *Nelumbo nucifera* Gaertn. | Nelumbonaceae | Embryos | Liensinine | Alkaloid | Jung et al., 2015 |
| | | Stamens | Cycloartenol | Terpenoid | Jung et al., 2010 |
| *Peganum nigellastrum* bunge | Zygophyllaceae | Seeds | Harmine, harmaline and harmol | Alkaloids | Zheng et al., 2009 |
| *Perilla frutescens* (L.) Britton | Lamiaceae | Whole plant | Rosmarinic acid | Phenolic acid | Choi et al., 2016 |
| *Perovskia atriplicifolia* Benth. | Lamiaceae | Roots | Rosmarinic acid | Phenolic acid | Ślusarczyk et al., 2020 |
| *Phagnalon saxatile* (L.) cass. | Asteraceae | Flowering aerial parts | Caffeic acid, and luteolin 3,5-dicaffeoylquinic acid | Phenolic acid, and flavonoid | Conforti et al., 2010 |
| *Pinus heldreichii* subsp. Leucodermis | Pinaceae | Needles | Terpinolene, beta-phellandrene, linalyl acetate, trans-caryophyllene, and terpinen-4-ol | Terpenoids | Bonesi et al., 2010 |
| *Piper bavinum* L. | Piperaceae | Aerial parts | Bavinol a | Phenolic | Dung et al., 2015 |

| | | | | | |
|---|---|---|---|---|---|
| *Piper nigrum* L. | Piperaceae | Whole plant | Piperine, piperettine and piperettyline | Alkaloids | Tappayuthpijarn et al., 2011 |
| *Salvia glutinosa* L. | Lamiaceae | Roots | Rosmarinic acid | Phenolic acid | Senol et al., 2017 |
| *Salvia leriifolia* Benth. | Lamiaceae | Aerial parts | Camphor, 1,8-cineole, camphene and alpha-pinene | Terpenoids | Loizzo et al., 2009 |
| *Salvia miltiorrhiza* Bunge | Lamiaceae | Roots | Cryptotanshinone | Terpenoids | Wong et al., 2010 |
| *Sarcococca* hookeriana Baill. | Buxaceae | Whole plant | Chonemorphine | Alkaloid | Devkota et al., 2010 |
| *Stemona sessilifolia* (Miq.) Miq. | Stemonaceae | Roots | Stenine b | Alkaloid | Lai et al., 2013 |
| *Stephania venosa* Spreng. | Menispermaceae | Tubers | Cyclanoline | Alkaloid | Ingkaninan et al., 2006 |
| *Stichoneuron caudatum* Ridl. | Stemonaceae | Roots | Sessilistemonamines e | Alkaloid | Ramli et al., 2014 |
| *Tabernaemontana australis* Müll.Arg. | Apocynaceae | Stalks | Coronaridine | Alkaloid | Andrade et al., 2005 |
| *Taxus baccata* L. | Taxaceae | Heart wood | Lariciresinol, taxiresinol, 3′-demethylisolariciresinol-9′-hydroxyisopro | Lignans | Erdemoglu et al., 2004 |

| | | | | | |
|---|---|---|---|---|---|
| | | | pylether, isolariciresinol, and 3-demethylisolariciresinol | | |
| *Triclisia sacleuxii* (Pierre) Diels | Menispermaceae | Roots, and leaves | Lindoldhamine | Alkaloid | Murebwayire et al., 2009 |
| *Vanilla planifolia* Andrews | Orchidaceae | Pods | Vanillin | Phenolic | Kundu and Mitra, 2013 |

## 1.6. Challenges and future prospects

Comprehensive clinical studies are needed to strengthen the evidence for using herbal remedies in AD. Although encouraging results have emerged from preclinical and minor clinical trials, yet comprehensive evidence for these herbal interventions is still limited. Future trials should assess the efficacy of herbal remedies in different patient groups and at multiple stages of AD (Kirubakaran, 2025). Some major challenges of herbal drugs are showed in the below figure:

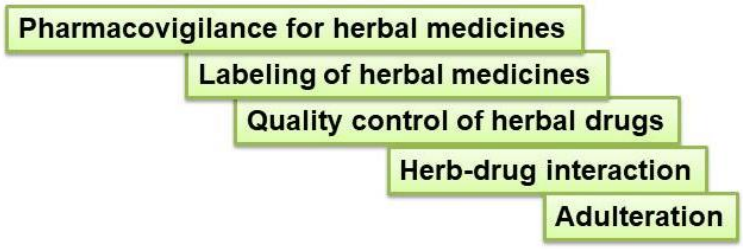


**Figure 1.2. Major challenges of herbal remedies to develop anti-Alzheimer's drug**

The progressive nature of AD highlights the need for long-term studies, since extended studies may clarify whether these treatments delay progression or enhance patient well-being. One of the main challenges in using herbal remedies for AD is the poor bioavailability of many active constituents. For example,

compounds such as curcumin extracted from the plant *Curcuma longa* and bacosides extracted from the plant *Bacopa monnieri* exhibited limited absorption, reducing their therapeutic potential. Developing formulations with improved bioavailability is therefore essential. These kinds of advanced herbal formulations may help to reduce the rapid metabolism of active compounds, extending their presence in the bloodstream. This prolonged bioavailability strengthens their neuroprotective effects and may lead to better clinical outcomes in AD, ultimately optimizing the therapeutic value of herbal remedies. Future research could also benefit from exploring combination approaches that unite herbal therapies with standard pharmaceutical treatments (Teja et al., 2022; Hampel et al., 2020).

## 1.7. Conclusion

The use of cholinesterase inhibitors has provided new therapeutic insights for managing neurodegenerative disorders associated with cholinergic neurotransmitter deficits. Both AChE and butyrylcholinesterase (BChE) play critical roles, making their evaluation equally important for the accurate and early diagnosis of AD. The concept of one compound acting on multiple targets has become an important strategy in modern drug discovery. By combining the ethnopharmacological wisdom with advanced tools, researchers have been able to find promising bioactive molecules from plant sources. These natural leads often exert a broad range of therapeutic effects and are associated with reduced adverse effects when compared to conventional synthetic drugs. Among these, alkaloid-rich fractions have frequently demonstrated superior potency. Consistent with structure-activity relationship concepts, most cholinesterase inhibitors contain nitrogen moieties within their core scaffold, aligning them with alkaloid chemistry. Notably, species from the Buxaceae, Amaryllidaceae, and Lycopodiaceae families have been reported to contain alkaloids and related phytochemicals. In addition, several non-nitrogenous compounds, including terpenoids, glycosides, and coumarins, have also shown significant inhibitory activity against cholinesterase. Based on these observations, the present dissertation explores cholinesterase inhibitors enriched medicinal plant,

highlighting diverse classes of bioactive compounds as safe and effective potential leads through in-vitro and in-vivo investigations. Ultimately, validating ethnobotanical claims with high-throughput screening strategies is expected to yield novel therapeutic candidates, thereby offering fresh perspectives for drug development and the treatment of neurodegenerative disorders such as AD.

# Chapter 2

## Chemo-diversity of ginger

2.1. Taxonomical study of ginger

2.2. Different varieties of ginger

2.3. Botanical description of ginger

2.4. Traditional uses of ginger

2.5. Phytochemistry of ginger

2.6. Conclusion

## 2.1. Taxonomical study of ginger

- Kingdom: Plantae.
- Clade: Tracheophytes.
- Clade: Angiosperms.
- Clade: Monocots.
- Clade: Commelinids.
- Order: Zingiberales.
- Family: Zingiberaceae.
- Genus: Zingiber.
- Species: *Zingiber officinale.*
- Binomial name: *Zingiber officinale* Roscoe.
- Vernacular names: Ginger (English), Shing (Manipuri), Ada (Assamese, Bengali, Oriya), Adu (Gujarati), Adrak (Hindi, Urdu), Shunti (Kannada, Konkani), Inji (Malayalam, Tamil), Aale (Marathi), Thingpuidum (Mizo), Singivera (Pali), Adaraka (Punjabi, Sanskrit), Allam (Telegu).

Family of the Zingiber genus is Zingiberaceae and the order of the genus Zingiber is Zingiberales while the tribe is Zingibereae. This tribe encompasses eight genera in total, including Zingiber along with Boesenbergia, Camptandra, Roscoea, Kaempferia, Amomum, Hedychium, and Curcuma (Kizhakkayil and Sasikumar, 2011). Although the precise evolutionary origin of *Zingiber officinale* remains a matter of scholarly debate, it is widely regarded as a domesticated species that traces its roots to the Indian subcontinent (Swamy, 2024). The Zingiberaceae family consists of roughly 50 genera and about 1,500 species of perennial herbaceous plants, predominantly thriving in tropical regions (Saensouk et al., 2016).

## 2.2. Different varieties of ginger

Ginger is a globally important spice and medicinal plant valued for its pungent aroma, characteristic flavor, and various therapeutic properties. While it is a single species, its morphological characters, flavor profiles, and phytochemical compositions vary significantly across different cultivars and places, leading to the recognition of multiple varieties adapted to specific agro-climatic conditions. These variations are influenced by factors such as soil type, altitude, rainfall, and cultivation practices, as well as genetic diversity preserved through traditional farming systems (Shaukat et al., 2023; Rai et al., 2006). Among the vast genera

and species of Zingiberaceae family, *Zingiber officinale* (ginger) stands out as the most extensively used species, primarily for its rhizome (Yang et al., 2025). Table below illustrates the different varieties of Zingiberaceae family (Table 2.1).

**Table 2.1. Different varieties of Zingiberaceae family and their short description**

| Scientific name | Common name | Description | Picture | References |
|---|---|---|---|---|
| *Zingiber officinale* Roscoe | Common ginger | This widely used culinary and medicinal herb thrives best under full sunlight. It holds immense value for both flavoring dishes and its therapeutic applications |  | https://powo.science.kew.org/taxon/urn:lsid:ipni.org:names:798372-1 |
| *Zingiber spectabile* Griff. | Beehive ginger | Also known as Malaysian ginger or Ginger wort, this plant is recognized by its characteristic beehive-like flower heads. It possesses several health benefits and is appreciated for its ornamental appeal |  | https://powo.science.kew.org/taxon/urn:lsid:ipni.org:names:798388-1 |

| | | | | |
|---|---|---|---|---|
| *Zingiber zerumbet* (L.) Roscoe ex Sm. | Bitter ginger | Commonly referred to as Pinecone ginger, Shampoo ginger, or Lempoyang, this variety emits a fragrant aroma from its foliage. Although slightly bitter, it enhances culinary flavors and is popularly used in hair care products |  | https://powo.science.kew.org/taxon/urn:lsid:ipni.org:names:798401-1 |
| *Zingiber mioga* (Thunb.) Roscoe | Myoga ginger | Also called Japanese ginger, the flower buds and young shoots of this plant are used in cooking. They offer a spicy, refreshing taste and a sharp fragrance |  | https://powo.science.kew.org/taxon/urn:lsid:ipni.org:names:798364-1 |
| *Cheilocostus speciosus* (J.Konig) C.D.Specht | Crepe ginger | Often known as Malay ginger or Cane reed, this species is characterized by its wrinkled white flowers that look like crepe paper. The buds and blossoms are edible and have a spicy flavour |  | https://indiaflora-ces.iisc.ac.in/FloraPeninsular/herbsheet.php?id=2932&cat=7 |

| | | | | |
|---|---|---|---|---|
| *Curcuma petiolata* Roxb. | Hidden ginger | Native to Malaysia, this plant is also called Queen lily, Siam tulip, or Hidden lily. Its spicy and slightly bitter flavor matches its colorful blooms in shades of red, orange, and pink |  | https://powo.science.kew.org/taxon/urn:lsid:ipni.org:names:796463-1 |
| *Hedychium coronarium* J.Koenig | Butterfly lily ginger | Known by names like White ginger lily, Mariposa blanca, and Dolan champa, it produces aromatic blossoms like butterflies. Its rhizomes are used for flavoring soups, and the essential oils are beneficial in treating fevers |  | https://powo.science.kew.org/taxon/urn:lsid:ipni.org:names:796836-1 |
| *Alpinia zerumbet* (Pers.) B.L.Burtt & R.M.Sm. | Shell ginger | Also called Variegated ginger or Getto plant, this ornamental variety has striped, oval leaves. Its fragrant flowers and edible vegetation are often included in culinary recipes |  | https://powo.science.kew.org/taxon/urn:lsid:ipni.org:names:872083-1 |

| | | | | |
|---|---|---|---|---|
| *Globba winitii* C.H.Wright | Dancing lady ginger | This ornamental species features delicate blossoms that resemble dancing figures swaying in the breeze. The flowers emit a sweet honeysuckle-like fragrance |  | https://powo.science.kew.org/taxon/urn:lsid:ipni.org:names:872574-1 |
| *Hedychium flavescens* Carey ex Roscoe | Yellow ginger | Referred to as Cream garland lily or Yellow ginger lily, this ginger is preferred for its ornamental and highly fragrant flowers. However, it is not as flavourful as other edible ginger types |  | https://powo.science.kew.org/taxon/urn:lsid:ipni.org:names:796848-1 |
| *Alpinia purpurata* (Vieill.) K.Schum. | Red ginger | Commonly known as Ostrich plume, Teuila flower, Jungle king, or Tahitian ginger, this plant has bright red or pink floral bracts. Though primarily ornamental, it also has a strong, spicy aroma |  | https://powo.science.kew.org/taxon/urn:lsid:ipni.org:names:795383-1 |

| | | | | |
|---|---|---|---|---|
| *Etlingera elatior* (Jack) R.M.Sm. | Torch ginger | Known by names like Wild ginger, Bunga kantan, Combrang, Red ginger lily, and Rose de porcelaine, this tropical species produces large, vibrant blossoms and is entirely edible, used in various cuisines worldwide |  | https://powo.science.kew.org/taxon/urn:lsid:ipni.org:names:942355-1 |
| *Curcuma amada* Roxb. | Mango ginger | Also called Mavina shunti, this variety resembles common ginger in appearance but lacks its pungency. Instead, it has a different raw mango flavour and is commonly used for pickles and chutneys in Indian cooking |  | https://efloraofindia.com/efi/curcuma-amada/ |
| *Hedychium gardnerianum* Sheph. ex Ker Gawl. | Kahili ginger | Sometimes referred to as Garland flower or Fragrant ginger lily, this Himalayan native is valued for its ornamental value. It is a tall, perennial species cultivated for its showy blooms |  | https://efloraofindia.com/efi/hedychium-gardnerianum/ |

| | | | | |
|---|---|---|---|---|
| *Alpinia galanga* (L.) Willd. | Thai ginger | Also known as Greater galangal, Lengkuas, Ginseng ginger, and Blue ginger, this type is essential in Southeast Asian cuisine and Unani medicine. Its rhizomes have a sharp aroma and a complex flavour of citrus, black pepper, and pine |  | https://powo.science.kew.org/taxon/urn:lsid:ipni.org:names:795279-1 |
| *Tapeinochilos ananassae* (Hassk.) K.Schum. | Pineapple ginger | Also called Lipstick ginger or Indonesian wax ginger, this tropical species features evergreen vegetation and red bracts housing bright yellow flowers. Its ornamental appeal makes it a popular indoor plant |  | https://powo.science.kew.org/taxon/urn:lsid:ipni.org:names:873025-1 |
| *Kaempferia rotunda* L. | Resurrection lily | Known by names such as Peacock ginger, Indian crocus, and Round-rooted galangal, this plant is known for its patterned leaves and fragrant, lily-like blooms. The tubers | 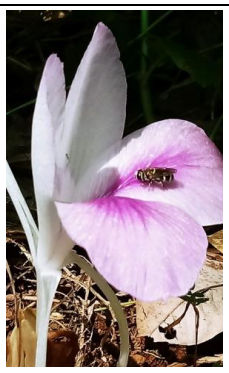 | https://efloraofindia.com/efi/kaempferia-rotunda/ |

| | | | | |
|---|---|---|---|---|
| | | have a mildly pungent flavour and are used similarly to ginger | | |
| *Curcuma alismatifolia* Gagnep. | Siam tulip | Also known as Summer tulip or Pink ginger tulip, this plant is known for its rosy bracts with reddish undertones. It is often grown indoors and used as a decorative cut flower |  | https://powo.science.kew.org/taxon/urn:lsid:ipni.org:names:796420-1 |
| *Alpinia calcarata* (Andrews) Roscoe | Snap ginger | Referred to as Indian ginger or Cardamom ginger, this species produces flowers resembling Snapdragons, with aromatic leaves showing a fragrance like cinnamon |  | https://powo.science.kew.org/taxon/urn:lsid:ipni.org:names:795225-1 |

## 2.3. Botanical description of ginger

*Zingiber officinale* Roscoe, commonly known as ginger, is a monocotyledonous, herbaceous perennial primarily cultivated for its aromatic rhizome. The plant possesses an underground system including a thick, fleshy, segmented rhizome with a pale yellow interior and a thin corky outer layer ranging from light yellow to reddish-brown. The rhizome grows horizontally just beneath the soil surface, with nodes bearing axillary buds that contribute to sympodial branching. From these nodes arise fibrous roots for nutrient absorption, as well as thicker supportive roots. The rhizome contains secretory cells rich in essential oils, responsible for

its characteristic aroma and flavor (Shahrajabian et al., 2019; Dhanik et al., 2017).

Above the ground, ginger grows pseudostems, which are upright, unbranched stems made from tightly packed leaf bases. These usually reach 60-150 cm in height. The leaves are narrow, lance-shaped, and arranged in two rows, measuring about 5-30 cm long and 8-20 mm wide, with a pointed tip and clear parallel veins. The upper surface is smooth, while the underside may have slight hairs. A ligule is present where the leaf blade meets the sheath. The leaf bases overlap to form the pseudostem (Maqbool et al., 2022; Sindhoora and Bhattacharjee, 2020).

The reproductive parts of ginger grow on special leafless stems called scapes, which come directly from the rhizome. The flowers are arranged in a dense, cone-like spike about 15-30 cm long, made up of overlapping oval to elliptical bracts. Inside each bract, there is one flower along with a small protective bracteole. The calyx is about 10-12 mm long, and the corolla tube is slightly longer, about 18-25 mm, ending in three uneven lobes: a curved dorsal lobe that bends over the anther, and two side lobes that bend backward (Ansari et al., 2021; Moghaddasi and Kashani, 2012).

The labellum is the most distinctive part of ginger flowers, yellow outside and deep purple or red inside, often spotted with a hairy center. Flowers have one fertile stamen, a slender style ending in a funnel-shaped stigma, and an inferior, three-chambered ovary with nectar glands. Fruits are rare, but when present, they are red capsules with black seeds in a white aril. Flowers are hermaphroditic, bilaterally symmetrical, and insect-pollinated. Ginger thrives in warm, humid tropical climates with loose, well-drained soils. Though perennial, it is cultivated as an annual crop. Apart from food and medicine, it is also valued as an ornamental plant (Ahmed and Jogdand, 2021; Adewale et al., 2021; Imtiyaz et al., 2013; Gavrilova et al., 2022).

## 2.4. Traditional uses of ginger

Since ancient times, the rhizome of ginger has been incorporated into diverse traditional medical systems, including those of Greece, Rome, India, China, the

Mediterranean basin, various regions of Asia, and the Arab world (Shahrajabian et al., 2019). Historical sources document its use for managing ailments such as colds, headaches, nausea, indigestion, gastrointestinal disturbances, diarrhea, arthritis, muscular discomfort, and other rheumatologic disorders (Verma and Bisen, 2022). Its carminative and antiflatulent actions have been widely known. In classical Greece and Rome, the characteristic aroma and pungent flavor of ginger were valued primarily for their medicinal rather than culinary properties. The eminent Greek physician Galen recommended ginger for body cleansing and for conditions believed to result from imbalances in the humoral system. Within African and West Indian traditions, the rhizome remains a key component of folk remedies (Bodagh et al., 2018). In contemporary contexts, particularly in the United States, ginger is frequently advocated to alleviate or prevent nausea. In traditional Chinese medicine, its recorded use extends back to at least the 4$^{th}$ century BCE, where it was regarded as an essential therapeutic root. Chinese practitioners prescribed it for a wide spectrum of health issues, including abdominal pain, nausea, diarrhea, cholera, respiratory conditions, asthma, cardiovascular complaints, toothaches, and rheumatic ailments. In Southeast Asian healing systems, ginger, both fresh and dried, has been extensively utilized for its therapeutic potential (Ernst and Pittler, 2000; Tiwari et al., 2025). In Arabian system of medicine, ginger is believed to enhance memory and has long been valued as a traditional remedy for boosting cognitive functions. In India, documented references to its medicinal application date back to the Vedic period, where it was honored with the description ‘Maha aushadhi’, meaning “Supreme medicine”. It occupies a prominent position in Ayurveda and is also incorporated into Siddha, Unani, Sri Lankan, Tibetan, and various indigenous healing practices. Traditionally, it has been recommended as a carminative, diaphoretic, antispasmodic, expectorant, circulatory stimulant, astringent, appetite stimulant, anti-inflammatory agent, diuretic, and digestive aid. Beyond its medicinal role, ginger is a staple in Indian cuisine, with an estimated per capita daily intake of 8-10 g, typically in the form of fresh paste or dried powder. It serves as a principal component of curry powders, sauces, and chutneys. More recently, it has been incorporated into a variety of food products, including confectionery, baked

goods, pickles, and beverages (Khodaie et al., 2015; Ajith et al., 2008; Saenghong et al., 2012).

## 2.5. Phytochemistry of ginger

Ginger contains diverse bioactive compounds, mainly essential oils and phenolics such as phenolic acids, flavonoids, gingerols. These metabolites are responsible for its pharmacological properties.

### *2.5.1. Flavonoids and phenolic acids*

Ginger contains phenolic acids such as gallic acid, ferulic acid, caffeic acid, syringic acid and flavonoids such as quercetin, rutin, luteolin, hesperidin, naringenin, kaempferol, etc. These compounds show strong antioxidant activity and are applied in pharmaceuticals and nutraceuticals. Their levels vary with extraction solvent, drying method, and temperature; ethanol extracts usually yield higher phenolic content. High-temperature drying increases antioxidant activity but degrades heat-sensitive compounds like 6-gingerol (Jan et al., 2022; Pawar et al., 2011).

### *2.5.2. Gingerols and derivatives*

Gingerols, shogaols, and paradols are key active phenolics. Major compounds include 6-gingerol, 6-shogaol, 8-gingerol, 10-gingerol, with strong antioxidant, anti-inflammatory, anticancer, and antiviral effects. 6-gingerol converts to 6-shogaol during heating, while paradols form in processed ginger. Processing thus alters concentrations, offering potential to optimize bioactive yield (Yudthavorasit et al., 2014; Tanaka et al., 2015).

### *2.5.3. Other metabolites*

Ginger also contains tannins, saponins, steroids, and alkaloids, which may work synergistically to enhance therapeutic effects (Momoh and Olaleye, 2022; Biswas et al., 2019).

## 2.6. Conclusion

*Zingiber officinale* Roscoe or ginger represents a plant of exceptional cultural and medicinal significance whose influence extends far beyond its value as a spice. Its place in diverse medical traditions reflects an long-term trust in its healing capacity, particularly in strengthening cognitive functions. Ancient medical systems, especially those of India, Arabia, and China, frequently highlighted its capacity to refresh the mind, sharpen memory, and other disorders linked to mental decline. Current scientific investigations support these traditional beliefs by showing that compounds like gingerols, shogaols, flavonoids, and phenolic acids can influence oxidative stress, reduce neuroinflammation, and help regulate neurotransmitter activity. By bridging the traditional practices with emerging pharmacological evidence, ginger emerges as a promising botanical resource for the management of neurodegenerative and memory-related conditions. Owing to its diverse actions supported by traditional use and modern scientific evidence, ginger is considered a promising natural option for managing conditions like AD and memory decline associated with aging. Consequently, ginger is not only a culinary component but a vital medicinal herb with considerable relevance in neuroprotective research and interventions aimed at preserving cognitive health.

# Chapter 3

## Scope, objective and plan of work

3.1. Scope of the study

3.2. Objective of the study

3.3. Plan of work

## 3.1. Scope of the study

The current research incorporates a comprehensive phytochemical and pharmacological evaluation of chemo-type *Zingiber officinale* (ginger) collected from nine distinct geographical locations across Northeast India, especially Manipur, a region recognized for its rich biodiversity and agro-climatic variation.

The phytochemical profiling will include determination of Total Phenolic Content (TPC) and Total Flavonoid Content (TFC), in-vitro antioxidant activity assays, and chromatographic characterization using High-Performance Liquid Chromatography (HPLC) and High Performance Thin Layer Chromatography (HPTLC). Statistical analysis through Pearson's correlation will be performed to establish relationships between phytochemical constituents and antioxidant activities.

Further, the extracts will be evaluated for their neuroprotective potential via in-vitro AChE and BChE enzyme inhibition assays. The most potent ginger sample, based on the analytical procedures and in-vitro screening, will be subjected to High-Resolution Liquid Chromatography-Mass Spectrometry (HR-LCMS) analysis to identify and characterize its major bioactive constituents and in-vivo anti-Alzheimer's evaluation using behavioral assays such as the Morris water maze, Y-maze, and Novel Object Recognition (NOR) test to assess memory and learning efficacy. Subsequent biochemical analysis will measure brain AChE, BChE, and ACh levels, along with antioxidant parameters, to elucidate the underlying mechanisms. Histopathological examination of brain tissue will provide further morphological evidence of neuroprotection. Molecular docking studies will be undertaken to predict interactions of major bioactive constituents with target enzymes, thus correlating in-silico results with experimental findings.

After an extensive review of literature covering articles indexed in Scopus, Google Scholar, and other scientific sources from 1987 to 2025, the present study is focused on phytochemical and preclinical investigations.

The scope of this study is confined to preclinical investigations by integrating the phytochemical, biochemical, behavioral, and computational approaches. Overall this research aims to identify and characterize region-specific ginger samples with the highest potential for AD management.

## 3.2. Objective of the study

The major objective of the present study is the evaluation and comparison of the phytochemical profiles, antioxidant activities, and neuroprotective potential of chemo-type ginger rhizomes collected from nine different geographical locations of Northeast India, with a view to identifying the most potent variety for the management of AD.

The main objectives of the present study are as follows:

- To collect ginger rhizomes from different geographical regions of Northeast India, especially from Manipur and authenticate the plant materials.
- To prepare extracts from the collected samples for phytochemical, in-vitro enzyme inhibition and pharmacological analysis.
- To determine the TPC and TFC of each ginger extract.
- To evaluate the in-vitro antioxidant activities of the ginger extracts using standard DPPH, hydroxyl and ABTS free radical scavenging activity.
- To evaluate the phytoconstituents of the ginger extracts using HPLC and HPTLC analysis.
- To perform the Pearson's correlation analysis between TPC, TFC, antioxidant activities, and HPLC analysis.
- To assess the in-vitro AChE and BChE enzyme inhibitory activities of each ginger extract.
- To select the most potent extract based on the phytochemical and in-vitro evaluations for further HR-LCMS and in-vivo studies.
- To perform the HR-LCMS analysis of the most potent ginger extract to know the major secondary metabolites present and responsible for the anti-Alzheimer's activity.
- To assess the in-vivo anti-Alzheimer's potential of the selected extract through behavioral assays (Morris water maze, Y-maze, and NOR test) in memory impaired Swiss albino mice model.
- To evaluate the brain biochemical parameters, including AChE, BChE, and ACh levels, along with antioxidant enzyme activities.
- To evaluate the pro-inflammatory marker in the brain tissues of experimental animals.

- To examine the brain histopathology for morphological changes associated with neurodegeneration.
- To conduct the molecular docking studies to predict interactions between major bioactive compounds and target enzymes relevant to Alzheimer's pathology.

## 3.3. Plan of work

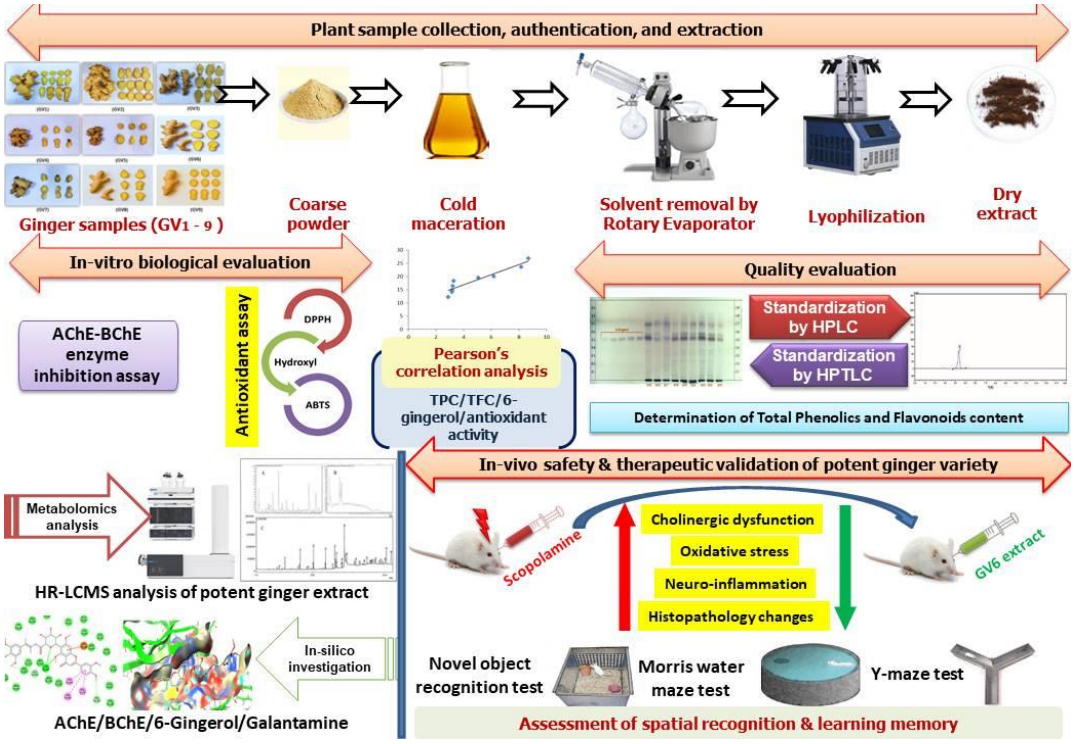


**Figure 3.1. Schematic representation of plan of work**

# Chapter 4

## Phytochemical profiling and in-vitro anti-Alzheimer's potential of chemo-typed ginger

4.1. Procurement, authentication and extraction

4.2. Phytochemical profile of ginger samples

4.3. In-vitro cholinesterase enzyme inhibition assay

4.4. Results and discussion

4.5. Conclusion

## 4.1. Procurement, authentication and extraction

Fresh rhizomes from nine (09) distinct ginger samples were gathered between August 16 and 19, 2021, from various geographic regions across Manipur, located in Northeast India, as detailed in Table 3.2. A botanist from the BRIC-Institute of Bioresources and Sustainable Development (IBSD), Imphal, Manipur, India, verified the plant specimens, and corresponding voucher samples were submitted to the IBSD herbarium for future reference and the 09 samples were denoted as GV1, GV2, GV3, GV4, GV5, GV6, GV7, GV8, and GV9.

The freshly collected ginger rhizomes were thoroughly washed using distilled water and subsequently shade-dried until a constant weight was achieved. The dried materials were then finely powdered. Precisely 100 g of each powdered sample were extracted through maceration by immersing in 500 mL of 80% methanol (methanol : water, 80 : 20 v/v) for a total duration of 72 hr, with occasional shaking every 24 hr to ensure thorough extraction (Ezez et al., 2021). After completion of the extraction period, the solvent was separated using Whatman No. 1 filter paper. The resulting filtrate was concentrated under reduced pressure using a rotary vacuum evaporator (IKA, Japan). The concentrated extracts were then freeze-dried using a lyophilizer (Instrumentation India, India) and the percentage yield of the extracts were calculated by the following formula:

$$\text{Extract yield (\% w/w)} = [W1 / W2] \times 100$$

Where, W1 = Weight of prepared extract and W2 = Weight of dry ginger rhizome

The extracts were then stored in an airtight container and kept at 4°C in a refrigerator until further analysis.

### Chemical and reagents

Methanol (≥ 99.5%, AR grade), Folin-Ciocalteu's reagent, sodium carbonate, and aluminium chloride ($AlCl_3$), 2,2-diphenyl-1-picrylhydrazyl (DPPH), deoxyribose, ferric chloride ($FeCl_3$), Ethylenediaminetetraacetic acid (EDTA), hydrogen peroxide ($H_2O_2$), trichloro acetic acid (TCA), thiobarbituric acid (TBA), sodium

hydroxide (NaOH), 2,2′-azinobis(3-ethylbenzothiazoline-6-sulfonic acid) (ABTS), and potassium persulfate were purchased from HiMedia, India. Standard gallic acid (≥ 98%), rutin (≥ 90%), ascorbic acid, 6-gingerol (≥ 99%), 5,5′-dithiobis(2-nitrobenzoic acid) DTNB, acetylthiocholine iodide (ATCI), butyrylthiocholine iodide (BTCI), AChE from bovine erythrocytes, BChE from equine serum, and galantamine were obtained from Sigma-Aldrich (MO, USA). HPLC grade methanol (≥ 99.8%), and all other reagents and chemicals were acquired from Merck (Darmstadt, Germany). Ultrapure water was obtained from Milli-Q system (Millipore, Bedford, MA, USA). All the working concentrations were prepared freshly on the day of experiment.

## 4.2. Phytochemical profile of ginger samples

### *4.2.1. Quantification of total phenolic content*

The TPC of the GV extracts was evaluated using a spectrophotometric method adapted from Wolfe et al., 2003, with minor modifications. The extract solutions (1 mg/mL) was mixed with 5 mL of Folin-Ciocalteu reagent, previously diluted tenfold with distilled water, and followed by the addition of 4 mL of 7.5% sodium carbonate solution. The mixture was vortexed for 15 sec and incubated at 40°C for 30 min to allow color development. The absorbance was then measured at 765 nm using a SpectraMax iD3 microplate reader (California, USA). A standard calibration curve was generated using gallic acid at concentrations ranging from 10-40 µg/mL. TPC was calculated and expressed as mg of gallic acid equivalents (GAE) per g of dry extract (mg GAE/g of dry extract).

### *4.2.2. Quantification of total flavonoid content*

The TFC of the GV extracts was quantified using a spectrophotometric method adapted from Quettier-Deleu et al., 2000. For this purpose, stock solutions (1 mg/mL) of each GV extract and rutin (used as a reference standard) were prepared in methanol. To initiate the reaction, 1 mL of the extract solution was mixed with an equal volume of 2% $AlCl_3$ solution in methanol. The resulting mixture was incubated at 28°C for 1 hr to allow complex formation. Absorbance

was then measured at 415 nm using a SpectraMax iD3 microplate reader (Molecular Devices, CA, USA). A standard calibration curve was constructed using rutin at concentrations ranging from 20-80 µg/mL. TFC was calculated and expressed as mg of rutin equivalent per g of dry extract (mg RUE/g dry extract).

### *4.2.3. Determination of antioxidant activity*

#### *4.2.3.1. DPPH radical scavenging assay*

The antioxidant potential of the GV extracts was assessed using the DPPH radical scavenging assay, following a modified protocol based on the method described by Das et al., 2020. The assay was carried out in a 96-well microplate reader. Briefly, 100 µL of various concentrations of the extracts (31.25, 62.5, 125, 250, 500, and 1000 µg/mL) and the reference antioxidant, ascorbic acid, were mixed with 100 µL of a 0.1 mM DPPH solution prepared in methanol. The mixtures were incubated in the dark at room temperature for 30 min to allow the reaction to occur. Subsequently, the absorbance was measured at 517 nm using a SpectraMax iD3 microplate reader (Molecular Devices, CA, USA). The percentage of radical scavenging activity was calculated using the following equation:

$$\% \text{ inhibition} = [(A1 - A0) / A1] \times 100$$

[Where A1 = absorbance of the control (DPPH solution without test sample) and A0 = absorbance in the presence of the test sample and standard].

#### *4.2.3.2. Hydroxyl radical scavenging assay*

The hydroxyl radical scavenging activity of the GV extracts was evaluated using a modified version of the deoxyribose degradation assay described by Halliwell et al., 1987, adapted for a 96-well microplate reader. In each well, the reaction mixture consisted of 10 µL of 28 mM deoxyribose dissolved in 50 mM phosphate buffer (pH 7.4), 10 µL of 1 mM $FeCl_3$, 10 µL of 1 mM EDTA, and 10 µL of 1 mM $H_2O_2$. To this, 100 µL of the GV extracts or standard ascorbic acid (at concentrations of 31.25, 62.5, 125, 250, 500, and 1000 µg/mL) was added. The

reaction mixtures were incubated at 42°C for 1 hr. Following incubation, 50 µL of 10% TCA and 50 µL of 0.5% TBA in 50 mM NaOH were added to each well. A second incubation was carried out at 42°C for 30 min. Absorbance was measured at 532 nm using a SpectraMax iD3 microplate reader (Molecular Devices, CA, USA). The percentage of hydroxyl radical scavenging activity was determined using the equation:

$$\% \text{ inhibition} = [(A1 - A0) / A1] \times 100$$

[Where A1 = absorbance of the control (reaction mixture without test sample) and A0 = absorbance in the presence of the test sample and standard].

#### *4.2.3.3. ABTS radical scavenging activity*

The ABTS radical scavenging activity of the GV extracts was assessed following the method outlined by Sridhar and Charles (2019), with slight modifications. The $ABTS^{+}$• working solution was prepared by mixing equal volumes of 7 mM ABTS stock solution with 2.45 mM potassium persulfate solution in distilled water. This mixture was kept in the dark at room temperature for 12 to 16 hr to allow the formation of stable $ABTS^{+}$• radicals. For the assay, 1 mL of the $ABTS^{+}$• solution was combined with 0.5 mL of the GV extracts or ascorbic acid (standard) at concentrations ranging from 31.25 to 1000 µg/mL. The reaction mixtures were incubated for exactly 10 min at room temperature in the dark. A control was prepared by mixing 1 mL of $ABTS^{+}$• solution with 0.5 mL of double-distilled water. The absorbance of the control was maintained within the range of $0.38 \pm 0.04$. The percentage of ABTS radical scavenging activity was calculated using the formula:

$$\% \text{ inhibition} = [(A1 - A0) / A1] \times 100$$

[Where A1 = absorbance of the control (reaction mixture without test sample) and A0 = absorbance in the presence of the test sample and standard].

### 4.2.4. *HPLC instrumentation and chromatographic conditions*

Quantitative estimation of 6-gingerol were carried out using a Reverse-Phase-High-Performance-Liquid-Chromatography (RP-HPLC) system (Shimadzu Prominence, Kyoto, Japan). The setup consisted of Shimadzu LC-20 AD UFLC pumps, a rheodyne manual injector equipped with a 20 µL sample loop, and a Shimadzu SPD-M20A Photodiode Array (PDA) detector. Chromatographic separation was achieved under isocratic conditions using a $C_{18}$ reverse-phase column (Phenomenex-Luna $C_{18}$, 250 × 4.6 mm, 5 µm particle size; Torrance, CA, USA) maintained at 25°C. The mobile phase comprised methanol (solvent A) and 1% acetic acid (solvent B), delivered at a constant flow rate of 1.0 mL/min. Data acquisition was performed at 280 nm, optimized for 6-gingerol detection.

Stock solutions of ginger extracts and standard 6-gingerol were prepared at a concentration of 1 mg/mL in methanol. Working solutions of the standard were obtained through serial dilutions. All samples and standards were filtered through 0.45 µm syringe filters before injection. Compound identification was conducted by comparing retention times and UV spectra with those of the reference standard (Harwansh et al., 2014).

The Limits of Detection (LOD) and Limits of Quantification (LOQ) were determined by injecting progressively diluted standard solutions until Signal-to-Noise (S/N) ratios of approximately 3 and 10 were achieved for LOD and LOQ, respectively. Intra-day precision was assessed by six repeated injections of the standard within a single day, whereas inter-day precision was evaluated over three consecutive days, each with triplicate analyses. Relative Standard Deviation (RSD) was calculated using the formula: RSD (%) = (Standard deviation / Mean) × 100. For accuracy assessment, recovery experiments were performed by spiking the samples with three different concentrations of 6-gingerol, followed by analysis to evaluate recovery percentages.

### *4.2.5. Pearson's correlation analysis*

Pearson's correlation coefficient is a statistical measure used to evaluate the strength and direction of a linear relationship between two continuous variables. In this study, Pearson's correlation analysis was conducted to assess the

associations among TPC, TFC, DPPH and hydroxyl free radical scavenging activities, and the percentage of 6-gingerol. This analysis aimed to determine how these phytochemical parameters and antioxidant activities are interrelated (Muflihah et al., 2021).

#### *4.2.6. HPTLC analysis*

Quantitative analysis of 6-gingerol content in the ginger samples (GV1-GV9) was performed using HPTLC with a CAMAG system (Muttenz, Switzerland), following a modified protocol based on Alqasoumi (2009). Standard stock solution of 6-gingerol (1 mg/mL) and GV extract solutions (10 mg/mL) were prepared in methanol, thoroughly vortexed until fully dissolved, and filtered through 0.45 µm syringe filters. A calibration curve was constructed using standard concentrations ranging from 0.2 to 1 µg/mL. Sample and standard solutions were applied as 6 mm bands on aluminium-backed silica gel 60 F254 HPTLC plates (10 × 20 cm, E. Merck, Germany) using a Linomat V applicator. Plate development was carried out in a twin-trough chamber with an optimized mobile phase. Post-development, the plates were scanned at 280 nm using a CAMAG TLC Scanner 4. For visualization, the developed plates were derivatized with anisaldehyde-sulphuric acid reagent. Quantification of 6-gingerol in the extracts was achieved by linear regression analysis of the calibration curve using visionCATS® software.

### 4.3. *In-vitro* cholinesterase enzyme inhibition assay

#### *4.3.1. AChE and BChE enzyme inhibition assay*

The assay procedure was adapted from the method reported by Das et al. (2023) with slight modifications. In summary, the reaction mixture consisted of 3 mM DTNB and 15 mM of either ATCI or BTCI, combined with varying concentrations of GV extracts (50-500 µg/mL) and the reference inhibitor galantamine (10-50 µg/mL), all prepared in phosphate buffer (pH 8.0). The mixtures were pre-incubated at 37°C for 10 min. Subsequently, AChE, 2 U/mL or BChE, 1 U/mL was added to the respective wells. The change in absorbance was monitored at

405 nm every 13 sec over a total period of 78 sec. The protocol for in-vitro AChE and BChE enzyme inhibition assay was illustrated in Figure 3.1.

### Statistical analysis

Statistical analysis was carried out using GraphPad Prism software version 8.0.2 (GraphPad Software, La Jolla, CA). A repeated measures one-way Analysis of Variance (ANOVA) was employed, followed by Tukey-Kramer post hoc tests for multiple comparisons. All experimental procedures were performed in triplicate, and the results are presented as mean values ± Standard Error of the Mean (SEM). Statistical significance was determined at a 95% confidence level, with p values less than 0.05 considered significant. The relationship between TPC, TFC, and 6-gingerol concentration with antioxidant activities was evaluated using Pearson's correlation analysis.

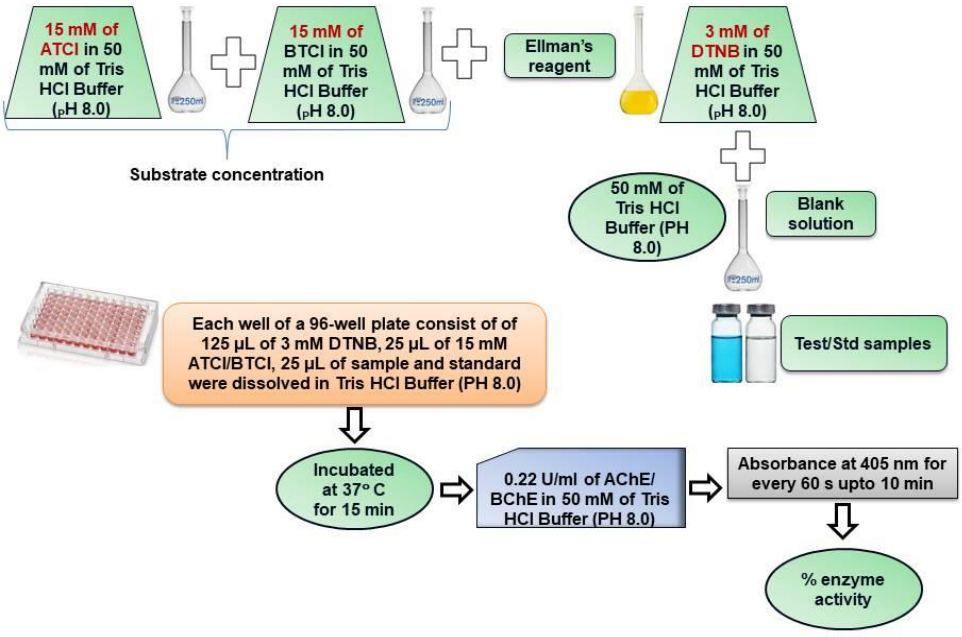


**Figure 4.1. Schematic representation of Ellman's method for in-vitro AChE and BChE inhibition assays**

## 4.4. Results and discussion

### *4.4.1. Collection details and extraction yields of the ginger samples*

Among the 09 ginger samples (Figure 3.2) GV5 showed the highest percentage yield (Table 3.2) of the extract with a value of 18.15% w/w followed by GV3 (17.59% w/w) > GV7 (17.39% w/w) > GV8 (16.51% w/w) > GV9 (16.04% w/w) > GV6 (15.83% w/w) > GV1 (15.61% w/w) > GV2 (13.52% w/w) > GV4 (12.86% w/w).

**Table 4.1. Sample ID, voucher specimen number, collection site, latitude, longitude and percentage extract yield of the nine ginger samples**

| Sl no. | Sample ID | Voucher specimen no. | Collection site | Latitude | Longitude | Extract yield (% w/w) |
|---|---|---|---|---|---|---|
| i. | GV1 | IBSD/C-221/A | Japhou village | 24°20'21.8"N | 25°00'22.4"E | 15.61 |
| ii. | GV2 | IBSD/C-221/B | Litan village | 28°42'23.18"N | 77°27'49.89"E | 13.52 |
| iii. | GV3 | IBSD/C-221/C | Mittong village | 24°22'05.6"N | 94°00'53.4"E | 17.59 |
| iv. | GV4 | IBSD/U-221/A | Hatha village | 25°01'54.6"N | 94°18'58.9"E | 12.86 |
| v. | GV5 | IBSD/U-221/B | Chaora village | 25°01'55.3"N | 94°19'08.3"E | 18.15 |
| vi. | GV6 | IBSD/U-221/C | Lopung village | 25°02'16.4"N | 94°18'57.5"E | 15.83 |
| vii. | GV7 | IBSD/M-221/A | Tadubi village | 25°28'51.6"N | 94°08'19.9"E | 17.39 |
| viii. | GV8 | IBSD/M-221/B | Tadubi village | 25°28'46.7"N | 94°08'18.2"E | 16.51 |
| ix. | GV9 | IBSD/M-221/C | Punanamei village | 25°31'57.9"N | 94°09'12.9"E | 16.04 |

The percentage yield of extracts among the nine ginger samples displayed marked variability, reflecting potential differences in phytochemical composition, moisture content and geographical influences on secondary metabolite biosynthesis. Similar variations in extraction yield have been reported in previous studies, often attributed to environmental factors such as soil composition, altitude, rainfall, and post-harvest handling, all of which influence metabolite accumulation in ginger rhizomes (Rawat et al., 2025; Golian et al., 2025; Khalil et al., 2020).

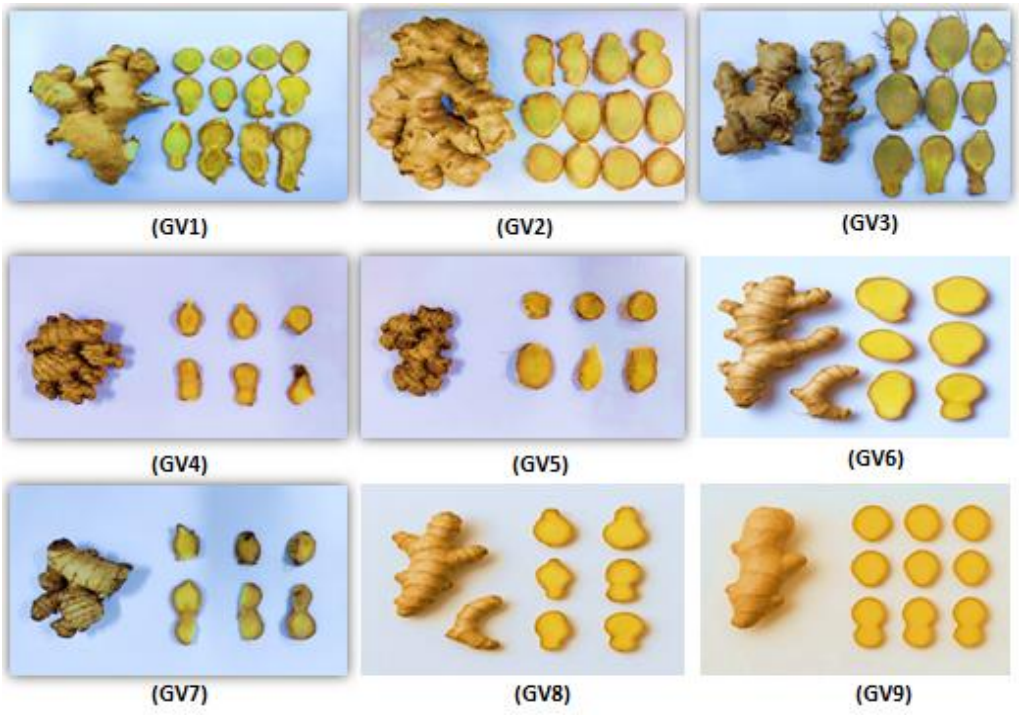


**Figure 4.2. Nine ginger samples collected from nine different locations of Manipur, India**

### *4.4.2. Quantification of TPC and TFC*

The TPC in the GV samples was quantified using gallic acid as the reference standard, and the results were expressed in terms of GAE based on the calibration curve equation: $y = 0.0084x + 0.0055$ ($R^2 = 0.92$). As presented in Table 3.3, the TPC values among the different ginger samples ranged from

12.18 ± 1.14 to 26.88 ± 1.47 mg GAE/g of dry extract. The TPC quantification indicates that GV6 may be richer in polar phenolic constituents, which are efficiently extracted under the chosen conditions. Since phenolic compounds are key contributors to antioxidant potential, such high TPC suggests that GV6 may possess enhanced bioactivity.

Similarly, the TFC was calculated using rutin as the standard and expressed as RUE, following the standard curve equation: y = 0.0029x - 0.0051 ($R^2$ = 0.98). The TFC values varied from 14.64 ± 1.54 to 24.38 ± 1.28 mg RUE/g of dry extract, as detailed in Table 3.3. Although TFC variation followed a broadly similar trend to TPC, certain samples such as, GV7 and GV8 exhibited proportionally higher flavonoid levels relative to their total phenolics, suggesting distinct phytochemical profiles and possible differences in phenolic subclass distribution.

**Table 4.2. TPC and TFC values of the GV samples**

| Sl no. | Sample ID | TPC (mg GAE/ g of dry extract)* | TFC (mg RUE/ g of dry extract)* |
|---|---|---|---|
| i. | GV1 | 14.16 ± 1.96 | 22.18 ± 1.57 |
| ii. | GV2 | 16.47 ± 1.34 | 20.74 ± 1.37 |
| iii. | GV3 | 18.38 ± 1.87 | 18.99 ± 1.29 |
| iv. | GV4 | 20.12 ± 1.47 | 16.28 ± 1.82 |
| v. | GV5 | 23.67 ± 1.76 | 14.73 ± 1.25 |
| vi. | GV6 | 26.88 ± 1.47 | 14.64 ± 1.54 |
| vii. | GV7 | 12.18 ± 1.14 | 24.38 ± 1.28 |
| viii. | GV8 | 14.86 ± 1.84 | 22.58 ± 1.16 |
| ix. | GV9 | 19.54 ± 1.05 | 16.83 ± 1.65 |
| * Values are presented as mean ± SEM (n = 3) | | | |

The variation in TPC and TFC among the ginger samples underscores the influence of geographical and environmental factors on phytoconstituent accumulation. Such differences are critical in selecting plant material for pharmacological evaluation, as phytochemical richness often correlates with biological efficacy (Zouine et al., 2024; Bin-Asal et al., 2025). These findings

provide a rational basis for prioritizing samples for further antioxidant and neuroprotective studies, including in-vitro cholinesterase inhibition and in-vivo behavioral assays.

### *4.4.3. Determination of antioxidant activity by DPPH, hydroxyl and ABTS free radical scavenging assay*

In this study, the antioxidant potential of various ginger extracts was evaluated based on their ability to donate electrons and neutralize free radicals. This was assessed through spectrophotometric measurements using three standard assays: DPPH, hydroxyl radical, and ABTS radical scavenging methods.

The $IC_{50}$ values, representing the concentration required to inhibit 50% of free radicals, were calculated for each assay. For the DPPH assay, the ginger extracts exhibited $IC_{50}$ values ranging from $31.24 \pm 1.08$ to $43.35 \pm 1.68$ µg/mL, while the reference compound, ascorbic acid, showed an $IC_{50}$ of $21.33 \pm 3.30$ µg/mL. In the hydroxyl radical scavenging assay, the $IC_{50}$ values of the ginger samples were between $44.52 \pm 1.14$ and $58.19 \pm 1.48$ µg/mL, compared to 25.11 µg/mL for the ascorbic acid.

For the ABTS assay, the $IC_{50}$ values of the ginger extracts ranged from $35.04 \pm 5.03$ to $77.03 \pm 3.09$ µg/mL, whereas ascorbic acid demonstrated a significantly lower $IC_{50}$ value of $18.34 \pm 4.07$ µg/mL. These findings collectively indicate that the ginger samples possess notable free radical scavenging capabilities, though slightly less potent than the standard antioxidant used.

The free radical scavenging activities of the ginger extracts along with the standard ascorbic acid are represented in figure 3.3.

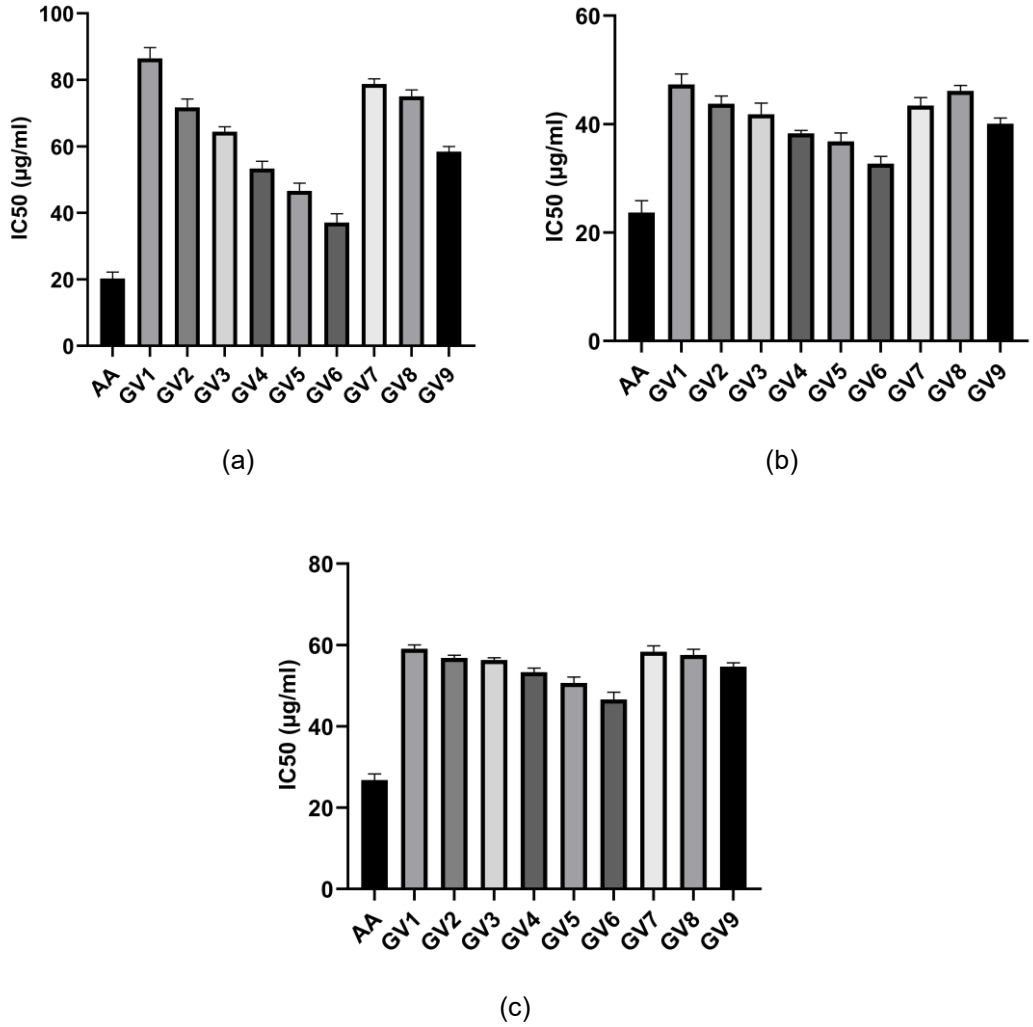


**Figure 4.3. Free radical scavenging activity of GV extracts (a) DPPH free radical scavenging activity (b) Hydroxyl free radical scavenging activity and (c) ABTS free radical scavenging activity. All values are expressed as mean ± SEM (n = 3)**

### *4.4.4. Calibration, LOD, and LOQ*

A calibration curve for 6-gingerol was established by analyzing six different concentrations, each in triplicate (n = 3). The curve was constructed by plotting the peak area against the corresponding concentration of 6-gingerol. A linear regression analysis was performed, generating an equation in the form y = ax + b, where x denotes the concentration of 6-gingerol, y is the measured peak area,

and $r^2$ represents the correlation coefficient. The analyte exhibited strong linearity over a broad concentration range (25-400 µg/mL), with an $r^2$ value of at least 0.9976 (Table 3.4).

**Table 4.3. Presentation of regression equation, test range, correlation coefficient, LOD, LOQ, % recovery, and %RSD of 6-gingerol**

| Analyte | Regression equation | $r^2$ | Test range (µg/ml) | LOD (µg/ml) | LOQ (µg/ml) | Recovery (%) | RSD (%) |
|---|---|---|---|---|---|---|---|
| 6-gingerol | y = 5745.5x + 114,585 | 0.9976 | 25-400 | 0.41 | 1.25 | 93.26 - 104.93 | 0.59 - 1.57 |

### *4.4.5. Precision and accuracy*

Method precision was evaluated through intra-day and inter-day repeatability studies. The % RSD values for both intra-day and inter-day assessments were found to be below 2%, indicating high precision and reproducibility of the analytical method (Table 3.5). Accuracy was assessed using recovery experiments, calculated using the formula:

Recovery (%) = [(measured amount - original amount) / spiked amount] × 100

The method demonstrated acceptable accuracy, with recovery rates for 6-gingerol ranging from 93.26% to 104.93%, confirming the reliability of the quantification procedure (Table 3.4).

**Table 4.4. Precision study of the quantitative HPLC method**

| Intra-day precision (n = 6) | | | | Inter-day precision (n = 6) | | | |
|---|---|---|---|---|---|---|---|
| RT (min) | | Response (AU) | | RT (min) | | Response (AU) | |
| Mean | % RSD | Mean | % RSD | Mean | % RSD | Mean | % RSD |
| 4.330 | 0.97 | 747,206 | 1.28 | 4.296 | 0.26 | 773,683 | 1.30 |
| 4.352 | 1.06 | 1,263,689 | 1.41 | 4.301 | 0.75 | 1,298,359 | 1.47 |

| | | | | | | | |
|---|---|---|---|---|---|---|---|
| 4.310 | 0.88 | 2,483,696 | 1.17 | 4.207 | 0.19 | 2,294,683 | 1.25 |
| *Values are presented as mean ± SEM (n = 3). AU: absorbance unit, % RSD: relative standard deviation, RT: retention time | | | | | | | |

### *4.4.6. Quantitative estimation of 6-gingerol content*

Figure 3.4 illustrates the chromatographic profiles of the standard 6-gingerol (Figure 3.4.a) and its detection in various ginger hydro-alcoholic extracts (Figure 3.4.b-j). As reported in Table 3.6 the concentration of 6-gingerol across the ginger samples ranged from 2.88% to 8.69% w/w. Among the tested samples, the GV6 variety exhibited the highest level of 6-gingerol, followed by GV5, GV4, GV9, GV3, GV2, GV8, GV1, and GV7, in descending order.

**Table 4.5. 6-gingerol content among the nine ginger samples**

| Sl no. | Sample ID | 6-gingerol content (% w/w) |
|---|---|---|
| i. | GV1 | 3.15 |
| ii. | GV2 | 3.22 |
| iii. | GV3 | 3.27 |
| iv. | GV4 | 6.17 |
| v. | GV5 | 8.17 |
| vi. | GV6 | 8.69 |
| vii. | GV7 | 2.88 |
| viii. | GV8 | 3.17 |
| ix. | GV9 | 5.05 |

The present investigation validated a reliable, and efficient RP-HPLC method for the quantification of 6-gingerol in ginger extracts. Quantitative findings demonstrated notable variation in 6-gingerol levels among ginger varieties sourced from different regions of Northeast India. These differences are likely influenced by geographical and environmental factors. Consistent with previous studies, such variations in 6-gingerol content are attributed to differences in

cultivar genetics, agronomic practices, environmental conditions, post-harvest handling, and storage duration (Pawar et al., 2011; Bailey-Shaw et al., 2008; Rafi et al., 2013).

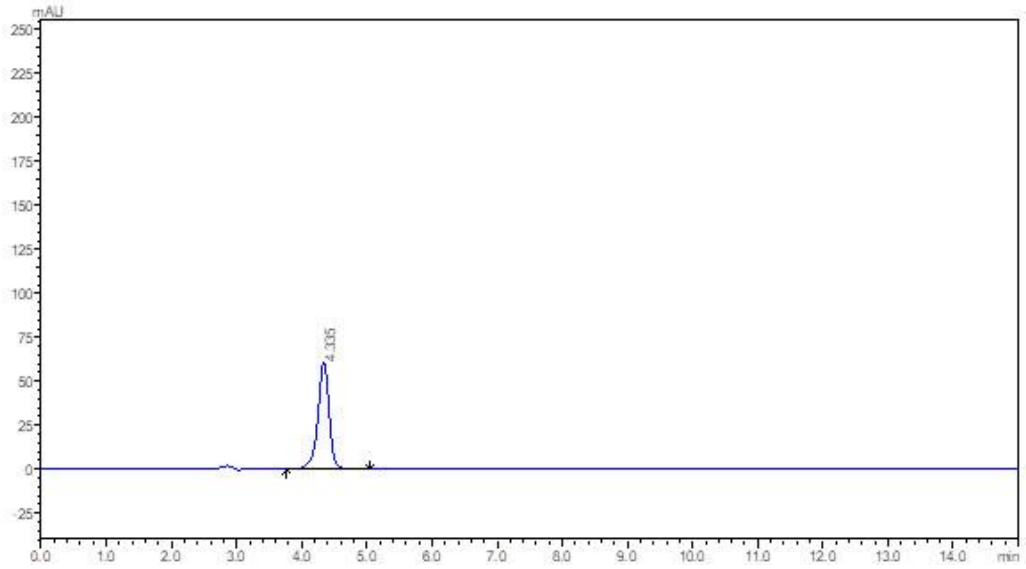


(a)

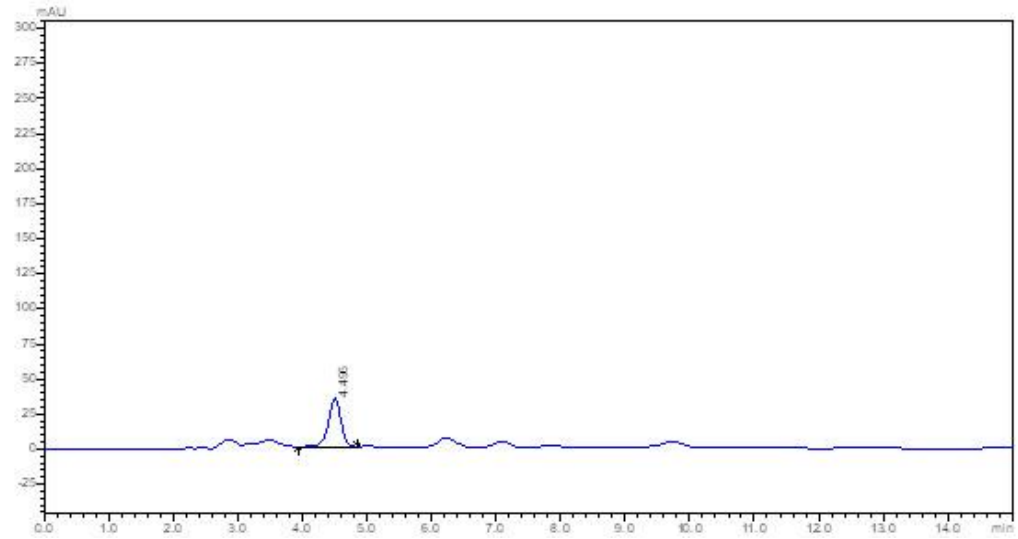


(b)

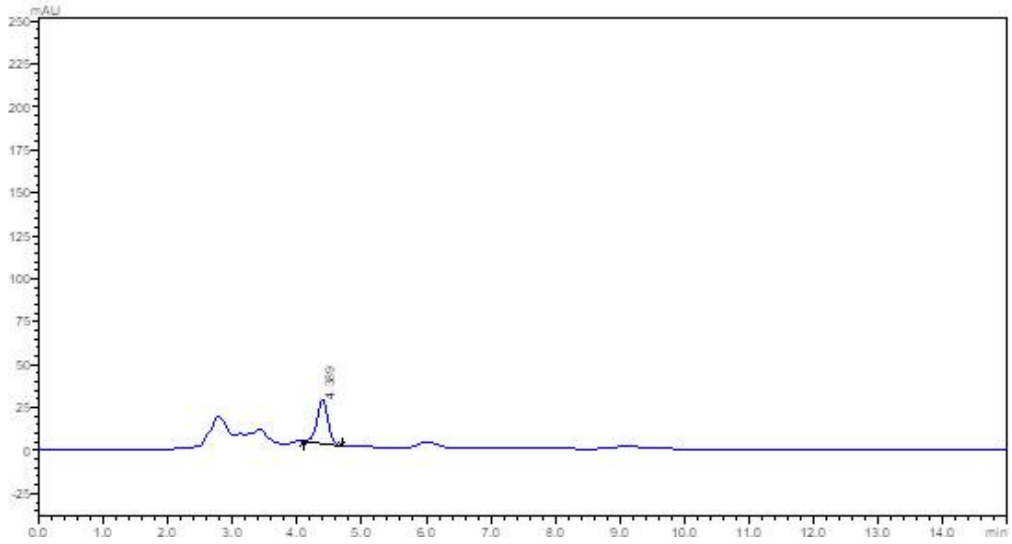


(c)

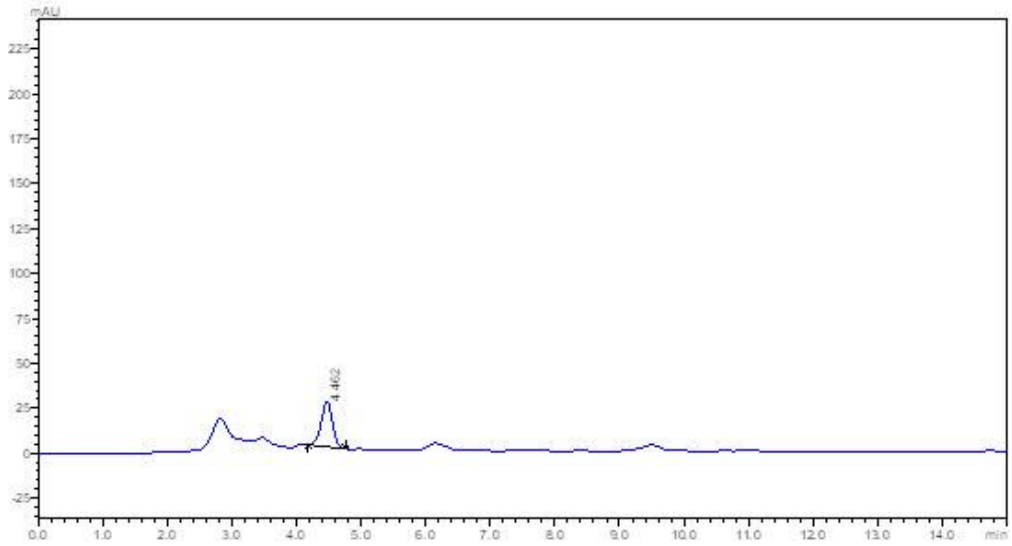


(d)

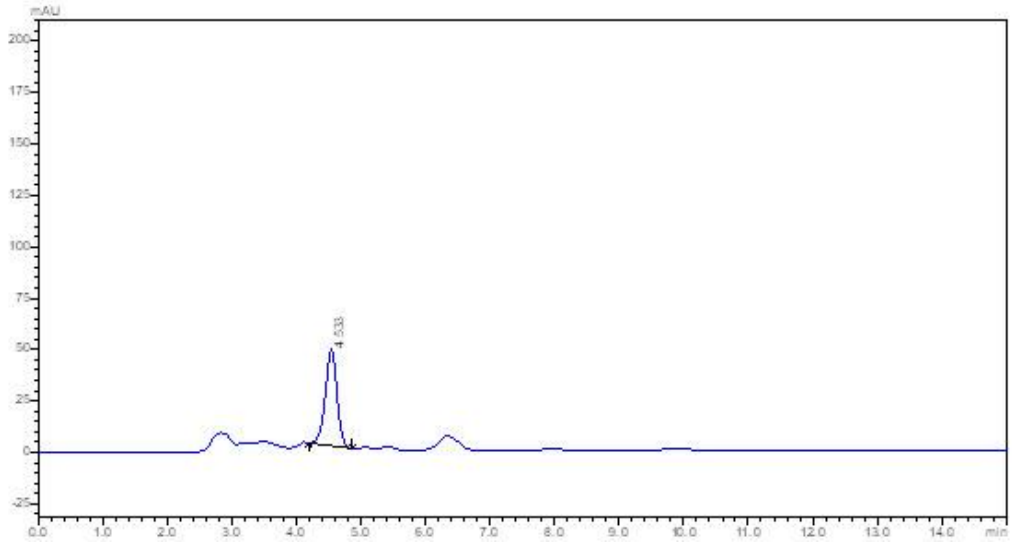


(e)

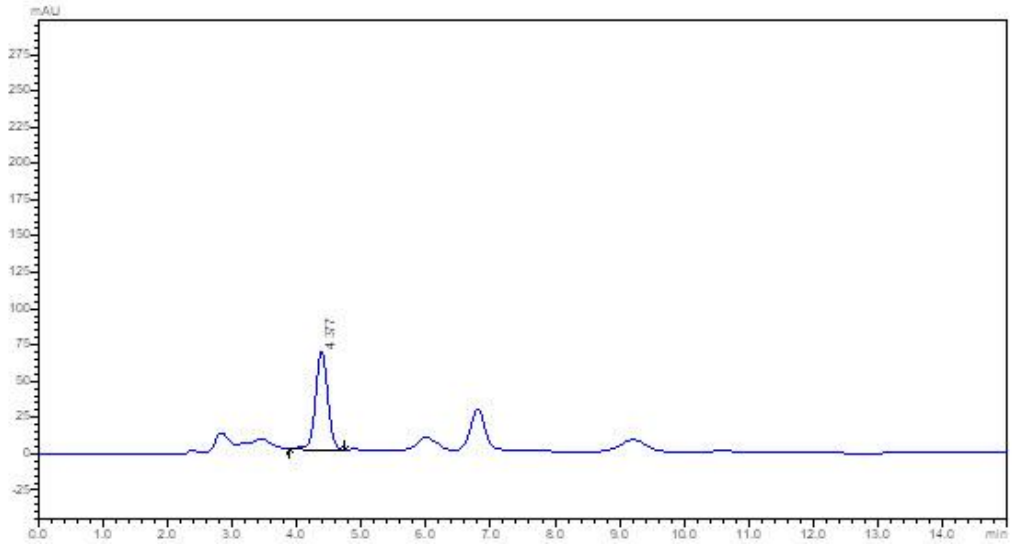


(f)

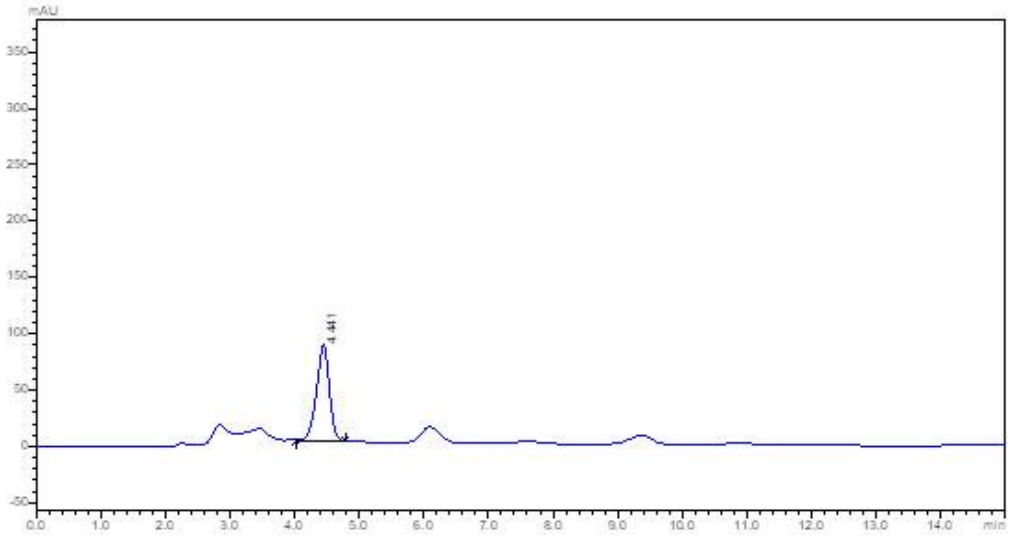


(g)

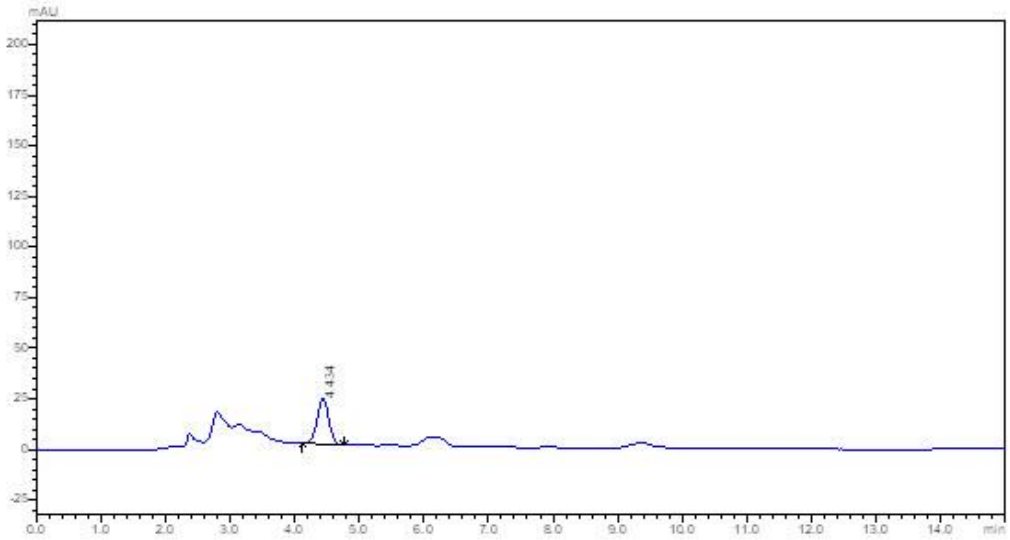


(h)

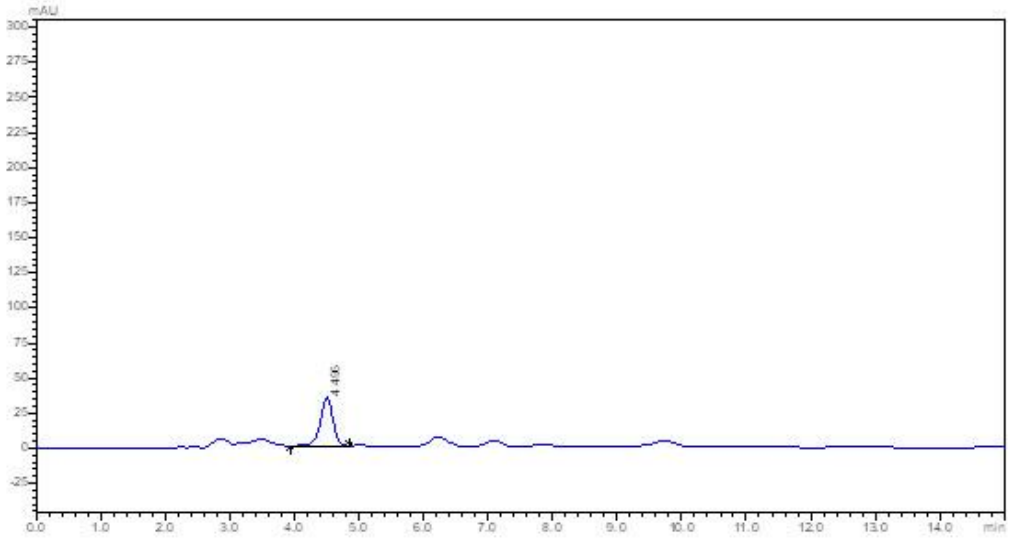


(i)

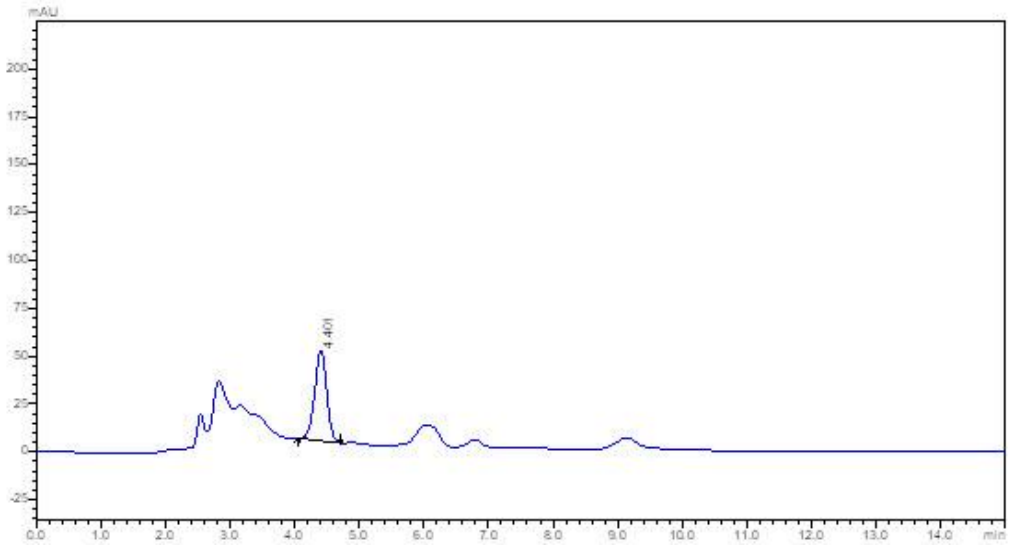


(j)

**Figure 4.4. RP-HPLC chromatograms illustrating the retention profiles of standard 6-gingerol and hydro-alcoholic extracts from nine ginger varieties. Traces correspond to: (a) pure 6-gingerol standard; (b) GV1; (c) GV2; (d) GV3; (e) GV4; (f) GV5; (g) GV6; (h) GV7; (i) GV8; and (j) GV9**

### *4.4.7. Pearson's correlation analysis*

Table 3.7 presents the results of Pearson's correlation analysis evaluating the relationships among 6-gingerol content (%), TPC, TFC, DPPH, and hydroxyl radical scavenging potential across all the ginger samples. The findings suggest that the presence of specific bioactive compounds contributes significantly to the overall antioxidant activity, thus reflecting the quality of the plant material. A positive correlation was observed between the levels of phenolics and flavonoids with antioxidant activities. Notably, TPC demonstrated stronger correlations with DPPH (r = 0.532) and hydroxyl radical scavenging activity (r = 0.580) compared to TFC, which showed r-values of 0.451 and 0.458, respectively. Additionally, 6-gingerol content exhibited a strong positive correlation with TPC (r = 0.880), as illustrated in Table 3.7. These results align with a previous findings which indicated that higher phenolic content contributes to enhanced antioxidant activity, and that a linear relationship exists between 6-gingerol levels and antioxidant potential (Pawar et al., 2011). Although the data support phenolics as the major contributors to antioxidant activity, as suggested by several earlier studies (Li et al., 2008; Mwamatopea et al., 2020; Lfitat et al., 2019), some reports have noted weak or inconsistent correlations between TPC and antioxidant effects (Chen et al., 2022a; Hou et al., 2020).

**Table 4.6. Pearson's correlation coefficient analysis to examine the relationships between TPC, TFC, and 6-gingerol concentration with the DPPH and hydroxyl radical scavenging potentials, across nine different ginger varieties**

| Analytes | TPC | TFC | DPPH | Hydroxyl |
|---|---|---|---|---|
| TPC | 1.000 | $0.912^{***}$ | $0.532^{**}$ | $0.580^{**}$ |
| TFC | $0.912^{***}$ | 1.000 | $0.451^{**}$ | $0.458^{**}$ |
| % 6-gingerol | $0.880^{***}$ | $0.810^{***}$ | $0.318^{ns}$ | $0.374^{ns}$ |

Pharmacokinetic investigations of ginger have revealed that its active constituents, particularly gingerols and shogaols, are rapidly absorbed and undergo extensive metabolism within the body. Some studies have reported a

Median Lethal Dose ($LD_{50}$) of approximately 250 mg/kg for certain ginger-derived compounds (Suekawa et al., 1984; Li et al., 2012). Given the potential for adverse effects at elevated doses, the establishment of clear safety guidelines is critical for the appropriate application of ginger constituents in both the food and pharmaceutical industries (Chiaramonte et al., 2021).

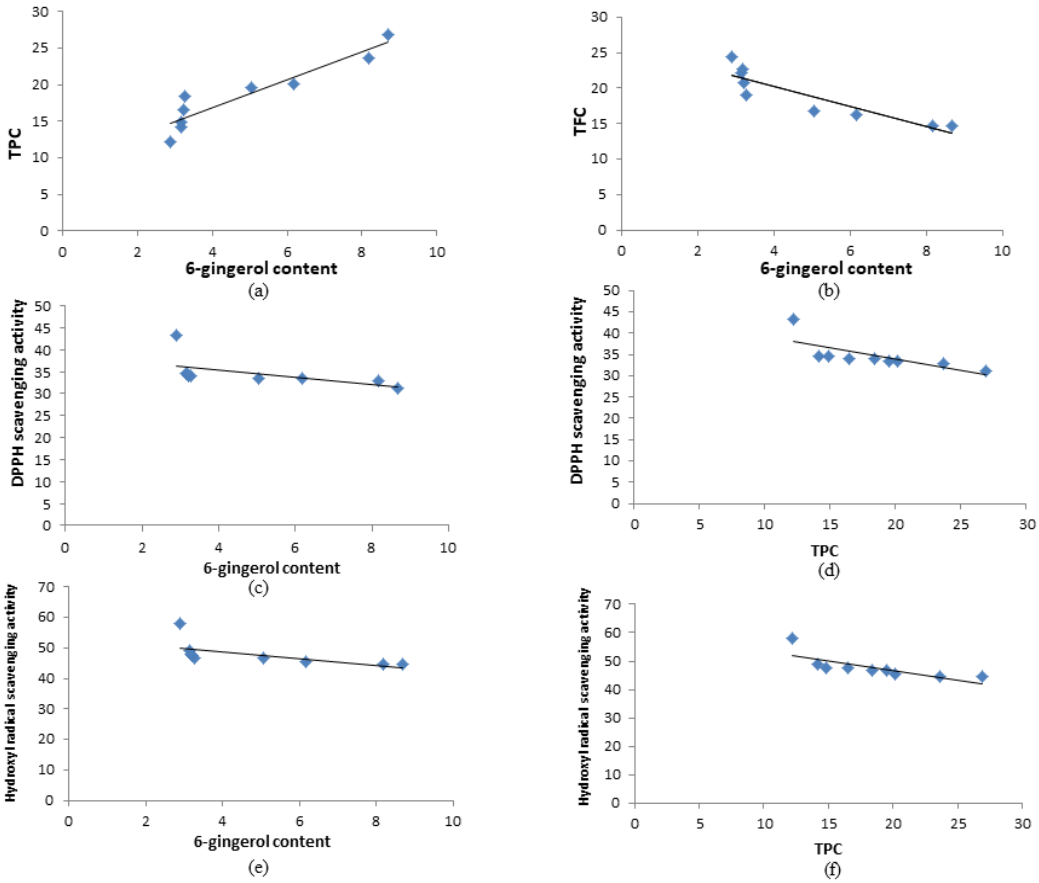

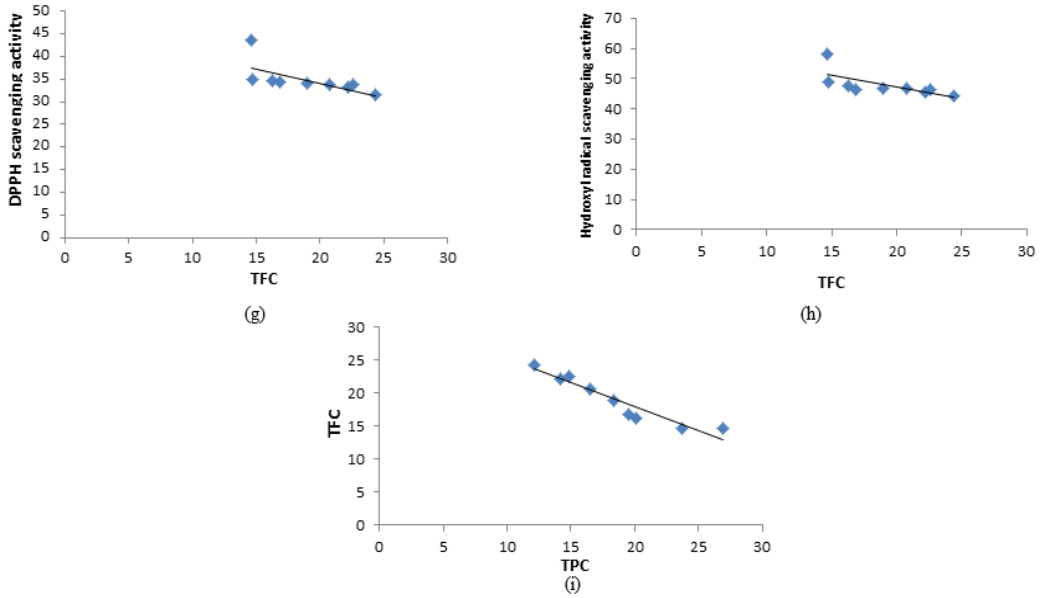


**Figure 4.5. Pearson correlation scatter plots illustrating the relationships between key phytochemical parameters and antioxidant activities across nine ginger varieties: (a) TPC vs. 6-gingerol content; (b) TFC vs. 6-gingerol content; (c) DPPH radical scavenging activity vs. 6-gingerol content; (d) hydroxyl radical scavenging activity vs. 6-gingerol content; (e) DPPH activity vs. TPC; (f) hydroxyl radical scavenging activity vs. TPC; (g) DPPH activity vs. TFC; (h) hydroxyl radical scavenging activity vs. TFC; and (i) TFC vs. TPC**

### *4.4.8. High-Performance-Thin-Layer-Chromatography analysis of ginger samples*

Quantitative analysis showed that the 6-gingerol content in the ginger samples ranged from 2.12% to 6.27% w/w, with GV6 containing the highest concentration and GV7 the lowest (Table 3.8).

**Table 4.7. 6-gingerol content (% w/w) present in the ginger samples by High-Performance-Thin-Layer-Chromatography analysis**

| Sl no. | Sample ID | 6-gingerol content (% w/w) |
|---|---|---|
| i. | GV1 | 2.82 |

| | | |
|---|---|---|
| ii. | GV2 | 3.44 |
| iii. | GV3 | 3.83 |
| iv. | GV4 | 5.06 |
| v. | GV5 | 5.66 |
| vi. | GV6 | 6.27 |
| vii. | GV7 | 2.12 |
| viii. | GV8 | 3.36 |
| ix. | GV9 | 4.74 |

The calibration curve for 6-gingerol was constructed by plotting peak areas against standard concentrations ranging from 0.5 to 1.7 µg/mL. A strong linear correlation was observed between concentration and peak area, with a correlation coefficient ($r^2 > 0.99$) and a Coefficient of Variation (CV) of 2.64 (Figure 3.6.a). The optimized mobile phase, consisting of n-hexane and ethyl acetate in a 4:6 (v/v) ratio, yielded a well-defined band for 6-gingerol at an $R_f$ value of 0.53. The image of the developed and derivatized plate was captured under white light using the CAMAG Reprostar 3 system (Figure 3.6.b). Densitometric profiles of the ginger extracts are illustrated in Figure 3.6.c.

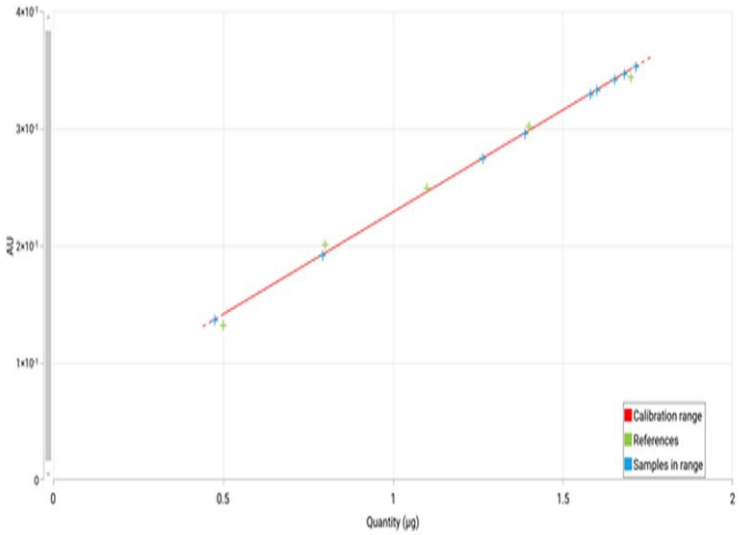
AU
Quantity (µg)
Calibration range
References
Samples in range

(a)

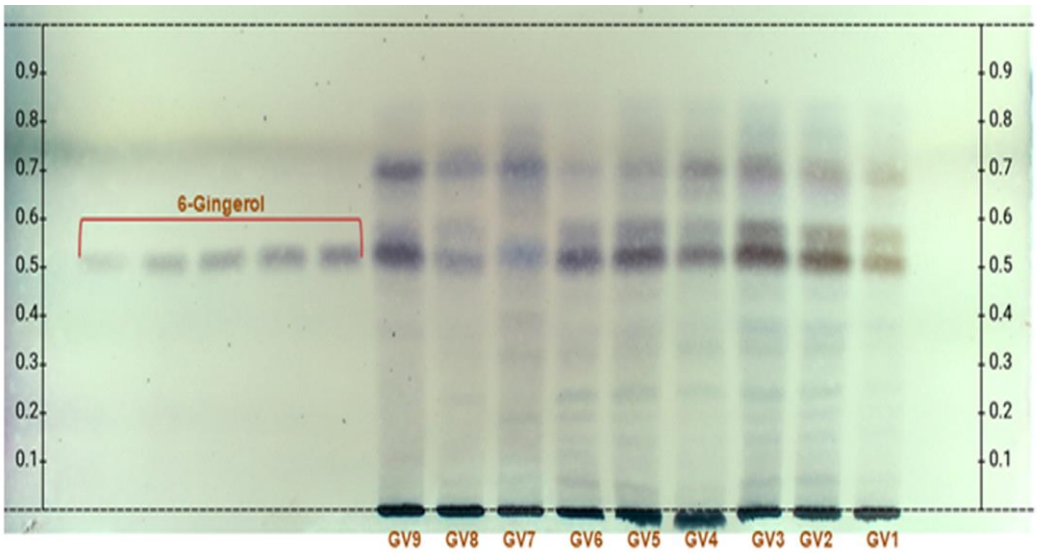
6-Gingerol
GV9
GV8
GV7
GV6
GV5
GV4
GV3
GV2
GV1

(b)

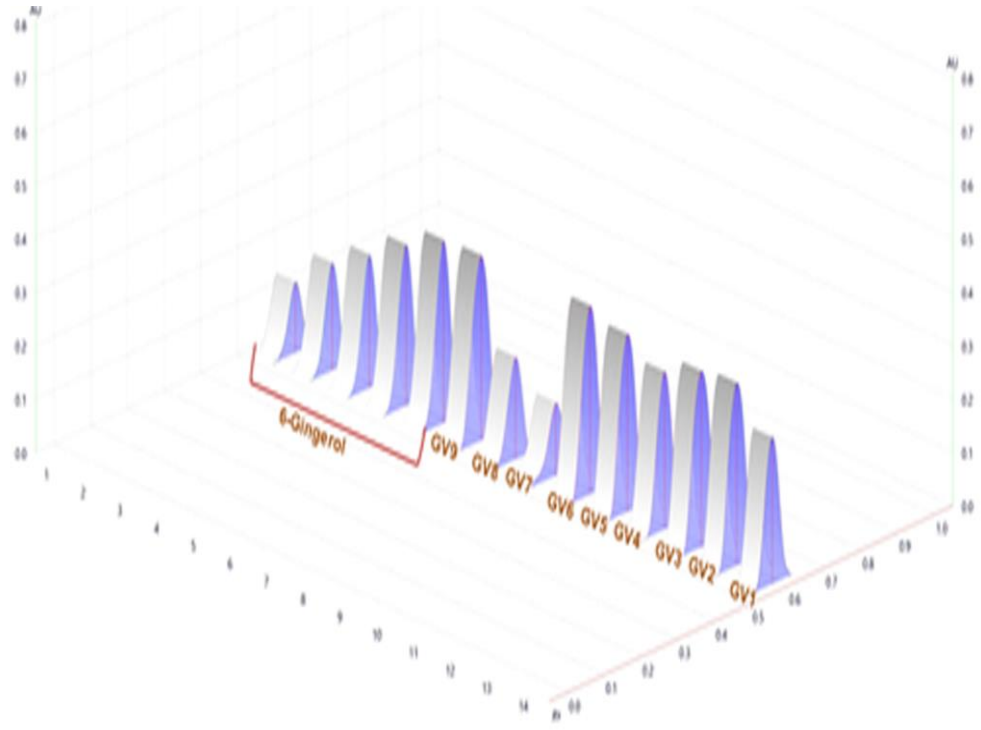


(c)

**Figure 4.6. HPTLC analysis of ginger chemo varieties showing (a) Calibration curve, (b) Picture of the developed plate taken at white light and (c) Densitometric chromatogram for quantitative estimation of 6-gingerol contents**

With the growing global confidence on herbal medicines, there is an urgent need to ensure their quality, safety, and therapeutic efficacy by employing advanced analytical techniques that align with International standards. Research has shown that geographical variations among ginger cultivars significantly affect the composition of their bioactive metabolites (Bayona et al., 2020). Manipur, a Northeastern state of India, is recognized for its rich biodiversity and serves as a hotspot for various ginger cultivars due to its unique ecological conditions (Devi et al., 2016). The present investigation utilized HPTLC analysis to assess the variation in 6-gingerol content across different ginger chemotypes collected from multiple regions within Manipur. Among them, the GV6 variety demonstrated the highest concentration of 6-gingerol. These analytical findings offer insight into the

phytochemical quality of the samples, particularly in relation to their potential therapeutic benefits.

### *4.4.9. Effect on the in-vitro cholinesterase enzymes*

The inhibitory effects of the ginger samples against AChE and BChE enzymes were evaluated and expressed in terms of their $IC_{50}$ values. Among the tested samples, GV6 exhibited the strongest AChE inhibitory activity with an $IC_{50}$ value of 305.19 ± 1.81 µg/mL, whereas GV7 showed the weakest inhibition, with an $IC_{50}$ of 521.46 ± 2.38 µg/mL (Table 3.9). A similar trend was observed for BChE inhibition, where GV6 again demonstrated the highest potency ($IC_{50}$ = 411.73 ± 4.03 µg/mL), and GV7 had the lowest inhibitory effect with an $IC_{50}$ of 602.81 ± 4.61 µg/mL. For comparison, the reference inhibitor galantamine exhibited significantly lower $IC_{50}$ values of 24.2 ± 1.85 µg/mL and 35.95 ± 3.05 µg/mL for AChE and BChE, respectively.

**Table 4.8. In-vitro AChE and BChE IC50 values of the 09 ginger samples. Data are presented as mean ± SEM (n = 3)**

| Sample Name | IC50 of AChE (µg/mL) | IC50 of BChE (µg/mL) |
|---|---|---|
| Galantamine (Reference standard) | 24.2 ± 1.85 | 35.95 ± 3.05 |
| GV1 | 474.46 ± 1.87 | 589.95 ± 3.04 |
| GV2 | 393.91 ± 2.20 | 546.64 ± 4.88 |
| GV3 | 384.59 ± 1.89 | 529.53 ± 3.58 |
| GV4 | 371.10 ± 3.22 | 486.94 ± 1.18 |
| GV5 | 368.02 ± 0.97 | 471.36 ± 2.18 |
| GV6 | 305.19 ± 1.81 | 411.73 ± 4.03 |
| GV7 | 521.46 ± 2.38 | 602.81 ± 4.61 |
| GV8 | 409.94 ± 1.29 | 576.10 ± 2.53 |
| GV9 | 378.37 ± 2.16 | 518.19 ± 2.73 |

## 4.5. Conclusion

The present findings validate the influence of geographical and ecological variations on the phytochemical richness and bioactivity of ginger cultivars. GV6, in particular, demonstrated potent extract due to higher phenolic content, greater antioxidant activities, higher 6-gingerol concentration, and highest cholinesterase inhibition compared to other ginger samples. The result highlights GV6 as a promising sample for further pharmacological exploration, particularly in the context of antioxidant and neuroprotective applications.

The study underscores the necessity of adopting robust phytochemical characterization and standardization strategies for herbal medicines, in alignment with International quality and safety standards. The present investigation not only link phytochemical diversity with biological activity but also advances the scientific understanding of ginger chemotypes to provide a basis for prioritize cultivars in drug discovery, and therapeutic interventions against neurodegenerative disorders.

## 4.6. Publications

### *4.6.1. Paper published*

Ghosh, S., Das, B., Haldar, P.K., Kar, A., Chaudhary, S.K., Singh, K.O., Bhardwaj, P.K., Sharma, N., Mukherjee, P.K., 2022. 6-Gingerol contents of several ginger varieties of Northeast India and correlation of their antioxidant activity in respect to phenolics and flavonoids contents. Phytochemical Analysis. 34, 259-268. https://doi.org/10.1002/pca.3201.

### *4.6.2. Paper presented*

**Ghosh, S.**, Das, B., Haldar, P.K., Kar, A., Chaudhary, S.K., Bhardwaj, P.K., Sharma, N., Mukherjee, P.K., "Quality evaluation of several ginger varieties of North-East India" at 9th Convention of SFE-INDIA and National Seminar on "Translational Research on Indian Medicinal Plants" at Jadavpur University, Kolkata during September 23-24, 2022.

# Chapter 5

## Neuroprotective effect of standardized extract of *Zingiber officinale* Roscoe. – Mechanistic insight

5.1. Metabolite profiling by HR-LCMS method

5.2. *In-vivo* neuroprotective activity

5.3. Molecular docking

5.4. Statistical analysis

5.5. Result and discussion

5.6. Conclusion

**Selection of the potent ginger sample to perform the metabolite profiling and *in-vivo* neuroprotective activity**

The GV6 sample was selected based on its quantified 6-gingerol content, and AChE, BChE inhibitory activities and was assessed for its metabolite profiling by HR-LCMS analysis and neuroprotective efficacy in a scopolamine-induced model of cognitive impairment in mice.

**Chemical and reagents**

Scopolamine, donepezil, ATCI, BTCI, DTNB, galantamine, AChE derived from bovine erythrocytes, BChE isolated from equine serum and the mouse Tumor Necrosis Factor- α (TNF-α) Enzyme-Linked Immunosorbent Assay (ELISA) kit were procured from Sigma-Aldrich (St. Louis, MO, USA). HPLC grade methanol (≥ 99.8%), formic acid and all other chemicals were purchased from Merck (Darmstadt, Germany). Ultrapure water was obtained from Milli-Q system (Millipore, Bedford, MA, USA). All the working concentrations were prepared freshly on the day of experiment.

## 5.1. Metabolite profiling by HR-LCMS method

### *5.1.1. Instrumentation*

The LC-MS analysis was performed using an Agilent 1290 Infinity II LC system (Agilent Technologies, Santa Clara, CA, USA) coupled with a Q-TOF 6545 mass spectrometer equipped with dual Electrospray Ionization (ESI) source. Chromatographic separation was carried out on a Waters BEH-$C_{18}$ column (2.1 × 150 mm, 1.8 µm) maintained at 30°C. The mobile phase consisted of solvent A (0.1% formic acid in water) and solvent B (0.1% formic acid in methanol), delivered at a flow rate of 0.30 mL/min. The gradient elution program was as follows: 0-10 min, 55% B; 10-30 min, 95% B; 30-34 min, 90% B; and 34-36 min, 55% B. Mass spectrometric detection was carried out in positive ESI mode with the following parameters: capillary voltage (VCap), 4000 V (positive) and 3500 V (negative); fragmentor, 125 V; skimmer, 65 V; octapole (OCT 1 RF Vpp), 750 V. The nebulizer pressure was set at 45 psi, with a drying gas flow rate of 11 L/min

at 320°C, and sheath gas temperature maintained at 350°C. The mass spectra were acquired in the m/z range of 100-3200. Data acquisition and processing were performed using Agilent MassHunter Qualitative Analysis.

### *5.1.2. Metabolite profiling*

For LC-MS analysis, 1 mg of the GV6 extract was dissolved in 1 mL of 70% methanol to prepare the stock solution. From this, 10 µL of the stock was diluted with 990 µL of 70% methanol. The resulting solution was filtered through a 0.22 µm PTFE syringe filter prior to injection. An aliquot of 20 µL of the filtered sample was introduced into the LC column via an autosampler. The processed LC-MS data were subsequently analysed to determine possible molecular formulas of the detected metabolites, which were identified and annotated using Agilent MassHunter software (Esquivel-Alvarado et al., 2022).

## 5.2. *In-vivo* neuroprotective activity

### *5.2.1. Animals and ethics*

Adult Swiss albino mice (8-12 weeks old) of either sex, weighing between 23-25 g, were procured from the West Bengal Livestock Development Corporation Ltd. (Kalyani, West Bengal, India). All experimental protocols involving animals were conducted in accordance with ethical standards and were approved by the Institutional Animal Ethics Committee (IAEC) of Jadavpur University, under the guidelines of the Committee for the Purpose of Control and Supervision of Experiments on Animals (CPCSEA) (Approval No.: JU/IAEC-22/10). The animals were housed in a controlled environment with a temperature of 22 ± 2°C, relative humidity of 60 ± 10%, and a 12-hr light/dark cycle. Standard laboratory food and water were provided *ad libitum*. Mice were allowed to acclimatize to these conditions for one week before the initiation of the study.

### *5.2.2. Acute oral toxicity study*

An acute oral toxicity study was conducted in accordance with Organization for Economic Co-operation and Development (OECD) guideline 425 (OECD, 2022).

Female mice (n = 6) received GV6 orally at a dose of 2000 mg/kg body weight (b.w.), while a separate control group (n = 6) received distilled water at 10 mL/kg. The low-dose and high-dose of the GV6 extract was selected based on the safety profile measured by the acute oral toxicity study.

### *5.2.3. Drug administration*

For the in-vivo investigation, a total of 30 Swiss albino mice were randomly allocated into five experimental groups, with six animals in each group (n = 6; 3 males and 3 females per group), as outlined below:

- Group I (Control): Received distilled water by oral (per os (p.o.)) and 0.9% normal saline intraperitoneal (i.p.);
- Group II (Scopolamine): Received scopolamine at a dose of 1 mg/kg b.w. via i.p. injection to induce cognitive dysfunction;
- Group III (Scopolamine + GV6 Low-dose): Received scopolamine (1 mg/kg, i.p.) and a low dose of the test extract GV6 (200 mg/kg, p.o.);
- Group IV (Scopolamine + GV6 High-dose): Received scopolamine (1 mg/kg, i.p.) in combination with a high dose of GV6 (400 mg/kg, p.o.);
- Group V (Scopolamine + Donepezil): Received scopolamine (1 mg/kg, i.p.) along with the standard drug donepezil (3 mg/kg, p.o.).

Donepezil served as the reference therapeutic agent, while scopolamine was employed to model memory impairment, as previously described by Wang et al. (2022). After a one-week acclimatization period, oral treatment with GV6 and donepezil commenced on day 8 and continued until the end of the study. Scopolamine administration began on day 13 and was given daily following a 20 min interval after the respective oral doses of test compounds or donepezil. The test extract of GV6 were prepared at concentrations of 20 mg/mL and 40 mg/mL, and donepezil at 0.03 mg/mL, with all oral doses administered at a volume of 10 mL/kg b.w.

### *5.2.4. Behavioral test*

To minimize potential carryover effects and ensure unbiased behavioral outcomes, a one-day gap was maintained between each behavioral assessment. Testing commenced 30 min post-treatment administration, following the protocol adapted from Nazari et al. (2022). Evaluation of spatial learning and memory was carried out using the Morris water maze test, which was conducted over a period of six consecutive days (from day 13 to day 18). Short-term memory performance was assessed using the Y-maze test on day 20. Subsequently, recognition memory and cognitive function were analyzed through the NOR test, conducted on the 22$^{nd}$ and 23$^{rd}$ days, following the procedure outlined by Mohamed et al. (2023).

#### *5.2.4.1. Morris water maze test*

The Morris water maze consisted of a round tank measuring 100 cm in diameter and 50 cm in height, which was conceptually divided into four equal quadrants named North, South, East, and West. A transparent escape platform, 12 cm in diameter perforated for better grip, was submerged in the centre of the southeast quadrant. The tank was filled with water, to which a non-toxic black dye was added for contrast. Additionally, skimmed milk powder was mixed into the water to give it a non-transparent, milky appearance. The water level was maintained 1 cm above the hidden platform surface, and the temperature was controlled at 25 ± 1°C throughout the experiment. The platform location remained unchanged for the duration of the study. To aid spatial orientation, prominent visual cues were positioned around the testing room. A digital video tracking system (ANY-maze, San Diego, USA) connected to an overhead camera and used to record and analyse the mouse movements, following the procedure adapted from Pisar et al. (2023).

- ***Training Phase***

Each animal underwent a training session once daily for five consecutive days. During each daily session, mice were subjected to four separate trials with 10 min intervals between them. For every trial, a mouse was released into the maze

facing the tank wall, with the starting quadrant varied randomly across trials. Mice were given 60 sec to locate the hidden platform and allowed to remain on it for 5 sec upon successful location. Escape latency (time taken to find the platform) and swimming paths were recorded for each attempt. If a mouse failed to locate the platform within the allotted time, it was gently guided to the platform and allowed to stay for 15 sec to aid learning. After each trial, the mouse was dried using a soft towel and returned to its home cage. This repeated exposure enabled the animals to gradually learn the spatial position of the hidden platform using external room cues.

- ***Probe trial***

On the sixth day, following the training phase, a probe trial was conducted to evaluate reference memory. For this, the hidden platform was removed from the tank, and each mouse was introduced into the maze from a fixed quadrant. Mice were allowed to swim freely for 60 sec. The time spent in the target quadrant, where the platform had previously been placed, and the searching trajectories were monitored and analyzed using the video tracking system. All behavioral assessments were conducted between 9:00 and 11:00 AM in a soundproof experimental room under consistent lighting and temperature conditions.

#### *5.2.4.2. Y-maze test*

The Y-maze test was conducted in accordance with the method outlined by da Costa Rodrigues et al. (2022), with slight modifications. The Y-maze apparatus was constructed from black acrylic and comprised three identical arms, each measuring 40 cm in length, 8 cm in width, and 15 cm in height, arranged at 120° angles from one another. During testing, each mouse was placed at the end of one designated arm (arm A), and allowed to explore the maze freely for a duration of 8 min. The total number of arm entries and sequences were recorded throughout the session. A spontaneous alternation was defined as consecutive entries into all three arms in a non-repetitive sequence (e.g., ABC, BCA, or CAB), indicating intact spatial working memory. An arm entry was counted when all four limbs of the mouse had fully crossed into an arm. The ability to alternate between

arms in overlapping triplet sequences was used as an index of working memory performance. To eliminate olfactory cues, the apparatus was thoroughly cleaned between each trial. The percentage of spontaneous alternations was calculated using the following formula:

$$\% \text{ alteration} = [(\text{Number of alternations} \times 3) / (\text{Total number of arm entries} - 2)] \times 100$$

### *5.2.4.3. NOR test*

The NOR test was conducted in a rectangular open-field box constructed from plywood (40 cm × 60 cm), with white acrylic walls and an open top to allow unobstructed observation. On the first day, mice underwent a habituation session where each animal was allowed to freely explore the empty arena for 5 min to acclimate to the environment. No objects were present during this session. On the second day, a brief re-habituation phase lasting 3 min was carried out, which included three successive phases: the acquisition trial, the inter-trial interval, and the retention trial. During the acquisition phase, mice were introduced into the arena containing two identical, biologically inert objects (labelled A1 and A2), positioned 10 cm away from the walls in the corners of the open field. The mice were allowed to explore these objects freely for 8 min. Following this, the animals were returned to their home cages for a 30 min inter-trial interval. In the subsequent retention phase, one familiar object (A1) and one novel object (B1) were placed in the same locations as in the acquisition phase, and mice were again allowed to explore for 8 min. Exploratory behaviors were defined as direct interactions such as sniffing, licking, or touching the objects, while behaviors such as leaning on the objects without active investigation were not considered (Lueptow, 2017). All trials were recorded using a video camera for further analysis. The recognition memory performance was quantified by calculating the Object Recognition (OR) index using the formula:

OR index = [(Time spent to explore the new object) - (Time spent to explore the familiar object)] / [(Time spent to explore the new object) + (Time spent to explore the familiar object)]

### *5.2.5. Assessment of biochemical and oxidative stress markers*

#### *5.2.5.1. Brain tissue collection*

As illustrated in Figure 5.1, on the 24$^{th}$ day of the experiment, mice were humanely euthanized via cervical dislocation. The entire brains were rapidly excised, rinsed with ice-cold Phosphate Buffer Saline (PBS), snap-frozen using dry ice, and subsequently stored at -80°C until further processing. Brain samples from three mice per group (n = 3) were used for the analysis of biochemical markers and oxidative stress-related parameters.

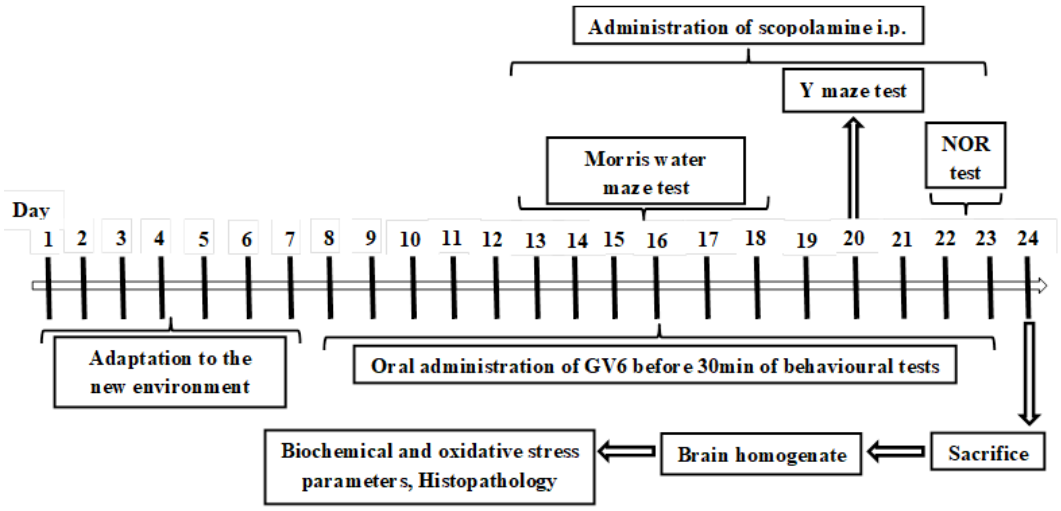


**Figure 5.1. Schematic representation of the experimental design. Following a 7-day acclimatization period, oral administration of GV6 commenced on day 8 and continued throughout the study. The i.p. injections of scopolamine began on day 12, administered 20 min after GV6 and 10 min prior to behavioral assessments. The Morris water maze test was conducted from days 13 to 18, followed by the Y-maze test on day 20, and the NOR test on days 22 and 23. On day 24, all animals were sacrificed, and brain tissues were collected for biochemical, oxidative stress, and histopathological analyses**

Each brain was homogenized in ice-cold 50 mM sodium phosphate buffer (pH 7.4) to prepare a 2% homogenate (w/v ratio of 1:10). The homogenates were centrifuged at 9000 g for 30 min at 4°C. The resulting supernatants were carefully collected and stored at -80°C for subsequent measurement of AChE and BChE enzyme activities, as well as ACh levels. The entire procedure was carried out on dry ice to prevent enzymatic degradation. (Phachonpai and Tongun, 2021).

### *5.2.5.2. AChE and BChE activity*

The enzymatic activities of AChE and BChE were determined using a modified method based on the protocol reported by Hussain et al. (2022), utilizing a 96-well microplate and a SpectraMax iD3 plate reader. In brief, each reaction well contained 75 µL of 50 mM Tris-HCl buffer (pH 8.0), 25 µL of either 15 mM ATCI for AChE or BTCI for BChE, and 0.1% Bovine Serum Albumin (BSA). This reaction mixture was combined with 100 µL of brain tissue supernatant and pre-incubated at 25°C for 5 min. Following incubation, 30 µL of 10 mM DTNB was added to initiate the enzymatic reaction. The change in absorbance was monitored at 412 nm for a total duration of 120 sec, with measurements recorded at 30 sec intervals. Enzymatic activity was calculated based on the rate of substrate hydrolysis and expressed as micromoles (µmol) of substrate hydrolyzed per min per milligram of protein (µmol/min/mg protein) for both AChE and BChE, respectively.

$$R = (\delta OD \times \text{total volume of assay} \times 1000) / (E \times \text{mg protein})$$

Where, δOD = change in absorbance per min, E = extinction coefficient ($1.36 \times 10^4$ $M^{-1}$ $cm^{-1}$).

### *5.2.5.3. ACh content estimation*

The concentration of ACh in brain tissue was quantified following a modified version of the method described by Bae et al. (2014). Briefly, 20 µL of brain supernatant was added to each well of a 96-well plate, followed by the addition of 50 µL of a freshly prepared 1% aqueous solution of hydroxylamine and

potassium hydroxide in a 1:1 ratio. The mixture was incubated at 25°C for 15 min. Subsequently, 250 µL of $FeCl_3$ solution prepared in 0.1 N HCl (pH 1.2) was added to each well to develop the color reaction. Absorbance was recorded at 540 nm using a microplate reader. The ACh content was calculated and expressed as micromoles per milligram of protein (µmol/mg protein). This method is based on the principle that ACh reacts with hydroxylamine in an alkaline medium to form acetohydroxamic acid, which, upon acidification with HCl and in the presence of Ferric ions ($Fe^{3+}$), yields a red-brown colored complex measurable spectrophotometrically (Karunakaran et al., 2022).

#### *5.2.5.4. Estimation of brain antioxidant content*

#### *Estimation of Malondialdehyde (MDA) levels*

Lipid peroxidation in brain tissues was assessed by measuring MDA levels using a modified Thiobarbituric Acid Reactive Substances (TBARS) method, as described by Babalola et al. (2023). Briefly, equal volumes of Trichloroacetic Acid (TCA) and Thiobarbituric acid (TBA) were mixed in a 1:1 ratio and added to the brain tissue supernatant. The reaction mixture was then heated in a boiling water bath for 15 min to facilitate the formation of the MDA-TBA adduct. After allowing the mixture to cool rapidly to room temperature, it was centrifuged at 3000 rpm for 10 min to remove any precipitates. The resulting supernatant, containing the pink chromogen formed by the reaction of MDA with TBA under acidic and high-temperature conditions, was measured spectrophotometrically at 532 nm. The MDA content was expressed as nanomoles per milligram of protein (nmol/mg protein).

#### *Determination of Superoxide Dismutase (SOD) activity*

SOD activity in brain tissue was assessed using a modified protocol adapted from Nunes et al. (2015). This assay is based on the principle that superoxide radicals react with 2,4-iodophenyl-3,4-nitrophenyl-5-phenyltetrazolium chloride to form a red-colored formazan dye, and the presence of SOD inhibits this reaction. A reaction mixture was prepared consisting of 3 mL of 500 µM xanthine, 3 mL of

200 µM Potassium cyanide (KCN), 7.44 mg of cytochrome c, 3 mL of 1 mM EDTA, and 18 mL of 0.05 M sodium phosphate buffer (pH 7.0). To initiate the assay, 975 µL of this reaction mixture was combined with 20 µL of brain tissue supernatant and 5 µL of xanthine oxidase. The reaction was allowed to proceed at room temperature for 7 min, after which the absorbance was measured at 550 nm. SOD activity was expressed as units per milligram of protein (U/mg protein), where one unit is defined as the amount of enzyme required to inhibit the rate of formazan formation by 50%.

***Estimation of Glutathione (GSH) content***

The reduced GSH level in brain tissues was estimated following a modified version of the method described by Lonita et al. (2017). This colorimetric assay is based on the reaction of GSH with DTNB, which results in the formation of Glutathione disulfide (GSSG) and a yellow-colored compound, 5-Thio-2-Nitrobenzoic acid (TNB). The intensity of the yellow coloration, measurable at 412 nm, is directly proportional to the GSH concentration in the sample.

In brief, 1 mL of brain tissue supernatant was diluted with 0.9 mL of PBS (pH 7.4), followed by the addition of 1 mL of 20% TCA to precipitate proteins. The mixture was incubated at room temperature for 20 min and then centrifuged at 10,000 rpm for 10 min. From the resulting supernatant, 0.75 mL was collected (after discarding 0.25 mL), and mixed with an equal volume of PBS. Subsequently, 2 mL of DTNB solution (600 µmol/L) was added, and the mixture was incubated for 10 min at room temperature. The absorbance was recorded at 412 nm, and the GSH levels were calculated and expressed as micromoles per milligram of protein (µmol/mg protein).

***Determination of Catalase (CAT) activity***

CAT activity in brain tissue was measured using a modified version of the colorimetric method described by Foyet et al. (2015). This assay is based on the formation of a yellow complex resulting from the reaction between unreacted

$H_2O_2$ and ammonium molybdate, which allows for indirect quantification of CAT activity by measuring the extent of $H_2O_2$ breakdown.

In a 96-well microplate, 50 µL of brain tissue supernatant was mixed with 50 µL of freshly prepared 50 mM $H_2O_2$ solution in 0.2 M sodium-potassium phosphate buffer (pH 7.4). The reaction mixture was incubated at 37°C for 3 min to allow the enzymatic degradation of $H_2O_2$. The reaction was then terminated by adding 100 µL of 64.8 mM ammonium molybdate prepared in Sulfuric acid. The absorbance of the resulting yellow complex was measured at 405 nm using a microplate reader. CAT activity was calculated and expressed as units per milligram of protein (U/mg protein).

***Estimation of Nitrate/nitrite (NOx) levels***

The concentration of NOx, a stable end-product of nitric oxide metabolism, was determined in brain tissue samples using the Griess reagent (Babalola et al. (2023). In brief, 100 µL of brain tissue supernatant was mixed with an equal volume (100 µL) of Griess reagent in a 96-well microplate. The reaction mixture was incubated at room temperature for 10 min to allow color development. The resulting pink-colored azo compound, indicative of NOx presence, was measured spectrophotometrically at 540 nm. NOx concentrations were determined from a standard curve prepared using known concentrations of sodium nitrite and expressed as micromolar per milligram of protein (µM/mg protein).

***Estimation of TNF-α levels***

TNF-α levels in the brain tissues of scopolamine-treated mice were quantified using a commercially available ELISA kit (Sigma-Aldrich, St. Louis, USA), following the manufacturer's instructions. All reagents and samples were prepared and processed as per the provided protocol, and absorbance was measured using a microplate reader. The concentration of TNF-α was calculated from the standard curve and expressed as pg/mg protein.

#### *5.2.5.5. Histological examination of brain tissue*

Brain tissues from three animals per group (n = 3) were utilized to assess morphological alterations. Following dissection, the whole brains were initially fixed in 10% neutral-buffered formalin. The samples were then subjected to a graded series of ethanol for dehydration, cleared with xylene, and post-fixed in 4% paraformaldehyde at 4°C overnight. After fixation, the tissues were embedded in paraffin wax and sectioned into 4 µm thick slices using a rotary microtome. For histological evaluation, the tissue sections were stained with Hematoxylin and Eosin (H&E), a standard technique for visualizing cellular and nuclear architecture. The stained sections were examined under a light microscope at 100x magnification. Images were captured using a DP-27 digital camera system and analyzed with Magvision software (Olympus, Japan), as previously described by Zeng et al. (2022).

### 5.3. Molecular docking

For the docking studies, the structural coordinates of the overlapping protein targets were employed as receptors, while the chemical structures of the selected bioactive ligands were retrieved from the PubChem database (https://pubchem.ncbi.nlm.nih.gov/). Molecular docking was performed using AutoDock Vina to evaluate the interactions between the ligands and their respective target proteins. Protein structures were prepared and visualized with PyMOL (v2.x) and BIOVIA Discovery Studio 2021, following established protocols (Seeliger and de Groot, 2010). Prior to docking, both receptor and ligand files were pre-processed using AutoDock Tools (ADT, v1.5.6). For the receptors, the binding sites were defined by generating grid boxes, with centers and dimensions set at coordinates (9.888244; −60.058399; −24.378703 for AChE) and (2.564882; 10.370544; 14.087385 for BChE). Receptor preparation involved removing non-essential molecules and cleaning the structures in PyMOL. Ligand preparation included assignment of torsional flexibility, root detection, and adjustment of charges. The processed receptor and ligand structures were then converted into .pdbqt format for docking. Semi-flexible

docking was carried out using the ligand expansion approach, with default parameters applied for exhaustiveness, energy range, and number of binding modes (Mukherjee et al., 2020). From the generated docking poses, the conformation with the lowest binding energy was selected for further interaction analysis. Hydrogen bonding and π–π/π–H stacking interactions were examined using visualization software to validate the binding orientation (Das et al., 2023).

## 5.4. Statistical analysis

Data analysis was performed using GraphPad Prism software (version 8.0.2, GraphPad Software Inc., La Jolla, CA, USA). All results are presented as mean ± Standard deviation (SD). Behavioral outcomes, as well as biochemical and oxidative stress parameters, were evaluated using one-way ANOVA with repeated measures. Post hoc comparisons between groups were conducted using Sidak's multiple comparisons test. A p-value of less than 0.05 was considered statistically significant.

## 5.5. Result and discussion

### *5.5.1. Chemical composition of GV6*

The chemical composition of GV6 was carried out by using HR-LCMS analysis. The total ion chromatogram revealed a total 39 compounds in positive ionization mode (Figure 5.2). The identified metabolites along with their molecular formula, mass, m/z, RT (min), error (ppm), and area are summarized in the below table (Table 5.1).

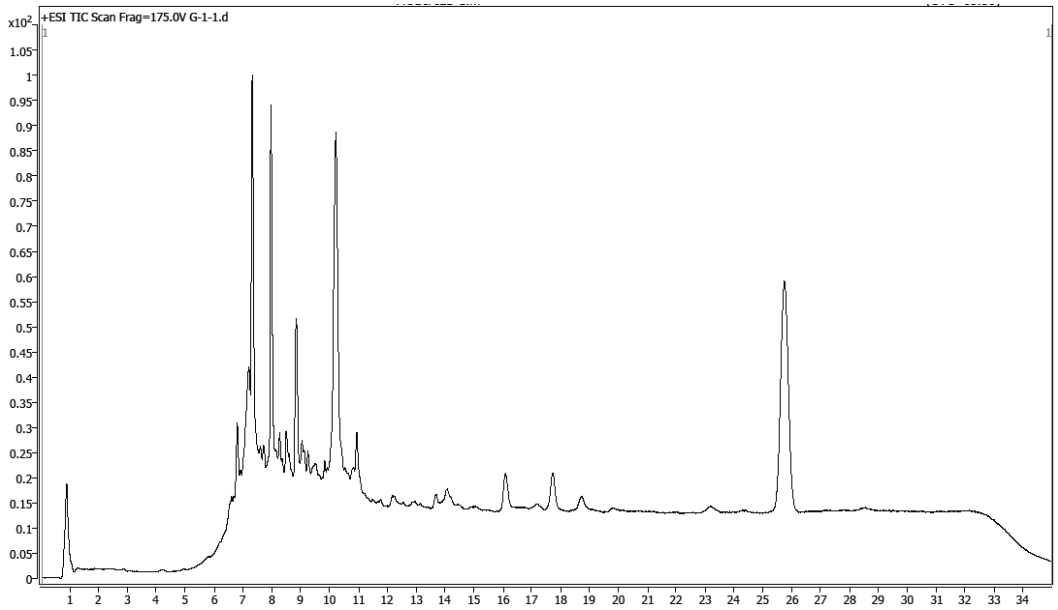


**Figure 5.2. Total ion chromatogram of the GV6 extract in positive ionization mode**

The molecular mass of the identified molecules ranged from 110.037 to 676.3638 while the m/z values ranged from 111.1291 to 677.4559. Various classes of compounds such as phenolics, flavonoid, diarylheptanoids, fatty acids, amino alcohols, and cinnamic acid derivatives were detected in various RT values.

**Table 5.1. Identified compounds with their molecular formula, mass, m/z value, RT, error and area in GV6 extract**

| Sl no. | Tentative identification | Molecular formula | Mass (g/mol) | m/z $[M+H]^+$ | RT (min) | Error (ppm) | Area |
|---|---|---|---|---|---|---|---|
| 1. | Methyl diacetoxy-[4]-gingerdiol | $C_{20}H_{30}O_6$ | 366.2033 | 367.2954 | 6.601 | -2.45 | 15019 |
| 2. | 6-paradol | $C_{17}H_{26}O_3$ | 278.1879 | 279.28 | 6.75 | -1.11 | 10126 |
| 3. | Rhamnetin | $C_{16}H_{12}O_7$ | 316.0589 | 317.151 | 6.929 | 1.89 | 11123 |
| 4. | 1-(3,4-dihydroxyphenyl)-7-(4-hydroxy-3- | $C_{20}H_{26}O_6$ | 362.1715 | 363.2636 | 7.05 | -3.84 | 9187 |

| | | | | | | | |
|---|---|---|---|---|---|---|---|
| | methoxyphenyl)-3,5-heptanediol | | | | | | |
| 5. | 5-hydroxy-1-(4-hydroxy-3-methoxyphenyl)-7-(4-hydroxyphenyl)-3-heptanone | $C_{20}H_{24}O_5$ | 344.1614 | 345.2535 | 7.083 | -2.73 | 222383 |
| 6. | Dehydrozingerone | $C_{11}H_{12}O_3$ | 192.0794 | 193.1715 | 7.282 | 3.87 | 128396 |
| 7. | Coumaric acid | $C_9H_8O_3$ | 164.0467 | 165.1388 | 7.316 | -3.95 | 37041 |
| 8. | 3,5-diacetoxy-1,7-bis(4-hydroxy-3-methoxyphenyl) heptane | $C_{25}H_{32}O_8$ | 460.2094 | 461.3015 | 7.399 | -0.71 | 111749 |
| 9. | Zingerone | $C_{11}H_{14}O_3$ | 194.0934 | 195.1855 | 7.532 | -4.44 | 4492 |
| 10. | 1,2-Oxidolinalool | $C_{10}H_{18}O_2$ | 170.1305 | 171.2226 | 7.798 | -1.05 | 5662 |
| 11. | Oxo-octadecenoic acid | $C_{23}H_{41}NO_2$ | 363.3148 | 364.4069 | 7.914 | 3.08 | 13010 |
| 12. | 6-gingerdione | $C_{17}H_{24}O_4$ | 292.1663 | 293.2584 | 7.947 | -3.89 | 7950 |
| 13. | 8-shogaol | $C_{19}H_{28}O_3$ | 304.2044 | 305.2965 | 7.98 | 1.69 | 43149 |
| 14. | Aminoeicosanediol | $C_{20}H_{43}NO_2$ | 329.3308 | 330.4229 | 8.18 | 4.39 | 1073619 |
| 15. | Aminooctadecenetriol | $C_{18}H_{37}NO_3$ | 315.2782 | 316.3703 | 8.28 | 2.66 | 3105 |
| 16. | Ubiquinol 10 | $C_{19}H_{28}O_4$ | 320.1992 | 321.2913 | 8.296 | 1.51 | 19078 |
| 17. | Oleamide | $C_{18}H_{35}NO$ | 281.2727 | 282.3648 | 8.329 | 3.09 | 34549 |
| 18. | 1-dehydro-6-gingerdione | $C_{17}H_{22}O_4$ | 290.1531 | 291.2452 | 8.545 | 4.55 | 359558 |
| 19. | Elemol | $C_{15}H_{26}O$ | 222.1987 | 223.2908 | 8.712 | 1.66 | 7615 |

| | | | | | | | |
|---|---|---|---|---|---|---|---|
| 20. | 10-shogaol | $C_{21}H_{32}O_3$ | 332.2361 | 333.3282 | 8.828 | 2.85 | 45010 |
| 21. | Geranial | $C_{10}H_{16}O$ | 152.1206 | 153.2127 | 8.894 | 3.4 | 11687 |
| 22. | 6-shogaol | $C_{17}H_{24}O_3$ | 276.1736 | 277.2657 | 9.26 | 3.65 | 158175 |
| 23. | 10-gingerdione | $C_{21}H_{32}O_4$ | 348.2293 | 349.3214 | 9.293 | -2.1 | 1225 |
| 24. | 8-paradol | $C_{19}H_{30}O_3$ | 306.2186 | 307.3107 | 9.46 | -3.01 | 1572 |
| 25. | 10-paradol | $C_{21}H_{34}O_3$ | 334.251 | 335.3431 | 9.526 | 0.65 | 6242 |
| 26. | 1-dehydro-8-gingerdione | $C_{19}H_{26}O_4$ | 318.1843 | 319.2764 | 9.676 | 3.72 | 141965 |
| 27. | Halaminol A | $C_{14}H_{29}NO$ | 227.2256 | 228.3177 | 10.158 | 2.98 | 20001 |
| 28. | Catechol | $C_6H_6O_2$ | 110.037 | 111.1291 | 10.64 | 2.11 | 4152 |
| 29. | Cymene | $C_{10}H_{14}$ | 134.1102 | 135.2023 | 10.656 | 4.75 | 27110 |
| 30. | Limonene | $C_{10}H_{16}$ | 136.1258 | 137.2179 | 10.673 | 4.59 | 96830 |
| 31. | Gingerglycolipid A | $C_{33}H_{56}O_{14}$ | 676.3638 | 677.4559 | 11.238 | -4.68 | 405057 |
| 32. | Geranyl acetate | $C_{12}H_{20}O_2$ | 196.1469 | 197.239 | 11.554 | 2.69 | 5138 |
| 33. | α-linolenic acid | $C_{18}H_{30}O_2$ | 278.2246 | 279.3167 | 12.168 | 0.1 | 19187 |
| 34. | Methyl-10-gingerol | $C_{22}H_{36}O_4$ | 364.2599 | 365.352 | 12.451 | -4 | 70438 |
| 35. | 12-gingerol | $C_{23}H_{38}O_4$ | 378.2773 | 379.3694 | 12.734 | 0.68 | 19982 |
| 36. | Palmitic acid | $C_{16}H_{32}O_2$ | 256.2413 | 257.3334 | 13.681 | 4.16 | 128804 |
| 37. | 6-gingerol | $C_{17}H_{26}O_4$ | 294.188 | 295.2801 | 13.698 | 1.54 | 25163 |
| 38. | Zingiberene | $C_{15}H_{24}$ | 204.1884 | 205.2805 | 25.531 | 2.75 | 4933 |
| 39. | Aminohexadecanediol | $C_{16}H_{35}NO_2$ | 273.2667 | 274.3588 | 25.88 | -0.2 | 7650 |

Among the 39 identified compounds, 12 compounds are having anti-alzheimer's properties, as described in previous studies. The structures of major metabolites responsible for anti-alzheimer's activity are presented in the (Figure 5.3).

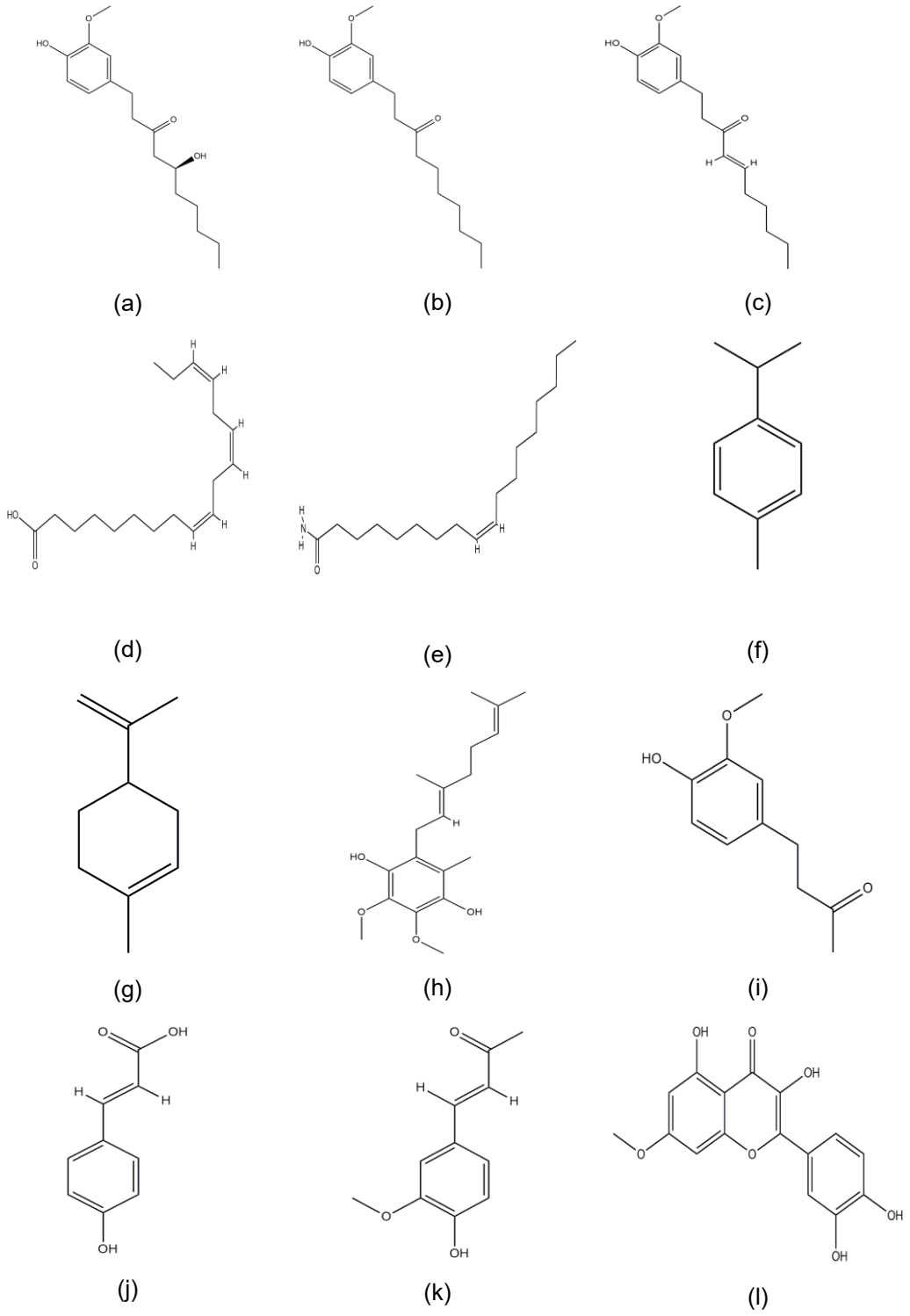


**Figure 5.3. Major metabolites present in GV6, responsible for the anti-Alzheimer's**

**activity (a) 6-gingerol, (b) 6-paradol, (c) 6-shogaol, (d) α-linolenic acid, (e) oleamide, (f) cymene, (g) limonene, (h) ubiquinol 10, (i) zingerone, (j) coumaric acid, (k) dehydrozingerone, (l) rhamnetin**

***Phenolic compounds***

A total of 16 phenolic compounds were identified based on the RT and m/z observed. The peak 10, 11, 31, 36, 38, 51, 56, 61, 62, 63, 64, 66, 70, 82, 83, and 86 showed an ion at m/z 367.2954, 279.28, 195.1855, 293.2584, 305.2965, 291.2452, 333.3282, 277.2657, 349.3214, 307.3107, 335.3431, 319.2764, 111.1291, 365.352, 379.3694, and 295.2801 corresponding to the molecular formula $C_{20}H_{30}O_6$, $C_{17}H_{26}O_3$, $C_{11}H_{14}O_3$, $C_{17}H_{24}O_4$, $C_{19}H_{28}O_3$, $C_{17}H_{22}O_4$, $C_{21}H_{32}O_3$, $C_{17}H_{24}O_3$, $C_{21}H_{32}O_4$, $C_{19}H_{30}O_3$, $C_{21}H_{34}O_3$, $C_{19}H_{26}O_4$, $C_6H_6O_2$, $C_{22}H_{36}O_4$, $C_{23}H_{38}O_4$, and $C_{17}H_{26}O_4$, identified as methyl diacetoxy-[4]-gingerdiol, 6-paradol, zingerone, 6-gingerdione, 8-shogaol, 1-dehydro-6-gingerdione, 10-shogaol, 6-shogaol, 10-gingerdione, 8-paradol, 10-paradol, 1-dehydro-8-gingerdione, catechol, methyl-10-gingerol, 12-gingerol, and 6-gingerol.

***Flavonoid compounds***

01 flavonoid compound was identified based on the RT and m/z observed. The peak 14 showed an ion at m/z 317.151 corresponding to the molecular formula $C_{16}H_{12}O_7$ and identified as rhamnetin.

***Terpenoids***

A total of 05 terpenoids were identified based on the RT and m/z value observed. The peak 4, 48, 55, 59, and 71 corresponding to the molecular formula $C_{10}H_{18}O_2$, $C_{15}H_{26}O$, $C_{10}H_{16}O$, $C_{10}H_{16}O$, $C_{10}H_{14}$, and identified as 1,2-oxidolinalool, elemol, geranial, cymene, and limonene.

***Diarylheptanoid***

A total of 03 diarylheptanoid compounds were identified based on the RT value and m/z value observed. The peak 16, 18, and 28 showed an ion at m/z

363.2636, 345.2535, and 461.3015 corresponding to the molecular formula $C_{20}H_{26}O_6$, $C_{20}H_{24}O_5$, $C_{25}H_{32}O_8$ and identified as 1-(3,4-dihydroxyphenyl)-7-(4-hydroxy-3-methoxyphenyl)-3,5-heptanediol, 5-hydroxy-1-(4-hydroxy-3-methoxyphenyl)-7-(4-hydroxyphenyl)-3-heptanone, and 3,5-diacetoxy-1,7-bis(4-hydroxy-3-methoxyphenyl)heptane.

***Fatty acid***

A total of 03 fatty acid derivatives were present based on the RT and m/z value observed. The peak 34, 81, and 85 showed an ion at m/z 364.4069, 279.3167 and 257.3334 corresponding to the molecular formula $C_{23}H_{41}NO_2$, $C_{18}H_{30}O_2$ and $C_{16}H_{32}O_2$ and identified as oxo-octadecenoic acid, α-linolenic acid and palmitic acid.

***Amino alcohol***

A total of 03 amino alcohol compounds were present based on the RT and m/z value observed. The peak 42, 67, and 93 showed an ion at m/z 330.4229, 228.3177 and 274.3588 corresponding to the molecular formula $C_{20}H_{43}NO_2$, $C_{14}H_{29}NO$ and $C_{16}H_{35}NO_2$ and identified as aminoeicosanediol, halaminol A and aminohexadecanediol.

***Cinnamic acid derivative***

A total of 02 cinnamic acid derivatives were present based on the RT and m/z value observed. The peak 22 and 25 showed an ion at m/z 193.1715 and 165.1388 corresponding to the molecular formula $C_{11}H_{12}O_3$ and $C_9H_8O_3$ and identified as dehydrozingerone, and coumaric acid.

***Other compounds***

Some other compounds such as 01 fatty amide, 01 alkanolamine, 01 co-enzyme Q10, and 01 galactosyl-glycerol derivative compound were present based on the RT and m/z value observed. The peak 46, 42, 45, and 75 showed an ion at m/z 282.3648. 330.4229, 321.2913, and 677.4559 corresponding to the molecular

formula $C_{18}H_{35}NO$, $C_{20}H_{43}NO_2$, $C_{19}H_{28}O_4$, $C_{33}H_{56}O_{14}$ and identified as oleamide, aminoeicosanediol, ubiquinol 10, and gingerglycolipid A.

HR-LCMS analysis of GV6 revealed a rich phytochemical profile, with phenolics being the most abundant class of compounds. In addition to phenolics, GV6 contained flavonoid, terpenoids, diarylheptanoids, fatty acids, amino alcohols, cinnamic acid derivatives, fatty amide, alkanolamine, coenzyme Q10, and galactosyl-glycerol derivatives.

Among the identified compounds, several demonstrated potent anti-amyloidogenic, antioxidant, anti-inflammatory, and neurotrophic activities in earlier studies. For example, flavonoid such as rhamnetin detected in GV6 and is well recognized for its multi-modal neuroprotective effects. These include attenuation of cognitive impairments and inhibition of inflammation and oxidative stress in the hippocampal tissue of traumatic brain injured rat models (Zhang et al., 2015). Study also investigated that rhamnetin significantly decreased the excitotoxicity induced by NMDA during ethanol exposure and showed improved neuroprotective activity (Lutz et al., 2015).

Other phenolic compounds, including 6-paradol, 6-shogaol, 6-gingerol, zingerone, and dehydrozingerone, have shown complementary anti-Alzheimer's effects, such as inhibition of secretase activities, disruption of Aβ fibril formation, suppression of glial activation, and upregulation of neurotrophic factors (Abdallah et al., 2024; Moon et al., 2014; Berntsson et al., 2021; Kim et al., 2018; Emeka et al., 2025).

Additionally, GV6 was found to contain coenzyme Q10, oleamide, cinnamic acid derivatives, cymene, limonene, and α-linolenic acid, all of which contribute to neuroprotection via distinct mechanisms. Coenzyme Q10 improved mitochondrial function, reduced amyloidogenesis, and enhanced BDNF expression (Nawar et al., 2024), while oleamide promoted hippocampal neurogenesis and microglial clearance of Aβ (Ano et al., 2015; Tao et al., 2022). Cinnamic acid promoted lysosomal biogenesis for toxic protein clearance (Chandra et al., 2019), and α-linolenic acid modulated oxidative and inflammatory pathways to protect hippocampal neurons (Tofighi et al., 2021).

Taken together, the metabolite profile of GV6 demonstrates a multi-target therapeutic potential against AD, attributable to the combined presence of phenolics, flavonoid, terpenoids, and other bioactive compounds. These molecules act synergistically by inhibiting Aβ and tau aggregation, reducing oxidative stress and enhancing antioxidant defenses, suppressing neuroinflammation, promoting synaptic plasticity and neurotrophic support and improving clearance of toxic aggregates and supporting mitochondrial/ lysosomal function.

Notably, among the identified metabolites, 6-gingerol deserves special emphasis due to its pharmacological relevance and its role as a marker compound in our previous phytochemical standardization studies using HPLC and HPTLC. As the principal pungent phenolic constituent of ginger, 6-gingerol is not only a reliable quality-control marker for ginger-based extracts but also a multifunctional neuroprotective agent against AD (Moon et al., 2014; Abdallah et al., 2024; Berntsson et al., 2021; Kim et al., 2018; Emeka et al., 2025). The fact that 6-gingerol was consistently detected in GV6 across LC-MS, HPLC, and HPTLC profiling not only validates the robustness of our phytochemical characterization but also underscores its importance as both a chemical marker and a therapeutic lead compound. Its presence, alongside other synergistic metabolites such as shogaols, paradols, zingerone, flavonoid, and phenolic acids, strengthens the neuroprotective portfolio of GV6. This dual significance of 6-gingerol as a quality marker and a potent anti-Alzheimer's molecule reinforces the translational potential of GV6 for standardized, reproducible, and clinically relevant applications in AD management.

Therefore, GV6 can be regarded as a potent anti-Alzheimer's extract with pleiotropic actions targeting multiple pathological hallmarks of AD. Its diverse phytoconstituents act in concert to provide neuroprotection, preserve memory, and mitigate disease progression, making it a promising candidate for further preclinical and clinical evaluation.

### *5.5.2. Acute oral toxicity test*

No mortality or observable toxic effects were noted at the tested dose, indicating a favourable safety profile for GV6 (Table 5.2 and Table 5.3).

**Table 5.2. Impact of GV6 on mortality, b.w., and organ-to-b.w. ratios in female mice during a 14-day observation (n = 6, mean ± SEM)**

| Dose 2000 mg/kg b.w. | |
|---|---|
| Death/mortality | 0/6 |
| b.w. day 0 (g) | 29 ± 2.12 |
| b.w. day 14 (g) | 30 ± 1.41 |
| Liver (%) | 2.23 ± 0.25 |
| Heart (%) | 0.14 ± 0.0017 |
| Spleen (%) | 0.16 ± 0.0019 |
| Kidney (%) | 0.3 ± 0.016 |
| Ovary (%) | 0.0261 ± 0.004 |
| Uterus (%) | 0.15 ± 0.013 |

In the experimental design, the control group served as the reference group.

**Table 5.3. Hematological and biochemical responses in female Swiss albino mice following 14-day GV6 extract administration at 2000 mg/kg b.w. (mean ± SEM, n = 6)**

| Serum parameters | Values | Reference value |
|---|---|---|
| **Haematological parameters** | | |
| Red Blood Cell (RBC) ($\times 10^6$/μL) | 7.28 ± 1.13 | 7.83 ± 0.48 |
| Hemoglobin (g/dL) | 11.74 ± 2.86 | 13.08 ± 0.47 |
| Hematocrit (%) | 40.07 ± 1.30 | 41.15 ± 1.30 |
| Mean Corpuscular Volume (MCV) (fL) | 56.26 ± 2.49 | 53.11 ± 2.04 |
| Mean Corpuscular Hemoglobin | 19.43 ± 2.41 | 16.31 ± 1.42 |

| | | |
|---|---|---|
| (MCH) (pg) | | |
| Mean Corpuscular Haemoglobin Concentration (MCHC) (%) | 30.26 ± 1.35 | 32.71 ± 2.11 |
| Platelets ($10^3$/ $mm^3$) | 1182 ± 82 | 1044 ± 78 |
| White Blood Cell (WBC) ($10^3$/ µL) | 18.4 ± 2.03 | 19.02 ± 1.12 |
| Neutrophils (%) | 17.1 ± 1.18 | 16.32 ± 3.27 |
| Lymphocytes (%) | 87.23 ± 5.93 | 85.29 ± 4.04 |
| Monocytes (%) | 1.02 ± 0.38 | 2.23 ± 1.27 |
| Eosinophils (%) | 0.4 ± 0.26 | 0.62 ± 0.83 |
| Basophils (%) | 0.24 ± 0.71 | 0.38 ± 0.19 |
| **Biochemical parameters** | | |
| Total protein (g/dL) | 5.61 ± 1.12 | 6.71 ± 2.01 |
| Alkaline phosphatase (U/L) | 61.32 ± 4.79 | 59.80 ± 6.04 |
| Aspartate aminotransferase (U/L) | 125.77 ± 4.18 | 122.10 ± 3.6 |
| Alanine aminotransferase (U/L) | 52.84 ± 3.20 | 49.19 ± 3.38 |

### *5.5.3. Effect of GV6 on spatial memory deficits assessed by the Morris water maze test*

The impact of GV6 on spatial learning and memory was evaluated using the Morris water maze test over a five-day training period. As illustrated in Figure 5.4a, animals treated with GV6 showed a progressive reduction in escape latency times compared to the scopolamine-treated group, indicating improved spatial learning across all treatment doses. Notably, GV6 administration led to a significant, dose-dependent increase in the time spent within the target quadrant during the probe trial, in contrast to the scopolamine group [$F(4, 35) = 68.76$, $p < 0.0001$], as shown in Figure 5.4b.

Furthermore, latency to locate the hidden platform was significantly prolonged in the scopolamine group compared to controls [$F(4, 35) = 13.04$, $p < 0.0001$], while GV6 treatment significantly reduced this latency in a dose-dependent manner (Figure 5.4c). Swimming speed, assessed to exclude motor dysfunction, did not differ significantly among the various experimental groups [$F(4, 25) = 0.09492$, $p > 0.05$], as shown in Figure 5.4d.

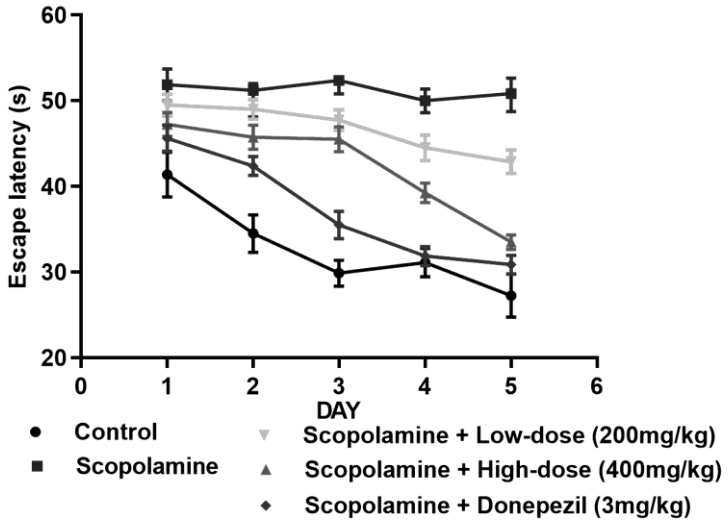


(a)

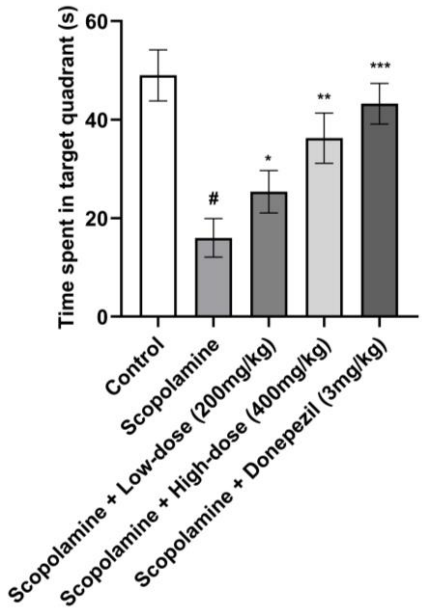


(b)

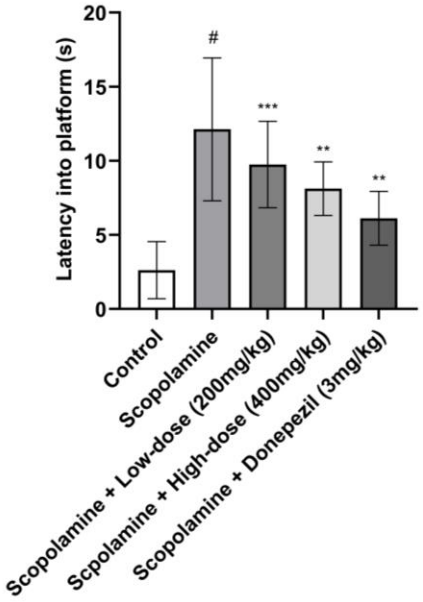


(c)

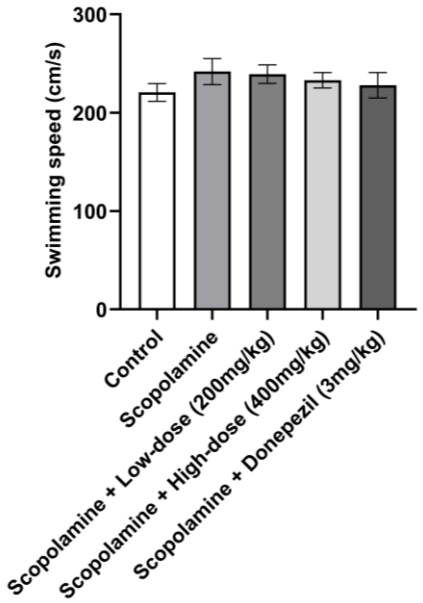


(d)

**Figure 5.4. Evaluation of GV6 effects on cognitive performance using Morris water maze test (a) progressive decline in escape latency over consecutive training days, indicating learning acquisition, (b) mice treated with GV6 spent significantly more time in the target quadrant during the probe trial, suggesting enhanced memory**

**retention, and (c) the latency into platform decreased in the GV6 treated mice compared to scopolamine treated mice whereas, (d) swimming speed remains roughly unchanged during the trial period**

On the sixth day of testing, the platform was removed to assess memory retention during a 60 sec probe trial. As depicted in Figure 5.5a-e, control animals predominantly navigated within the target quadrant, demonstrating intact spatial memory. In contrast, scopolamine-treated mice exhibited disoriented swimming patterns, lacking quadrant preference. GV6-treated animals showed a dose-related increase in time spent within the target quadrant, indicating improved memory retention.

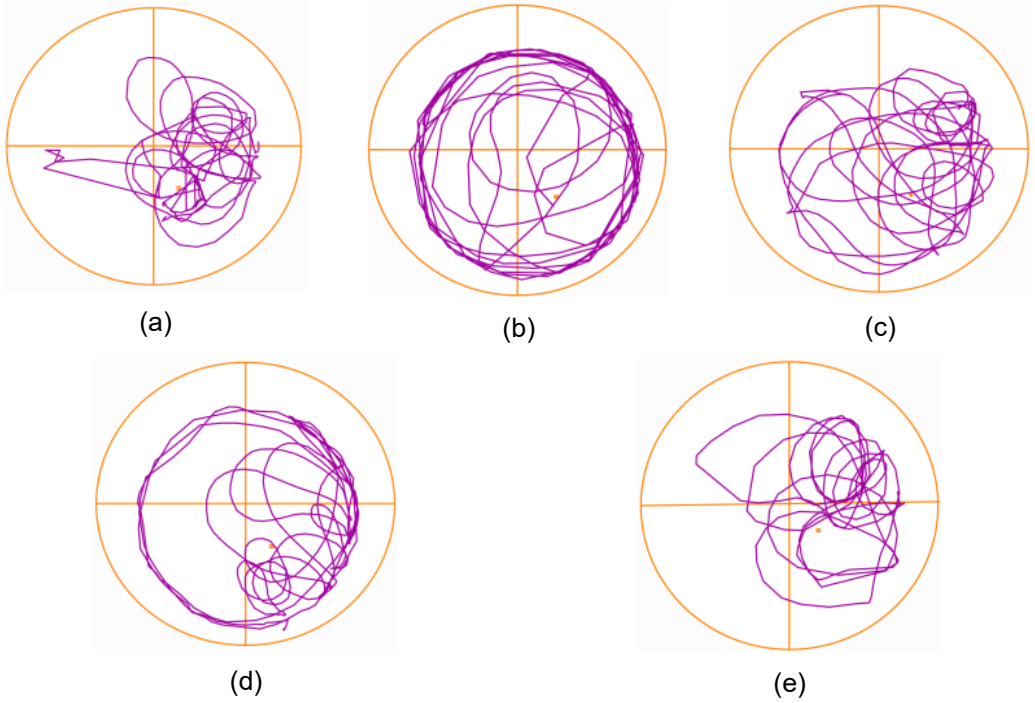


**Figure 5.5. Representative swim paths of mice during the Morris water maze test illustrating the effect of GV6 treatment. The trajectories depict the spatial navigation patterns observed across different experimental groups: (a) control (b) scopolamine (c) scopolamine + GV6 Low-dose (d) scopolamine + GV6 High-dose (e) scopolamine + Donepezil. GV6 administration led to a noticeable reduction in escape latency, indicating improved learning and memory performance during the test phase**

Scopolamine, a known muscarinic receptor antagonist, disrupts cholinergic neurotransmission, thereby impairing memory and learning ability (Gul et al., 2023). In the current study, scopolamine administration led to increased latency in reaching the target zone and reduced time spent in the preferred arm, indicating spatial learning deficits. Morris water maze results revealed that GV6 treated mice showed no significant improvement during the initial days of training; however, by the $4^{th}$ and $5^{th}$ days, notable improvements in spatial memory were observed. Mice receiving GV6 spent more time in the target quadrant and exhibited decreased latency in locating the hidden platform compared to the scopolamine group.

### *5.5.4. Effect of GV6 on spatial and short-term memory in the Y-maze test*

The Y-maze test was employed to evaluate the effects of GV6 on spatial and short-term memory performance. As shown in Figure 5.6, scopolamine administration led to a significant reduction in the percentage of spontaneous alternations compared to the control group [$F(4, 35) = 20.63$, $p < 0.0001$], indicating notable impairment in spatial and working memory. Treatment with GV6 markedly reversed this deficit by significantly increasing the spontaneous alternation percentage relative to the scopolamine-treated group, suggesting an improvement in cognitive performance. The effect was found to be dose-dependent, highlighting the memory-enhancing potential of GV6.

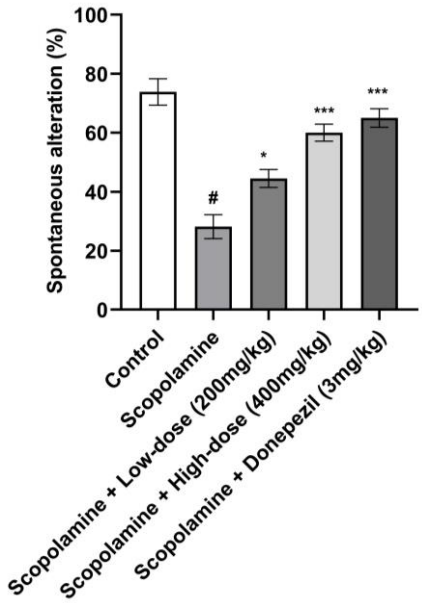


**Figure 5.6. Assessment of GV6 on spatial and short-term memory using the Y-maze test (a) treatment with GV6 resulted in a significant increase in the percentage of spontaneous alternation behavior**

The Y-maze performance demonstrated improved short-term memory in the GV6 treated group, as indicated by an increased percentage of spontaneous alternation. These results are in line with earlier reports where 6-gingerol treatment improved spatial and working memory in similar models (Kim et al., 2018; Huh et al., 2018).

### *5.5.5. Effect of GV6 on long-term and cognitive memory impairment in the NOR test*

The NOR test was used to assess the impact of GV6 on recognition memory. As illustrated in Figure 5.7a, mice treated with scopolamine exhibited a significant reduction in the percentage of time spent exploring the novel object compared to the control group [$F(4, 25) = 380.0$, $p < 0.0001$], indicating impaired long-term and recognition memory. Concurrently, as shown in Figure 5.7b, the scopolamine group showed a marked increase in exploration time toward the familiar object [$F(4, 25) = 223.8$, $p < 0.0001$], further supporting cognitive dysfunction.

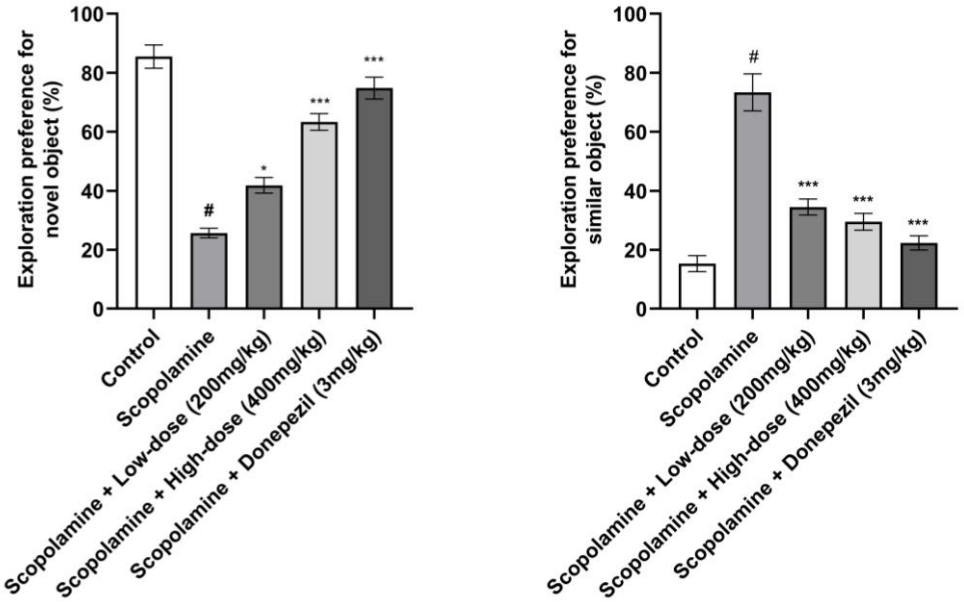


(a) (b)

**Figure 5.7. Evaluation of GV6 on cognitive deficits using the NOR test (a) GV6-treated mice demonstrated a higher percentage of exploration time for the novel object (b) exploration of the familiar object was reduced in the GV6 groups compared to scopolamine-treated mice**

Administration of GV6 significantly restored recognition memory in a dose-dependent manner, as evidenced by an increase in novel object exploration and a corresponding decrease in familiar object preference when compared to the scopolamine-treated group. These findings suggest that GV6 effectively mitigates memory impairments induced by scopolamine.

The NOR test further supported the cognitive enhancing potential of GV6, as treated mice showed increased preference for the novel object over the familiar one, suggesting enhanced recognition memory (Sener et al., 2022). This observation aligns with findings by Lim et al. (2014), where ginger-derived compounds improved hippocampal dependent cognitive functions in scopolamine treated mice.

### *5.5.6. Effect of GV6 on cholinergic neurotransmission*

To evaluate the influence of GV6 on cholinergic function, the activities of AChE and BChE, along with ACh levels, were assessed in brain tissues from control, scopolamine, GV6, and donepezil treated groups. As shown in Figure 5.8a and 5.8b, scopolamine administration significantly elevated AChE and BChE activities compared to the control group [$F(4, 25) = 81.80$, $p < 0.0001$ for AChE; $F(4, 25) = 58.19$, $p < 0.0001$ for BChE], indicating cholinergic dysfunction. GV6 treatment resulted in a dose dependent suppression of both AChE and BChE enzymatic activities, suggesting a protective effect on cholinergic signaling. Furthermore, as illustrated in Figure 5.8c, scopolamine treated mice exhibited a substantial reduction in brain ACh content [$F(4, 25) = 86.60$, $p < 0.0001$] relative to controls. GV6 administration at doses of 200 and 400 mg/kg b.w. significantly restored ACh levels. These findings collectively indicate that GV6 has a beneficial modulatory effect on cholinergic neurotransmission, likely contributing to its memory-enhancing properties.

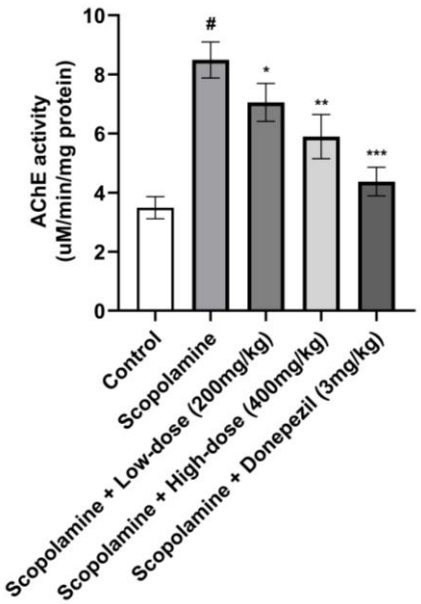


(a)

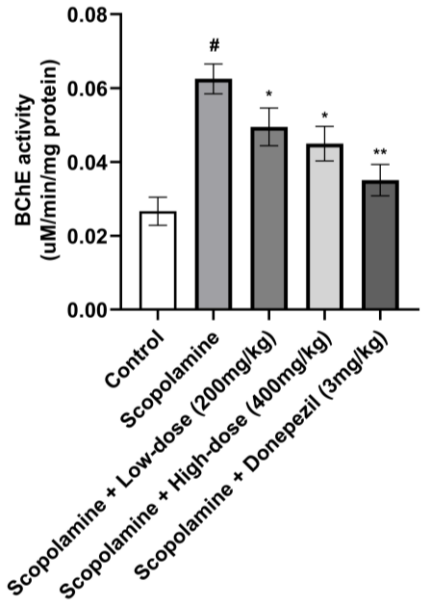


(b)

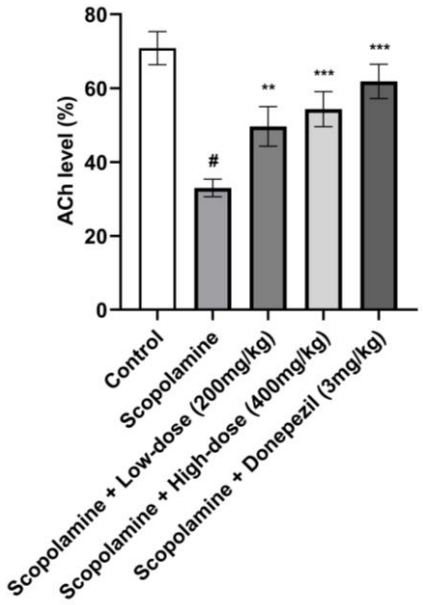


(c)

**Figure 5.8. Impact of GV6 on the cholinergic system in the brains of experimental mice (a) AChE activity (b) BChE activity (c) ACh level**

Biochemical analyses showed that GV6 treatment significantly restored cholinergic function by lowering elevated AChE and BChE activity and increasing ACh levels in the brain. These results are consistent with earlier studies reporting the capacity of ginger extract to inhibit cholinesterase enzymes and boost ACh concentration (Joshi and Parle, 2006).

### *5.5.7. Effect of GV6 on oxidative stress markers*

This study highlights the antioxidant potential of GV6 in mitigating oxidative stress in the brain, as evidenced by its modulatory effects on MDA, SOD, GSH, CAT, and NOx levels. As shown in Figure 5.9a, scopolamine administration led to a significant elevation in MDA levels [$F(4, 25) = 98.87$, $p < 0.0001$] compared to the control group, indicating enhanced lipid peroxidation. Treatment with GV6 at both 200 and 400 mg/kg doses markedly reduced MDA levels relative to the scopolamine group. Figure 5.9b reveals that scopolamine significantly suppressed SOD activity [$F(4, 25) = 67.26$, $p < 0.0001$]. However, GV6 treatment

effectively restored SOD activity in a dose dependent manner. Moreover, GV6 administration counteracted the scopolamine induced decline in both GSH and CAT activities [$F(4, 25) = 30.53$, $p < 0.0001$ and $F(4, 25) = 89.49$, $p < 0.0001$, respectively], particularly at the 400 mg/kg dose (Figure 5.9c and 5.9d). Additionally, GV6 significantly reduced the elevated $NO_x$ levels caused by scopolamine [$F(4, 25) = 53.27$, $p < 0.0001$], as shown in Figure 5.9e. While the higher dose (400 mg/kg) showed significant improvement in GSH, CAT, and $NO_x$ levels, the 200 mg/kg dose did not produce statistically significant changes compared to the scopolamine treated group. These results suggest that GV6 confers neuroprotection by enhancing the brain's antioxidant defense mechanisms and reducing oxidative damage.

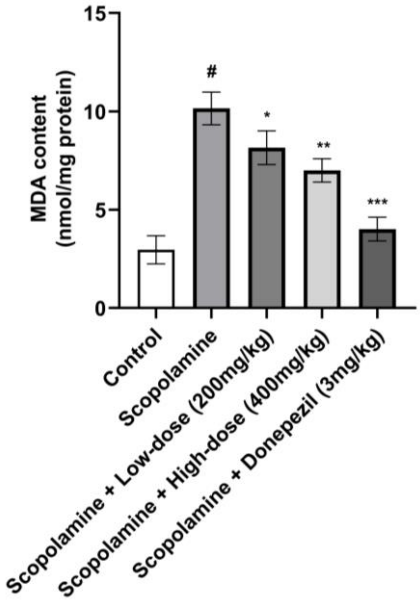


(a)

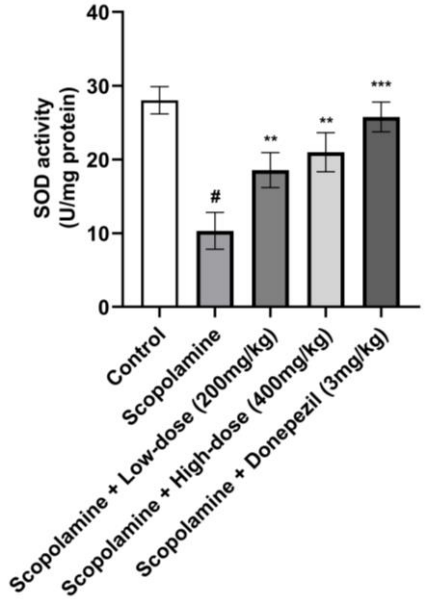


(b)

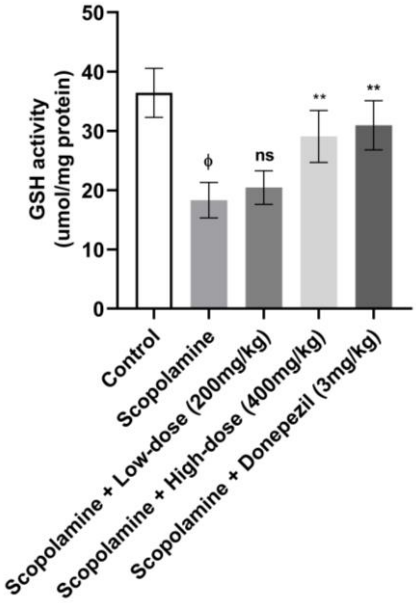


(c)

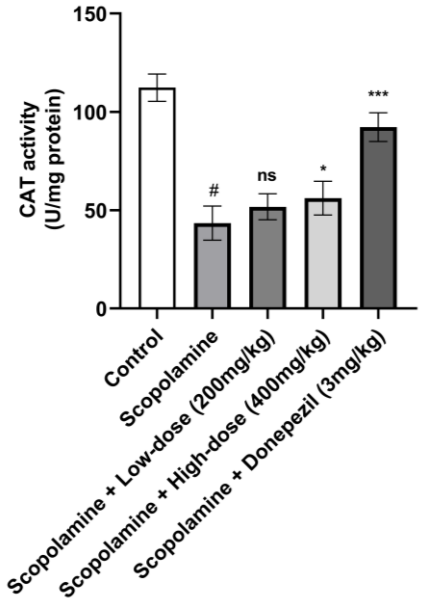


(d)

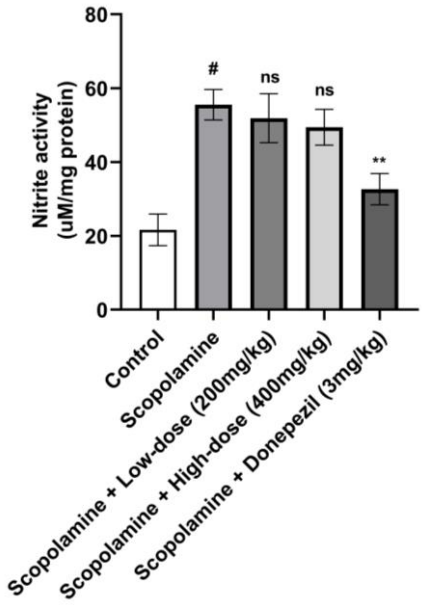


(e)

**Figure 5.9. Effect of GV6 on oxidative stress markers in the brains of experimental mice (a) MDA level (b) SOD activity (c) GSH activity (d) CAT activity (e) Nitrite activity**

Since oxidative stress is a key contributor to neurodegeneration, the antioxidant profile was also assessed. GV6 reduced MDA levels, indicating decreased lipid peroxidation, and increased levels of key antioxidant enzymes SOD, GSH, and CAT, along with normalization of NOx levels. These improvements suggest enhanced oxidative defense, reducing the risk of ROS induced neuronal damage (Simunkova et al., 2019; Rao et al., 2021; Youssef et al., 2018). Similar antioxidant effects have been previously attributed to 6-gingerol in cerebral ischemic models (Kongsui and Jittiwat, 2023).

### *5.5.8. Effect of GV6 on TNF-α levels*

Figure 5.10. illustrates the impact of GV6 on TNF-α, a pro-inflammatory cytokine. Scopolamine administration significantly elevated TNF-α levels in the brain tissue compared to the control group [$F(4, 25) = 68.67$, $p < 0.0001$], indicating pronounced neuroinflammation. Notably, treatment with GV6 at doses of 200 and 400 mg/kg b.w. markedly attenuated the scopolamine-induced rise in TNF-α, demonstrating the anti-inflammatory potential of the extract.

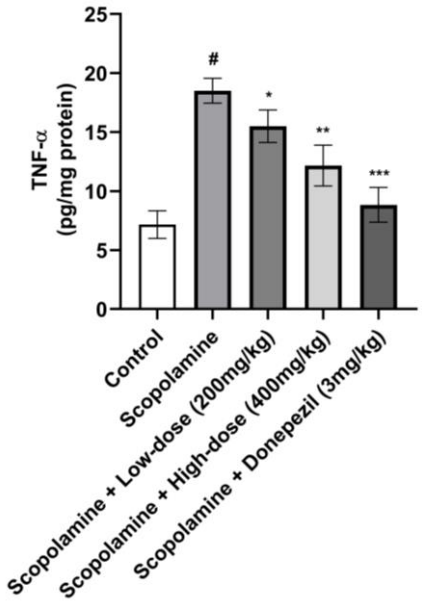


**Figure 5.10. Effect of GV6 on TNF-α levels in the brains of experimental mice**

Neuroinflammatory processes, particularly the elevation of pro-inflammatory cytokines like TNF-α, are known to exacerbate cognitive decline in AD and related models (Roy et al., 2023). Scopolamine administration significantly increased TNF-α levels, whereas GV6 treatment markedly reduced its concentration, indicating an anti-inflammatory effect. This aligns with Tripathi et al. (2007), who demonstrated the anti-inflammatory activity of 6-gingerol in LPS activated macrophages.

### *5.5.9. Histopathological observations*

As presented in Figure 5.11a-e, histological evaluation revealed that scopolamine administration resulted in notable neurodegenerative changes in the hippocampal region. These alterations included neuronal shrinkage, loss of cellular architecture, pyknotic nuclei, karyolysis, and evidence of spongiosis characterized by vacuolar formation. In contrast, treatment with GV6 notably preserved hippocampal integrity by maintaining neuronal density and restoring the normal histoarchitecture. These findings indicate that GV6 exerts a neuroprotective effect against scopolamine-induced histopathological damage.

Histopathological examination of hippocampal tissue further corroborated the neuroprotective effect of GV6. While scopolamine treated brains exhibited cellular shrinkage, neuronal loss, and structural disorganization, GV6 administration preserved neuronal integrity, restored cell density, and maintained normal histo-architecture. These observations support the role of the GV6 extract in mitigating structural damage associated with cognitive deficits (Chen et al., 2022b; Maurer and Williams, 2017).

Collectively, these findings highlight the multifaceted neuroprotective potential of 6-gingerol rich GV6 extract. It enhances cognitive function by restoring cholinergic balance, reducing oxidative stress, suppressing neuroinflammation, and preserving neuronal morphology. The study design, where GV6 was administered both prior to and during scopolamine exposure, simulates a preventive approach, underscoring its relevance in early intervention strategies

for neurodegenerative diseases like AD. This aligns with current therapeutic goals aimed at delaying the progression of cognitive impairments.

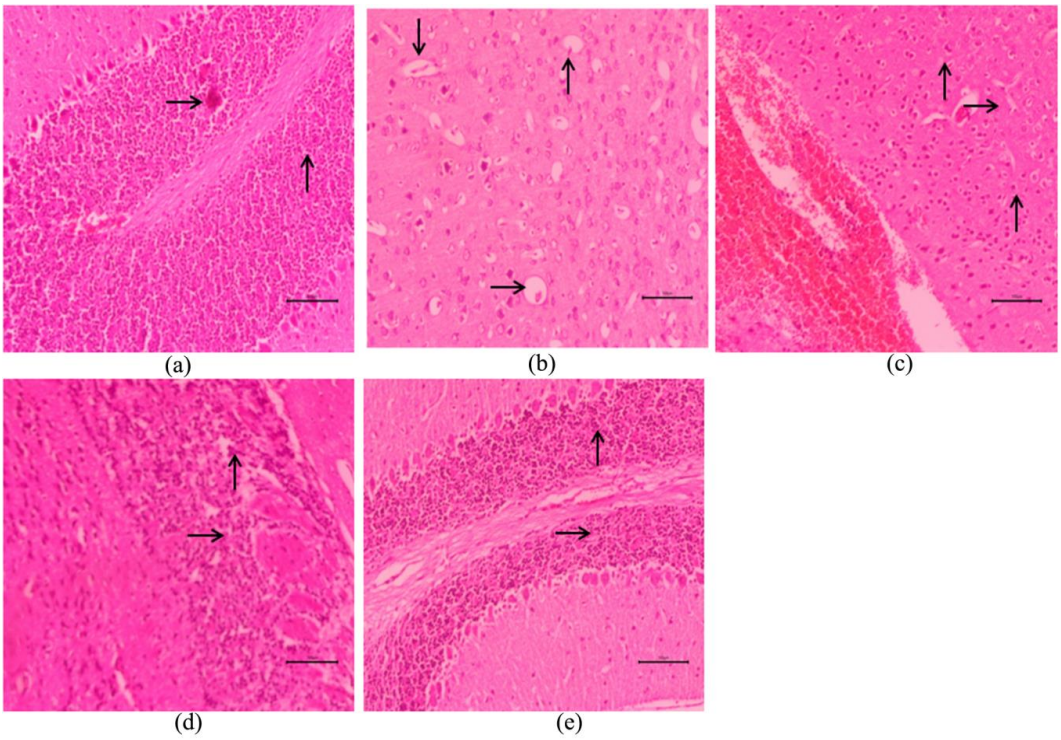


**Figure 5.11. Histopathological analysis of brain sections from experimental mice highlighting neuronal morphological changes (a) black arrows indicate intact and healthy neuronal architecture in the normal control group (b) the scopolamine-treated group shows pronounced neuronal degeneration, including cell loss, shrinkage, and spongiosis (c) GV6 treatment exhibits marked restoration of neuronal structure, with cells appearing closer to normal morphology (d) Similar neuroprotective effects are observed in the donepezil-treated group, as indicated by the black arrows**

### *5.5.10. Molecular docking analysis*

Crystal structures of human AChE (AChE, PDB ID: 4M0E) and BChE (BChE, PDB ID: 5K5E), both co-crystallized with ligands, were obtained from the Protein Data Bank and used as receptor macromolecules for docking studies with 6-gingerol and galantamine. The docking analysis revealed negative binding energies (Kcal/mol), suggesting that both compounds could spontaneously

interact with the respective protein targets. Against AChE, 6-gingerol and galantamine exhibited docking scores of -7.5 and -7.3, respectively (Table 5.4).

**Table 5.4. Molecular docking outcomes of 6-gingerol and galantamine with AChE (PDB ID: 4M0E) and BChE (PDB ID: 5K5E), showing binding affinity scores, hydrogen bonds, π-interactions, and key active site residues involved in ligand binding**

| Compound | Docking score | Conventional - H Bond | π - interaction | Active site pocket residues |
|---|---|---|---|---|
| AChE | | | | |
| 6-gingerol | -7.5 | PHE295, ARG296(2), TYR72(2) | TRP286(2), TYR341, TYR337, PHE338, PHE297 | PHE295, ARG296, TYR72, TRP286, TYR341, TYR337, PHE338, PHE297, LEU289, SER293, THR75, VAL294, TYR124 |
| Galantamine | -7.3 | TYR72(3) | TRP286(2) | TYR72, TRP286, LEU76, THR75, ASP74, SER293, TYR341 |
| BChE | | | | |
| 6-gingerol | -7.3 | GLU197, TYR128, ASP70, TYR332 | HIS438, PRO285, TYR332(2), TRP82 | GLU197, TYR128, ASP70, TYR332, HIS438, PRO285, TRP82, ILE442, GLY439, SER79, GLY121, GLY115, TYR114 |
| Galantamine | -8.5 | TRP82 | HIS438, TRP82(3), ALA328 | TRP82, HIS438, TRP82, ALA328, GLY116, ILE442, GLY439, GLU197, TYR440, MET437, TRP430, |

| | | | | |
|---|---|---|---|---|
| | | | | GLY78, TYR332, SER79, ASP70, THR120 |

These ligands established multiple hydrogen bonds with active site residues, in addition to several π-type interactions. The key amino acids involved included TYR72, TRP286, TYR341, THR75, and SER293 (Figure 5.12).

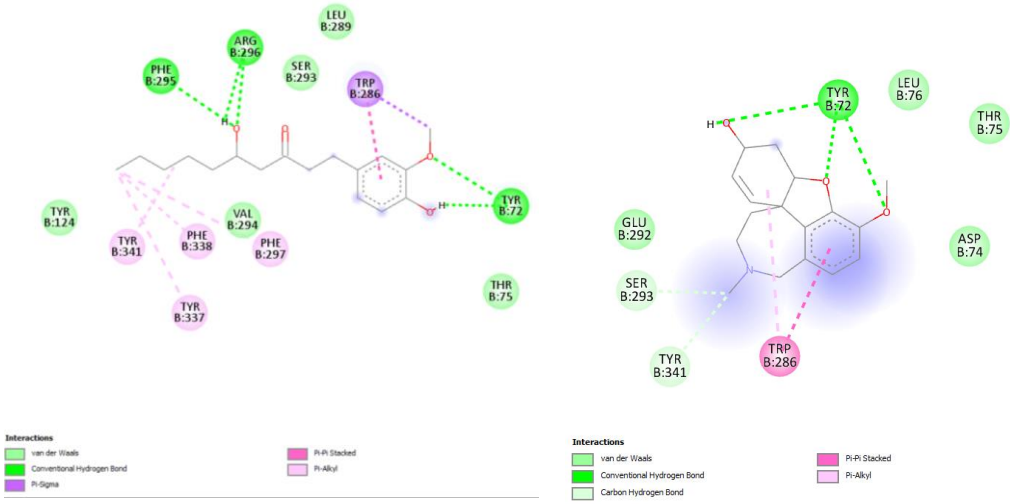


(a) (b)

**Figure 5.12. 2D depiction showing interactions of (a) 6-gingerol and (b) galanthamine with AChE (PDB ID: 4M0E)**

Similarly, favorable interactions were also observed with BChE, where galantamine and 6-gingerol showed binding energies of -8.5 and -7.3, respectively. In this case, the ligands engaged in hydrogen bonding as well as π–π and π–H interactions with residues located in the active site. The most significant interacting residues were GLU197, ASP70, TYR332, HIS438, TRP82, ILE442, GLY439, and SER79 (Figure 5.13).

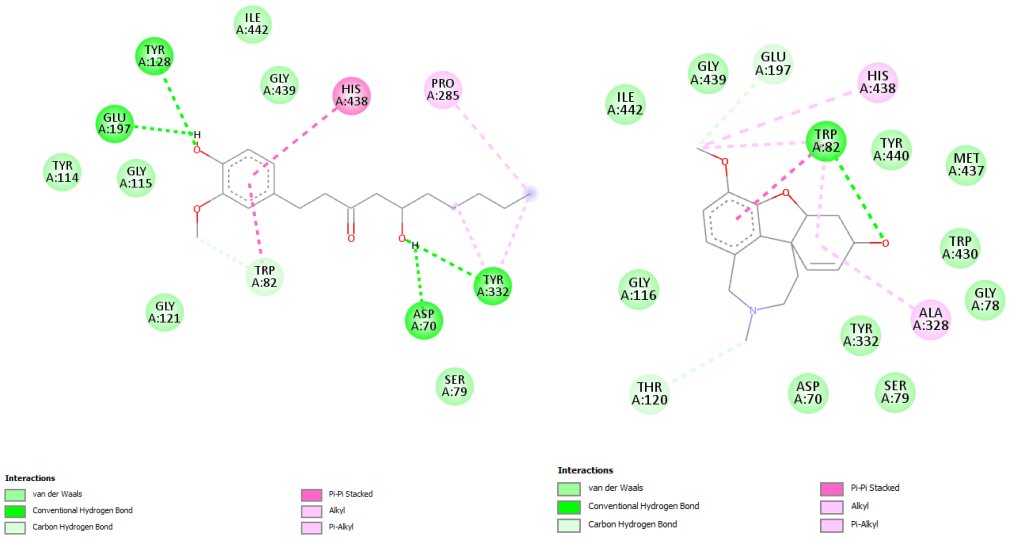


(a) (b)

**Figure 5.13. 2D depiction showing interactions of (a) 6-gingerol and (b) galantamine with BChE (PDB ID: 5K5E)**

The molecular docking studies performed against the catalytic sites of the selected cholinesterase enzymes demonstrated that both galantamine (reference standard) and 6-gingerol exhibited favorable binding interactions. Among them, galantamine, a well-established cholinesterase inhibitor, displayed the most stable affinity towards BChE. In the case of AChE, key amino acid residues including TYR72, TRP286, THR75, SER293, and TYR341 were found to play critical roles in stabilizing ligand binding within the active pocket. For BChE, significant contacts were observed with residues such as TRP82, ILE442, GLY439, and GLY115, suggesting their importance in ligand recognition and stabilization. Taken together, these findings provide insight into the possible mechanistic basis of action, supporting the hypothesis that GV6 possesses multitargeted potential against AD by modulating cholinesterase activity.

## 5.6. Conclusion

Among the identified metabolites, 6-gingerol deserves special emphasis due to its pharmacological relevance and its role as a marker compound in our previous

phytochemical standardization studies using HPLC and HPTLC. As the principal pungent phenolic constituent of ginger, 6-gingerol is not only a reliable quality-control marker for ginger-based extracts but also a multifunctional neuroprotective agent against AD. The fact that 6-gingerol was consistently detected in GV6 across LC-MS, HPLC, and HPTLC profiling not only validates the robustness of our phytochemical characterization but also underscores its importance as both a chemical marker and a therapeutic lead compound. Its presence, alongside other synergistic metabolites such as shogaols, paradols, zingerone, flavonoids, and phenolic acids, strengthens the neuroprotective portfolio of GV6. This dual significance of 6-gingerol as a quality marker and a potent anti-Alzheimer's molecule reinforces the translational potential of GV6 for standardized, reproducible, and clinically relevant applications in AD management.

The present findings support the preclinical neuroprotective potential of GV6 in alleviating AD-related symptoms. This effect was demonstrated by the attenuation of scopolamine-induced cognitive deficits, as reflected in behavioral assessments, enhanced cholinergic activity in the brain, antioxidant efficacy, anti-inflammatory responses, and histopathological improvements. Furthermore, in-silico molecular docking revealed the strong affinity and selectivity of 6-gingerol toward cholinergic enzymes. Considering the diverse biological activities of plant-derived secondary metabolites, it may be inferred that herbs rich in polyphenols are promising candidates for preventing neurodegeneration. Accordingly, ginger from Northeast India, noted for its high sensorial qualities, could serve as a valuable source of bioactive constituents with the potential to be developed into nutraceuticals for managing AD-like symptoms and associated neurotoxicity.

## Publications

### Paper published

**Ghosh, S.**, Das, B., Jana, S., Singh, K.O., Sharma, N., Mukherjee, P.K., Haldar, P.K., 2025. Mechanistic insight into neuroprotective effect of standardized ginger chemo varieties from Manipur, India in scopolamine induced learning and memory impaired mice. Metabolic Brain Disease 40, 101, 1-17. https://doi.org/10.1007/s11011-025-01535-8.

# Chapter 6

# Summary and conclusion

6.1 Summary

6.2 Conclusion

## 6.1. Summary

The present work comprehensively explored the significance of chemo-variety of *Zingiber officinale* Roscoe (ginger) from multiple perspectives, combining the phytochemical, and experimental evidence to highlight its therapeutic potential, particularly in the context of neurodegenerative disease such as AD. The chemo-diversity of ginger represents one of its most defining attributes, making it both a valuable culinary spice and a medicinal plant of global importance. With an overview of Alzheimer's pathology and herbal approaches, the work progressed through an ethnobotanical and pharmacological analysis of ginger, culminating in experimental investigations on its phytochemical diversity and in-vitro cholinesterase inhibitory potential. Collectively, the chapters establish that the ginger sample GV6 collected from Lopung village (25◦02'16.4"N; 94◦18'57.5"E) as a promising medicinal plant in the point of view of modern scientific validation.

The chapter 1 focused on AD, providing an overview of its global epidemiology, pathophysiological mechanisms, and current treatment strategies. The discussion highlighted the role of oxidative stress, Aβ aggregation, tau hyperphosphorylation and cholinergic dysfunction in disease progression. The chapter also reviewed the role of herbal medicine and bioactive phytochemicals, underscoring their neuroprotective effects through antioxidant, anti-inflammatory and cholinesterase inhibitory activities. Overall, the chapter provided basis for further exploring ginger as a possible medicinal resource.

Chapter 2 explores the chemo-diversity of ginger, focusing on its phytochemical profile and in-vitro anti-Alzheimer's potential. The chapter begins with a taxonomical study, botanical description, and overview of different ginger varieties, followed by traditional medicinal uses across different cultures. The phytochemical section highlights essential bioactive compounds, particularly phenolic acids, flavonoids, gingerols, shogaols, and other metabolites responsible for the therapeutic effects of ginger.

Chapter 3 outlines the scope and research plan of the study, highlighting its specific objectives. A structured framework was developed in alignment with the objectives, and the chapter further presents a detailed description of the experiments carried out.

Chapter 4 presents the collection of ginger samples from different locations, authentication, extraction and investigation of the phytochemical properties. To evaluate the properties, nine ginger samples from different regions of Manipur were collected, authenticated, and extracted using hydroalcoholic solvents. Phytochemical profiling involved quantifying TPC, TFC and antioxidant activities through DPPH, hydroxyl, and ABTS radical scavenging assays. Advanced chromatographic methods such as HPLC and HPTLC were employed to determine 6-gingerol content, revealing notable variability among the samples. Pearson's correlation analysis showed strong positive relationships between phenolic content, 6-gingerol content, and antioxidant potential. Further, the in-vitro cholinesterase inhibition assay demonstrated the neuroprotective potential of the ginger extracts. Among the samples, GV6 exhibited the highest phenolic content, antioxidant activity, 6-gingerol content, and strongest AChE and BChE inhibition. Collectively, the chapter highlights the importance of robust phytochemical characterization and standardization of herbal medicine to ensure quality, safety, and efficacy.

Chapter 5 presents the metabolite profiling, in-vivo neuroprotective activity, and molecular docking studies of the selected potent ginger sample, GV6. The sample was chosen for its high 6-gingerol content and strong inhibitory activity against AChE and BChE. LC-MS analysis identified 39 metabolites in GV6, including phenolics, flavonoid, terpenoids, diarylheptanoids, fatty acids, and amino alcohols. Among these, 12 compounds were reported with known anti-Alzheimer's properties. Key metabolites such as, 6-gingerol, 6-paradol, 6-shogaol, α-linolenic acid, oleamide, cymene, limonene, ubiquinol 10, zingerone, coumaric acid, dehydrozingerone, rhamnetin were highlighted for their

antioxidant, anti-Aβ, anti-inflammatory, and neurotrophic activities. GV6 was evaluated in a scopolamine-induced memory impairment model in Swiss albino mice. Acute oral toxicity test showed no adverse effects at 2000 mg/kg, confirming a favourable safety profile. Behavioural tests, including Morris water maze, Y-maze, and NOR test demonstrated that GV6 significantly improved spatial learning, short-term, and recognition memory in a dose-dependent manner. Biochemical analysis revealed that GV6 reduced AChE and BChE activities, restored ACh levels, enhanced antioxidant defense, and lowered TNF-α levels. Histopathological studies confirmed that GV6 preserved hippocampal neuronal structure against scopolamine-induced damaged. Docking studies with AChE and BChE demonstrated strong binding affinities of 6-gingerol, comparable to the reference drug galantamine. The interactions involved multiple hydrogen bonds and π-interactions with key catalytic residues, supporting its cholinesterase inhibitory activity. Collectively, the chapter concludes that GV6, rich in 6-gingerol and other synergistic phytochemicals, exhibits potent multi-target anti-Alzheimer's activity.

## 6.2. Conclusion

The present study highlights the significance of the chemo-diversity of *Zingiber officinale* Roscoe (ginger), demonstrating its potential as a multi-target therapeutic resource for the management of AD. By integrating phytochemical characterization, experimental validation, and biological assessments, the work establishes that the variability in chemical composition of ginger plays a pivotal role in its pharmacological efficacy. Among the evaluated samples, GV6 emerged as a particularly promising variety, enriched with bioactive metabolites such as 6-gingerol, phenolic and other compounds that collectively contribute to its strong antioxidant, anti-inflammatory, cholinesterase inhibitory, and neuroprotective effects. The findings confirm the global importance of ginger as both culinary spice and a medicinal plant, while also providing modern scientific validation for its ethnomedicinal relevance. Overall, the study underscores the therapeutic promise of ginger, particularly GV6, as a safe and effective candidate for further

research and development in the prevention and management of complex neurodegenerative disorders such as AD.

# Chapter 7

# References

Abdallah, H.M., El-Halawany, A.M., El-Sayed, N.S., El-Dine, R.S., 2024. 6-paradol modulates the amyloidogenic pathway and cognitive decline in a streptozotocin mouse model of sporadic Alzheimer's disease; in-vivo and in silico studies. Egypt. J. Chem. 67, 105-114.

Adair, T., Temple, J., Anstey, K.J., Lopez, A.D. 2022. Is the rise in reported dementia mortality real? Analysis of multiple-cause-of-death data for Australia and the United States. Am. J. Epidemiol. 191, 1270-1279.

Adewale, A., Ifeoluwa, A.P., Olusoji, O.A., Bukunmi, A.A., Simeon, O.O., 2021. Historical, botanical and medicinal perspectives on ginger (Zingiber officinale). J. Complement. Altern. Med. Res. 15, 44-67.

Adsersen, A., Gauguin, B., Gudiksen, L., Jager, K.A., 2006. Screening of plants used in Danish folk medicine to treat memory dysfunction for acetylcholinesterase inhibitory activity. J. Ethnopharmacol. 104, 418-422.

Agarwal, M., Alam, M.R., Haider, M.K., Malik, M.Z., Kim, D.K., 2020. Alzheimer's disease: An overview of major hypotheses and therapeutic options in nanotechnology. Nanomaterials (Basel). 11, 59.

Ahmad, H., Ahmad, S., Khan, S., Shahzad, S., Ali, M., Tahir, M.N., Shaheen, F., Ahmad, M., 2017. Isolation, crystal structure determination and cholinesterase inhibitory potential of isotalatizidine hydrate from Delphinium denudatum. Pharm. Biol. 55, 680-686.

Ahmad, H., Ahmad, S., Shah, S.A.A., Khan, H.U., Khan, F.A., Ali, M., Latif, A., Shaheen, F., Ahmad, M., 2018. Selective dual cholinesterase inhibitors from Aconitum leave. J. Asian Nat. Prod. Res. 20, 172-181.

Ahmad, M., Tahir, M., Hong, Z., Zia, M.A., Rafeeq, H., Ahmad, M.S., Rehman, S.U., Sun, J., 2025. Plant and marine-derived natural products: Sustainable pathways for future drug discovery and therapeutic development. Front. Pharmacol. 15, 1497668.

Ahmad, S., Ullah, F., Ayaz, M., Sadiq, A., Imran, M., 2015. Antioxidant and anticholinesterase investigations of Rumex hastatus D. Don: Potential effectiveness in oxidative stress and neurological disorders. Biol. Res. 48, 20.

Ahmad, W., Ahmad, B., Ahmad, M., Zafar, I., Nisar, M., Ahmad, M., 2003. In vitro inhibition of acetylcholinesterase, butyrylcholinesterase and lipoxygenase by crude extract of Myricaria elegans Royle. J. Biol. Sci. 3, 1046–1049.

Ahmed, A.A., Jogdand, S., 2021. Medicinal properties of Zingiber officinale. J. Pharm. Res. Int. 33, 3341-3347.

Ahmed, H.H., Salem, A.M., Sabry, G.M., Husein, A.A., Kotob, S.E., 2013. Possible therapeutic uses of Salvia triloba and Piper nigrum in Alzheimer's disease-induced rats. J. Med. Food.16, 437-446.

Aissi, O., Boussaid, M., Messaoud, C., 2016. Essential oil composition in natural populations of Pistacia lentiscus L. from Tunisia: Effect of ecological factors and incidence on antioxidant and antiacetylcholinesterase activities. Ind. Crops Prod. 91, 56-65.

Ajith, T.A., Aswathy, M.S., Hema, U., 2008. Protective effect of Zingiber officinale roscoe against anticancer drug doxorubicin-induced acute nephrotoxicity. Food Chem. Toxicol. 46, 3178-3181.

Ali, M.Y., Jung, H.A., Choi, J.S., 2015. Anti-diabetic and anti-Alzheimer's disease activities of Angelica decursiva. Arch. Pharmacal. Res. 38, 2216-2227.

ALNasser, M.N., Alboraiy, G.M., Alsowig, E.M., Alqattan, F.M., 2025. Cholinesterase inhibitors from plants and their potential in Alzheimer's treatment: Systematic review. Brain Sci. 15, 215.

Alqasoumi, S.I., 2009. Quantification of 6-gingerol in Zingiber officinale extract, ginger-containing dietary supplements, teas and commercial creams by validated HPTLC densitometry. FABAD J. Pharm. Sci. 34, 33-42.

Andersen, K., Nielsen, H., Lolk, A., Andersen, J., Becker, I., Kragh-Sorensen, P., 1999. Incidence of very mild to severe dementia and Alzheimer's disease in Denmark: The Odense study. Neurology. 52, 85-90.

Andrade, M.T., Lima, J.A., Pinto, A.C., Rezende, C.M., Carvalho, M.P., Epifanio, R.A., 2005. Indole alkaloids from Tabernaemontana australis (Muell. Arg) Miers that inhibit acetylcholinesterase enzyme. Bioorg. Med. Chem. 13, 4092-4095.

Andrade-Guerrero, J., Santiago-Balmaseda, A., Jeronimo-Aguilar, P., Vargas-Rodríguez, I., Cadena-Suárez, A.R., Sánchez-Garibay, C., Pozo-Molina, G., Méndez-Catalá, C.F., Cardenas-Aguayo, M.D., Diaz-Cintra, S., Pacheco-Herrero, M., Luna-Muñoz, J., Soto-Rojas, L.O., 2023. Alzheimer's disease: An updated overview of its genetics. Int. J. Mol. Sci. 24, 1-23.

Andrews, S.J., Fulton-Howard, B., Goate, A., 2020. Interpretation of risk loci from genome-wide association studies of Alzheimer’s disease. Lancet Neurol. 19, 326-335.

Ano, Y., Ozawa, M., Kutsukake, T., Sugiyama, S., Uchida, K., Yoshida, A., Nakayama, H., 2015. Preventive effects of a fermented dairy product against Alzheimer's disease and identification of a novel oleamide with enhanced microglial phagocytosis and anti-inflammatory activity. PLoS One. 10, e0118512.

Ansari, F.R., Chodhary, K.A., Ahad, M., 2021. A review on ginger (Zingiber officinale Rosc) with Unani perspective and modern pharmacology. J. Med. Plants Stud. 9, 101-104.

Ayaz, M., Ullah, F., Sadiq, A., Kim, M. O., & Ali, T., 2019. Editorial: natural products-based drugs: potential therapeutics against alzheimer's disease and other neurological disorders. Front. Pharmacol. 10, 1417.

Babalola, K.T., Oyebanjo, O., Adekoya, V.A., Adeniyi, I.A., Ajayi, A.M., Ona sanwo, S.A., 2023. Protective effect of methanol leaf extract of Cnidoscolus aconitifolius against lipopolysaccharides-induced cortico-hippocampal neuroinfammation, oxidative stress and memory impairment. Adv. Tradit. Med. 23, 145-155.

Bachman, D.L., Wolf, P.A., Linn, R.T., Knoefel, J.E., Cobb, J.L., Belanger, A.J., White, L.R., D'Agostino, R.B., 1993. Incidence of dementia and probable Alzheimer's disease in a general population: The Framingham study. Neurology. 43, 515-519.

Bae, D., Kim, Y., Kim, J., Kim, Y., Oh, K., Jun, W., Kim, S., 2014. Neuroprotective effects of Eriobotrya japonica and Salvia Miltiorrhiza Bunge in in vitro and in vivo models. Anim. Cells Syst. 18, 119 134.

Bahrani, H., Mohamad, J., Paydar, M., Rothan, H.A., 2014. Isolation and characterisation of acetylcholinesterase inhibitors from Aquilaria subintegra for the treatment of Alzheimer's disease (AD). Curr. Alzheimer Res. 11, 206-214.

Bailey-Shaw, Y.A., Williams, L.A.D., Junor, G.A.O., Green, C.E., Hibbert, S.L., Salmon, C.N.A., Smith, A.M., 2008 Changes in the contents of oleoresin and pungent bioactive principles of Jamaican ginger (Zingiber officinale roscoe.) during maturation. J. Agric. Food Chem. 56, 5564-5571.

Bakthir, H., Ali, N.A., Arnold, N., Teichert, A., Wessjohann, L., 2011. Anticholinesterase activity of endemic plant extracts from Soqotra. Afr. J. Tradit. Complement. Altern. Med. 8, 296-299.

Bayona, L.M., van Leeuwen, G.V., Erol, O., Swierts, T., van der Ent, E., de Voogd, N.J., Choi, Y.H., 2020. Influence of geographical location on the metabolic production of giant barrel sponges (Xestospongia spp.) revealed by metabolomics tools. ACS Omega. 5, 12398-12408.

Bellenguez, C., Charbonnier, C., Grenier-Boley, B., Quenez, O., Le Guennec, K., Nicolas, G., Chauhan, G., Wallon, D., Rousseau, S., Richard, A.C., Boland, A., Bourque, G., Munter, H.M., Olaso, R., Meyer, V., Rollin-Sillaire, A., Pasquier, F., Letenneur, L., Redon, R., Dartigues, J.F., Tzourio, C., Frebourg, T., Lathrop, M., Deleuze, J.F., Hannequin, D., Genin, E., Amouyel, P., Debette, S., Lambert, J.C., Campion, D., CNR MAJ Collaborators, 2017. Contribution to Alzheimer's disease risk of rare variants in TREM2, SORL1, and ABCA7 in 1779 cases and 1273 controls. Neurobiol. Aging. 59, 220.e1-220.e9.

Bello, O.M., Jagaba, S.M., Bello, O.E., Ogbesejana, A.B., Dada, O.A., Adetunji, C.O., Abubakar, S.M., 2019. Phytochemistry, pharmacology and perceived health uses of non- cultivated vegetable Cyphostemma adenocaule (Steud. ex A. Rich.) Desc. ex Wild & R.B. Drumm: A review. Sci. Afr. 2, e00053.

Berntsson, E., Paul, S., Sholts, S.B., Jarvet, J., Barth, A., Gräslund, A., Wärmländer, S.K.T.S., 2021. 6-gingerol interferes with amyloid-beta (Aβ) peptide aggregation. bioRxiv. 1-16.

Bhadra, S., Mukherjee, P.K., Bandyopadhyay, A., 2012. Cholinesterase inhibition activity of Marsilea quadrifolia Linn. an edible leafy vegetable from West Bengal, India. Nat. Prod. Res. 26, 1519-1522.

Bin-Asal, F.S.N., Saeed, A.A.M., Yahia, A.R.A.B., 2025. Ceropegia variegata: Phytochemical profiling, antioxidant prowess, and antimicrobial potential. Clin. Trad. Med. Pharmacol. 6, 200194.

Biswas, M., Borah, P., Bora, M., Saikia, M., 2019. Pharmacognostic evaluation, phytochemical screening and antimicrobial activity of rhizome of Zingiber officinale Roscoe (cv Moran). Res. Rev. Biotech. Biosci. 6, 05-14.

Bodagh, M.N., Maleki, I., Hekmatdoost, A., 2018. Ginger in gastrointestinal disorders: A systematic review of clinical trials. Food Sci. Nutr. 7, 96-108.

Boga, M., Hacıbekiroğlu, I., Kolak, U., 2011. Antioxidant and anticholinesterase activities of eleven edible plants. Pharm. Biol. 49, 290-295.

Bonesi, M., Loizzo, M.R., Conforti, F., Passalacqua, N.G., Saab, A., Menichini, F., Tundis, R., 2013. Berberis aetnensis and B. libanotica: A comparative study on the chemical composition, inhibitory effect on key enzymes linked to Alzheimer's disease and antioxidant activity. J. Pharm. Pharmacol. 65, 1726-1735.

Bonesi, M., Menichini, F., Tundis, R., Loizzo, M.R., Conforti, F., Passalacqua, N.G., Statti, G.A., Menichini, F., 2010. Acetylcholinesterase and butyrylcholinesterase inhibitory activity of Pinus species essential oils and their constituents. J. Enzym. Inhib. Med. Chem. 25, 622-628.

Boubakri, A., Leri, M., Bucciantini, M., Najjaa, H., Ben Arfa, A., Stefani, M., Neffati, M., 2020. Allium roseum L. extract inhibits amyloid beta aggregation and toxicity involved in Alzheimer's disease. PLoS ONE. 15, e0223815.

Cacace, R., Sleegers, K., Van Broeckhoven, C., 2016. Molecular genetics of early-onset Alzheimer's disease revisited. Alzheimer's Dement. 12, 733-748.

Chaiyana, W., Okonogi, S., 2012. Inhibition of cholinesterase by essential oil from food plants. Phytomedicine. 19, 836-839.

Chandra, S., Roy, A., Jana, M., Pahan, K., 2019. Cinnamic acid activates PPARα to stimulate Lysosomal biogenesis and lower Amyloid plaque pathology in an Alzheimer's disease mouse model. Neurobiol. Dis. 124, 379-395.

Chandra, V., Pandav, R., Dodge, H.H., Johnston, J.M., Belle, S.H., DeKosky, S.T., Ganguli, M., 2001. Incidence of Alzheimer's disease in a rural community in India: The Indo-US study. Neurology. 57, 985-989.

Cheenpracha, S., Jitonnom, J., Komek, M., Ritthiwigrom, T., Laphookhieo, S., 2016. Acetylcholinesterase inhibitory activity and molecular docking study of steroidal alkaloids from Holarrhena pubescens barks. Steroids. 108, 92-98.

Chen, X., Wang, H., Huang, X., Xia, S., Chen, C., Nie, Q., Nie, S., 2022. Efficient enrichment of total flavonoids from kale (Brassica oleracea L. var. acephala L.) extracts by NKA-9 resin and antioxidant activities of flavonoids extract in vitro. Food Chem. 374, 131508.

Chen, Z.R., Huang, J.B., Yang, S.L., Hong, F.F., 2022. Role of cholinergic signaling in Alzheimer's disease. Molecules. 27, 1-23.

Chethana, K.R., Sasidhar, B.S., Naika, M., Keri, R.S., 2018. Phytochemical composition of Caesalpinia crista extract as potential source for inhibiting cholinesterase and β-amyloid aggregation: Significance to Alzheimer's disease. Asian Pac. J. Trop. Biomed. 8, 500-512.

Chethana, K.R., Senol, F.S., Orhan, I.E., Anilakumar, K.R., Keri, R.S., 2017. Cassia tora Linn.: A boon to Alzheimer's disease for its anti-amyloidogenic and cholinergic activities. Phytomedicine. 33, 43-52.

Chiaramonte, M., Bonaventura, R., Costa, C., Zito, F., Russo, R., 2021. [6] gingerol dose-dependent toxicity, its role against lipopolysaccharide insult in sea urchin (Paracentrotus lividus Lamarck), and antimicrobial activity. Food Biosci. 39, 100833.

Cho, N., Lee, H.K., Jeon, B.J., Kim, H.W., Kim, H.P., Lee, J.H., Kim, Y.C., Sung, S.H., 2014. The effects of Betula platyphylla bark on amyloid beta-induced learning and memory impairment in mice. Food Chem. Toxicol. 74, 156-63.

Choi, J.Y., Cho, E.J., Lee, H.S., Lee, J.M., Yoon, Y.H., Lee, S., 2013. Tartary buckwheat improves cognition and memory function in an in vivo amyloid-β-induced Alzheimer model. Food Chem. Toxicol. 53, 105-111.

Choi, S.J., Oh, S.S., Kim, C.R., Kwon, Y.K., Suh, S.H., Kim, J.K., Park, G.G., Son, S.Y., Shin, D.H., 2016. Perilla frutescens extract ameliorates acetylcholinesterase and trimethyltin chloride-induced neurotoxicity. J. Med. Food. 19, 281-289.

Chowdhury, S., Das Gupta, B., Ghosh, S., Gayen, S., Kar, A., Mukherjee, P.K., Haldar, P.K., 2025. Metabolite profiling and neuroprotective potential of Clitoria ternatea L. through in-vitro and in-vivo experimental models. Fitoterapia. 185, 106772.

Conforti, F., Rigano, D., Formisano, C., Bruno, M., Loizzo, M.R., Menichini, F., Senatore, F., 2010. Metabolite profile and in vitro activities of Phagnalon saxatile (L.) Cass. relevant to treatment of Alzheimer's disease. J. Enzym. Inhib. Med. Chem. 25, 97-104.

Cornutiu, G., 2015. The epidemiological scale of Alzheimer's disease. J. Clin. Med. Res. 7, 657-666.

Cortes, N., Sierra, K., Alzate, F., Osorio, E.H., Osorio, E., 2018. Alkaloids of amaryllidaceae as inhibitors of cholinesterases (AChEs and BChEs): An Integrated bioguided study. Phytochem. Anal. 29, 217-227.

Costa, P., Goncalves, S., Grosso, C., Andrade, P.B., Valentao, P., Bernardo-Gil, M.G., Romano, A., 2012. Chemical profiling and biological screening of Thymus lotocephalus extracts obtained by supercritical fluid extraction and hydrodistillation. Ind. Crops Prod. 36, 246-256.

da Costa Rodrigues, K., de Oliveira, R.L., da Silva Chaves, J., da Rocha, V.M.E., dos Santos, B.F., Fronza, M.G., de Campos Domingues, N.L., Savengnago, L., Wilhelm, E.A., Luchese, C., 2022. A new arylsulfanyl-benzo-2,1,3-thiadiazoles derivative produces an anti-amnesic effect in mice by modulating acetylcholinesterase activity. Chem. –Biol. Interact. 351, 1-13.

da Silva Barbosa, D.C., Holanda, V.N., de Assis, C.R.D., de Oliveira Farias de Aguiar, J.C.R., doNascimento, P.H., da Silva W.V., do Amaral Ferraz Navarro D.M., daSilva M.V., de Menezes Lima V.L., dos Santos Correia M.T., 2020. Chemical composition and acetylcholinesterase inhibitory potential, in silico, of Myrciaria floribunda (H. West ex Willd.) O. Berg fruit peel essential oil. Ind. Crops Prod. 151, 112372.

Dalai, M.K., Bhadra, S., Chaudhary, S.K., Bandyopadhyay, A., Mukherjee, P.K., 2014. Anti-cholinesterase potential of Cinnamomum tamala (Buch.-Ham.) T.Nees & Eberm. Leaves. Indian J. Trad. Knowledge. 13, 691-697.

Das, A., Shanker, G., Nath, C., Pal, R., Singh, S., Singh, H. K., 2002. A comparative study in rodents of standardized extracts of Bacopa monniera and Ginkgo biloba anticholinesterase and cognitive enhancing activities. Pharmacol. Biochem. Behav. 73, 893-900.

Das, B., Bhardwaj, P.K., Sharma, N., Sarkar, A., Haldar, P.K., Mukherjee, P.K., 2023. Evaluation of Mollugo oppositifolia Linn. as cholinesterase and β-secretase enzymes inhibitor. Front. Pharmacol. 13, 1-13.

Das, B., Kar, A., Matsabisa, M., Mukherjee, P.K., 2020. Anti-cholinesterase potential of standardized extract of PHELA a traditional South African medicine formulation. J. Herb. Med. 22, 100348.

Dastmalchi, K., Ollilainen, V., Lackman, P., af Gennäs, G.B., Dorman, H.D., Järvinen, P.P., Yli-Kauhaluoma, J., Hiltunen, R., 2009. Acetylcholinesterase inhibitory guided fractionation of Melissa officinalis L. Bioorg. Med. Chem. 17, 867-871.

de Oliveira, P.C.O., da Silva, G.M., de Moraes, Q.B.C.M.C., Cardoso, C.L., 2024. Natural products as a source of cholinesterase inhibitors. Pharmacol. Res.- Nat. Prod. 5, 100099.

de Pedro-Cuesta, J., Virues-Ortega, J., Vega, S., Seijo-Martinez, M., Saz, P., Rodriguez, F., Rodriguez-Laso, A., Rene, R., de las Heras, S.P., Mateos,

R., Martinez-Martin, P., Manubens, J.M., Mahillo-Fernandez, I., Lopez-Pousa, S., Lobo, A., Regla, J.L., Gascon, J., García, F.J., Fernandez-Martinez, M., Boix, R., Bermejo-Pareja, F., Bergareche, A., Benito-Leon, J., de Arce, A., del Barrio, J.L., 2009. Prevalence of dementia and major dementia subtypes in Spanish populations: A reanalysis of dementia prevalence surveys, 1990-2008. BMC Neurol. 9, 55.

Demirezer, L.O., Gürbüz, P., Uğur, E.P.K., Bodur, M., Özenver, N., Uz, A., Güvenalp, Z., 2015. Molecular docking and ex vivo and in vitro anticholinesterase activity studies of Salvia sp. and highlighted rosmarinic acid. Turk. J. Med. Sci. 45, 1141-1148.

DeTure, M.A., Dickson, D.W., 2019. The neuropathological diagnosis of Alzheimer's disease. Mol. Neurodegener. 14, 1-18.

Devi, N.B., Singh, P.K., Das, A.K., 2016. Wilderness and biodiversity of gingers in the valley district, Manipur. Int. J. Sci. Tech. Res. 5, 286-291.

Dhanik, J., Arya, N., Nand, V., 2017. A review on Zingiber officinale. J. Pharmacog. Phytochem. 6, 174-184.

Di Liegro, C.M., Schiera, G., Proia, P., Di Liegro, I., 2019. Physical activity and brain health. Genes (Basel). 10, 720.

Diniz Pereira, J., Gomes Fraga, V., Morais Santos, A.L., Carvalho, M.D.G., Caramelli, P., Braga Gomes, K., 2021. Alzheimer's disease and type 2 diabetes mellitus: A systematic review of proteomic studies. J. Neurochem. 156, 753-776.

Dohi, S., Terasaki, M., Makino, M., 2009. Acetylcholinesterase inhibitory activity and chemical composition of commercial essential oils. J. Agric. Food Chem. 57, 4313-4318.

Dung, H.V., Cuong, T.D., Chinh, N.M., Quyen, D., Kim, J.A., Byeon, J.S., Woo, M.H., Choi, J.S., Min, B.S., 2015. Compounds from the aerial parts of

Piper bavinum and their anti-cholinesterase activity. Arch. Pharmacal. Res. 38, 677-682.

Durazzo, T.C., Mattsson, N. and Weiner, M.W., 2014. Smoking and increased Alzheimer's disease risk: A review of potential mechanisms. Alzheimer's Dement. 10, S122–S145.

Eldeen, I.M.S., Elgorashi, E.E., Staden, J.V., 2005. Antibacterial, anti-inflammatory, anti-cholinesterase and mutagenic effects of extracts obtained from some trees used in South African traditional medicine. J. Ethnopharmacol. 102, 457-464.

Elendu, C., 2024. The evolution of ancient healing practices: From shamanism to hippocratic medicine: A review. Medicine (Baltimore). 103, e39005.

Elgorashi, E.E., Stafford, G.I., Staden, J.V., 2004. Acetylcholinesterase enzyme inhibitory effects of Amaryllidaceae alkaloids. Planta. Med. 70, 260-262.

Emeka, A.G., Augustine, O., Chidinma, O.E., Nto, N.J., 2023. Zingerone improves memory impairment in Wistar rats exposed to cadmium via modulation of redox imbalance. J. Krishna Institute Med. Sci. University. 12, 1-16.

Erdemoglu, N., Sahin, E., Sener, B., Ide, S., 2004. Structural and spectroscopic characteristics of two lignans from Taxus baccata L. J. Mol. Struc. 692, 57-62.

Ernst, E., Pittler, M.H., 2000. Efficacy of ginger for nausea and vomiting: A systematic review of randomized clinical trials. Br. J. Anaesth. 84, 367-371.

Ernst, R.L, Hay, J.W., 1994. The US economic and social costs of Alzheimer's disease revisited. Am. J. Public Health. 84, 1261-1264.

Esfandiary, E., Karimipour, M., Mardani, M., Ghanadian, M., Alaei, H.A., Mohammadnejad, D., Esmaeili, A., 2015. Neuroprotective effects of Rosa

damascena extract on learning and memory in a rat model of amyloid-β-induced Alzheimer's disease. Adv. Biomed. Res. 4, 131.

Esquivel-Alvarado, D., Zhang, S., Hu, C., Zhao, Y., Sang, S., 2022. Using metabolomics to identify the exposure and functional biomarkers of ginger. J. Agric. Food Chem. 70, 12029-12040.

Ezez, D., Tefera, M., 2021. Effects of solvents on total phenolic content and antioxidant activity of ginger extracts. J. Chem. 2021, 1-5.

Ferreira, A., Proenca, C., Serralheiro, M.L.M., Araujo, M.E.M., 2006. The in vitro screening for acetylcholinesterase inhibition and antioxidant activity of medicinal plants from Portugal. J. Ethnopharmacol. 108, 31-37.

Foyet, H.S., Abaissou, H.H.N., Wado, E., Acha, E.A., Alin, C., 2015. Emilia coccinae (SIMS) G extract improves memory impairment, cholinergic dysfunction, and oxidative stress damage in scopolamine treated rats. BMC Complement. Altern. Med. 15, 333.

Gavrilova, A., Gavrilov, G., Trifonova, D., 2022. Contribution to the microscopic identification of Zingiber officinale. Pharmacia. 69, 93-97.

Geissler, T., Brandt, W., Porzel, A., Schlenzig, D., Kehlen, A., Wessjohann, L., Arnold, N., 2010. Acetylcholinesterase inhibitors from the toadstool Cortinarius infractus. Bioorg. Med. Chem. 18, 2173-2177.

Ghahremanitamadon, F., Shahidi, S., Zargooshnia, S., Nikkhah, A., Ranjbar, A., Soleimani Asl, S.S., 2014. Protective effects of Borago officinalis extract on amyloid β-peptide(25-35)-induced memory impairment in male rats: A behavioral study. Biomed. Res. Int. 2014, 798535.

Goldman, J.S., Hou, C.E., 2004. Early-onset Alzheimer disease: When is genetic testing appropriate? Alzheimer Dis. Assoc. Disord. 18, 65-67.

Golian, M., Tancinova, D., Lakatosova, J., Mrvova, M., Gazo, J., Borsanyi, P., 2025. Effect of altitude on biomass production and essential oil composition of selected medicinal plants. Ind. Crops Prod. 233, 21475.

Grodzicki, W., Dziendzikowska, K., 2020. The role of selected bioactive compounds in the prevention of Alzheimer's disease. Antioxidants (Basel). 9, 229.

Gul, S., Attaullah, S., Alsugoor, M.H., Bawazeer, S., Shah, S.A., Khan, S., Salahuddin, H.S., Ullah, M., 2023. Folicitin abrogates scopolamine induced oxidative stress, hyperlipidemia mediated neuronal synapse and memory dysfunction in mice. Heliyon. 9, e16930.

Guo, Z., Cupples, L.A., Kurz, A., Auerbach, S.H., Volicer, L., Chui, H., Green, R.C., Sadovnick, A.D., Duara, R., DeCarli, C., Johnson, K., Go, R.C., Growdon, J.H., Haines, J.L., Kukull, W.A., Farrer, L.A. 2000. Head injury and the risk of AD in the MIRAGE study. Neurology. 54, 1316-1323.

Gupta, V.B., Indi, S.S., Rao, K.S.J., 2009. Garlic extract exhibits antiamyloidogenic activity on amyloid-beta fibrillogenesis: Relevance to Alzheimer’s disease. Phytother. Res. 23, 111-115.

Habtemariam, S., 2011. The therapeutic potential of Berberis darwinii stem-bark: Quantification of berberine and in vitro evidence for Alzheimer’s disease therapy. Nat. Prod. Commun. 6, 1089-1090.

Halliwell, B., Gutteridge, J.M.C., Aruoma, O.I., 1987. The deoxyribose method: A simple “test-tube” assay for determination of rate constants for reactions of hydroxyl radicals. Anal. Biochem. 165, 215-219.

Hampel, H., Mesulam, M.M., Cuello, A.C., Farlow, M.R., Giacobini, E., Grossberg, G.T., Khachaturian, A.S., Vergallo, A., Cavedo, E., Snyder, P.J., Khachaturian, Z.S., 2018. The cholinergic system in the pathophysiology and treatment of Alzheimer's disease. Brain. 141, 1917-1933.

Harwansh, R.K., Mukherjee, K., Bhadra, S., Kar, A., Bahadur, S., Mitra, A., Mukherjee, P.K., 2014. Cytochrome P450 inhibitory potential and RP-HPLC standardization of trikatu- A rasayana from Indian Ayurveda. J. Ethnopharmacol. 153, 674-681.

Heinrich, M., 2010b. Ethnopharmacology and drug discovery. In: Liu H-W, Mander L, editors. Comprehensive Natural Products II: chemistry and biology. Elsevier; Oxford. 3, 351-381.

Ho, Y.S., Yu, M.S., Lai, C.S., So, K.F., Yuen, W.H., Chang, R.C., 2007. Characterizing the neuroprotective effects of alkaline extract of Lycium barbarum on beta-amyloid peptide neurotoxicity. Brain Res. 1158, 123-134.

Hou, M., Hu, W., Xiu, Z., Shi, Y., Hao, K., Cao, D., Guan, Y., Yin, H., 2020. Efficient enrichment of total flavonoids from Pteris ensiformis Burm extracts by macroporous adsorption resins and in vitro evaluation of antioxidant and antiproliferative activities. J. Chromatogr. B. 1138, 121960.

Hritcu, L., Noumedem, J.A., Cioanca, O., Hancianu, M., Kuete, V., Mihasan, M., 2014. Methanolic extract of Piper nigrum fruits improves memory impairment by decreasing brain oxidative stress in amyloid beta(1-42) rat model of Alzheimer's disease. Cell. Mol. Neurobiol. 34, 437-449.

Huang, S.H., Lin, C.M., Chiang, B.H., 2008. Protective effects of Angelica sinensis extract on amyloid beta-peptide-induced neurotoxicity. Phytomedicine. 15, 710-721.

Huh, E., Lim, S., Kim, H.G., Ha, S.K., Park, H.Y., Huh, Y., Oh, M.S., 2018. Ginger fermented with Schizosaccharomyces pombe alleviates memory impairment via protecting hippocampal neuronal cells in amyloid beta1-42 plaque injected mice. Food Funct. 9, 171-178.

Hussain, H., Ahmad, S., Shah, S.W.A., Ullah, A., Ali, N., Almehmadi, M., Ahmad, M., Khalil, A.A.K., Jamal, S.B., Ahmad, H., Halawi, M., 2022. Attenuation of scopolamine-induced amnesia via cholinergic modulation in mice by synthetic curcumin analogs. Molecules. 27, 2468.

Imtiyaz, S., Rahman, K., Sultana, A., Tariq, M., Chaudhary, S.S., 2013. Zingiber officinale Rosc.: A traditional herb with medicinal properties. TANG Human. Trad. Med. 3, e26.

Ingkaninan, K., Phengpa, P., Yuenyongsawad, S., Khorana, N., 2006. Acetylcholinesterase inhibitors from Stephania venosa tuber. J. Pharm. Pharmacol. 58, 695-700.

Ingkaninan, K., Temkitthawon, P., Chuenchom, K., Yuyaem, T., Thongnoi, W., 2003. Screening for acetylcholinesterase inhibitory activity in plants used in Thai traditional rejuvenating and neurotonic remedies. J. Ethnopharmacol. 89, 261-264.

J.M. Garg, eFlora of India, 2024. Curcuma amada Roxb. eFlora of India. Available at: https://efloraofindia.com/efi/curcuma-amada/. (accessed 08 August 2025).

J.M. Garg, eFlora of India, 2024. Hedychium gardnerianum Sheppard ex Ker Gawl. eFlora of India. Available at: https://efloraofindia.com/efi/hedychium-gardnerianum/. (accessed 08 August 2025).

J.M. Garg, eFlora of India, 2024. Kaempferia rotunda L. eFlora of India. Available at: https://efloraofindia.com/efi/kaempferia-rotunda/. (accessed 08 August 2025).

Jan, R., Gani, A., Dar, M.M., Bhat, N.A., 2022. Bioactive characterization of ultrasonicated ginger (Zingiber officinale) and licorice (Glycyrrhiza Glabra) freeze dried extracts. Ultrason. Sonochem. 88, 106048.

Jansen, C., Baker, J.D., Kodaira, E., Ang, L., Bacani, A.J., Aldan, J.T., Shimoda, L.M.N., Salameh, M., Small-Howard, A.L., Stokes, A.J., Turner, H., Adra, C.N., 2021. Medicine in motion: Opportunities, challenges and data analytics-based solutions for traditional medicine integration into western medical practice. J. Ethnopharmacol. 267, 113477.

Joshi, H., Parle, M., 2006. Zingiber officinale: evaulation of its nootropic effect in mice. Afr. J. Tradit. Complement. Altern. Med. 3, 64-74.

Jung, H.A., Ali, M.Y., Jung, H.J., Jeong, H.O., Chung, H.Y., Choi, J.S., 2016. Inhibitory activities of major anthraquinones and other constituents from Cassia obtusifolia against β-secretase and cholinesterases. J. Ethnopharmacol. 191, 152-160.

Jung, H.A., Jung, Y.J., Hyun, S.K., Min, B.S., Kim, D.W., Jung, J.H., Choi, J.S., 2010. Selective cholinesterase inhibitory activities of a new monoterpene diglycoside and other constituents from Nelumbo nucifera stamens. Biol. Pharm. Bull. 33, 267-272.

Jung, H.A., Karki, S., Kim, J.H., Choi, J.S., 2015. BACE1 and cholinesterase inhibitory activities of Nelumbo nucifera embryos. Arch. Pharmacal. Res. 38, 1178-1187.

Karakaya, S., Yilmaz, S., Koca, M., Demirci, B., Sytar, O., Pal, L., 2019. Screening of non-alkaloid acetylcholinesterase inhibitors from extracts and essential oils of Anthriscus nemorosa (M. Bieb.) Spreng. (Apiaceae). S. Afr. J. Bot. 125, 261-269.

Karunakaran, K.B., Thiyagaraj, A., Santhakumar, K., 2022. Novel insights on acetylcholinesterase inhibition by Convolvulus Pluricaulis, scopolamine and their combination in zebrafish. Nat. Prod. Bio. Prospect. 12, 1-15.

Khalid, A., Azim, M.K., Parveen, S., Rahman, A., Choudhary, M.I., 2005. Structural basis of acetylcholinesterase inhibition by triterpenoidal alkaloids. Biochem. Biophys. Res. Commun. 331, 1528-1532.

Khalil, N., El-Jalel, L., Yousif, M., Gonaid, M., 2020. Altitude impact on the chemical profile and biological activities of Satureja thymbra L. essential oil. BMC Complement. Med. Ther. 20, 186.

Khan, A.A., Janardhanan, R., Kishore, J., Awasthi, A.A., Parveen, S., Saeed, S., Shannawaz, M., Selvamurthy, W., 2022. Awareness and utilization of Unani medicine among the adult population from East Delhi: A cross sectional survey. J. Pharm. Bioallied Sci. 14, 157-161.

Khan, R.A., Khan, M.R., Sahreen, S., 2012. Protective effects of Sonchus asper against KBrO3 induced lipid peroxidation in rats. Lipids Health Dis. 11, 164.

Khattak, S., Rehman, S.U., Shah, H.U., Khan, T., Ahmad, M., 2005. In vitro enzyme inhibition activities of crude ethanolic extracts derived from medicinal plants of Pakistan. Nat. Prod. Res. 19, 567-571.

Khodaie, L., Sadeghpoor, O., 2015. Ginger from ancient times to the new outlook. Jundishapur J. Nat. Pharm. Prod. 10, e18402.

Kim, C.Y., Seo, Y., Lee, C., Park, G.H., Jang, J.H., 2018. Neuroprotective effect and molecular mechanism of [6]-gingerol against scopolamine-induced amnesia in C57BL/6 mice. Evid. Based Complement. Alternat. Med. 2018, 8941564.

Kim, D.K., 2002. Inhibitory effect of corynoline isolated from the aerial parts of Corydalis incisa on the acetylcholinesterase. Arch. Pharm. Res. 25, 817-819.

Kirubakaran, D., 2025. Herbal remedies for Alzheimer's disease: neuroprotective mechanisms and cognitive enhancement potential. Dig. Chinese Med. 8, 183-195.

Kizhakkayil, J., Sasikumar, B., 2011. Diversity, characterization and utilization of ginger: A review. Plant Genet. Res. 9, 464-477.

Kohoude, M.J., Gbaguidi, F., Agbani, P., Ayedoun, M.A., Cazaux, S., Bouajila, J., 2017. Chemical composition and biological activities of extracts and essential oil of Boswellia dalzielii leaves. Pharm. Biol. 55, 33-42.

Kongsui, R., Jittiwat, J., 2023. Ameliorative effects of 6-gingerol in cerebral ischemia are mediated via the activation of antioxidant and anti-inflammatory pathways. Biomed. Rep. 18, 1-10.

Konrath, E.L., Neves, B.M., Passos, C.S., Lunardi, P.S., Ortega, M.G., Cabrera, J.L., Goncalves, C., Henriques, A.T., 2012. Huperzia quadrifariata and Huperzia reflexa alkaloids inhibit acetylcholinesterase activity in vivo in mice brain. Phytomedicine. 19, 1321-1324.

Kuanhuta, W., Aree, T., Pornpakakul, S., Sawasdee, P., 2014. Novel cucurbitane triterpenoids and anti-cholinesterase activities of constituents from Momordica charantia L. Nat. Prod. Commun. 9, 765-769.

Kuk, E.B., Jo, A.R., Oh, S.I., Sohn, H.S., Seong, S.H., Roy, A., Choi, J.S., Jung, H.A., 2017. Anti-Alzheimer's disease activity of compounds from the root bark of Morus alba L. Arch. Pharmacal. Res. 40, 338-349.

Kumar, G.P., Khanum, F., 2012. Neuroprotective potential of phytochemicals. Pharmacogn. Rev. 6, 81-90.

Kundu, A., Mitra, A., 2013. Flavoring extracts of Hemidesmus indicus roots and Vanilla planifolia pods exhibit in vitro acetylcholinesterase inhibitory activities. Plant Foods Hum. Nutr. 68, 247-253.

Kushwah, S., Maurya, N.S., Kushwaha, S., Scotti, L., Chawade, A., Mani, A., 2023. Herbal therapeutics for Alzheimer's disease: Ancient Indian medicine system from the modern viewpoint. Curr. Neuropharmacol. 21, 764-776.

Kwon, S.H., Lee, H.K., Kim, J.A., Hong, S.I., Kim, S.Y., Jo, T.H., Park, Y.I., Lee, C.K., Kim, Y.B., Lee, S.Y., Jang, C.G., 2011. Neuroprotective effects of

Eucommia ulmoides Oliv. Bark on amyloid beta(25-35)-induced learning and memory impairments in mice. Neurosci. Lett. 487, 123-127.

Lai, D.H., Yang, Z.D., Xue, W.W., Sheng, J., Shi, Y., Yao, X.J., 2013. Isolation, characterization and acetylcholinesterase inhibitory activity of alkaloids from roots of Stemona sessilifolia. Fitoterapia. 89, 257-264.

Lanoiselee, H.M., Nicolas, G., Wallon, D., Rovelet-Lecrux, A., Lacour, M., Rousseau, S., Richard, A.C., Pasquier, F., Rollin-Sillaire, A., Martinaud, O., Quillard-Muraine, M., de la Sayette, V., Boutoleau-Bretonniere, C., Etcharry-Bouyx, F., Chauvire, V., Sarazin, M., le Ber, I., Epelbaum, S., Jonveaux, T., Rouaud, O., Ceccaldi, M., Felician, O., Godefroy, O., Formaglio, M., Croisile, B., Auriacombe, S., Chamard, L., Vincent, J.L., Sauvee, M., Marelli-Tosi, C., Gabelle, A, Ozsancak, C., Pariente, J., Paquet, C., Hannequin, D., Campion, D., Collaborators of the CNR-MAJ Project, 2017. APP, PSEN1, and PSEN2 mutations in early-onset Alzheimer disease: A genetic screening study of familial and sporadic cases. PLOS Med. 14, e1002270.

Lfitat, A., Zejli, H., Bousraf, F.Z., Bousselham, A., Atki, Y.E., Gourch, A., Lyoussi, B., Abdellaoui, A., 2019. Comparative assessment of total phenolics content and in vitro antioxidant capacity variations of macerated leaf extracts of Olea europaea L. and Argania spinosa (L.) Skeels. Mater. Today Proc. 45, 7271-7277.

Li, H.B., Wong, C.C., Cheng, K.W., Chen, F., 2008. Antioxidant properties in vitro and total phenolic contents in methanol extracts from medicinal plants. LWT. 41, 385-390.

Li, N.M., Liu, K.F., Qiu, Y.J., Zhang, H.H., Nakanishi, H., Qing, H., 2019. Mutations of beta-amyloid precursor protein alter the consequence of Alzheimer's disease pathogenesis. Neural. Regen. Res14, 658-665.

Li, Q., Tu, Y., Zhu, C., Luo, W., Huang, W., Liu, W., Li, Y., 2017. Cholinesterase, β -amyloid aggregation inhibitory and antioxidant capacities of Chinese medicinal plants. Ind. Crops Prod. 108, 512-519.

Li, Y., Tran, V.H., Duke, C.C., Roufogalis, B.D., 2012. Preventive and protective properties of Zingiber officinale (ginger) in diabetes mellitus, diabetic complications, and associated lipid and other metabolic disorders: a brief review. Evid. Based Complement. Alt. Med. 2012, 516870.

Lim, S., Moon, M., Oh, H., Kim, H.G., Kim, S.Y., Oh, M.S., 2014. Ginger improves cognitive function via NGF-induced ERK/CREB activation in the hippocampus of the mouse. J. Nutr. Biochem. 25, 1058-1065.

Liu, D., Du, D., 2020. Mulberry fruit extract alleviates cognitive impairment by promoting the clearance of amyloid-β and inhibiting neuroinflammation in Alzheimer's disease mice. Neurochem. Res. 45, 2009-2019.

Loizzo, M.R., Ben Jemia, M., Senatore, F., Bruno, M., Menichini, F., Tundis, R., 2013a. Chemistry and functional properties in prevention of neurodegenerative disorders of five Cistus species essential oils. Food Chem. Toxicol. 59, 586-594.

Loizzo, M.R., Bonesi, M., Di Lecce, G., Boselli, E., Tundis, R., Pugliese, A., Menichini, F., Frega, N.G., 2013b. Phenolics, aroma profile, and in vitro antioxidant activity of Italian dessert passito wine from Saracena (Italy). J. Food Sci. 78, 703-708.

Loizzo, M.R., Menichini, F., Tundis, R., Bonesi, M., Conforti, F., Nadjafi, F., Statti, G.A., Frega, N.G., Menichini, F., 2009. In vitro biological activity of Salvia leriifolia Benth essential oil relevant to the treatment of Alzheimer's disease. J. Oleo. Sci. 58, 443-446.

Long, J.M., Holtzman, D.M., 2019. Alzheimer disease: An update on pathobiology and treatment strategies. Cell. 179, 312-339.

Lonita, R., Postu, P.A., Beppe, G.J., Mihasan, M., Petre, B.A., Hancianu, M., Cioanca, O., Hritcu, L., 2017. Cognitive-enhancing and antioxidant activities of the aqueous extract from Markhamia tomentosa (Benth.) K. Schum. stem bark in a rat model of scopolamine. Behav. Brain Funct. 13, 5.

López, S., Bastida, J., Viladomat, F., Codina, C., 2002. Acetylcholinesterase inhibitory activity of some Amaryllidaceae alkaloids and Narcissus extracts. Life Sci. 71, 2521-2529.

Lueptow, L.M., 2017. Novel object recognition test for the investigation of learning and memory in mice. J. Vis. Exp. 126, 1-9.

Lutz, J.A., Carter, M., Fields, L., Barron, S., Littleton, J.M., 2015. The dietary flavonoid rhamnetin inhibits both inflammation and excitotoxicity during ethanol withdrawal in rat organotypic hippocampal slice cultures. Alcohol Clin. Exp. Res. 39, 2345-2353.

Ma, Y., Ma, B., Shang, Y., Yin, Q., Hong, Y., Xu, S., Shen, C., Hou, X., Liu, X., 2018. Flavonoid-rich ethanol extract from the leaves of Diospyros kaki attenuates cognitive deficits, amyloid-beta production, oxidative stress, and neuroinflammation in APP/PS1 transgenic mice. Brain Res. 1678, 85-93.

Maqbool, I., Ali, A., Ashraf, M., Rehman, N.U., Khalid, I., Talib, S., Jameel, F., Hussain, A., 2022 The multi characteristics values of ginger (Zingiber officinale) in human nutrition and disease prevention. GSC. Biol. Pharm. Sci. 21, 127-134.

Martins, M.M., Branco, P.S., Ferreira, L.M., 2023. Enhancing the therapeutic effect in Alzheimer's disease drugs: The role of polypharmacology and cholinesterase inhibitors. ChemistrySelect. 8, e202300461.

Maurer, S.V., Williams, C.L., 2017. The cholinergic system modulates memory and hippocampal plasticity via its interactions with non neuronal cells. Front. Immunol. 8, 1489.

McNeil, M.J., Porter, R.B.R., Rainford, L., Dunbar, O., Francis, S., Laurieri, N., Delgoda, R., 2018. Chemical composition and biological activities of the essential oil from Cleome rutidosperma DC. Fitoterapia. 129, 191-197.

Mekinić, I.G., Šimat, V., Ljubenkov, I., Burčul, F., Grga, M., Mihajlovski, M., Loncar, R., Katalinić, V., Skroza, D., 2018. Influence of the vegetation period on sea fennel, Crithmum maritimum L. (Apiaceae), phenolic composition, antioxidant and anticholinesterase activities. Ind. Crops Prod. 124, 947-953.

Menichini, F., Loizzo, M.R., Bonesi, M., Conforti, F., De Luca, D., Statti, G.A., de Cindio, B., Menichini, F., Tundis, R., 2011. Phytochemical profile, antioxidant, anti-inflammatory and hypoglycemic potential of hydroalcoholic extracts from Citrus medica L. cv Diamante flowers, leaves and fruits at two maturity stages. Food Chem. Toxicol. 49, 1549-1555.

Min, B.S., Cuong, T.D., Lee, J.S., Shin, B.S., Woo, M.H., Hung, T.M., 2010. Cholinesterase inhibitors from Cleistocalyx operculatus buds. Arch. Pharmacal. Res. 33, 1665-1670.

Mocan, A., Zengin, G., Uysal, A., Gunes, E., Mollica, A., Degirmenci, N.S., Alpsoy, L., Aktumsek, A., 2016. Biological and chemical insights of Morina persica L.: A source of bioactive compounds with multifunctional properties. J. Func. Food. 25, 94-109.

Moghaddasi, M.S., Kashani, H.H., 2012. Ginger (Zingiber officinale): A review. J. Med. Plants Res. 6, 4255-4258.

Mohamed, S.M., Shalaby, M.A., Al-Mokaddem, A.K., El-Banna, A., El Banna, H.A., Nabil, G., 2023. Evaluation of anti-alzheimer activity of Echinacea

purpurea extracts in aluminum chloride-induced neurotoxicity in rat model. J. Chem. Neuroanat. 128, 1-11.

Mohebali, N., Shahzadeh Fazeli, S.A., Ghafoori, H., Farahmand, Z., MohammadKhani, E., Vakhshiteh, F., Ghamarian, A., Farhangniya, M., Sanati, M.H., 2018. Effect of flavonoids rich extract of Capparis spinosa on inflammatory involved genes in amyloid-beta peptide injected rat model of Alzheimer's disease. Nutr. Neurosci. 21, 143-150.

Momoh, J.O., Olaleye, O.N., 2022. Evaluation of secondary metabolites profiling of ginger (Zingiber officinale Roscoe) rhizome using GC-MS and its antibacterial potential on Staphylococcus aureus and Escherichia coli. Microbiol. Res. J. Int. 32, 07-31.

Monfared, A.A.T., Byrnes, M.J., White, L.A., Zhang, Q., 2022. Alzheimer's disease: Epidemiology and clinical progression. Neurol. Ther. 11, 553-569.

Moon, M., Kim, H.G., Choi, J.G., Oh, H., Lee, P.K., Ha, S.K., Kim, S.Y., Park, Y., Huh, Y., Oh, M.S., 2014. 6-shogaol, an active constituent of ginger, attenuates neuroinflammation and cognitive deficits in animal models of dementia. Biochem. Biophys. Res. Commun. 449, 8-13.

Moore, K.B.E., Hung, T.J., Fortin, J.S., 2023. Hyperphosphorylated tau (p-tau) and drug discovery in the context of Alzheimer's disease and related tauopathies. Drug Discov. Today. 28, 103487.

Morzelle, M.C., Salgado, J.M., Telles, M., Mourelle, D., Bachiega, P., Buck, H.S., Viel, T.A., 2016. Neuroprotective effects of pomegranate peel extract after chronic infusion with amyloid-β peptide in mice. PLoS One. 11, e0166123.

Muflihah, Y.M., Gollavelli, G., Ling, Y.C., 2021. Correlation study of antioxidant activity with phenolic and flavonoid compounds in 12 Indonesian indigenous herbs. Antioxidants (Basel). 10, 1530.

Mukherjee, P.K., Banerjee, S.K., Kar, A., 2021. Molecular combination networks in medicinal plants: Understanding synergy by network pharmacology in Indian traditional medicine. Phytochem. Rev. 20, 693-703.

Mukherjee, P.K., Kumar, V., Mal, M., Houghton, P.J., 2007. Acetylcholinesterase inhibitors from plants. Phytomedicine. 14(4), 289-300.

Mura, T., Dartigues, J.F., Berr, C., 2010. How many dementia cases in France and Europe? Alternative projections and scenarios 2010-2050. Eur. J. Neurol. 17, 252-259.

Murebwayire, S., Ingkaninan, K., Changwijit, K., Frédérich, M., Duez, P., 2009. Triclisia sacleuxii (Pierre) Diels (Menispermaceae), a potential source of acetylcholinesterase inhibitors. J. Pharm. Pharmacol. 61, 103-107.

Mwamatopea, B., Tembo, D., Chikowe, I., Kampira, E., Nyirenda, C., 2020. Total phenolic contents and antioxidant activity of Senna singueana, Melia azedarach, Moringa Oleifera and Lannea discolor herbal plants. Sci. Africa. 9, e00481.

Najmi, A., Javed, S.A., Al Bratty, M., Alhazmi, H.A., 2022. Modern approaches in the discovery and development of plant-based natural products and their analogues as potential therapeutic agents. Molecules. 27, 349.

Namdaung, U., Athipornchai, A., Khammee, T., Kuno, M., Suksamrarn, S., 2018. 2-Arylbenzofurans from Artocarpus lakoocha and methyl ether analogs with potent cholinesterase inhibitory activity. Eur. J. Med. Chem. 143, 1301-1311.

Nasb, M., Tao, W., Chen, N., 2024. Alzheimer's disease puzzle: Delving into pathogenesis hypotheses. Aging Dis. 15, 43-73.

Nawar, N.F., Beltagy, D.M., Mohamed, T.M., Tousson, E.M., El-Keey, M.M., 2024. Anti-oxidant activity of coenzyme Q10 against AlCl3/D-galactose in

albino rat induced cognitive dysfunctions: Behavioral, biochemical, and BACE-1/GSK-3β alterations. Toxicol. Res. (Camb) 13, tfae131.

Nazari, L., Komaki, S., Salehi, I., Raoufi, S., Golipoor, Z., Kourosh-Arami, M., Komaki, A., 2022. Investigation of the protective effects of lutein on memory and learning using behavioral methods in a male rat model of Alzheimer's disease. J. Funct. Foods. 99, 1-12.

Nillert, N., Pannangrong, W., Welbat, J.U., Chaijaroonkhanarak, W., Sripanidkulchai, K., Sripanidkulchai, B., 2017. Neuroprotective effects of aged garlic extract on cognitive dysfunction and neuroinflammation induced by-amyloid in rats. Nutrients. 9, 24.

Nudelman, K.N.H., Jackson, T., Rumbaugh, M., Eloyan, A., Abreu, M., Dage, J.L., Snoddy, C., Faber, K.M., Foroud, T., Hammers, D.B., DIAN/DIAN-TU Clinical/Genetics Committee, Taurone, A., Thangarajah, M., Aisen, P., Beckett, L., Kramer, J., Koeppe, R., Kukull, W.A., Murray, M.E., Toga, A.W., Vemuri, P., Atri, A., Day, G.S., Duara, R., Graff-Radford, N.R., Honig, L.S., Jones, D.T., Masdeu, J.C., Mendez, M., Musiek, E., Onyike, C.U., Riddle, M., Rogalski, E., Salloway, S., Sha, S.J., Turner, R.S., Wingo, T.S., Wolk, D.A., Carrillo, M.C., Dickerson, B.C., Rabinovici, G.D., Apostolova, L.G., LEADS Consortium, 2023. Pathogenic variants in the longitudinal early-onset Alzheimer's disease study cohort. Alzheimers Dement. 19, S64-S73.

Nunes, G.B.L., Costa, L.M., Gutierrez, S.J.C., Satyal, P., de Freitas, R.M., 2015. Behavioral tests and oxidative stress evaluation in mitochondria isolated from the brain and liver of mice treated with riparin A. Life Sci. 121, 57-64.

Oh, M., Houghton, P., Whang, W., Cho, J., 2004. Screening of Korean herbal medicines used to improve cognitive function for anti-cholinesterase activity. Phytomedicine. 11, 544-548.

Organization for Economic Co-operation and Development (OECD). OECD guideline for testing of chemicals 425: Acute Oral Toxicity – Up-and-Down Procedure. Paris: OECD Publishing; 2022.

Orhan, I., Kartal, M., Kan, Y., Sener, B., 2008. Activity of essential oils and individual components against acetyl- and butyrylcholinesterase. Z. Naturforsch. C. J. Biosci. 63, 547-553.

Orhan, I., Sener, B., Choudhary, M.I., Khalid, A., 2004. Acetylcholinesterase and butyrylcholinesterase inhibitory activity of some Turkish medicinal plants. J. Ethnopharmacol. 91, 57-60.

Orhan, I., Senol, F.S., Gülpinar, A.R., Kartal, M., Sekeroglu, N., Deveci, M., Kan, Y., Sener, B., 2009. Acetylcholinesterase inhibitory and antioxidant properties of Cyclotrichium niveum, Thymus praecox subsp. Caucasicus var. Caucasicus, Echinacea purpurea and E. pallida. Food Chem. Toxicol. 47, 1304-1310.

Orhan, I.E., Gulyurdu, F., Akkol, E.K., Senol, F.S., Anul, S.A., Tatli, I.I., 2016. Anticholinesterase, antioxidant, analgesic and anti-inflammatory activity assessment of Xeranthemum annuum L. and isolation of two cyanogenic compounds. Pharm. Biol. 54, 2643-2651.

Othman, W.N.N.W., Liew, S.Y., Khaw, K.Y., Murugaiyah, V., Litaudon, M., Awang, K., 2016. Cholinesterase inhibitory activity of isoquinoline alkaloids from three Cryptocarya species (Lauraceae). Bioorg. Med. Chem. 24, 4464-4469.

Pawar, N., Pai, S., Nimbalkar, M., Dixit, G., 2011. RP-HPLC analysis of phenolic antioxidant compound 6-gingerol from different ginger cultivars. Food Chem. 126, 1330-1336.

Penumala, M., Zinka, R.B., Shaik, J.B., Mallepalli, S.K.R., Vadde, R., Amooru, D.G., 2018. Phytochemical profiling and in vitro screening for anticholinesterase, antioxidant, antiglucosidase and neuroprotective effect

of three traditional medicinal plants for Alzheimer's Disease and Diabetes Mellitus dual therapy. BMC Complement. Altern. Med. 18, 77.

Pereira, J.D., Fraga, V.G., Santos, A.L.M., Carvalho, M.D.G., Caramelli, P., Gomes, K.B., 2021. Alzheimer's disease and type 2 diabetes mellitus: A systematic review of proteomic studies. J. Neurochem. 156, 753-776.

Peterson, D.W., George, R.C., Scaramozzino, F., LaPointe, N.E., Anderson, R.A., Graves, D.J., Lew, J., 2009. Cinnamon extract inhibits tau aggregation associated with Alzheimer's disease in vitro. J. Alzheimers Dis. 17, 585-597.

Petrović, G.M., Stamenković, J.G., Kostevski, I.R., Stojanović, G.S., Mitić, V.D., Zlatković, B.K., 2017. Chemical composition of volatiles; antimicrobial, antioxidant and cholinesterase inhibitory activity of Chaerophyllum aromaticum L. (Apiaceae) essential oils and extracts. Chem Biodivers. 14, e1600367.

Phachonpai, W., Tongun, T., 2021. Cognition enhancing effects of Clausena lansium (lour.) Peel extract attenuate chronic restraint stress-induced memory deficit in rats. Heliyon. 7, 1-7.

Pintać, D., Četojević-Simin, D., Berežni, S., Orčić, D., Mimica-Dukić, N., Lesjak, M., 2019. Investigation of the chemical composition and biological activity of edible grapevine (Vitis vinifera L.) leaf varieties. Food Chem. 286, 686-695.

Piri, A., Sahebzadeh, N., Zibaee, A., Sendi, J.J., Shamakhi, L., Shahriari, M., 2020. Toxicity and physiological effects of ajwain (Carum copticum, Apiaceae) essential oil and its major constituents against Tuta absoluta (Meyrick) (Lepidoptera: Gelechiidae). Chemosphere. 256, 127103.

Pisano, M.B., Cosentino, S., Viale, S., Spanò, D., Corona, A., Esposito, F., Tramontano, E., Montoro, P., Tuberoso, C.I.G., Medda, R., 2016.

Biological activities of aerial parts extracts of Euphorbia characias. BioMed. Res. Int. 2016, 1538703.

Pisar, M.M., Chee, B.J., Long, I., Osman, A., 2023. Protective effects of Centella asiatica extract on spatial memory and learning deficits in animal model of systemic inflammation induced by lipopolysaccharide. Ann. Med. 55, 1-16.

Polatoglu, K., Karakoç, Ö., Yücel, Y., Demirci, B., Gören, N., Baser, K.H.C., 2015. Composition, insecticidal activity and other biological activities of Tanacetum abrotanifolium Druce. essential oil. Ind. Crops Prod. 71, 7-14.

Quettier-Deleu, C., Gressier, B., Vasseur, J., Dine, T., Brunet, C., Luyckx, M., Cazin, M., Cazin, J.C., Bailleul, F., Trotin, F., 2000. Phenolic compounds and antioxidant activities of buckwheat (Fagopyrum esculentum Moench) hulls and flour. J. Ethnopharmacol. 72, 35-42.

Rafi, M., Lim, L.W., Takeuchi, T., Darusman, L.K., 2013. Simultaneous determination of gingerols and shogaol using capillary liquid chromatography and its application in discrimination of three ginger varieties from Indonesia. Talanta. 103, 28-32.

Rahman, A., Parveen, S., Khalid, A., Farooq, A., Choudhury, M.I., 2001. Acetyl and butyrylcholinestarase-inhibiting triterpenoid alkaloids from Buxus papillosa. Phytochemistry. 58, 963-968.

Rahman, A., Wahab, A.T., Nawaz, S.A., Choudhary, I.M., 2004. New cholinesterase inhibiting bisbenzyl isoquinoline alkaloids from Cocculus pendulus. Chem. Pharm. Bull. 52, 802-806.

Rai, S., Mukherjee, K., Mal, M., Wahile, A., Saha, B.P., Mukherjee, P.K., 2006. Determination of 6-gingerol in ginger (Zingiber officinale) using high-performance thin-layer chromatography. J. Sep. Sci.29, 2292-2295.

Raman, S., Brookhouser, N., Brafman, D.A., 2020. Using human induced pluripotent stem cells (hiPSCs) to investigate the mechanisms by which

Apolipoprotein E (APOE) contributes to Alzheimer's disease (AD) risk. Neurobiol. Dis. 138, 1-17.

Ramli, R.A., Lie, W., Pyne, S.G., 2014. Alkaloids from the roots of Stichoneuron caudatum and their acetylcholinesterase inhibitory activities. J. Nat. Prod. 77, 894-901.

Ramshini, H., Ebrahim-Habibi, A., Aryanejad, S., Rad, A., 2015 Effect of Cinnamomum verum extract on the amyloid formation of hen egg-white lysozyme and study of its possible role in Alzheimer's disease. Basic Clin. Neurosci. 6, 29-37.

Rao, S.M., Bonner-Jackson, A., Nielson, K.A., Seidenberg, M., Smith, J.C., Woodard, J.L., Durgerian, S., 2015. Genetic risk for Alzheimer's disease alters the five-year trajectory of semantic memory activation in cognitively intact elders. NeuroImage. 111, 136-146.

Rao, Y.L., Ganaraja, B., Marathe, A., Manjrekar, P.A., Joy, T., Ullal, S., Pai, M.M., Murlimanju, B.V., 2021. Comparison of malondialdehyde levels and superoxide dismutase activity in resveratrol and res veratrol/donepezil combination treatment groups in Alzheimer's disease induced rat model. 3 Biotech. 11, 329.

Rawat, P., Sehar, U., Bisht, J., Selman, A., Culberson, J., Reddy, P.H., 2022. Phosphorylated tau in Alzheimer's disease and other tauopathies. Int. J. Mol. Sci. 23, 12841.

Rocha, M.I., Rodrigues, M.J., Pereira, C., Pereira, H., da Silva, M.M., da Rosa Neng, N., Nogueira, J.M.F., Varela, J., Barreira, L., Custódio, L., 2017. Biochemical profile and in vitro neuroprotective properties of Carpobrotus edulis L., a medicinal and edible halophyte native to the coast of South Africa. S. Afr. J. Bot. 111, 222-231.

Roy, R.G., Mandal, P.K., Maroon, J.C., 2023. Oxidative stress occurs prior to amyloid Aβ plaque formation and tau phosphorylation in Alzheimer's

disease: Role of glutathione and metal ions. ACS Chem. Neurosci. 14, 2944-2954.

Royal Botanic Garden, Herbarium JCB, 2019. Flora of Peninsular India. FloraPeninsular (Digital Flora of Peninsular India by Herbarium JCB), Indian Institute of Science (IISc), Bangalore. Available at: https://indiaflora-ces.iisc.ac.in/FloraPeninsular/herbsheet.php?id=2932&cat=7. (accessed 08 August 2025).

Royal Botanic Gardens, Kew, 2025. [Species name unavailable]. Plants of the World Online [POWO entry inaccessible]. Available at: https://powo.science.kew.org/taxon/urn:lsid:ipni.org:names:795279-1. (accessed 08 August 2025).

Royal Botanic Gardens, Kew, 2025. Alpinia calcarata (Haw.) Roscoe. Plants of the World Online [POWO entry not accessible]. Available at: https://powo.science.kew.org/taxon/urn:lsid:ipni.org:names:795225-1. (accessed 08 August 2025).

Royal Botanic Gardens, Kew, 2025. Alpinia purpurata (Vieill.) K.Schum. Plants of the World Online [no entry available for LSID ipni.org:names:795383-1]. Available at: https://powo.science.kew.org/taxon/urn:lsid:ipni.org:names:795383-1. (accessed 08 August 2025).

Royal Botanic Gardens, Kew, 2025. Alpinia zerumbet (Pers.) B.L.Burtt & R.M.Sm. Plants of the World Online. Available at: https://powo.science.kew.org/taxon/urn:lsid:ipni.org:names:872083-1. (accessed 08 August 2025).

Royal Botanic Gardens, Kew, 2025. Curcuma alismatifolia Gagnep. Plants of the World Online. Available at:

https://powo.science.kew.org/taxon/urn:lsid:ipni.org:names:796420-1. (accessed 08 August 2025).

Royal Botanic Gardens, Kew, 2025. Curcuma petiolata Roxb. Plants of the World Online. Available at: https://powo.science.kew.org/taxon/urn:lsid:ipni.org:names:796463-1. (accessed 08 August 2025).

Royal Botanic Gardens, Kew, 2025. Etlingera elatior (Jack) R.M.Sm. Plants of the World Online [POWO entry not available]. Available at: https://powo.science.kew.org/taxon/urn:lsid:ipni.org:names:942355-1. (accessed 08 August 2025).

Royal Botanic Gardens, Kew, 2025. Globba winitii C.H.Wright. Plants of the World Online. Available at: https://powo.science.kew.org/taxon/urn:lsid:ipni.org:names:872574-1. (accessed 08 August 2025).

Royal Botanic Gardens, Kew, 2025. Hedychium coronarium J.Koenig. Plants of the World Online. Available at: https://powo.science.kew.org/taxon/urn:lsid:ipni.org:names:796836-1. (accessed 08 August 2025).

Royal Botanic Gardens, Kew, 2025. Hedychium flavescens Carey ex Roscoe. Plants of the World Online. Available at: https://powo.science.kew.org/taxon/urn:lsid:ipni.org:names:796848-1. (accessed 08 August 2025).

Royal Botanic Gardens, Kew, 2025. Plants of the World Online. Available at: https://powo.science.kew.org/taxon/urn:lsid:ipni.org:names:798372-1. (accessed 08 August 2025).

Royal Botanic Gardens, Kew, 2025. Plants of the World Online. Available at: https://powo.science.kew.org/taxon/urn:lsid:ipni.org:names:798388-1. (accessed 08 August 2025).

Royal Botanic Gardens, Kew, 2025. Plants of the World Online. Available at: https://powo.science.kew.org/taxon/urn:lsid:ipni.org:names:798401-1. (accessed 08 August 2025).

Royal Botanic Gardens, Kew, 2025. Tapeinochilos ananassae (Hassk.) K.Schum. Plants of the World Online. Available at: https://powo.science.kew.org/taxon/urn:lsid:ipni.org:names:873025-1. (accessed 08 August 2025).

Royal Botanic Gardens, Kew, 2025. Zingiber officinale Roscoe. Plants of the World Online. Available at: https://powo.science.kew.org/taxon/urn:lsid:ipni.org:names:798364-1. (accessed 08 August 2025).

Sadaoui, N., Bec, N., Barragan-Montero, V., Kadri, N., Cuisinier, F., Larroque, C., Arab, K., Khettal, B., 2018. The essential oil of Algerian Ammodaucus leucotrichus Coss. & amp; Dur. and its effect on the cholinesterase and monoamine oxidase activities. Fitoterapia. 130, 1-5.

Sadeer, N.B., Llorent-Martínez, E.J., Bene, K., Mahomoodally, M.F., Mollica, A., Sinan, K.I., Stefanucci, A., Ruiz-Riaguas, A., Cordova, M.L.F., Zengin, G., 2019. Chemical profiling, antioxidant, enzyme inhibitory and molecular modelling studies on the leaves and stem bark extracts of three African medicinal plants. J. Pharm. Biomed. Anal. 174, 19-33.

Saenghong, N., Wattanathorn, J., Muchimapura, S., Tongun, T., Piyavhatkul, N., Banchonglikitkul, C., Kajsongkram, T., 2012. Zingiber officinale improves cognitive function of the middle-aged healthy women. Evid. Based Complement. Alternat. Med. 2012, 383062.

Saensouk, S., Saensouk, P., Pasorn, P., Chantaranothai, P., 2016. Diversity and uses of Zingiberaceae in Nam nao National park, Chaiyaphum and Phetchabun provinces, Thailand, with a new record for Thailand. Agri. Nat. Res. 50, 445-453.

Saleem, H., Zengin, G., Ahmad, I., Htar, T.T., Naidu, R., Mahomoodally, M.F., Ahemad, N., 2020. Therapeutic propensities, phytochemical composition, and toxicological evaluation of Anagallis arvensis (L.): A wild edible medicinal food plant. Food Res. Int. 137, 109651.

Saliu, J.A., Olabiyi, A.A., 2017. Aqueous extract of Securidaca longipendunculata Oliv. and Olax subscropioidea inhibits key enzymes (acetylcholinesterase and butyrylcholinesterase) linked with Alzheimer's disease in vitro. Pharm. Biol. 55, 252-257.

Sancheti, S., Sancheti, S., Um, B.-H., Seo, S.-Y., 2010. 1,2,3,4,6-penta-O-galloyl-β-d-glucose: A cholinesterase inhibitor from Terminalia chebula. S. Afr. J. Bot. 76, 285-288.

Seeliger, D., de Groot, B., 2010. Ligand docking and binding site analysis with PyMOL and Autodock/Vina. J. Comput. Aided Mol. Des. 24, 417-422.

Sener, G., Karakadıoglu, G., Ozbeyli, D., Ede, S., Yanardag, R., Sacan, Q., Aykac, A., 2022. Petroselinum crispum extract ameliorates scopolamine-induced cognitive dysfunction: Role on apoptosis, inflammation and oxidative stress. Food Sci. Hum. Wellness. 11, 1290-1298.

Senol, F.S., Ślusarczyk, S., Matkowski, A., Pérez-Garrido, A., Girón-Rodríguez, F., Cerón-Carrasco, J.P., den-Haan, H., Peña-García, J., Pérez-Sánchez, H., Domaradzki, K., 2017. Selective in vitro and in silico butyrylcholinesterase inhibitory activity of diterpenes and rosmarinic acid isolated from Perovskia atriplicifolia Benth. and Salvia glutinosa L. Phytochemistry. 133, 33-44.

Seo, S.M., Kim, J., Kang, J., Koh, S.H., Ahn, Y.J., Kang, K.S., Park, I.K., 2014. Fumigant toxicity and acetylcholinesterase inhibitory activity of 4 Asteraceae plant essential oils and their constituents against Japanese termite (Reticulitermes speratus Kolbe). Pestic. Biochem. Physiol. 113, 55-61.

Shahrajabian, M.H., Sun, W., Cheng, Q., 2019. Clinical aspects and health benefits of ginger (Zingiber officinale) in both traditional Chinese medicine and modern industry. Acta Agric. Scand, Sect. B Soil Plant Sci. 69, 546-556.

Sharifi-Rad, M., Varoni, E.M., Salehi, B., Sharifi-Rad, J., Matthews, K.R., Ayatollahi, S.A., Kobarfard, F., Ibrahim, S.A., Mnayer, D., Zakaria, Z.A., Sharifi-Rad, M., Yousaf, Z., Iriti, M., Basile, A., Rigano, D., 2017. Plants of the genus Zingiber as a source of bioactive phytochemicals: From tradition to pharmacy. Molecules. 22, 2145.

Shaukat, M.N., Nazir, A., Fallico, B., 2023. Ginger bioactives: A comprehensive review of health benefits and potential food applications. Antioxidants. 12, 2015.

Siebert, D.A., Tenfen, A., Yamanaka, C.N., de Cordova, C.M.M., Scharf, D.R., Simionatto, E.L., Alberton, M.D., 2015. Evaluation of seasonal chemical composition, antibacterial, antioxidant and anticholinesterase activity of essential oil from Eugenia brasiliensis Lam. Nat. Prod. Res. 29, 289-292.

Simunkova, M., Alwasel, S.H., Alhazza, I.M., Jomova, K., Kollar, V., Rusko, M., Valko, M., 2019. Management of oxidative stress and other pathologies in Alzheimer's disease. Arch. Toxicol. 93, 2491-2513.

Sindhoora, D., Bhattacharjee, A., 2020. A brief review on pharmacological profile of Zingiber officinale. RGUHS J. Pharm. Sci. 10, 01-06.

Singh, S., Singh, D., Ansari, A.H., Singh, S., 2025. Autonomic nervous system dysregulation in neurodegenerative diseases: Bridging brain and heart. Prog. Brain Res. 294, 47-73.

Slot, R.E., Sikkes, S.A., Berkhof, J., Brodaty, H., Buckley, R., Cavedo, E., Dardiotis, E., Guillo-Benarous, F., Hampel, H., Kochan, N.A., 2019. Subjective cognitive decline and rates of incident Alzheimer's disease and non-Alzheimer's disease dementia. Alzheimer's Dement. 15, 465-476.

Ślusarczyk, S., Senol Deniz, F.S., Abel, R., Pecio, Ł., Pérez-Sánchez, H., Cerón-Carrasco, J.P., den-Haan, H., Banerjee, P., Preissner, R., Krzyżak, E., Oleszek, W., Orhan, I.E., Matkowski, A., 2020. Norditerpenoids with selective anti-cholinesterase activity from the roots of Perovskia atriplicifolia Benth. Int. J. Mol. Sci. 21:4475.

Sonibare, M.A., Ayoola, I.O., Elufioye, T.O., 2017. Antioxidant and acetylcholinesterase inhibitory activities of leaf extract and fractions of Albizia adianthifolia (Schumach) WF Wright. J. Basic Clin. Physiol. Pharmacol. 28, 143-148.

Soodi, M., Saeidnia, S., Sharifzadeh, M., Hajimehdipoor, H., Dashti, A., Sepand, M.R., Moradi, S., 2016. Satureja bachtiarica ameliorate beta-amyloid induced memory impairment, oxidative stress and cholinergic deficit in animal model of Alzheimer's disease. Metab. Brain Dis. 31, 395-404.

Sridhar, K., Charles, A.L., 2019. In vitro antioxidant activity of Kyoho grape extracts in DPPH and ABTS assays: Estimation methods for EC50 using advanced statistical programs. Food Chem. 275, 41-49.

Suekawa, M., Ishige, A., Yuasa, K., Sudo, K., Aburada, M., Hosoya, E., 1984. Pharmacological studies on ginger. I. pharmacological actions of pungent constituents, (6)-gingerol and (6)-shogaol. J. Pharmacobiodyn. 7, 836-848.

Suganthy, N., Devi, K.P., 2016. In vitro antioxidant and anti-cholinesterase activities of Rhizophora mucronata. Pharm. Biol. 54, 118-129.

Suganthy, N., Pandian, S.K., Devi, K.P., 2009. Cholinesterase inhibitory effects of Rhizophora lamarckii, Avicennia officinalis, Sesuvium portulacastrum and Suaeda monica: Mangroves inhabiting an Indian coastal area (Vellar Estuary). J. Enzym. Inhib. Med. Chem. 24, 702-707.

Swamy, K.R.M., 2024. Origin, distribution, taxonomy, botanical description, genetics and cytogenetics, genetic diversity and breeding of ginger. Int. J. Curr. Res. 16, 29179-29201.

Tanaka, K., Arita, M., Sakurai, H., Ono, N., Tezuka, Y., 2015. Analysis of chemical properties of edible and medicinal ginger by metabolomics approach. BioMed. Res. Int. 2015, 671058.

Tao, R., Huang, S., Zhou, J., Ye, L., Shen, X., Wu, J., Qian, L., 2022. Neonatal supplementation of oleamide during suckling promotes learning ability and memory in adolescent mice. J. Nutr. 152, 889-898.

Tappayuthpijarn, P., Itharat, A., Makchuchit, S., 2011. Acetylcholinesterase inhibitory activity of Thai traditional nootropic remedy and its herbal ingredients. J. Med. Assoc. Thail. Chotmaihet. Thangphaet. 94, S183-S189.

Taqui, R., Debnath, M., Ahmed, S., Ghosh, A., 2022. Advances on plant extracts and phytocompounds with acetylcholinesterase inhibition activity for possible treatment of Alzheimer's disease. Phytomed. Plus. 2, 100184.

Teja, P.K., Mithiya, J., Kate, A.S., Bairwa, K., Chauthe, S.K., 2022. Herbal nanomedicines: Recent advancements, challenges, opportunities and regulatory overview. Phytomedicine. 96, 153890.

Tiwari, V.K., Thimmaraju, M., Malik, J.K., Gupta, V., Singh, G., 2025. Ginger (Zingiber officinale) in traditional Chinese medicine: A comprehensive review of its anti-inflammatory properties and clinical applications. Int. J. Pham. Sci. Med. 3, 32-42.

Tofighi, N., Asle-Rousta, M., Rahnema, M., Amini, R., 2021. Protective effect of alpha-linoleic acid on Aβ-induced oxidative stress, neuroinflammation, and memory impairment by alteration of α7 nAChR and NMDAR gene expression in the hippocampus of rats. Neurotoxicology. 85, 245-253.

Tripathi, S., Maier, K.G., Bruch, D., Kittur, D.S., 2007. Effect of 6-gingerol on pro-inflammatory cytokine production and costimulatory molecule expression in murine peritoneal macrophages. J. Surg. Res. 138, 209-213.

Uddin, M.N., Afrin, R., Uddin, M.J., Uddin, M.J., Alam, A., Rahman, A.A., Sadik, G., 2015. Vanda roxburghii chloroform extract as a potential source of polyphenols with antioxidant and cholinesterase inhibitory activities: Identification of a strong phenolic antioxidant. BMC Complement. Altern. Med. 15, 195.

Van Acker, Z.P., Bretou, M., Annaert, W., 2019. Endo-lysosomal dysregulations and late-onset Alzheimer's disease: Impact of genetic risk factors. Mol. Neurodegener. 14, 1-20.

Verma, R., Bisen, P.S., 2022. Ginger- A potential source of therapeutic and pharmaceutical compounds. J. Food Bioact. 18.

Verma, R.S., Joshi, N., Padalia, R.C., Singh, V.R., Goswami, P., Verma, S.K., Iqbal, H., Chanda, D., Verma, R.K., Darokar, M.P., Chauhan, A., Kandwal, M.K., 2018. Chemical composition and antibacterial, antifungal, allelopathic and acetylcholinesterase inhibitory activities of cassumunar-ginger. J. Sci. Food Agric. 98, 321-327.

Vladimir-Knežević, S., Blažeković, B., Kindl, M., Vladić, J., Lower-Nedza, A.D., Brantner, A.H., 2014. Acetylcholinesterase inhibitory, antioxidant and phytochemical properties of selected medicinal plants of the Lamiaceae family. Molecules. 19, 767-782.

Wang, H.N., Mei, W.L., Dong, W.H., Kong, F.D., Li, W., Yuan, J.Z., Dai, H.F., 2018. Two new 2-(2-Hydroxy-2-phenylethyl) chromens from agarwood originating from Aquilaria crassna. J. Asian Nat. Prod. Res. 20, 122-127.

Wang, M., Huang, W., Huang, J., Luo, Y., Huang, N., 2025. Natural bioactive compounds form herbal medicine in Alzheimer's disease: from the perspective of GSK-3β. Front. Pharmacol. 16, 1497861.

Wang, Z., Lian, W., He, J., He, X., Wang, Y., Pan, C., Li, M., Zhang, W., Liu, L., Xu, J., 2022. Cornuside ameliorates cognitive impairments in scopolamine induced AD mice: involvement of neurotransmitter and oxidative stress. J. Ethnopharmacol. 293, 1-10.

Wolfe, K., Wu, X., Liu, R.H., 2003. Antioxidant activity of apple peels. J. Agric. Food Chem. 51, 609-614.

Wong, K.K.K., Ho, M.T.W., Lin, H.Q., Lau, K.F., Rudd, J.A., Chung, R.C.K., Fung, K.P., Shaw, P.C., Wan, D.C.C., 2010. Cryptotanshinone, an acetylcholinesterase inhibitor from Salvia miltiorrhiza, ameliorates scopolamine-induced amnesia in Morris water maze task. Planta Med. 76, 228-234.

Wszelaki, N., Kuciun, A., Kiss, A.K., 2010. Screening of traditional European herbal medicines for acetylcholinesterase and butyrylcholinesterase inhibitory activity. Acta Pharm. 60, 119-128.

Xing, H., Yue, S., Qin, R., Du, X., Wu, Y., Zhangsun, D., Luo, S., 2025. Recent advances in drug development for Alzheimer's disease: A comprehensive review. Int. J. Mol. Sci. 26, 3905.

Xu, C., Apostolova, L.G., Oblak, A.L., Gao, S., 2020. Association of hypercholesterolemia with Alzheimer's disease pathology and cerebral amyloid angiopathy. J. Alzheimer's Dis. 73, 1305-1311.

Yaffe, K., Vittinghoff, E., Hoang, T., Matthews, K., Golden, S.H., Zeki Al Hazzouri, A., 2021. Cardiovascular risk factors across the life course and cognitive decline: A pooled cohort study. Neurology. 96, e2212-e2219.

Yang, H.Y., Yang, L., Wang, Y.L., Hu, Y.S., Li, Y., Qu, H., Wei, W.L., Yang, H.Y., Bi, Q.R., Zhang, J.Q., Guo, D.A., 2025. A systematic comparative analysis of ginger-related varieties from three dimensions based on HS-SPME-GC-Q-TOF MS and UHPLC-LTQ-Orbitrap MS. Food Res. Int. 203, 115820.

Yiannopoulou, K.G., Papageorgiou, S.G., 2020. Current and future treatments in Alzheimer disease: An update. J. Cent. Nerv. Syst. Dis. 12, 1179573520907397.

Youssef, P., Chami, B., Lim, J., Middleton, T., Sutherland, G.T., Witting, P., 2018. Evidence supporting oxidative stress in a moderately affected area of the brain in Alzheimer's disease. Sci. Rep. 8, 11553.

Yudthavorasit, S., Wongravee, K., Leepipatpiboon, N., 2014. Characteristic fingerprint based on gingerol derivative analysis for discrimination of ginger (Zingiber officinale) according to geographical origin using HPLC-DAD combined with chemometrics. Food Chem. 158, 101-111.

Zeng, Z., Chen, C., Situ, Y., Shen, Z., Chen, Y., Zhang, Z., Tang, C., Jiang, T., 2022. Anoectochilus roxburghii flavonoids extract ameliorated the memory decline and reduced neuron apoptosis via modulating SIRT1 signaling pathway in senescent mice. J. Ethnopharmacol. 296, 115361.

Zhang, H., Wei, W., Zhao, M., Ma, L., Jiang, X., Pei, H., Cao, Y., Li, H., 2021. Interaction between Aβ and Tau in the pathogenesis of Alzheimer's Disease. Int. J. Biol. Sci. 17, 2181-2192.

Zhang, W., Li, B., Guo, Y., Bai, Y., Wang, T., Fu, K., Sun, G., 2015. Rhamnetin attenuates cognitive deficit and inhibits hippocampal inflammatory response and oxidative stress in rats with traumatic brain injury. Cent. Eur. J. Immunol. 40, 35-41.

Zhang, X., Wang, X., Hu, X., Chu, X., Li, X., Han, F., 2019. Neuroprotective effects of a Rhodiola crenulata extract on amyloid-β peptides (Aβ1-42) - induced cognitive deficits in rat models of Alzheimer's disease. Phytomedicine. 57, 331-338.

Zhang, X.D., Liu, X.Q., Kim, Y.H., Whang, W.K., 2014. Chemical constituents and their acetyl cholinesterase inhibitory and antioxidant activities from leaves

of Acanthopanax henryi: Potential complementary source against Alzheimer's disease. Arch. Pharmacal. Res. 37, 606-616.

Zheng, X.Y., Zhang, Z.J., Chou, G.X., Wu, T., Cheng, X.M., Wang, C.H., Wang, Z.T., 2009. Acetylcholinesterase inhibitive activity-guided isolation of two new alkaloids from seeds of Peganum nigellastrum Bunge by an in vitro TLC-bioautographic assay. Arch. Pharmacal. Res. 32, 1245-1251.

Zouine, N., Ghachtouli, N.E., Abed, S.E., Koraichi, S.I., 2024. A comprehensive review on medicinal plant extracts as antibacterial agents: Factors, mechanism insights and future prospects. Sci. Afr. 26, e02395.

Received: 28 October 2022 | Revised: 2 November 2022 | Accepted: 2 November 2022

DOI: 10.1002/pca.3201

RESEARCH ARTICLE

Phytochemical Analysis WILEY

# 6-Gingerol contents of several ginger varieties of Northeast India and correlation of their antioxidant activity in respect to phenolics and flavonoids contents

Suparna Ghosh[1] | Bhaskar Das[1,2] | Pallab Kanti Haldar[1] | Amit Kar[2] | Sushil K. Chaudhary[2] | Keithellakpam Ojit Singh[2] | Pardeep K. Bhardwaj[2] | Nanaocha Sharma[2] | Pulok K. Mukherjee[1,2]

[1]School of Natural Product Studies, Department of Pharmaceutical Technology, Jadavpur University, Kolkata, India

[2]Institute of Bioresources and Sustainable Development, Imphal, India

**Correspondence**
Pulok K. Mukherjee, PhD, FAScT, FNAAS, FRSC, FNASc; Institute of Bioresources and Sustainable Development, Department of Biotechnology, Government of India, Imphal-795001, Manipur, India.
Email: naturalproductm@gmail.com and director.ibsd@nic.in

**Funding information**
Jadavpur University

## Abstract

**Introduction:** Ginger constitutes the rhizome part of the plant *Zingiber officinale* from the Zingiberaceae family. A large number of ginger varieties with high sensorial and functional quality are found in Northeast India. Hence, phytopharmacological screening of different ginger varieties is essential that will serve as a guideline in applied research to develop high-end products and improve economical margins.

**Objective:** To determine the variation in total phenolics content (TPC), total flavonoids content (TFC), and antioxidant activities and correlate that with 6-gingerol contents of different ginger varieties collected from Northeast India using Pearson's correlation analysis.

**Materials and Methods:** The TPC and TFC values were determined using standard methods. Antioxidant activities were measured using the 2,2-diphenyl-1-picrylhydrazyl (DPPH) and hydroxyl radical scavenging assays, while reversed-phase high-performance liquid chromatography (RP-HPLC) analysis was utilised for quantitative determination of 6-gingerol content.

**Results:** The result revealed that ginger variety 6 (GV6) contains the highest 6-gingerol content and TPC value showing maximum antioxidant activity, followed by GV5, GV4, GV9, GV3, GV2, GV8, GV1, and GV7. The findings also suggested that the antioxidant activity has much better correlations with TPC as compared with TFC values. Pearson's correlation analysis showed a significant correlation between 6-gingerol contents and TPC values.

**Conclusion:** This work underlines the importance of ginger varieties from Northeast India as a source of natural antioxidants with health benefits.

KEYWORDS
antioxidant activity, ginger varieties, Northeast India, Pearson's correlation, RP-HPLC

## 1 | INTRODUCTION

Ginger constitutes the rhizome part of the plant *Zingiber officinale* from the Zingiberaceae family and has been globally used as a herbal medicine and spice owing to its medical and culinary properties.[1,2] In the last few decades, ginger intake has increased, and ginger has become one of the 20 top selling herbal supplements in the USA.[3] The herb possesses pharmacological and physiological activities

  

including analgesic, anti-inflammatory, anti-diabetic, cardioprotective, anti-cancer, anti-viral, anti-hyperlipidemic and, immunomodulatory properties.[4,5] Ginger has been documented over 2500 years in the Ayurvedic, traditional Chinese, and Unani system of medicines to treat sore throats, constipation, nausea, fever, arthritis, helminthiasis, muscular aches, and infectious diseases.[4,6]

Phenols and flavonoids are major secondary metabolites, have antioxidant properties, and may protect and modulate the organ functions from oxidative stress-induced damage and reduce the progression of related disorders.[7,8] Gingerols are the pungent component that are the major contributors to therapeutic applications of ginger.[9] Additionally, ginger contains other antioxidant compounds such as terpenoids and β-carotene.[10] 6-Gingerol is present as a major metabolite along with other phenolic compounds such as 7-, 8-, and 10-gingerols; 4-, 6-, 8-, 10-, and 12-shogaols; 7-, 8-, 9-, 10-, 11-, and 13-paradols.[11,12] 6-Gingerol offers therapeutic benefits in preventing anxiety, diabetes-related complications, neurodegenerative disorders, inflammation, and oxidative damage condition in the ovary.[13,14] The Northeast region of India covers almost 50% of the country's biodiversity and is considered the geographical gateway for the majority of Indian endemic flora and fauna due to its wide range of eco-climatic and physiographic conditions.[15] This region is one of the highest ginger producing areas in the world and is emerging as India's organic ginger hub. Ginger locally known as "shing" in Manipur has been used by local herbal healers for ethnomedicinal purposes.[16] Considering its widespread uses, authentication of ginger samples remains a difficult problem because of its heterogeneity and adulteration with alike commercial samples. Thus, to maintain preferred quality during the manufacture of reliable herbal dietary supplements, a valid and proper authentication of the crude materials should be a main focus.[17] Hence, phytopharmacological screening of different ginger varieties is essential that will serve as a guideline in applied research to develop a high-end product and improve economical margins.[18]

The present study aimed to develop a validated reversed-phase high-performance liquid chromatography (RP-HPLC) method for quantitative estimation of 6-gingerol content in ginger samples together with the determination of total phenolics content (TPC) and total flavonoids content (TFC). The in vitro antioxidant activity was measured using 2,2-diphenyl-1-picrylhydrazyl (DPPH) and hydroxyl radical scavenging assay. Pearson's correlation analysis was applied to correlate the percentage 6-gingerol contents, TPC, and TFC with the antioxidant activity.

## 2 | EXPERIMENTAL

### 2.1 | Chemicals and reagents

Standard 6-gingerol (≥99%), gallic acid (≥98%), rutin (≥90%), ascorbic acid, DPPH, and $H_2O_2$ were obtained from Sigma-Aldrich (MO, USA). Folin–Ciocalteu's reagent, HPLC grade methanol (≥99.8%), and all other reagents and chemicals were acquired from Merck (Darmstadt, Germany). Ultrapure water was obtained from Milli-Q system (Millipore, Bedford, MA, USA). All the working concentrations were prepared freshly on the day of experiment.

### 2.2 | Plant material collection and authentication

Fresh rhizome part of nine different ginger varieties was collected during 16–19 August 2021 from different geographical locations of Manipur, Northeast India, as mentioned in Table 3. The botanist from the Institute of Bioresources and Sustainable Development (IBSD), Imphal, Manipur, India authenticated the plant specimens, and the voucher specimens were deposited at IBSD, Imphal, Manipur, India for future reference.

### 2.3 | Extract preparation

Freshly collected rhizomes were cleaned with distilled water and shade dried until constant weight was obtained. The dried crude samples were ground. Accurately weighed 100 g of each sample was subjected to maceration by soaking in 500 mL of 80% methanol in water for 72 h (24 h × 3) to perform exhaustive extraction.[19] The filtrate was collected using Whatman No. 1 filter paper and concentrated in rotary vacuum evaporator (IKA, Japan). It was further lyophilised (Instrumentation India, India) and packed in a container. This was stored in a refrigerator (−4°C) for further use. The percentage yields of different ginger samples are shown in Table 3.

### 2.4 | Reversed-phase HPLC instrumentation and chromatographic conditions

Quantitative analysis and separation of 6-gingerol were performed using an RP-HPLC system (Shimadzu Prominence, Kyoto, Japan) built with Shimadzu LC-20 AD ultrafast high-performance liquid chromatography (UFLC) reciprocating pumps, a rheodyne manual injector of 20 µL loop size, and a variable Shimadzu SPD-M20A Prominence photodiode array (PDA) detector. The chromatographic separation was performed in isocratic conditions with the help of a $C_{18}$ RP column (250 × 4.6 mm, 5 µm) (Phenomenex-Luna $C_{18}$, Torrance, CA, USA) maintained at 25°C. The mobile phase consisted of solvent A (methanol) and solvent B (1% acetic acid). The flow rate was maintained at 1.0 mL/min. The chromatograms were acquired at 280 nm for analysis of 6-gingerol.

Stock solutions of 1 mg/mL for each ginger variety and standard 6-gingerol were prepared in methanol. The standard stock solution was further diluted to obtain desired concentrations, and prior to injection all the sample and standard solutions were filtered through 0.45-µm syringe filters. The compound identification was performed based on retention times and UV absorption spectra.[20]

The limit of detection (LOD) and limit of quantification (LOQ) were calculated by injecting a series of standard solutions until the signal-to-noise (S/N) ratio was around 3 for LOD and 10 for LOQ,

respectively. The intra-day precision was studied by analysing six replicates of the standard on the same day, while inter-day precision was studied in triplicate on three successive days.

Relative standard deviation (%RSD) was calculated as RSD (%) = (SD/mean) × 100%. For accuracy study, three different concentrations of 6-gingerol were added to the sample and then analysed for recovery test.

## 2.5 | Quantification of TPC and TFC

Total phenolics content was determined spectrophotometrically following the protocol by Wolfe et al with slight modifications.[21] The extracts (1 mg/mL) were mixed with Folin–Ciocalteu's reagent diluted with water at a ratio of 1:10 v/v (5 mL) and 4 mL of 7.5% sodium carbonate was added to it. Lastly the mixture was vortexed for 15 s and kept at 40°C for 30 min for colour development. Absorbance was recorded at 765 nm measured using SpectraMax iD3 reader (CA, USA). Gallic acid (10–40 μg/mL) was used as standard to prepare calibration curve. The TPC was expressed in terms of gallic acid equivalent (GAE) (mg of GAE/g of dry extract).

Total flavonoids content was determined spectrophotometrically as mentioned by Quettier et al.[22] For the study, 1 mg/mL stock solution of each ginger extract and rutin were prepared in methanol. To start the reaction, 1 mL of the test extract solution was mixed with 1 mL 2% $AlCl_3$ solution in methanol. The mixture was incubated at 28°C for 1 h, and the absorbance was recorded at 415 nm using SpectraMax iD3 reader (CA, USA). A calibration curve was prepared using rutin as standard (20–80 μg/mL). The TPC values were mentioned in terms of rutin equivalent (RUE) (mg of RUE/g of dry extract).

## 2.6 | Determination of antioxidant activity

### 2.6.1 | DPPH radical scavenging assay

To evaluate the antioxidant activity, DPPH radical scavenging assay was performed in a 96-well microplate with some modification as mentioned by Das et al.[23] Briefly, 100 μL of the ginger extracts (31.25, 62.5, 125, 250, 500, and 1000 μg/mL) and standard ascorbic acid were added to 100 μL of 0.1 mM DPPH radical solution in methanol and incubated for 30 min in the dark at room temperature. Then, the absorbance was measured at 517 nm using Spectramax iD3 reader (CA, USA). The % inhibitions were calculated using the formula:

$$\%\ \text{inhibition} = \frac{(A1 - A0)}{A1} \times 100$$

(where $A_1$ = absorbance of the control and $A_0$ = absorbance of the samples).

### 2.6.2 | Hydroxyl radical scavenging assay

To determine the antioxidant activity, hydroxyl radical scavenging assay was performed in a 96-well microplate with slight modification as mentioned by Halliwell et al.[24] A reaction aliquot was prepared by mixing 10 μL of deoxyribose (28mM) in phosphate buffer (50mM, pH 7.4), 10 μL of $FeCl_3$ (1mM), 10 μL of ethylenediaamine tetra-acetic acid (EDTA) (1mM) and 10 μL of $H_2O_2$ (1mM). Then, 100 μL of ginger extract and standard ascorbic acid (31.25, 62.5, 125, 250, 500, and 1000 μg/mL) were added to each well. The mixture aliquot was incubated for 1 h at 42°C, and 50 μL of 10% TCA and 50 μL of 0.5% thiobarbituric acid (TBA) in NaOH solution (50mM) were added. The mixture aliquot was again incubated for 30 min at 42°C. The absorbance was recorded at 532 nm using SpectraMax iD3 reader (CA, USA).

The hydroxyl radical scavenging activity of the extracts was calculated using the formula:

$$\%\ \text{inhibition} = \frac{(A1 - A0)}{A1} \times 100$$

(where $A_1$ = absorbance of the control and $A_0$ = absorbance of the samples).

## 2.7 | Statistical analysis

The statistical data were implemented using GraphPad Prism software. Repeated measures analysis of variance (ANOVA) was performed (Tukey–Kramer multiple comparisons tests). The correlation of TPC, TFC, and 6-gingerol content with antioxidant capacity was done by using Pearson's correlation. All experiments were conducted in triplicate and the data obtained were expressed as mean ± standard error mean (SE). The confidence limits in this study were based on 95% ($p < 0.05$).

# 3 | RESULTS AND DISCUSSION

## 3.1 | Reversed-phase HPLC analysis

### 3.1.1 | Calibration, LOD, and LOQ

To acquire the calibration curve, six different concentrations of 6-gingerol were analysed ($n = 3$). The calibration curve was drawn by plotting the peak area vs. the quantity of each sample analysed and the obtained regression equation written as $y = ax + b$ ($x$ represents the quantity of 6-gingerol, $y$ is the peak area, and $r^2$ denotes the correlation coefficient). The calibration curve of the analyte revealed good linearity ($r^2 \geq 0.9976$) in relatively wide dynamic ranges (25–400 μg/mL) (Table 1).

**TABLE 1** Regression equation, test range, correlation coefficient, limit of detection (LOD), limit of quantification (LOQ), % recovery, and relative standard deviation (%RSD) of 6-gingerol

| Analyte | Regression equation | Test range (μg/mL) | $r^2$ | LOD (μg/mL) | LOQ (μg/mL) | Recovery (%) | RSD (%) |
|---|---|---|---|---|---|---|---|
| 6-gingerol | $y = 5745.5x + 114{,}585$ | 25–400 | 0.9976 | 0.41 | 1.25 | 93.26–104.93 | 0.59–1.57 |

**TABLE 2** Precision of the quantitative HPLC method

| Intra-day precision ($n = 6$) | | | | Inter-day precision ($n = 6$) | | | |
|---|---|---|---|---|---|---|---|
| RT (min) | | Response (AU) | | RT (min) | | Response (AU) | |
| Mean | %RSD | Mean | %RSD | Mean | %RSD | Mean | %RSD |
| 4.330 | 0.97 | 747,206 | 1.28 | 4.296 | 0.26 | 773,683 | 1.30 |
| 4.352 | 1.06 | 1,263,689 | 1.41 | 4.301 | 0.75 | 1,298,359 | 1.47 |
| 4.310 | 0.88 | 2,483,696 | 1.17 | 4.207 | 0.19 | 2,294,683 | 1.25 |

*Values are presented as mean ± SEM (n = 3).
Abbreviations: AU, absorbance units; %RSD, relative standard deviation; RT, retention time.

### 3.1.2 | Precision and accuracy

To determine precision variations, intra- and inter-day precisions were used. It can be seen that %RSD was less than 2% for the intra- and inter-day analyses, and this demonstrates good precision of this method (Table 2). The % recoveries were determined using the formula: recovery (%) = [(acquired amount − original amount) / amount spiked] × 100. The quantitative method in the present study showed suitable accuracy with the overall recoveries of the analyte ranging from 93.26% to 104.93% (Table 1).

## 3.2 | Quantitative estimation of 6-gingerol content

The chromatograms for the standard 6-gingerol and its presence in ginger hydro-alcohol extracts are presented in Figure 1(A) and 1(B-J), respectively. As mentioned in Table 3, 6-gingerol content varied from 2.88% to 8.69% w/w. The GV6 variety had the highest 6-gingerol content, followed by GV5, GV4, GV9, GV3, GV2, GV8, GV1, and GV7 (Table S1). The present study confirms an accurate, simple, rapid, and reproducible RP-HPLC method that was successfully applied to quantify 6-gingerol in ginger extracts. The quantitative analysis data showed variation in 6-gingerol content among the ginger varieties collected from different regions of Northeast India. Accumulating data suggest that geographical variations of different cultivars greatly influence the metabolite compositions in natural products. Similarly, several findings showed the difference in 6-gingerol content in ginger samples that vary with the diversity of agronomic conditions, origins, storage methods, and ages.[25–27]

## 3.3 | Total phenolics content and total flavonoids content estimation

The TPC was expressed in terms of gallic acid equivalent ($y = 0.0084x + 0.0055$; $r^2 = 0.92$). As mentioned in Table 4, the TPC in the ginger varieties varied from 12.18 ± 1.14 to 26.88 ± 1.47 mg GAE/g of extract.

The TFC present in different ginger varieties was expressed as rutin equivalent ($y = 0.0029x - 0.0051$; $r^2 = 0.98$). The amounts varied from 14.64 ± 1.54 to 24.38 ± 1.28 mg RUE/g of extract (Table 4). Phenols and flavonoids are extensively present in plant materials and are regarded as substantial contributors of antioxidants, mostly due to their distinctive redox properties.[28,29]

## 3.4 | Antioxidant activity

Free radicals play a significant role in combating many pathological manifestations. A disparity between reactive oxygen species (ROS) and the body intrinsic antioxidant capacity directed the use of dietary supplements in disease conditions.[30] Antioxidants help to protect us from several diseases caused by free radicals either by ROS scavenging or improving the antioxidant defence mechanisms.[31] The World Health Organization (WHO) has also recommended the use of antioxidants from natural sources that can delay or hinder the oxidation by inhibiting oxidative chain reactions.[32] In the present study, the electron-donating capability of plant products was measured spectrophotometrically by both DPPH and hydroxyl radical scavenging assays. Ascorbic acid was used as a standard antioxidant. The $IC_{50}$ values for all the ginger varieties were within the range of 31.24 ± 1.08 to 43.35 ± 1.68 μg/mL for DPPH and 44.52 ± 1.14 to 58.19 ± 1.48 μg/ml for hydroxyl radical scavenging assay (Figure 2). The comparative free radical scavenging assay of all the ginger varieties implied that the sample GV6 showed the highest inhibition potential with $IC_{50}$ values of 31.24 ± 1.08 for DPPH and 44.52 ± 1.14 μg/mL for hydroxyl radical scavenging assay, whereas GV7 showed the least inhibitory activity, showing $IC_{50}$ values of 43.35 ± 1.68 and 58.19 ± 1.48 μg/mL, respectively. The GV6 variety contains the highest TPC value and maximum antioxidant activity, followed by GV5, GV4, GV9, GV3, GV2, GV8, GV1, and GV7.

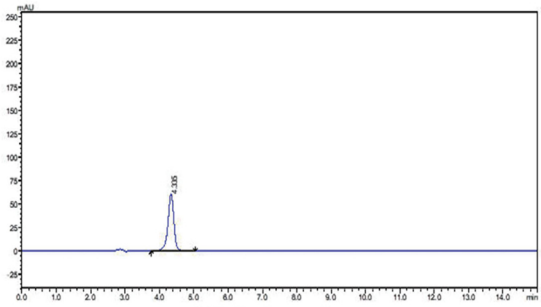


(A) 6-gingerol

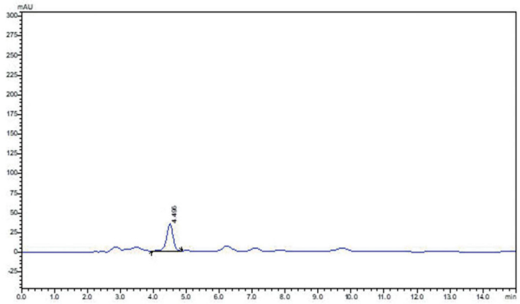


(B) GV1

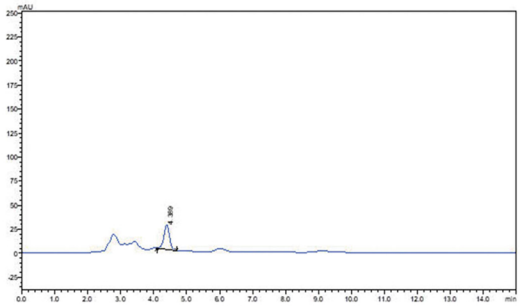


(C) GV2

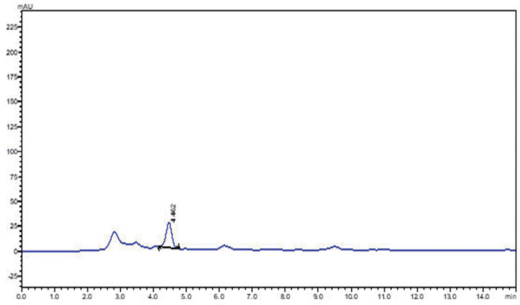


(D) GV3

**FIGURE 1** Reversed-phase high-performance liquid chromatography (RP-HPLC) chromatograms of standard 6-gingerol and its presence in different ginger varieties showing retention times (RT). (A) 6-gingerol, (B) GV1, (C) GV2, (D) GV3, (E) GV4, (F) GV5, (G) GV6 (H), GV7, (I) GV8, (J) GV9 [Colour figure can be viewed at wileyonlinelibrary.com]

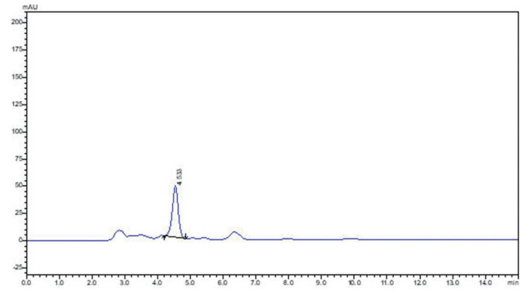

(E) GV4

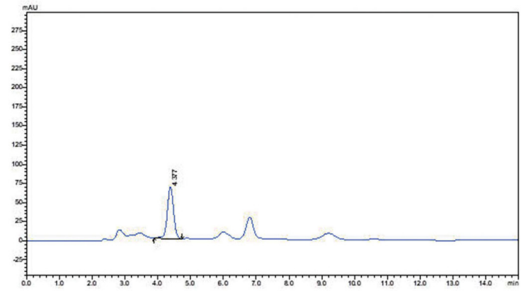

(F) GV5

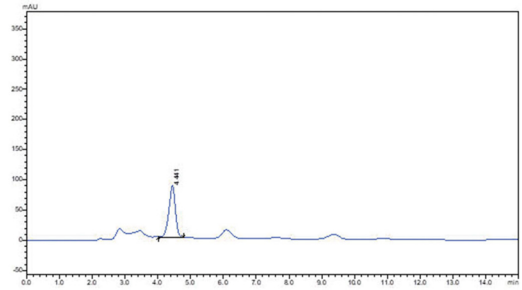

(G) GV6

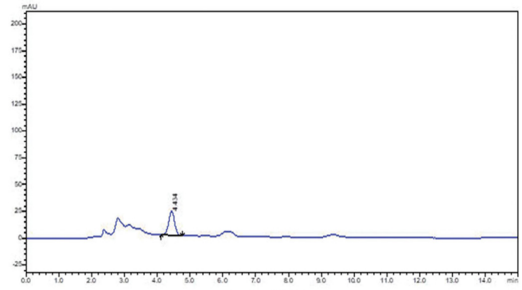

(H) GV7

**FIGURE 1** (Continued)

It may be assumed that the TPC is majorly responsible for the antioxidant activity of the selected ginger varieties.[19,25,33] The antioxidant potential of Zingiberaceae family plants is mainly known for richness in TPC and TFC as vital antioxidant constituents.[32] Plant products rich in phenolics and flavonoids are being used in the food industry, as they hinder oxidative

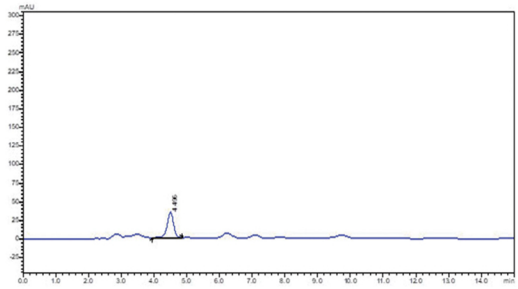

(I) GV8

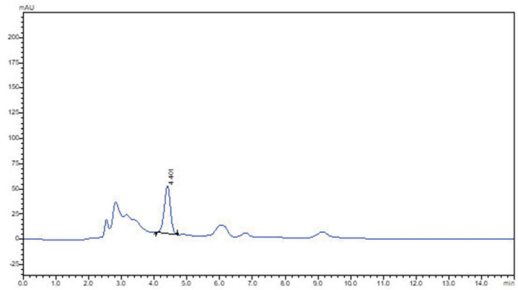

(J) GV9

**FIGURE 1** (Continued)

**TABLE 3** Sample ID, voucher specimen number, collection site, latitude, longitude, extract yield, and 6-gingerol content of ginger varieties

| Sample ID | Voucher specimen no. | Collection site | Latitude | Longitude | Extract yield (%w/w) | 6-Gingerol content (%w/w) |
|---|---|---|---|---|---|---|
| **GV1** | IBSD/C-221/A | Japhou village | 24°20′21.8″N | 25°00′22.4″E | 15.61 | 3.15 |
| **GV2** | IBSD/C-221/B | Litan village | 28°42′23.18″N | 77°27′49.89″E | 13.52 | 3.22 |
| **GV3** | IBSD/C-221/C | Mittong village | 24°22′05.6″N | 94°00′53.4″E | 17.59 | 3.27 |
| **GV4** | IBSD/U-221/A | Hatha village | 25°01′54.6″N | 94°18′58.9″E | 12.86 | 6.17 |
| **GV5** | IBSD/U-221/B | Chaora village | 25°01′55.3″N | 94°19′08.3″E | 18.15 | 8.17 |
| **GV6** | IBSD/U-221/C | Lopung village | 25°02′16.4″N | 94°18′57.5″E | 15.83 | 8.69 |
| **GV7** | IBSD/M-221/A | Tadubi village | 25°28′51.6″N | 94°08′19.9″E | 17.39 | 2.88 |
| **GV8** | IBSD/M-221/B | Tadubi village | 25°28′46.7″N | 94°08′18.2″E | 16.51 | 3.17 |
| **GV9** | IBSD/M-221/C | Punanamei village | 25°31′57.9″N | 94°09′12.9″E | 16.04 | 5.05 |

degradation of lipids and increase the quality and nutritive value of food.[34]

## 3.5 | Pearson's correlation analysis

Pearson's correlation analysis among percentage 6-gingerol contents, TPC, TFC, DPPH, and hydroxyl radical scavenging potential among all the tested ginger varieties is shown in Table 5. The study implied the quality of herb by specific compounds in light of their bioactivities. A positive correlation between phenolics and flavonoids contents with the antioxidant activities can be seen. The TPC values showed better correlation with DPPH and hydroxyl radical scavenging activity (0.532 and 0.580) compared with the TFC values (0.451 and 0.458). The percentage 6-gingerol contents also showed significant correlation (0.880) with the TPC (Figure S1). The present findings showed similar results to those previously reported by Pawar et al, namely that higher phenolics content contributed to higher antioxidant activity, and also a linear correlation can be seen between the bioactive compounds, that is, 6-gingerol and antioxidant activity.[25] However, the

**TABLE 4** Total phenolics content (TPC) and total flavonoids content (TFC) values for ginger varieties

| Sample ID | TPC (mg GAE/g of dry extract)* | TFC (mg RUE/g of dry extract)* |
|---|---|---|
| **GV1** | 14.16 ± 1.96 | 22.18 ± 1.57 |
| **GV2** | 16.47 ± 1.34 | 20.74 ± 1.37 |
| **GV3** | 18.38 ± 1.87 | 18.99 ± 1.29 |
| **GV4** | 20.12 ± 1.47 | 16.28 ± 1.82 |
| **GV5** | 23.67 ± 1.76 | 14.73 ± 1.25 |
| **GV6** | 26.88 ± 1.47 | 14.64 ± 1.54 |
| **GV7** | 12.18 ± 1.14 | 24.38 ± 1.28 |
| **GV8** | 14.86 ± 1.84 | 22.58 ± 1.16 |
| **GV9** | 19.54 ± 1.05 | 16.83 ± 1.65 |

*Values are presented as mean ± SEM ($n = 3$).
Abbreviations: GAE, gallic acid equivalent; RUE, rutin equivalent.

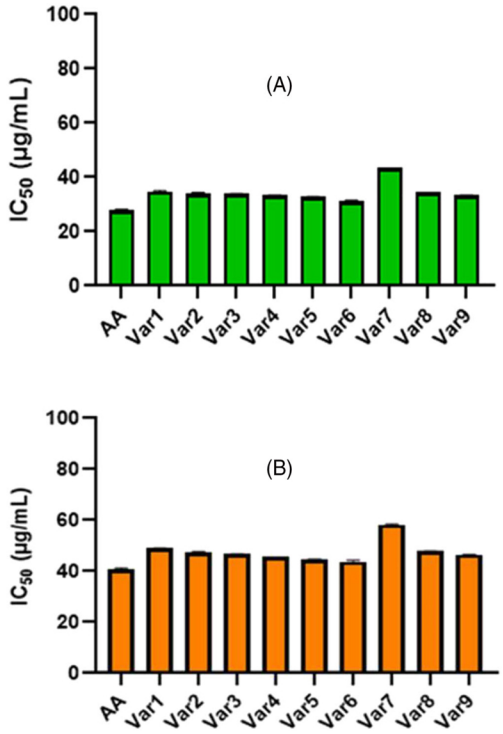


**FIGURE 2** $IC_{50}$ values f or ginger varieties by (A) 2,2-diphenyl-1-picrylhydrazyl (DPPH) and (B) hydroxyl radical scavenging assay. All values are expressed as mean ± SEM ($n = 3$) [Colour figure can be viewed at wileyonlinelibrary.com]

study also suggested that the principal antioxidant components responsible might be the phenolics.[35–37] However, a few studies showed very little correlation between the antioxidant activity and TPC values.[38,39]

**TABLE 5** Pearson's correlation coefficient analysis of total phenolics content (TPC), total flavonoids content (TFC), and 6-gingerol content with 2,2-diphenyl-1-picrylhydrazyl (DPPH) and hydroxyl radical scavenging activity of nine ginger varieties

| Analytes | TPC | TFC | DPPH | Hydroxyl |
|---|---|---|---|---|
| **TPC** | 1.000 | 0.912*** | 0.532** | 0.580** |
| **TFC** | 0.912*** | 1.000 | 0.451** | 0.458** |
| **% 6-Gingerol** | 0.880*** | 0.810*** | 0.318ns | 0.374ns |

nsnot significant,
**significant at $p < 0.05$,
***extremely significant at $p < 0.001$.

Pharmacokinetics study of *Z. officinale* showed that gingerols and shogaols are taken up by the body rapidly and metabolised extensively. Some researchers reported that the compound has an $LD_{50}$ value of 250 mg/kg.[40,41] Thus proper guidelines are essential for its use in food or drug industry because ginger compounds may exert toxic effects at higher doses.[42]

In summary, the study showed the variation and correlation between TPC, TFC, and antioxidant potentials of ginger varieties from the Northeast region of India with 6-gingerol content as major metabolite. The developed analytical method for quantitative evaluation will help to minimise the unwanted effects of the herbal supplements as content variation of metabolites considering the diversity of geographical conditions. Pearson's correlation analysis also implies that TPC values show much better correlation with the antioxidant activities than TFC values. This suggests that phenolics are majorly responsible for the antioxidant properties. This approach may be convenient for antioxidant studies, as it can enable a more thoughtful understanding of results from biological assays, instrumental analyses, and their correlation to acquire more comprehensive explanations.

## ACKNOWLEDGEMENTS

The authors are thankful to the State Government Research Fellowship Scheme of Jadavpur University, West Bengal for providing financial support. The authors are also thankful to the Institute of Bioresources and Sustainable Development, Imphal, Manipur India for providing necessary help and support through the IBSD-JU joint collaboration programme.

## CONFLICTS OF INTEREST

The authors declare that they have no conflicts of interest.

## DATA AVAILABILITY STATEMENT

The data that support the findings of this study are available as supporting information.

## ORCID

*Suparna Ghosh* https://orcid.org/0000-0002-8596-7485
*Pallab Kanti Haldar* https://orcid.org/0000-0001-8734-7346
*Sushil K. Chaudhary* https://orcid.org/0000-0002-7964-0021
*Pardeep K. Bhardwaj* https://orcid.org/0000-0002-3681-3391

## REFERENCES


1. Abolaji AO, Ojo M, Afolabi TT, Arowoogun MD, Nwawolor D, Farombi EO. Protective properties of 6-gingerol-rich fraction from *Zingiber officinale* (ginger) on chlorpyrifos-induced oxidative damage and inflammation in the brain, ovary and uterus of rats. *Chem Biol Interact*. 2017;270:15-23. doi:10.1016/j.cbi.2017.03.017
2. Ko MJ, Nam HH, Chung MS. Conversion of 6-gingerol to 6-shogaol in ginger (*Zingiber officinale*) pulp and peel during subcritical water extraction. *Food Chem*. 2019;270:149-155. doi:10.1016/j.foodchem.2018.07.078
3. Salmon CNA, Bailey-Shaw YA, Hibbert S, Green C, Smith AM, Williams LAD. Characterisation of cultivars of Jamaican ginger (*Zingiber officinale* roscoe) by HPTLC and HPLC. *Food Chem*. 2012;131(4):1517-1522. doi:10.1016/j.foodchem.2011.09.115
4. Srinivasan K. Ginger rhizomes (*Zingiber officinale*): a spice with multiple health beneficial potentials. *PharmaNutrition*. 2017;5(1):18-28. doi:10.1016/j.phanu.2017.01.001
5. Menon V, Elgharib M, El-awady R, Saleh E. Ginger: from serving table to salient therapy. *Food Biosci*. 2021;41:100934. doi:10.1016/j.fbio.2021.100934
6. Sharifi-Rad M, Varoni EM, Salehi B, et al. Plants of the genus *Zingiber* as a source of bioactive phytochemicals: from tradition to pharmacy. *Molecules*. 2017;22(12):2145. doi:10.3390/molecules22122145
7. Xia JX, Zhao BB, Zan JF, Wang P, Chen LL. Simultaneous determination of phenolic acids and flavonoids in *Artemisiae argyi* folium by HPLC-MS/MS and discovery of antioxidant ingredients based on relevance analysis. *J Pharm Biomed Anal*. 2019;175:112734. doi:10.1016/j.jpba.2019.06.031
8. Deng M, Jia X, Dong L, et al. Structural elucidation of flavonoids from Shatianyu (*Citrus grandis* L. Osbeck) pulp and screening of key antioxidant components. *Food Chem*. 2022;366:130605. doi:10.1016/j.foodchem.2021.130605
9. Sanwal SK, Rai N, Singh J, Buragohain J. Antioxidant phytochemicals and gingerol content in diploid and tetraploid clones of ginger (*Zingiber officinale* roscoe). *Sci Horti*. 2010;124(2):280-285. doi:10.1016/j.scienta.2010.01.003
10. Ghafoor K, Juhaimi FA, Ozcan MM, Uslu N, Babiker EE, Ahmed IAM. Total phenolics, total carotenoids, individual phenolics and antioxidant activity of ginger (*Zingiber officinale*) rhizome as affected by drying methods. *LWT*. 2020;126:109354. doi:10.1016/j.lwt.2020.109354
11. Magdy AM, Fahmy EM, Al-Ansary AERMF, Awad G. Improvement of 6-gingerol production in ginger rhizomes (*Zingiber officinale* roscoe) plants by mutation breeding using gamma irradiation. *Appl Radiat Isot*. 2020;162:109193. doi:10.1016/j.apradiso.2020.109193
12. Ali BH, Blunden G, Tanira MO, Nemmar A. Some phytochemical, pharmacological and toxicological properties of ginger (*Zingiber officinale* roscoe): a review of recent research. *Food Chem Toxicol*. 2008;46(2):409-420. doi:10.1016/j.fct.2007.09.085
13. Sampath C, Zhu Y, Sang S, Ahmedna M. Bioactive compounds isolated from apple, tea, and ginger protect against dicarbonyl induced stress in cultured human retinal epithelial cells. *Phytomedicine*. 2016;23(2):200-213. doi:10.1016/j.phymed.2015.12.013
14. Simon A, Darcsi A, Kery A, Riethmuller E. Blood-brain barrier permeability study of ginger constituents. *J Pharm Biomed Anal*. 2020;177:112820. doi:10.1016/j.jpba.2019.112820
15. Roy A, Das SK, Tripathi AK, Singh NU, Barman HK. Biodiversity in north East India and their conservation. *Prog Agric*. 2015;15(2):182-189. doi:10.5958/0976-4615.2015.00005.8
16. Tushar B, Basak S, Sarma GC, Rangan L. Ethnomedical uses of Zingiberaceous plants of Northeast India. *J Ethnopharmacol*. 2010;132(1):286-296. doi:10.1016/j.jep.2010.08.032
17. Jiang H, Xie Z, Koo H, Mclaughlin SP, Timmermann B, Gang D. Metabolic profiling and phylogenetic analysis of medicinal *Zingiber* species: tools for authentication of ginger (*Zingiber officinale* Rosc.). *Phytochemistry*. 2006;67(15):1673-1685. doi:10.1016/j.phytochem.2005.08.001
18. Shukla A, Goud VV, Das C. Antioxidant potential and nutritional compositions of selected ginger varieties found in Northeast India. *Ind Crops Prod*. 2019;128:167-176. doi:10.1016/j.indcrop.2018.10.086
19. Ezez D, Tefera M. Effects of solvents on total phenolic content and antioxidant activity of ginger extracts. *J Chem*. 2021;2021:6635199-5. doi:10.1155/2021/6635199
20. Harwansh RK, Mukherjee K, Bhadra S, et al. Cytochrome P450 inhibitory potential and RP-HPLC standardization of *trikatu*- a *Rasayana* from Indian *Ayurveda*. *J Ethnopharmacol*. 2014;153(3):674-681. doi:10.1016/j.jep.2014.03.023
21. Wolfe K, Wu X, Liu RH. Antioxidant activity of apple peels. *J Agric Food Chem*. 2003;51(3):609-614. doi:10.1021/jf020782a
22. Quettier-Deleu D, Gressier B, Vasseur J, et al. Phenolic compounds and antioxidant activities of buckwheat (*Fagopyrum esculentum* Moench) hulls and flour. *J Ethnopharmacol*. 2000;72(1–2):35-42. doi:10.1016/S0378-8741(00)00196-3
23. Das B, Kar A, Matsabisa MG, Mukherjee PK. Anti-cholinesterase potential of standardized extract of PHELA a traditional south African medicine formulation. *J Herb Med*. 2020;22:100348. doi:10.1016/j.hermed.2020.100348
24. Halliwell B, Gutteridge JMC, Aruoma OI. The deoxyribose method: a simple "test-tube" assay for determination of rate constants for reactions of hydroxyl radicals. *Anal Biochem*. 1987;165(1):215-219. doi:10.1016/0003-2697(87)90222-3
25. Pawar N, Pai S, Nimbalkar M, Dixit G. RP-HPLC analysis of phenolic antioxidant compound 6-gingerol from different ginger cultivars. *Food Chem*. 2011;126(3):1330-1336. doi:10.1016/j.foodchem.2010.11.090
26. Bailey-Shaw YA, Williams LAD, Junor GAO, et al. Changes in the contents of oleoresin and pungent bioactive principles of Jamaican ginger (*Zingiber officinale* roscoe.) during maturation. *J Agric Food Chem*. 2008;56(14):5564-5571. doi:10.1021/jf072782m
27. Rafi M, Lim LW, Takeuchi T, Darusman LK. Simultaneous determination of gingerols and shogaol using capillary liquid chromatography and its application in discrimination of three ginger varieties from Indonesia. *Talanta*. 2013;103:28-32. doi:10.1016/j.talanta.2012.09.057
28. Muflihah YM, Gollavelli G, Ling YC. Correlation study of antioxidant activity with phenolic and flavonoid compounds in 12 Indonesian indigenous herbs. *Antioxidants*. 2021;10(10):1530. doi:10.3390/antiox10101530
29. Li M, Pare PW, Zhang J, et al. Antioxidant capacity connection with phenolic and flavonoid content in Chinese medicinal herbs. *Rec Nat Prod*. 2018;12(3):239-250. doi:10.25135/rnp.24.17.08.138
30. Gulcin I. Antioxidant activity of food constituents: an overview. *Arch Toxicol*. 2012;86(3):345-391. doi:10.1007/s00204-011-0774-2
31. Lobo V, Patil A, Phatak A, Chandra N. Free radicals, antioxidants and functional foods: impact on human health. *Pharmacogn Rev*. 2010;4(8):118-126. doi:10.4103/0973-7847.70902
32. Mastorci F, Vassalle C, Chatzianagnostou K, et al. Undernutrition and overnutrition burden for diseases in developing countries: the role of oxidative stress biomarkers to assess disease risk and interventional strategies. *Antioxidants*. 2017;6(2):41. doi:10.3390/antiox6020041
33. Ali AMA, El-Nour MEM, Yagi SM. Total phenolic and flavonoid contents and antioxidant activity of ginger (*Zingiber officinale* Rosc.) rhizome, callus and callus treated with some elicitors. *J Genet Eng Biotechnol*. 2018;16(2):677-682. doi:10.1016/j.jgeb.2018.03.003
34. Saeed N, Khan MR, Shabbir M. Antioxidant activity, total phenolic and total flavonoid contents of whole plant extracts *Torilis leptophylla* L. *BMC Complement Alternat Med*. 2012;12(1):221. doi:10.1186/1472-6882-12-221

35. Li HB, Wong CC, Cheng KW, Chen F. Antioxidant properties *in vitro* and total phenolic contents in methanol extracts from medicinal plants. *LWT*. 2008;41(3):385-390. doi:10.1016/j.lwt.2007.03.011
36. Mwamatopea B, Tembo D, Chikowe I, Kampira E, Nyirenda C. Total phenolic contents and antioxidant activity of *Senna singueana*, *Melia azedarach*, *Moringa Oleifera* and *Lannea discolor* herbal plants. *Sci Afr*. 2020;9:e00481.
37. Lfitat A, Zejli H, Bousraf FZ, et al. Comparative assessment of total phenolics content and *in vitro* antioxidant capacity variations of macerated leaf extracts of *Olea europaea* L. and *Argania spinosa* (L.) Skeels. *Mater Today: Proc*. 2019;45(8):7271-7277.
38. Chen X, Wang H, Huang X, et al. Efficient enrichment of total flavonoids from kal(*Brassica oleracea* L. *var. acephala* L.) extracts by NKA-9 resin and antioxidant activities of flavonoids extract *in vitro*. *Food Chem*. 2022;374:131508. doi:10.1016/j.foodchem.2021.131508
39. Hou M, Hu W, Xiu Z, et al. Efficient enrichment of Total flavonoids from *Pteris ensiformis* Burm extracts by macroporous adsorption resins and *in vitro* evaluation of antioxidant and Antiproliferative activities. *J Chromatogr B*. 2020;1138:121960.
40. Suekawa M, Ishige A, Yuasa K, Sudo K, Aburada M, Hosoya E. Pharmacological studies on ginger. I. Pharmacological actions of pungent constituents, (6)-gingerol and (6)-shogaol. *J Pharmacobiodyn*. 1984;7(11):836-848. doi:10.1248/bpb1978.7.836
41. Li Y, Tran VH, Duke CC, Roufogalis BD. Preventive and protective properties of *Zingiber officinale* (ginger) in diabetes mellitus, diabetic complications, and associated lipid and other metabolic disorders: a brief review. *Evid Based Complement Alt Med*. 2012;2012:516870.
42. Chiaramonte M, Bonaventura R, Costa C, Zito F, Russo R. [6]-Gingerol dose-dependent toxicity, its role against lipopolysaccharide insult in sea urchin (*Paracentrotus lividus* Lamarck), and antimicrobial activity. *Food Biosci*. 2021;39:100833. doi:10.1016/j.fbio.2020.100833

## SUPPORTING INFORMATION

Additional supporting information can be found online in the Supporting Information section at the end of this article.

**How to cite this article:** Ghosh S, Das B, Haldar PK, et al. 6-Gingerol contents of several ginger varieties of Northeast India and correlation of their antioxidant activity in respect to phenolics and flavonoids contents. *Phytochemical Analysis*. 2023;1-10. doi:10.1002/pca.3201

Metabolic Brain Disease (2025) 40:101
https://doi.org/10.1007/s11011-025-01535-8

RESEARCH

# Mechanistic insight into neuroprotective effect of standardized ginger chemo varieties from Manipur, India in scopolamine induced learning and memory impaired mice

**Suparna Ghosh[1] · Bhaskar Das[2] · Sandipan Jana[1] · Keithellakpam Ojit Singh[2] · Nanaocha Sharma[2] · Pulok K. Mukherjee[1,2] · Pallab Kanti Haldar[1]**

Received: 11 September 2024 / Accepted: 10 January 2025


**Abstract**

Alzheimer's disease is a complex neurodegenerative disease characterized by progressive decline in cognitive function and behaviour. Ginger is the rhizome of the plant *Zingiber officinale* Roscoe, has been an important ingredient of many Ayurveda formulations to treat neurological disorders. The present study aims to estimate the variation of 6-gingerol content in nine different ginger samples collected from Manipur, India, investigate the neuroprotective potential of the most potent ginger sample against scopolamine-induced cognitively impaired mice, and validate the therapeutic claim by molecular docking analysis. High Performance Thin Layer Chromatography (HPTLC) analysis suggested that the sample GV6 had the highest 6-gingerol content with potent in vitro acetylcholnesterase (AChE) (IC50 = 336.10 µg/mL) and butyrylcholinesterase (BChE) (IC50 = 411.73 µg/mL) enzyme inhibitory activity. The neuroprotective potential of GV6 was tested in scopolamine-induced cognitively impaired mice (200 and 400 mg/kg). The behavioral analysis showed that GV6 alleviated the spatial recognition, and short-term and long-term memory in the experimental mice model. GV6 significantly improved brain AChE and BChE activity, acetylcholine (ACh) level, markedly alleviated the antioxidant parameters, and reversed the neuroinflammation. Brain histopathological observations confirmed the presence of organized nerve fibers, improvement of neuronal cell density, and reverse the nucleus shrinkage. Further molecular docking analysis showed that 6-gingerol and galantamine exhibited stable interaction with AChE (-7.5 and −7.3 kcaL/moL) and BChE (-7.3 and −8.5 kcaL/moL). The present study emphasizes the quality-related therapeutic importance of ginger samples from Northeast India and demonstrates that administration of GV6 may improve brain cognitive functions by restoring neurotransmitter levels and inflammatory and antioxidant parameters in scopolamine-induced cognitively impaired mice.

**Keywords** Ginger · Neuroprotection · Memory impairment · Inflammation · Oxidative stress · Cognition · 6-gingerol · Scopolamine

✉ Pallab Kanti Haldar
pallab.haldar@jadavpuruniversity.in;
pallabkanti2007@gmail.com

Suparna Ghosh
supghosh8@gmail.com

Bhaskar Das
mailmebhaskar007@gmail.com

Sandipan Jana
sandipan.jana95@gmail.com

Keithellakpam Ojit Singh
ojit1999@gmail.com

Nanaocha Sharma
sharma.nanaocha@gmail.com

Pulok K. Mukherjee
naturalproductm@gmail.com; pulok.m@ibsd.gov.in

[1] School of Natural Product Studies, Department of Pharmaceutical Technology, Jadavpur University, Kolkata 700 032, India

[2] Department of Biotechnology, BRIC-Institute of Bioresources and Sustainable Development (BRIC-IBSD), Government of India, Imphal, Manipur 795001, India

Published online: 15 January 2025

## Introduction

Memory is a fundamental component of cognition, playing a crucial role in various cognitive processes such as learning, problem solving, reasoning, and decision-making. Short-term memory allows for the temporary holding of information necessary for immediate tasks, while long-term memory includes the information storage over an extended period, enabling the accumulation of knowledge and experiences that shape the cognitive abilities (Ano et al. 2019; Norris 2017). Disruptions in memory, therefore, can have profound effects on overall cognitive functioning, causing Alzheimer's disease (AD)-like symptoms or other forms of dementia (Avila-Villanueva et al. 2022). Cholinergic inhibitors are mostly used to improve the cognitive dysfunction in AD patients by improving the cholinergic functioning (Easton et al. 2013). Oxidative stress is another significant component causing neuronal deterioration, resulting in mild cognitive impairment that typically develops to dementia (Ionescu-Tucker and Cotman 2021). Several findings have suggested that chronic neuroinflammation driven by tumor necrosis factor-alpha (TNF-α) accelerates the accumulation of amyloid-β plaques and neurofibrillary tangles, further impairing cognitive functions (Sartori et al. 2012; Hennessy et al. 2017).

Medicinal plants have served as the foundation of healthcare worldwide since the earliest days of civilization. The discovery of early pharmaceuticals from plant resources, such as galantamine and physostigmine, marked a remarkable achievement in the field of medicine against AD (Orhan and Senol 2013). Other drug candidates like huperzine A, resveratrol, nicotine, and curcumin from natural resources are under different phases of clinical trial to treat AD (Ayaz et al. 2019).

Ginger is the rhizome of *Zingiber officinale* Roscoe belongs to the Zingiberaceae family. It is one of the ingredients in the memory-enhancing Ayurveda formulation, Sarasvata ghrita (Shelar et al. 2018). Besides the cognition improvement properties, it has also been mentioned in Unani and traditional Persian medicine to treat various disorders such as diabetes, fever, nausea, sorethroats, constipation, nerve problems, infections, stroke, worm infestation, dyspepsia, gingivitis etc. (Talebi et al. 2021). A study by Okesola et al. mentioned that co-administration of ginger extract restored the antioxidant parameters in lead-induced brain damage of rodents (Okesola et al. 2019). Another study mentioned that the presence of phenolics and anthocyanins may contribute to its neuroprotective effects (Fadaki et al. 2017). The plant is reported to contain gingerols, shogaols, gingerdione, zingerones, paradol, pinene, cumene, camphene, bisabolene, borneol, and zingiberol as major metabolites (Liu et al. 2019). Among them, 6-gingerol is the major pungent phenol contributing to its various pharmacological activities (Promdam and Panichayupakaranant 2022).

In this context, the present study aimed to estimate the variation of 6-gingerol content in several ginger chemovarieties by HPTLC analysis and in vitro investigation of AChE and BChE enzyme inhibitory potential followed by in vivo validation of the neuroprotective mechanism of the potent ginger variety in scopolamine-induced cognitively impaired mice model through assessment of brain cholinergic functions, inflammation, and antioxidant parameters. Additionally, in silico molecular docking analysis was performed to understand the interaction potential of 6-gingerol with AChE and BChE.

## Materials and methods

### Chemical and reagents

Standard 6-gingerol (≥99%), ascorbic acid, (2,2′-azino-bis-(3-ethylbenzothiazoline-6-sulfonic) acid) (ABTS), scopolamine, donepezil, acetyl thiocholine iodide (ATCI), butyryl thiocholine iodide (BTCI), 5,5′-dithiobis [2-nitrobenzoic acid] (DTNB), galantamine, and AChE from bovine erythrocytes, BChE from equine serum, and mouse TNF-α enzyme linked immunosorbent assay (ELISA) kit were obtained from Sigma Aldrich, St. Louis (USA).

### Procurement of plant material and extract preparation

The fresh rhizomes of 09 different ginger samples were collected from different locations of Manipur, India which are named as GV1, GV2, GV3, GV4, GV5, GV6, GV7, GV8, and GV9 (Table 1). All the collected plant samples were authenticated by the botanist Dr. Biseshwori Thongam, Scientist E, Plant Systematic and Conservation Laboratory, Institute of Bioresources and Sustainable Development (IBSD), Imphal, Manipur, India. The voucher specimens were maintained in the herbarium at IBSD, Imphal, Manipur, India, for future reference. The details of the samples, voucher specimen no., collection site and latitude, longitude are mentioned in table no. 1. After grinding the dried crude ginger samples, 100 g of each sample was macerated using 500 mL of 80% methanol for 72 h. Then the mixtures were filtered through Whatman filter paper and the filtrate was concentrated by a rotary vacuum evaporator (IKA, Japan). The lyophilized (Instrumentation India, India) extracts were maintained in a refrigerator at 4°C for further use (Ghosh et al. 2023).

**Table 1** Sample code, their respective voucher specimen no., collection site, latitude/longitude, 6-gingerol content (% w/w) present in the ginger samples by HPTLC analysis and in vitro AChE and BChE $IC_{50}$ values. Data are presented as mean ± SEM ($n = 3$)

| Sample name | Voucher specimen no. | Collection site | Latitude/Longitude | 6-gingerol content | AChE (µg/mL) | BChE (µg/mL) |
|---|---|---|---|---|---|---|
| Galantamine | - | - | - | - | 24.2 ± 1.85 | 35.95 ± 3.05 |
| GV1 | IBSD/C-221/A | Japhou village | 24°20'21.9"N/25°00'22.4"E | 3.83 | 474.46 ± 1.87 | 589.95 ± 3.04 |
| GV2 | IBSD/C-221/B | Litan village | 28°42'23.8"N/77°27'49.89"E | 4.27 | 393.91 ± 2.20 | 546.64 ± 4.88 |
| GV3 | IBSD/C-221/C | Mittong village | 24°22'05.6"N/94°00'53.4"E | 4.6 | 384.59 ± 1.89 | 529.53 ± 3.58 |
| GV4 | IBSD/U-221/A | Hatha village | 25°01'54.6"N/94°18'58.9"E | 4.16 | 371.10 ± 3.22 | 486.94 ± 1.18 |
| GV5 | IBSD/U-221/B | Chaora village | 25°01'55.3"N/94°19'08.3"E | 4.41 | 368.02 ± 0.97 | 471.36 ± 2.18 |
| GV6 | IBSD/U-221/C | Lopung village | 25°02'16.4"N/94°18'57.5"E | 6.27 | 305.19 ± 1.81 | 411.73 ± 4.03 |
| GV7 | IBSD/M-221/A | Tadubi village | 25°28'51.6"N/94°08'19.9"E | 2.71 | 521.46 ± 2.38 | 602.81 ± 4.61 |
| GV8 | IBSD/M-221/B | Tadubi village | 25°28'46.7"N/94°08'18.2"E | 3.36 | 409.94 ± 1.29 | 576.10 ± 2.53 |
| GV9 | IBSD/M-221/C | Punanamei village | 25°31'57.9"N/94°09'12.9"E | 4.74 | 378.37 ± 2.16 | 518.19 ± 2.73 |

## HPTLC analysis

The variation of 6-gingerol content within the ginger samples was determined using HPTLC (Camag, Muttenz, Switzerland) as mentioned by Alqasoumi 2009. The stock solution for standard 6-gingerol (1 mg/mL) and nine ginger extracts (GV1-GV9) (10 mg/mL) were prepared in methanol. All the solutions were vortexed till dissolved and filtered using a 0.45 µm syringe filter. The standard calibration curve was prepared in a concentration range of 0.2–1 µg/mL. The solutions were applied on 10 × 20 cm aluminium-backed HPTLC plates of silica gel 60 F254 (E.Merck, Germany) at a band length of 6 mm using a Linomat V applicator. The plate was developed in a twin-trough chamber using a suitable mobile phase. After development, the plate was scanned by CAMAG TLC scanner 4 at 280 nm. For photo documentation, the developed plate was derivatized using an anisaldehyde-sulphuric acid reagent. The quantity of the standard within the extract samples was assessed by a calibration curve using linear regression through visionCATS® software.

## Cholinesterase enzyme inhibition assay

The assay was performed as described in a previous report by Das et al. (2023). Briefly, 3 mM DTNB, 15 mM ATCI, or BTCI were mixed with the ginger samples and standard galantamine, dissolved in phosphate buffer pH 8.0 (at concentrations of 50–500 µg/mL and 10–50 µg/mL, respectively). After that, the plate was incubated for 10 min at 37°C followed by the addition of AChE (2 U/mL) or BChE (1 U/mL) to each well, respectively. The absorbance was measured at 405 nm at an interval of 13s for 78s.

## Animals and ethics

Swiss albino adult mice (8–12 weeks) of either sex, weighing 23–25 g, were purchased from West Bengal Livestock Development Co. Ltd. (Kalyani, West Bengal, India). All animal experiments performed were approved by the Institutional Animal Ethics Committee, The Committee for the Purpose of Control and Supervision of Experiments on Animals (Approval Number: JU/IAEC-22/10). The animals were acclimatized under controlled conditions (22 ± 2°C; 60 ± 10% relative humidity; 12 h light-dark cycle; water and food *ad libitum*) in the animal house, Jadavpur University, Kolkata for one week prior to the experiments.

Based on the activity it presented on the inhibition of AChE and BChE and its concentration of 6-gingerol, GV6 was further validated for its neuroprotective potential in scopolamine induced learning and memory impaired mice model. An acute oral toxicity study was performed according to the Organization for Economic Cooperation and Development (OECD) guideline 425 (OECD (2022)). Female mice ($n = 6$) were orally administered GV6 at a dose of 2000 mg/kg and a control group of female mice ($n = 6$) were orally administered water at a dose of 10 mL/kg. From the study, it was found that up to 2000 mg/kg body weight (b.w.) of the GV6 extract didn't show any sign of mortality. Details are given in Online Resource Tables S1 and S2. In this study, the control group referred as reference group.

## Drug administration

For the in vivo study, 30 mice were divided into 5 groups ($n = 6$, 3 female and 3 male), as follows: Group I (Ctrl): Control [received distilled water, p.o. (per os) + 0.9% saline solution, intraperitoneal (i.p.)]; Group II (Scop): Scopolamine (1 mg/kg, b.w., i.p.); Group III (Scop + GV6-LD): Scopolamine (1 mg/kg, b.w., i.p.) + test sample, low-dose (200 mg/kg, b.w., p.o.); Group IV (Scop + GV6-HD): Scopolamine (1 mg/kg, b.w., i.p.) + test sample, high-dose (400 mg/kg, b.w., p.o.); Group V (Scop + Dnp): Scopolamine (1 mg/kg, b.w., i.p.) + donepezil (3 mg/kg, b.w., p.o.).

Donepezil was used as the reference standard drug, and scopolamine was used as a cognitive impairment-inducing agent (Wang et al. 2022). After one week of adaptation, oral administration of donepezil and test samples was continued

from the 8th day to the end of the experiment, as shown in Fig. 1. Scopolamine was administered from the 13th day to the last day of the experiment after 20 min of the test samples and donepezil administration. Test samples (20 and 40 mg/mL) and donepezil (0.03 mg/mL) were administered with a volume of 10 mg/mL, b.w. (p.o.).

## Behavioral test

The behavioral tests were conducted with a one-day interval between each test to prevent any unsolicited influence of preceding data on subsequent behavioral performance after 30 min of dosing (Nazari et al. 2022). The spatial memory was evaluated using the Morris water maze (from days 13 to 18) and the Y maze test for short-term memory (on day 20), followed by an assessment of long-term and cognitive memory using the novel object recognition test (on days 22nd and 23rd ) (Mohamed et al. 2023).

### Morris water maze test

The maze comprised of a circular tank (length 100 cm × height 50 cm), divided with four conjectural equal quadrants, and labelled as North, South, East and West, respectively. One small transparent platform of 12 cm diameter was hidden in the center of the southeast quadrant, having holes on the top for easy grasp of the mice. The maze was filled with water, and non-toxic black dye was used to cover the maze. To achieve an opaque appearance, skim milk powder was introduced into the maze water. The water temperature was maintained at 25 ± 1°C, and the water level was adjusted 1 cm above the hidden platform. The position of the hidden platform remained the same throughout the experiment. Some visual cues were present at the room during the experiment to facilitate the orientation sense of the mice. A camera was mounted at the top of the water maze tank to track the movement of the experimental mice, which were converted to digital form by using a video tracking system (ANY-maze software, San Diego, USA).

**Acquisition phase** Throughout the five consecutive days, every mouse were underwent the test four times daily, with a 10-minute interval between each session. Each mouse was placed into the water maze facing the wall, and each time starting from a different quadrant. The mice were allowed to search the platform for 60 s and allowed to stand on the platform for 5s and recorded its escape latency along with the escape routes. Throughout the acquisition phase, mice can escape from swimming by climbing up the hidden platform. The escape behavior will allow the mice to learn the spatial location of the hidden platform from any point in the four quadrants. Each day, the starting positions were rearranged in a different order. The animals are gently guided to the platform if they cannot find it and allowed to stand for 15 s

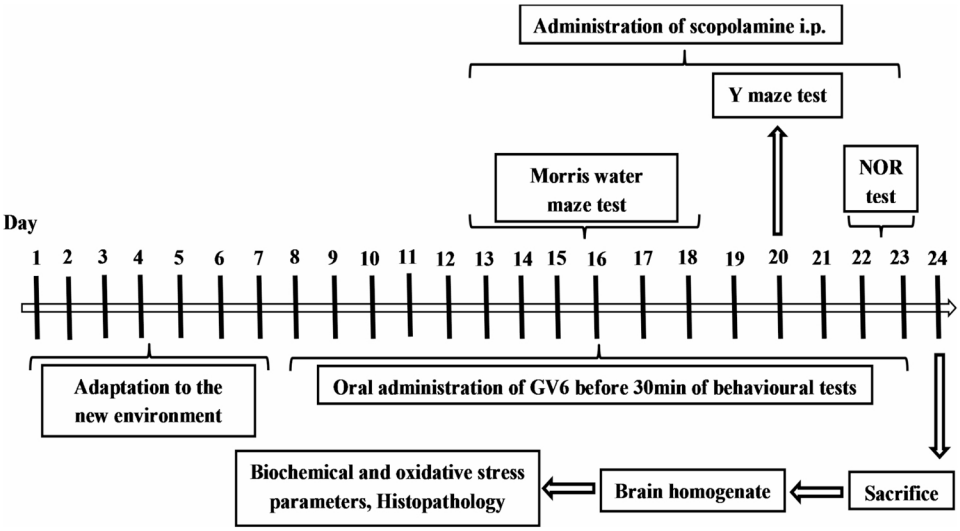


**Fig. 1** Schematic diagram of the experimental study. After seven days of adaptation the oral administration of GV6 was continued from 8th day to the end. From 12th day i.p. administration of scopolamine was continued, after 20 min of oral administration of GV6 and 10 min prior to behavioural test. Morris water maze test was performed from 13th day to 18th day, Y maze test was performed in the 20th day and NOR test was performed on the 22nd and 23rd day. On day 24 all mice were sacrificed and brain homogenates were collected to perform the biochemical and oxidative stress parameters and histopathology

training; each mouse was dried with a towel and returned to their cages.

**Probe trial** After the five-day training session, a one-day test session was applied to determine the reference memory. The hidden platform was removed from the water maze, and the mice were allowed to swim for 60s, starting from a single quadrant. The searching routes and time spent in the target quadrant (in which quadrant the hidden platform was placed previously) were analyzed by the video tracking system. All tests were performed during daylight hours between 09 AM and 11 AM, within a soundproof laboratory (Pisar et al. 2023).

### Y-maze test

The Y-maze task was performed as previously described by da Costa Rodrigues et al. 2022. The Y-maze apparatus consists of three horizontal arms (long 40 cm, wide 8 cm, and height 15 cm), made up of black acrylic material and separated symmetrically with 120° angles. Each mouse was placed in one arm (A), and the number of sequences and arm entries were recorded for 8-minute session. An alteration was defined as an entry of each animal in all three consecutive arm choices (ABC, BCA, CAB). A successive entry was defined as the entry of each paw into the boundaries of each arm. The alternating entries into the three arms reflect the working memory capacity of the mice. This capacity was assessed by observing successive entries into the three arms within overlapping triplet sets, where each set includes entry into three different arms. To remove the residual smells, all the arms were cleaned properly in between every test. Percentage alterations were calculated by using the equation as follows: % alteration = [(No. of alterations × 3) / (total arm entries −2) × 100].

### Novel object recognition test

The test is performed in a plywood box (40 cm × 60 cm) consisting of white acrylic walls and an open upper portion. A habituation trial was performed on the 1st day of the test by allowing each mouse in the open field to explore freely during 5-minute session. During the trial, no objects were placed in the open field. The 2nd day of the test was the re-habituation period for an additional 3 min. The rehabituation period was divided into three trials: The acquisition trial, the inter-trial interval and the retention trial. During the acquisition trial, the mice were given the opportunity to freely explore two identical objects (A1 and A2) made up of biologically inert substances in the open field for 8 min. The objects were placed in the corner of the open field at a distance of 10 cm from the wall. In the inter-trial interval period, the mice were placed in the home cage for 30 min. In the retention trial, two objects (A1 and B1), one of which is familiar with the previous object, were placed in the same place, and the mice were allowed to explore the objects for 8 min (Lueptow 2017).

Sniffing, licking, touching, and not the leaning on the objects were subjected to exploration of the objects. The acquisition, inter-trial, and retention trial periods were recorded by using a video recorder, and the memory discrimination index (OR) was calculated as follows:

$$\mathrm{OR} = [(\text{Time spent to explore the new object}) - (\text{Time spent to explore the familiar object})]/[(\text{Time spent to explore the new object}) + (\text{Time spent to explore the familiar object})].$$

## Evaluation of biochemical markers and oxidative stress parameters

### Collection of brain tissues

As shown in Fig. 1, the mice were sacrificed on day 24 by cervical dislocation, and the whole brains were immediately removed and washed with ice-cold PBS, frozen on dry ice, and stored at −80°C for further analysis. Brains of 3 mice ($n$=3) from each group was used to evaluate the biochemical and oxidative stress parameters. The whole brain of the mice was homogenized in 50 mM ice-cold sodium phosphate buffer (2% homogenate or 1:10 w/v), pH 7.4, and centrifuged at 9000 g for 30 min at 4 °C. The supernatants were stored at −80 °C to evaluate the AChE, BChE activity, and ACh level. To avoid any enzymatic degradation, dry ice was used for the process (Phachonpai and Tongun 2021). Brains of 3 mice from each group was used to eval.

### AChE and BChE activity

The AChE and BChE activity was measured as described by Hussain et al. with some modifications in a 96-well microplate by using a spectramax iD3 (Hussain et al. 2022). Briefly, 75 µL of 50 mM Tris-HCl buffer pH 8.0, 25 µL of 15 mM ATCI and BTCI, and 0.1% BSA were added to 100 µL of brain supernatant, and the mixture aliquot was incubated at 25 °C for 5 min. After that, 0.03 mL of 10 mM DTNB was added to it to start the reaction, and the absorbance was measured at 412 nm for 120 s at an interval of 30 s. The AChE and BChE activity was measured by using the following equation and expressed as µmol ACh hydrolized/min/mg protein and µmol BCh hydrolized/min/mg protein, respectively.

$$R = (\delta OD \times \text{total volume of assay} \times 1000) / (E \times \text{mg protein})$$

Where $\delta$OD is the change in absorbance/min and E is the extinction coefficient ($1.36 \times 10^4\ M^{-1}\ cm^{-1}$).

### ACh content estimation

ACh content of the brain tissues were analysed as described by Bae et al. with some modifications (Bae et al. 2014). In each well, 20 µL of brain supernatant and 50 µL of 1% aqueous hydroxylamine and aqueous potassium hydroxide (1:1) were added. The plate was then incubated for 15 min at 25°C and 250 µL of ferric chloride ($FeCl_3$) in 0.1 N hydrochloric acid (HCl), pH 1.2, was added to each well. The absorbance was measured at 540 nm and expressed as µmoL/mg protein. The principal is that the hydroxylamine reacts with the substrate ACh in a strong alkaline medium to produce acetohydroxamic acid, which forms a red-brown complex when acidified with HCl and ferric chloride ($Fe^{3+}$) ions (Karunakaran et al. 2022).

### MDA level

To determine the MDA level, TCA, and TBA were mixed at a 1:1 ratio and added to the brain supernatants. The above mixture was heated for 15 min and after a rapid cooling, the mixture was centrifuged (3000 rpm) for 10 min. The MDA reacts with TBA in the acidic environment at boiling temperature to form pink coloration, which was then measured at an absorbance of 532 nm and expressed as nmol/mg protein (Babalola et al. 2023).

### Superoxide dismutase (SOD) activity

In this method, 2,4-iodophenyl-3,4-nitrophenyl-5-phenyltetrazolium chloride reacts with the free radicals to produce a red formazan dye. Initially, a mixture of 3 mL of 500µM xanthine, 3 mL of 200 µM KCN, 7.44 mg cytochrome c, 3 mL of 1 mM EDTA, and 18 mL of 0.05 M sodium phosphate buffer pH 7.0 was prepared. Finally, 975 µL of the mixture aliquot was added to 20 µL of the brain supernatant and 5 µL of xanthine oxidase. The absorbance was measured after 7 min at 550 nm and the results were expressed as U/mg protein (Nunes et al. 2015).

### Glutathione reductase (GSH) content

The glutathione content was estimated by a previous study stated by Lonita et al. 2017; with some modifications. In this method, DTNB oxidized the GSH to produce glutathione disulfide (GSSG) and a yellow-colored 5-thio-2-nitrobenzoic acid (TNB), which is directly proportional with the GSH level in the test sample. Briefly, 0.9 mL of phosphate buffer was used to dilute 1 mL of brain supernatant. To this, 1 mL of 20% trichloroacetic acid (TCA) was mixed. The mixture was incubated at room temperature for 20 min and after that, the mixture was centrifuged for 10 min at 10,000 rpm. From this mixture, 0.25 mL was discarded and 0.75 mL of phosphate buffer was added. Finally, 600 µmol/L of 2 mL DTNB was added to it and incubated at room temperature for 10 min and the absorbance was measured at 412 nm. The GSH content was expressed as µmol/mg protein.

### Catalase (CAT) activity

The catalase assay was performed by following the method described by Foyet et al. 2015; with some modifications. In this colorimetric assay, a yellow complex was formed with the mixture of molybdate and $H_2O_2$, which was measured to determine the catalase inhibition. Briefly, in a 96-well microplate, 50 µL of the brain supernatant was added to 50 µL of 50 mM $H_2O_2$ prepared in 0.2 M sodium-potassium phosphate buffer (pH 7.4) and incubated (37° C) for 3 min. The enzymatic reaction was stopped by adding 100 µL of 64.8 mM ammonium molybdate prepared in $H_2SO_4$, and the absorbance was recorded at 405 nm. The catalase level was expressed as U/mg protein.

### Nitrate (NOx) level

Griess reagent was used to determine the nitrite levels in experimental mice brain. Briefly, 100µL mice's brains supernatant was combined with 100 µL Griess reagent and then incubated at room temperature for 10 min. The absorbance was recorded at 540 nm. The nitrite level concentration was expressed as µM/mg protein from a standard curve of sodium nitrite (Babalola et al. 2023).

### TNF-α level

The level of TNF-α released from the scopolamine-induced brains was measured by using the ELISA kit obtained from Sigma-Aldrich (St. Louis, USA), according to the protocol provided by the manufacturers.

## Histological analysis

Brains of 3 mice ($n = 3$) from each group was used to observe the morphological changes. The whole brains of experimental animals were preserved with 10% neutral buffered formalin, washed with ethyl alcohol of various grades, and xylene. Finally, the brain tissues were fixed in a 4% paraformaldehyde solution at 4°C, overnight embedded in paraffin wax, and then sectioned at a thickness of 4 µm by using a

microtome. A standard staining method, haematoxylin and eosin (H&E), was used to stain the nucleus of the 4 µm sections brain tissues. The slides were observed under a light microscope at 100x magnification equipped with the DP-27 digital camera and Magvision software (Olympus, Japan) (Zeng et al. 2022).

### Molecular docking

The structural files of the overlapping targets were used and screened as receptors to dock with the ligands. The chemical structures of active compounds (ligands) were extracted from the https://pubchem.ncbi.nlm.nih.gov/ database. Inter actions between the ligand and pivotal targets within were confirmed by molecular docking using AutoDock Vina. PyMOL (V2.x) and BIOVIA Discovery Studio 2021 visualization tools were used for analyzing proteins (Seeliger and de Groot 2010). The receptor and ligand were pre-processed using auto dock tools (ADT, v1.5.6), and the Gridbox's center and dimensions (9.888244; −60.058399; −24.378703 for AChE and 2.564882; 10.370544; 14.087385 for BChE) were ascertained. PyMOL was used to clean the receptor. The ligand was processed by selecting torsions, detecting roots, and adjusting charges. Next, the receptor's original ligand structures along with protein were separately saved as PDB file formats, respectively, and imported into ADT. The processed protein is then saved as a.pdbqt file for docking, and the original ligand is treated similarly to the docking ligand. Semi-flexible docking was carried out using the ligand expansion method; keeping exhaustiveness, energy range, and numbers of modes were among the default parameters (Forli et al. 2016). To further analyze the H-bond and π-π/π-H interaction, the result with the lowest binding energy was chosen (Das et al. 2023).

### Statistical analysis

All the data were analyzed by using GraphPad Prism version 8.0.2 (GraphPad Software, La Jolla, CA) and expressed as mean ± SD. The behavioural data and changes in biochemical and oxidative stress markers were analyzed by one-way analysis of variance (ANOVA) with repeated measures followed by Sidak's multiple comparisons test. The P value less than 0.05 is adopted as significant.

## Results

### HPTLC analysis of ginger samples

A standard calibration curve was prepared by plotting peak areas against different concentrations ranging from 0.5 to1.7 µg/mL. A good linear relation was obtained between peak areas and concentrations with the correlation coefficient ($r^2 > 0.99$) and a CV value of 2.64 (Online Resource Fig. S1a). The mobile phase n-hexane: ethyl acetate (4:6 v/v), produced a compact spot for the standard 6-gingerol at $R_f$ 0.53. The contents of the standard were found to be within the range of 2.12 to 6.27% w/w where the sample GV6 showed the highest and GV7 had the least 6-gingerol content (Table 1). The picture of the derivatized developed plate was taken by CAMAG Reprostar 3 at white light (Online Resource Fig. S1b). Online Resource Fig S1c represents the densitometric chromatograms of ginger samples.

### Effect on the in vitro cholinesterase enzymes

The AChE and BChE enzyme inhibition activity of the ginger samples were expressed by their respective $IC_{50}$ values. The most potent $IC_{50}$ value for AChE inhibitory activity was found to be 305.19 ± 1.81 µg/mL for GV6, and the least $IC_{50}$ value for AChE inhibitory activity was found to be 521.46 ± 2.38 µg/mL for GV7 (Table 1). The $IC_{50}$ values for BChE enzyme inhibitory activity of the ginger samples were given in Table 1, where GV6 also showed the potent inhibition for BChE activity with an $IC_{50}$ value of 411.73 ± 4.03 µg/mL, while, GV7 showed the least potency ($IC_{50}$ = 602.81 ± 4.61 µg/mL). The $IC_{50}$ value for galantamine was found to be 24.2 ± 1.85 and 35.95 ± 3.05 µg/mL for AChE and BChE enzymes, respectively.

### Effect of GV6 on memory and learning impairment

#### Effect of GV6 on the spatial memory impairment by the Morris water maze test

During the five-day training session of the Morris water maze test, the escape latency progressively decreased compared to the scopolamine-treated group, as depicted in Fig. 2a, with varying degrees of reduction observed in each group.

Treatment with GV6 resulted in a gradual increase in the exploring time spent in the target quadrant compared to the scopolamine-treated group [F (4, 35) = 68.76, $p < 0.0001$], showing a dose-dependent effect (Fig. 2b). Additionally, Fig. 2c demonstrated that scopolamine-treated mice experienced a significant increase in latency [F (4, 35) = 13.04, $p < 0.0001$] to reach the platform compared to the control group, while GV6 treatment dose-dependently decreased the latency period into the platform. Figure 2d revealed no significant difference in swimming speeds [F (4, 25) = 0.09492, p value is not significant] among the control, scopolamine, GV6, and donepezil-treated groups.

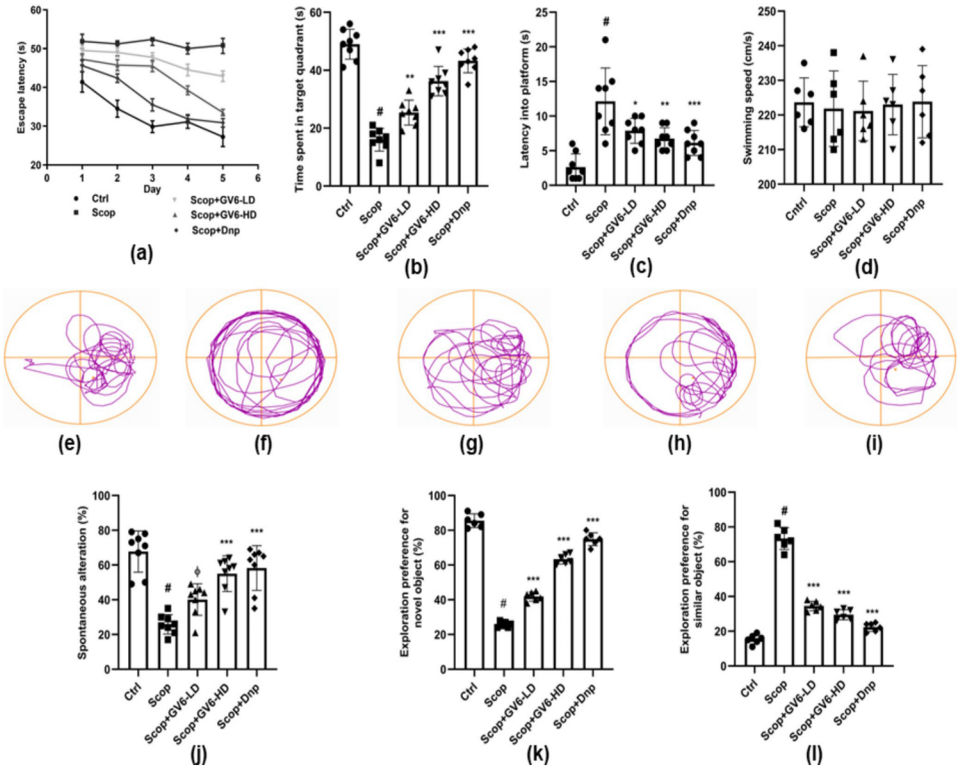


**Fig. 2** Assessment of GV6 influence on Morris water maze, Y-maze and Novel object recognition test parameters. In Morris water maze test (**a**) the escape latency decreased as training progressed during the navigation trials, (**b**) the time spent in target quadrant increased, and (**c**) the latency into platform decreased in the GV6 treated mice compared to scopolamine treated mice whereas, (**d**) Swimming speed remains roughly unchanged during the trial period, (**e-i**) representative routes during the test session where GV6 decreased the latency into platform during the test period (control, scopolamine, scopolamine + Low dose, scopolamine + High dose, scopolamine + Donepezil). In Y-maze test GV6 (**j**) increased the % spontaneous alteration, and in the Novel object recognition test GV6 (**k**) increased the % exploration preference for novel object and (**l**) decreased the % exploration preference for similar object, compared to scopolamine treated group. $^{\#}p<0.0001$ vs. control group, $^{\Phi}p<0.05$, $^{*}p<0.01$, $^{**}p<0.001$ and $^{***}p<0.0001$ vs. scopolamine group. Data are presented as mean ± SD ($n=6$)

On the 6th day of the test session, the platform was removed, and the exploring route was recorded while mice freely swam for 60 s, as illustrated in Fig. 2e-i. The control group mice spent more time in the target quadrant, whereas mice in the scopolamine-treated group exhibited movement across all four quadrants without a specific direction. GV6-treated group gradually increased the time spent in the target quadrant, dose-dependently.

### Effect of GV6 on the spatial and short-term memory performance by the Y-maze test

In the Y-maze test, scopolamine administration significantly decreased the percentage spontaneous alteration [$F(4, 35)=20.63$, $p<0.0001$], as shown in Fig. 2j, compared to the control, which indicated that scopolamine impaired the spatial and short-term memory function. Treatment with GV6 improved the impairment of spatial and short-term memory function by significantly increasing the percentage spontaneous alteration compared to the scopolamine-treated group.

### Effect of GV6 on the long-term and cognition memory impairment by the novel object recognition test

As shown in Fig. 2k, in the novel object recognition test, the scopolamine-treated group showed a significant decrease in percentage exploration preference for novel objects [$F(4, 25)=380.0$, $p<0.0001$], while the percentage exploration preference for familiar objects was increased [F (4,

25) = 223.8, $p < 0.0001$], as shown in Fig. 2l, compared with the control group, which also indicated the memory impairment by scopolamine. Treatment with GV6 significantly reverses the percentage exploration preference for novel as well as familiar objects, dose-dependently.

### Effect of GV6 on the cholinergic neurotransmission

The cholinergic neurotransmission was investigated by measuring the AChE, BChE activity, and the ACh level and compared among control, scopolamine, GV6, and donepezil-treated mice brains. Figure 3a and b depicted that the AChE and BChE activities were significantly increased in the scopolamine-treated group [F (4, 25) = 81.80, $p < 0.0001$] and [F (4, 25) = 58.19, $p < 0.0001$], respectively. Treatment with GV6 inhibited both the AChE and BChE enzymatic activity, dose-dependently. As shown in Fig. 3c, scopolamine-treated group significantly reduced the brain ACh level [F (4, 25) = 86.60, $p < 0.0001$] compared with control group. GV6 treatment significantly increased the ACh level at both 200 and 400 mg/kg b.w. Therefore, it can be emphasized that GV6 demonstrated a significant influence on cholinergic neurotransmission.

### Effect of GV6 on the oxidative stress parameters

The present study exhibited the potency of GV6 to improve the brain antioxidant parameters by modulating the MDA, SOD, GSH, CAT, and NOx levels. As shown in Fig. 4a, scopolamine administration significantly increased MDA levels [F (4, 25) = 98.87, $p < 0.0001$] in mice brains compared to the control group. GV6 significantly decreased the MDA levels at both doses, respectively compared to scopolamine-treated mice. Figure 4b illustrates that scopolamine administration significantly reduced SOD activity [F (4, 25) = 67.26, $p < 0.0001$] in the mice brain compared to the control group. Administration of GV6 extract at 200 and 400 mg/kg, b.w., significantly reversed the reduction in SOD activity compared to scopolamine-treated mice.

Additionally, administration of the GV6 extract increased the scopolamine-induced reduction of both the GSH and CAT activities [F (4, 25) = 30.53, $p < 0.0001$] and [F (4, 25) = 89.49, $p < 0.0001$], respectively, and decreased the scopolamine induced increment of the NOx activities [F (4, 25) = 53.27, $p < 0.0001$] respectively at a dose of 400 mg/kg (Fig. 4c and e). In contrast, the group that received GV6 at a dose of 200 mg/kg exhibited non-significant changes in the GSH, CAT, and NOx activities compared to the scopolamine-treated group.

### Effect of GV6 on the TNF-α level

Figure 5 shows the results of the inflammatory cytokine TNF-α level. In the whole brain of group that received scopolamine, the levels of TNF- α were dramatically increased [F (4, 25) = 68.67, $p < 0.0001$] when compared to the control group. Interestingly, our study showed that the groups received the GV6 at doses of 200 and 400 mg/kg, b.w., exerted a lower level of the inflammatory cytokine TNF-α.

### Histopathology observations

The results obtained, as shown in Fig. 6a and e, showed that scopolamine administration led to neuronal cell loss and shrinkage in the hippocampus, as evidenced by the presence of pyknotic nuclei and karyolysis changes. Spongiosis was also observed, with vacuoles present in the hippocampus section, when compared to control. However, administration of

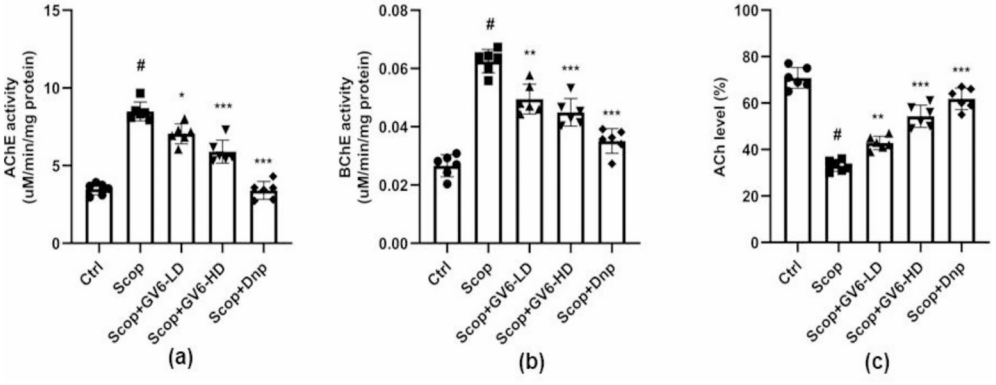


**Fig. 3** Effect of GV6 on the cholinergic system of experimental mice brain. GV6 (**a**) decreased the activity of AChE and (**b**) BChE whereas, (**c**) increased the ACh levels compared to scopolamine treated mice brain. $^{\#}p < 0.0001$ vs. control group, $^{*}p < 0.01$, $^{**}p < 0.001$ and $^{***}p < 0.0001$ vs. scopolamine group. Data are presented as mean ± SD ($n = 6$)

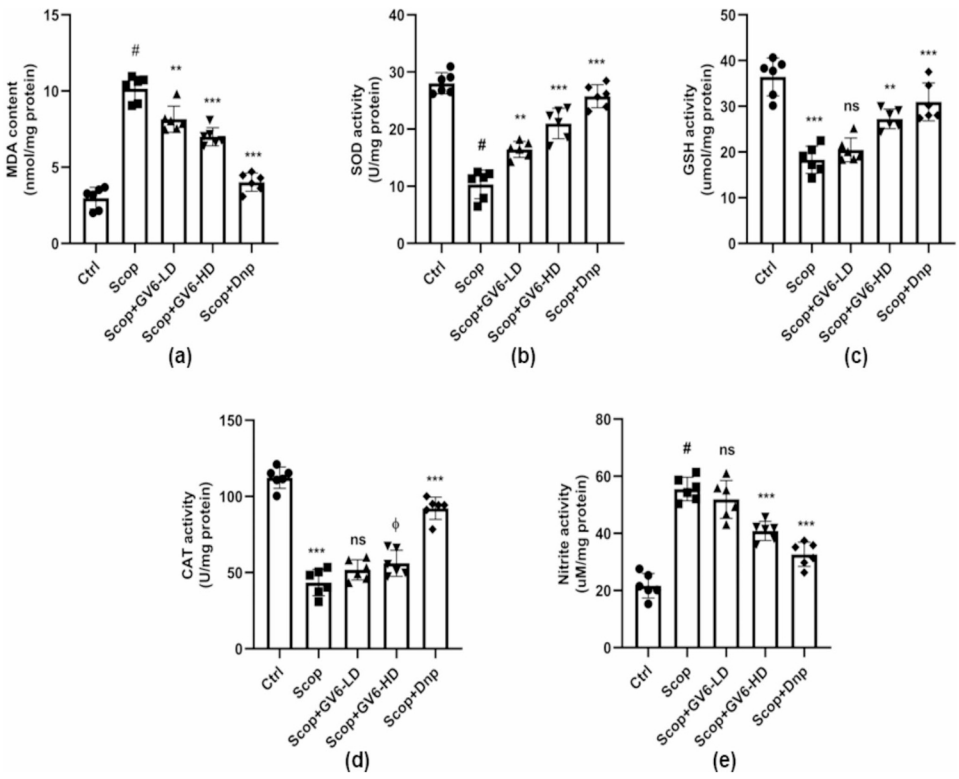


**Fig. 4** Effect of GV6 on the antioxidant parameters in experimental mice brain. GV6 (**a**) decreased the level of MDA, and increased the levels of (**b**) SOD, (**c**) GSH, and (**d**) CAT and also increased the (**e**) Nitrite activity compared to scopolamine treated mice brain. $^{\#}p<0.0001$ vs. control group, $^{\phi}p<0.05$, $^{*}p<0.01$, $^{**}p<0.001$, $^{***}p<0.0001$ and ns = not significant vs. scopolamine group. Data are presented as mean ± SD ($n=6$)

GV6 demonstrated significant restoration of neuronal cells, density, and normal structure in mice's hippocampus and proved to exhibit a protective effect against scopolamine-induced memory and cognitive impairment.

## Molecular docking analysis

Human crystal structures containing co-crystal ligands of AChE (PDB ID: 4M0E) and BChE (PDB ID: 5K5E) were retrieved from the PDB database as macromolecules for docking with 6-gingerol and galantamine. The negative binding energy (kcal/moL) indicated the compounds could interact with the macromolecule spontaneously. The docking results showed that 6-gingerol and galantamine showed docking scores of −7.5 and −7.3, respectively, against AChE (Table 2). Both the compounds formed multiple H-bonds with the active site residues of the key targets. The compounds also formed different π interactions. The crucial amino acid residues were TYR72, TRP286, TYR341, THR75, and SER293 (Online Resource Fig. S2).

Both the compounds also showed a good docking score against BChE. The docking scores were found to be −8.5 for galantamine and −7.3 for 6-gingerol (Table 2). In addition, both compounds found to form H-bonds and π–interactions with the target macromolecule. The pivotal amino acids within the active site that predominantly interact with the ligand molecules include GLU197, ASP70, TYR332, HIS438, TRP82, ILE442, GLY439, and SER79 (Online Resource Fig. S3).

## Discussion

Considering the increased demand for herbal medicines globally, there is a call to ensure the quality, safety, and efficacy using current analytical methods to satisfy the

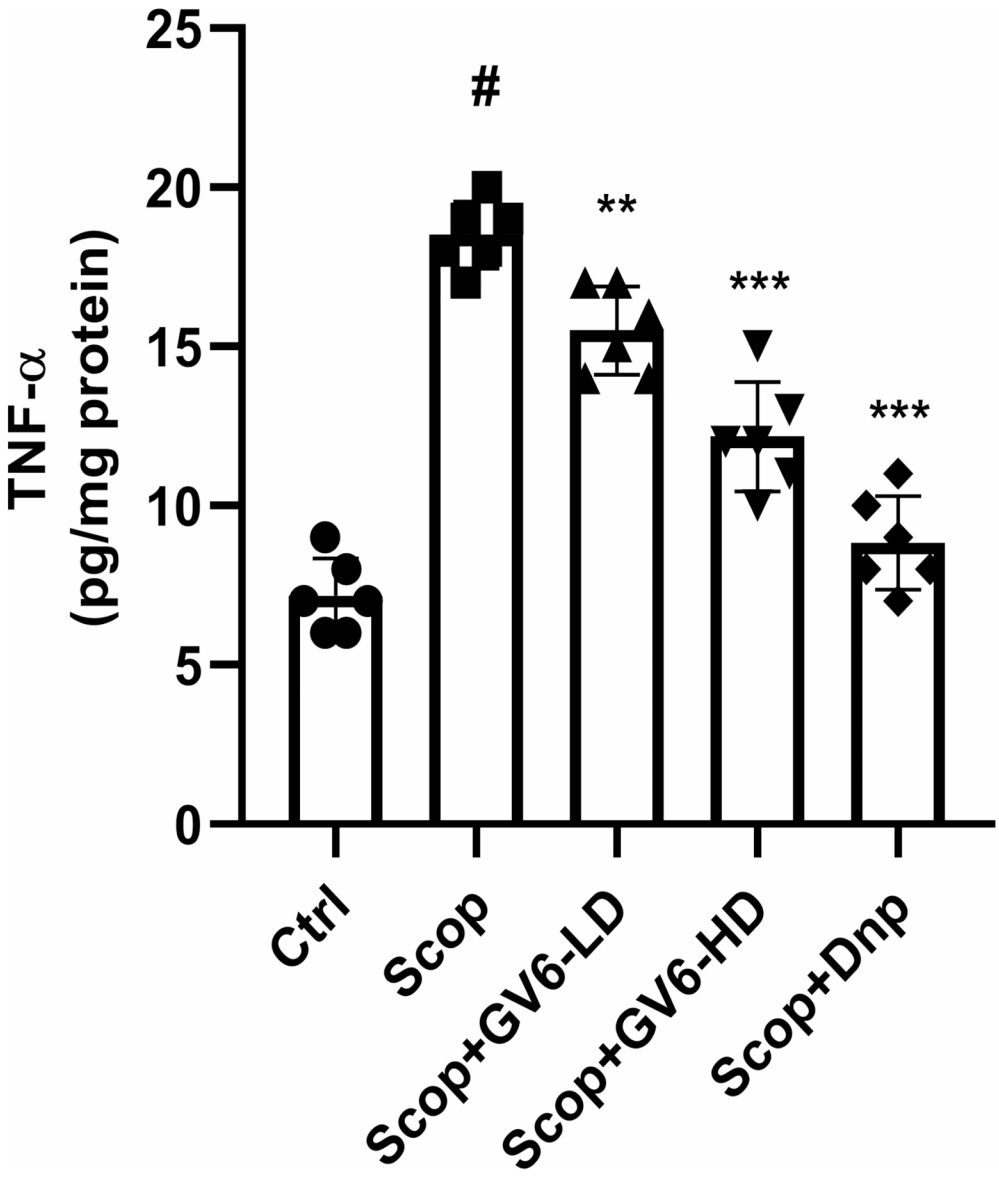


**Fig. 5** Effects of GV6 on TNF-α level in experimental mice brain. GV6 decreased the TNF-α level compared to scopolamine treated mice brain. $^{\#}p<0.0001$ vs. control group, $^{**}p<0.001$ and $^{***}p<0.0001$ vs. scopolamine group. Data are presented as mean ± SD ($n=6$)

international standards. It has been proven that the geographical variations among different ginger cultivars significantly influence the metabolite compositions in natural products (Bayona et al. 2020). Manipur, India, is renowned for its unique ecological landscape with diverse flora and fauna, including a hot spot of several gingers cultivars (Devi et al. 2016). The present study establishes evidence for variation of 6-gingerol content in ginger chemo varieties collected from different locations of Manipur by HPTLC analysis, where the chemo variety GV6 showed the highest

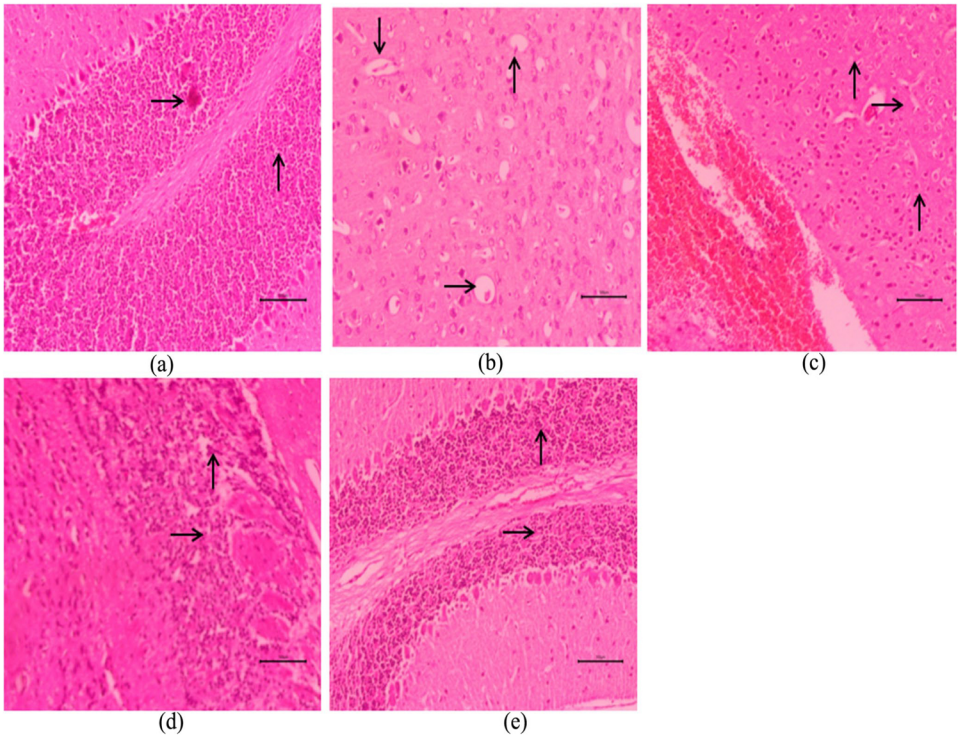


**Fig. 6** Histopathological observations on experimental mice brain showing the morphological changes. Black arrows indicates (**a**) the normal neuronal cell structure in normal control group, (**b**) neuronal cell loss and cell shrinkage, spongiosis in scopolamine treated group whereas, black arrows in GV6 treated group indicates the (**c**) restoration of neuronal cells towards the normal as well as in (**d**) donepezil treated group

6-gingerol content. The HPTLC data will help to understand the quality of the herb for the presence of specific compounds in light of their therapeutic efficacies.

Rabiei et al. mentioned that progression of AD is associated with memory impairment, learning difficulties, and behavioral as well as cognitive alterations in affected individuals (Rabiei et al. 2014). Abnormalities in cholinergic neurotransmission associated with AChE/BChE deficiency, neuro-inflammation, and oxidative stress (Chen et al. 2022; Greig et al. 2005). The importance of 6-gingerol as a cholinesterase inhibitor against AD pathogenicity has been highlighted in several studies (Zeng et al. 2015; Lee et al. 2011). Scientific evidence indicates that consumption of foods rich in polyphenols might slow down the advancement of AD through the inhibition of the harmful impact of free radicals. Thus, incorporation of antioxidant substances holds significant importance to improve cognitive functions (Khorrami et al. 2015). A study suggested that ginger cultivars that had the highest 6-gingerol content also exerted the strongest antioxidant property (Pawar et al. 2011). In the present study, the GV6 variety showed the highest cholinesterase inhibition potency, as evident by in vitro AChE and BChE enzyme inhibition assays. Considering the cholinesterase enzyme inhibitory potential together with the HPTLC data suggested that the GV6 variety may serve as an effective lead for the development of value added nutraceutical products against AD.

The ameliorative effect of the extract was further validated in an experimental animal model using scopolamine-induced learning and memory-impaired mice. Scopolamine causes blocking of the muscarinic acetylcholine receptor that hinders cholinergic neurotransmission, causing memory and learning impairments (Gul et al. 2023). In the present study, administration of scopolamine increased the latency time of mice to enter the preferred arm, resulting in a reduction in time passed in the preferred arm in the disease control group. Based on the Morris water maze test, the GV6-administered group showed no significant effect on the spatial memory of amnesic mice on the first, second, and third days, however, on days four and five, it

**Table 2** Details of molecular docking studies of 6-gingerol and galantamine on AChE (PDB ID: 4M0E) and BChE (PDB ID: 5K5E) which include Docking score, conventional H- bonds, π- interactions, and active site pocket residues

| Compound | Docking score | Conventional – H Bond | π – interaction | Active site pocket residues |
|---|---|---|---|---|
| AChE | | | | |
| 6-gingerol | −7.5 | PHE295, ARG296(2), TYR72(2) | TRP286(2), TYR341, TYR337, PHE338, PHE297 | PHE295, ARG296, TYR72, TRP286, TYR341, TYR337, PHE338, PHE297, LEU289, SER293, THR75, VAL294, TYR124 |
| Galantamine | −7.3 | TYR72(3) | TRP286(2) | TYR72, TRP286, LEU76, THR75, ASP74, SER293, TYR341 |
| BChE | | | | |
| 6-gingerol | −7.3 | GLU197, TYR128, ASP70, TYR332 | HIS438, PRO285, TYR332(2), TRP82 | GLU197, TYR128, ASP70, TYR332, HIS438, PRO285, TRP82, ILE442, GLY439, SER79, GLY121, GLY115, TYR114 |
| Galantamine | −8.5 | TRP82 | HIS438, TRP82(3), ALA328 | TRP82, HIS438, TRP82, ALA328, GLY116, ILE442, GLY439, GLU197, TYR440, MET437, TRP430, GLY78, TYR332, SER79, ASP70, THR120 |

showed an effective improvement in the spatial memory. The extract-treated groups spent more time and reduced the time to latency into platform in target quadrant than the amnesic mice group. There was also improved short-term memory impairment in scopolamine-induced amnesic mice by increasing the percentage alteration by the Y-maze test in the extract-treated group. In a different study, Kim et al. showed an improvement of spatial memory and short-term working memory impairment in 6-gingerol-treated groups (Kim et al. 2018). Another study mentioned that ginger may improve the spatial and short-term working memory of scopolamine- and Aβ1–42-induced AD models (Huh et al. 2018). A novel object recognition test was performed to judge the cognitive memory function of the amnesic mice by determining the interest of the mice in new objects (Sener et al. 2022). The present experimental data showed improvement of cognitive impairment in the scopolamine-induced learning and memory impaired mice after extract treatment. Another study reported that treatment with 6-gingerol and 6-shogaol-enriched ginger extract enhanced cognitive impairment in the hippocampus of scopolamine-induced mice (Lim et al. 2014). Scopolamine-induced elevated brain AChE and BChE activity as well as brain ACh level were also restored to the normal level after treatment with GV6 extract. This finding is consistent with Joshi and Parle, where treatment with ginger extract significantly reduced the brain cholinesterase enzyme activity together with an improvement in ACh levels (Joshi and Parle 2006).

Excessive production of ROS can result in cognitive decline and neuronal cell damage in the brain. Reports indicate that patients with learning and memory impairments exhibit an imbalance between oxidant and antioxidant levels, increasing the risk of AD (Simunkova et al. 2019). The present study demonstrated that treatment with GV6 extract significantly improved the antioxidant defense system in scopolamine-treated amnesic mice brains by normalizing the increased MDA and NO levels and decreasing SOD, GSH, and CAT levels. The brain, composed mainly of lipids, is susceptible to damage from ROS-induced lipid peroxidation. Therefore, the reduction of MDA levels suggests a reduction in oxidative stress. NO production is well associated with the malformation of memory in hippocampus regions (Rao et al. 2021). Therefore, reversing the decreased level of NO improves learning and memory abilities in amnesic mice's brains. Furthermore, it has been reported that increased SOD, GSH, and CAT are key components of the antioxidant defense system in converting ROS into harmless components (Youssef et al. 2018). A study mentioned that treatment with 6-gingerol improved the oxidative stress condition by altering the free radical levels in the brain of a focal cerebral ischemic mouse model (Kongsui and Jittiwat 2023).

Neuroinflammation plays a key role in learning and memory impairment by increasing the levels of pro-inflammatory cytokines such as TNF-α, which involves oxidative

stress, amyloid-β, and tau pathology (Roy et al. 2023). In contrast, several studies mentioned that scopolamine may elevate the pro-inflammatory cytokine level in experimental rodent models (Heneka et al. 2015). In the present study, we found that oral administration of GV6 extract significantly reduced the level of TNF-α in cognitive mice towards the normal level. This finding correlated with Tripathi et al. where treatment with 6-gingerol inhibited the level of pro-inflammatory cytokine (TNF-α) in LPS-activated macrophages (Tripathi et al. 2007).

This is further apparent by histopathology observation of mice hippocampus tissues, where the scopolamine caused cellular damage evident by neuronal cell loss and shrinkage in the hippocampus. However, treatment with GV6 significantly restored the neuronal cell density to a normal level and proved to exhibit a protective effect against scopolamine-induced memory and cognitive impairment. Furthermore, nucleus shrinkage and disorganized nerve fibers reverted to their normal condition in the extract-treated group. Evidence suggests that learning and memory impairment may lead to nerve cell damage as well as reduced neurotransmitter levels affecting the hippocampus region (Chen et al. 2022; Maurer and Williams 2017). The present findings confirm the role of GV6 extract treatment in memory and learning abilities, including improvement of neuronal cell structure and increasing the activities of neurotransmitters.

In the present study, 6-gingerol-rich GV6 demonstrated neuroprotective effects through multiple mechanisms, including the restoration of cholinergic neurotransmitter levels, reduction of oxidative stress, and prevention of inflammation in the brain. The experimental paradigms, where GV6 was administered before and during scopolamine treatment, mirrors a preventive strategy as it counteract the onset of cognitive impairments. In the context of AD, this is particularly relevant, as early intervention and prevention of cognitive decline are critical areas of research. Many current AD treatments focus on slowing the progression of cognitive symptoms, which aligns with the preventive approach used in our study.

The in silico molecular docking analysis towards the active site of the respective target enzymes suggested that standard galantamine as well as 6-gingerol showed good interactions with the target enzymes. The standard cholinesterase inhibitor galantamine was found to form the most stable interaction with the BChE enzyme. The amino acid residues, namely TYR72, TRP286, THR75, SER293, and TYR341, were identified as essential for the establishment of strong interaction within the binding pocket of AChE. Similarly, TRP82, ILE442, GLY439, and GLY115 were identified as the active site residues in the binding site of BChE. Considering a potential mechanistic overview of the primary factors implicated in the neurodegenerative disorder, our findings suggest that GV6 may act as a multi-targeted agent against AD.

In the present study, we focused on the selection of a ginger sample with high 6-gingerol content and AChE/BChE inhibitory activity to evaluate the in vivo neuroprotective effects in scopolamine-induced memory impaired mice. 6-gingerol has been extensively studied for its diverse biological activities, and several clinical trials are currently underway to confirm its neuroprotective properties. 6-gingerol is present in much higher quantities in fresh ginger rhizomes compared to other ginger components (Ahmed et al. 2021). However, other bioactive compounds in ginger, such as 6-shogaol and 6-paradol, have also shown strong in vivo neuroprotective effects. Studies have demonstrated that 6-shogaol and 6-paradol enriched ginger extracts could also modulate the neuroinflammation, and have been shown to have neuroprotective effects (Ha et al. 2012; Choi et al. 2017). Additionally, while our study focused on the specific mechanisms of AChE and BChE inhibition, other pathways and molecular targets involved in the neuroprotective effects of GV6 remain to be fully explored. Future research should consider the inclusion of a broader range of GV6 bioactive compounds and examine their combined or synergistic effects in neuroprotection.

## Conclusion

Plants have become more appealing as potential therapeutic candidates as neuroprotective agents. As the number of cases of dementia rises, we must find an effective therapeutic strategy to treat the condition. Looking ahead, a natural source could be a superior option due to its varied secondary metabolite composition. The current findings may be accepted to justify the preclinical neuroprotective role of GV6 in AD-related symptoms, which could potentially alleviate scopolamine-induced impaired cognitive functions as evidenced by the behavioral tests, improved brain cholinergic functions, antioxidant potency, anti-inflammatory activity, and histopathology observations. Additionally, the in silico molecular docking analysis exposed the affinity and selectivity of 6-gingerol toward cholinergic target enzymes. Given the multifaceted uses of plant secondary metabolites, it might be assumed that herbs with high polyphenols would be better options for preventing neurodegeneration. Therefore, ginger from Northeast India with high sensorial values may have a potential source of moieties that have the ability to be developed as a nutraceutical for the management of AD-like symptoms and neurotoxicity.

**Supplementary Information** The online version contains supplementary material available at https://doi.org/10.1007/s11011-025-01535-8.

**Acknowledgements** The authors are thankful to the University Grants Commission (UGC) for providing financial support through SJSGC fellowship at Jadavpur University, Kolkata, West Bengal, India. The authors are also thankful to the Institute of Bioresources and Sustainable Development, Imphal, Manipur, India, for providing necessary help and support through the Himalayan Bioresource Mission project sanctioned by the Department of Biotechnology (DBT), Govt. of India, New Delhi.

**Author contributions** S.G. wrote the original manuscript, methodology, collected the data and analyzed the data. B.D. prepared all the figures and tables. S.J. analyzed the manuscript. K.O.S. and N.S. provided the resources. P.K.M. provided the concept and supervised the manuscript. P.K.H. provided the concept, resources, supervised, reviewed and edited the manuscript.

**Funding** The authors declare that no funds, grants, or other support were received during the preparation of this manuscript.

**Data availability** No datasets were generated or analysed during the current study.

## Declarations

**Ethics approval** This study was performed according to The Committee for the Purpose of Control and Supervision of Experiments on Animals. Approval was granted by the Institutional Animal Ethics Committee (Approval Number: JU/IAEC-22/10).

**Competing interests** The authors declare no competing interests.

## References

Ahmed SHH, Gonda T, Hunyadi A (2021) Medicinal chemistry inspired by ginger: exploring the chemical space around 6-gingerol. RSC Adv 11:26687–26699. https://doi.org/10.1039/D1RA04227K

Alqasoumi SI (2009) Quantification of 6-gingerol in Zingiber officinale extract, ginger-containing dietary supplements, teas and commercial creams by validated HPTLC densitometry. FABAD J Pharm Sci 34:33–42

Ano Y, Kutsukake T, Sasaki T, Uchida S, Yamada K, Kondo K (2019) Identification of a novel peptide from β-casein that enhances spatial and object recognition memory in mice. J Agric Food Chem 67:8160–8167. https://doi.org/10.1021/acs.jafc.9b02495

Avila-Villanueva M, Dolado AM, Gomez-Ramirez J, Fernandez-Blazquez M (2022) Brain structural and functional changes in cognitive impairment due to Alzheimer's disease. Front Psychol 13:1–13. https://doi.org/10.3389/fpsyg.2022.886619

Ayaz M, Ullah F, Sadiq A, Kim MO, Ali T (2019) Editorial: natural products-based drugs: potential therapeutics against alzheimer's disease and other neurological disorders. Front Pharmacol 10:1–5. https://doi.org/10.3389/fphar.2019.01417

Babalola KT, Oyebanjo O, Adekoya VA, Adeniyi IA, Ajayi AM, Onasanwo SA (2023) Protective effect of methanol leaf extract of Cnidoscolus aconitifolius against lipopolysaccharides–induced cortico–hippocampal neuroinfammation, oxidative stress and memory impairment. Adv Tradit Med 23:145–155. https://doi.org/10.1007/s13596-021-00578-3

Bae D, Kim Y, Kim J, Kim Y, Oh K, Jun W, Kim S (2014) Neuroprotective effects of Eriobotrya japonica and Salvia Miltiorrhiza Bunge in in vitro and in vivo models. Anim Cells Syst 18:119–134. https://doi.org/10.1080/19768354.2014.903856

Bayona LM, van Leeuwen GV, Erol O, Swierts T, van der Ent E, de Voogd NJ, Choi YH (2020) Influence of geographical location on the metabolic production of giant barrel sponges (Xestospongia spp.) revealed by metabolomics tools. ACS Omega 5:12398–12408. https://doi.org/10.1021/acsomega.0c01151

Chen ZR, Huang JB, Yang SL, Hong FF (2022) Role of cholinergic signaling in Alzheimer's disease. Molecules 27:1–23. https://doi.org/10.3390/molecules27061816

Choi JW, Park HY, Oh MS, Yoo HH, Lee SH, Ha SK (2017) Neuroprotective effect of 6-paradol enriched ginger extract by fermentation using Schizosaccharomyces Pombe. J Funct Foods 31:304–310. https://doi.org/10.1016/j.jff.2017.02.010

da Costa Rodrigues K, de Oliveira RL, da Silva Chaves J, da Rocha VME, dos Santos BF, Fronza MG, de Campos Domingues NL, Savengnago L, Wilhelm EA, Luchese C (2022) A new arylsulfanyl-benzo-2,1,3-thiadiazoles derivative produces an anti-amnesic effect in mice by modulating acetylcholinesterase activity. Chem -Biol Interact 351:1–13. https://doi.org/10.1016/j.cbi.2021.109736

Das B, Bhardwaj PK, Sharma N, Sarkar A, Haldar PK, Mukherjee PK (2023) Evaluation of Mollugo Oppositifolia Linn. As cholinesterase and β-secretase enzymes inhibitor. Front Pharmacol 13:1–13. https://doi.org/10.3389/fphar.2022.990926

Devi NB, Singh PK, Das AK (2016) Wilderness and biodiversity of gingers in the valley district, Manipur. Int J Sci Tech Res 5:286–291

Easton A, Sankaranarayanan S, Tanghe A, Terwel D, Lin AX, Hoque N, Bourin C, Gu H, Ahlijanian M, Bristow L (2013) Effects of sub-chronic donepezil on brain abeta and cognition in a mouse model of Alzheimer's disease. Psychopharmacol 230:279–289. https://doi.org/10.1007/s00213-013-3152-3

Fadaki F, Modaresi M, Sajjadian I (2017) The effects of ginger extract and diazepam on anxiety reduction in animal model. Indian J Pharm Educ Res 51:S159–S162. https://doi.org/10.5530/ijper.51.3s.4

Forli S, Huey R, Pique ME, Sanner MF, Goodsell DS, Olson AJ (2016) Computational protein–ligand docking and virtual drug screening with the AutoDock suite. Nat Protoc 11:905–919. https://doi.org/10.1038/nprot.2016.051

Foyet HS, Abaissou HHN, Wado E, Acha EA, Alin C (2015) Emilia coccinae (SIMS) G Extract improves memory impairment, cholinergic dysfunction, and oxidative stress damage in scopolamine-treated rats. BMC Complement Altern Med 15:333. https://doi.org/10.1186/s12906-015-0864-4

Ghosh S, Das B, Haldar PK, Kar A, Chaudhary SK, Singh KO, Bhardwaj PK, Sharma N, Mukherjee PK (2023) 6-gingerol contents of several ginger varieties of Northeast India and correlation of their antioxidant activity in respect to phenolics and flavonoids contents. Phytochem Anal 34:259–268. https://doi.org/10.1002/pca.3201

Greig NH, Utsuki T, Ingram DK, Wang Y, Pepeu G, Scali C, Yu QS, Mamczarz J, Holloway HW, Giordano T, Chen D, Furukawa K, Sambamurti K, Brossi A, Lahiri DK (2005) Selective butyrylcholinesterase inhibition elevates brain acetylcholine, augments learning and lowers Alzheimer-amyloid peptide in rodent. Proc Natl Acad Sci 102:17213–17218. https://doi.org/10.1073/pnas.0508575102

Gul S, Attaullah S, Alsugoor MH, Bawazeer S, Shah SA, Khan S, Salahuddin HS, Ullah M (2023) Folicitin abrogates scopolamine induced oxidative stress, hyperlipidemia mediated neuronal synapse and memory dysfunction in mice. Heliyon 9:e16930. https://doi.org/10.1016/j.heliyon.2023.e16930

Ha SK, Moon E, Ju MS, Kim DH, Ryu JH, Oh MS, Kim SY (2012) 6-shogaol, a ginger product, modulates neuroinflammation: a

new approach to neuroprotection. Neuropharmacol 63:211–223. https://doi.org/10.1016/j.neuropharm.2012.03.016

Heneka MT, Carson MJ, El Khoury J, Landreth GE, Brosseron F, Feinstein DL, Jacobs AH, Wyss-Coray T, Vitorica J, Ransohoff RM, Herrup K, Frautschy SA, Finsen B, Brown GC, Verkhratsky A, Yamanaka K, Koistinaho J, Latz E, Halle A, Petzold GC, Town T, Morgan D, Shinohara ML, Perry VH, Holmes C, Bazan NG, Brooks DJ, Hunot S, Joseph B, Deigendesch N, Garaschuk O, Boddeke E, Dinarello CA, Breitner JC, Cole GM, Golenbock DT, Kummer MP (2015) Neuroinflammation in Alzheimer's disease. Lancet Neurol 14:388–405. https://doi.org/10.1016/S1474-4422(15)70016-5

Hennessy E, Gormley S, Lopez-Rodriguez AB, Murray C, Murray C, Cunningham C (2017) Systemic TNF-α produces acute cognitive dysfunction and exaggerated sickness behavior when superimposed upon progressive neurodegeneration. Brain Behav Immun 59:233–244. https://doi.org/10.1016/j.bbi.2016.09.011

Huh E, Lim S, Kim HG, Ha SK, Park HY, Huh Y, Oh MS (2018) Ginger fermented with Schizosaccharomyces Pombe alleviates memory impairment via protecting hippocampal neuronal cells in amyloid beta1-42 plaque injected mice. Food Funct 9:171–178. https://doi.org/10.1039/c7fo01149k

Hussain H, Ahmad S, Shah SWA, Ullah A, Ali N, Almehmadi M, Ahmad M, Khalil AAK, Jamal SB, Ahmad H, Halawi M (2022) Attenuation of scopolamine-induced amnesia via cholinergic modulation in mice by synthetic curcumin analogs. Molecules 27:2468. https://doi.org/10.3390/molecules27082468

Ionescu-Tucker A, Cotman CW (2021) Emerging roles of oxidative stress in brain aging and Alzheimer's disease. Neurobiol Aging 107:86–95. https://doi.org/10.1016/j.neurobiolaging.2021.07.014

Joshi H, Parle M (2006) Zingiber officinale: evaulation of its nootropic effect in mice. Afr J Tradit Complement Altern Med 3:64–74. https://doi.org/10.4314/ajtcam.v3i1.31140

Karunakaran KB, Thiyagaraj A, Santhakumar K (2022) Novel insights on acetylcholinesterase inhibition by Convolvulus Pluricaulis, scopolamine and their combination in zebrafish. Nat Prod Bioprospect 12:1–15. https://doi.org/10.1007/s13659-022-00332-5

Khorrami A, Ghanbarzadeh S, Mahmoudi J, Nayebi A, Maleki-Dizaji N, Garjani A (2015) Investigation of the memory impairment in rats fed with oxidized-cholesterol-rich diet employing passive avoidance test. Drug res 65:231–237. https://doi.org/10.1055/s-0034-1370950

Kim CY, Seo Y, Lee C, Park GH, Jang JH (2018) Neuroprotective effect and molecular mechanism of [6]-gingerol against scopolamine-induced amnesia in C57BL/6 mice. Evid Based Complement Alternat Med 2018:8941564. https://doi.org/10.1155/2018/8941564

Kongsui R, Jittiwat J (2023) Ameliorative effects of 6–gingerol in cerebral ischemia are mediated via the activation of antioxidant and anti–inflammatory pathways. Biomed Rep 18:1–10. https://doi.org/10.3892/br.2023.1608

Lee C, Park GH, Kim CY, Jang JH (2011) [6]-Gingerol attenuates β-amyloid-induced oxidative cell death via fortifying cellular antioxidant defense system. Food Chem Toxicol 49:1261–1269. https://doi.org/10.1016/j.fct.2011.03.005

Lim S, Moon M, Oh H, Kim HG, Kim SY, Oh MS (2014) Ginger improves cognitive function via NGF-induced ERK/CREB activation in the hippocampus of the mouse. J Nutr Biochem 25:1058–1065. https://doi.org/10.1016/j.jnutbio.2014.05.009

Liu Y, Liu J, Zhang Y (2019) Research progress on chemical constituents of Zingiber officinale Roscoe. Biomed Res Int 2019:1–21. https://doi.org/10.1155/2019/5370823

Lonita R, Postu PA, Beppe GJ, Mihasan M, Petre BA, Hancianu M, Cioanca O, Hritcu L (2017) Cognitive-enhancing and antioxidant activities of the aqueous extract from Markhamia tomentosa (Benth.) K. Schum. Stem bark in a rat model of scopolamine. Behav Brain Funct 13:5. https://doi.org/10.1186/s12993-017-0123-6

Lueptow LM (2017) Novel object recognition test for the investigation of learning and memory in mice. J Vis Exp 126:1–9. https://doi.org/10.3791/55718

Maurer SV, Williams CL (2017) The cholinergic system modulates memory and hippocampal plasticity via its interactions with non-neuronal cells. Front Immunol 8:1489. https://doi.org/10.3389/fimmu.2017.01489

Mohamed SM, Shalaby MA, Al-Mokaddem AK, El-Banna A, El-Banna HA, Nabil G (2023) Evaluation of anti-alzheimer activity of Echinacea purpurea extracts in aluminum chloride-induced neurotoxicity in rat model. J Chem Neuroanat 128:1–11. https://doi.org/10.1016/j.jchemneu.2023.102234

Nazari L, Komaki S, Salehi I, Raoufi S, Golipoor Z, Kourosh-Arami M, Komaki A (2022) Investigation of the protective effects of lutein on memory and learning using behavioral methods in a male rat model of Alzheimer's disease. J Funct Foods 99:1–12. https://doi.org/10.1016/j.jff.2022.105319

Norris D (2017) Short-term memory and long-term memory are still different. Psychol Bull 143:992–1009. https://doi.org/10.1037/bul0000108992

Nunes GBL, Costa LM, Gutierrez SJC, Satyal P, de Freitas RM (2015) Behavioral tests and oxidative stress evaluation in mitochondria isolated from the brain and liver of mice treated with riparin A. Life Sci 121:57–64. https://doi.org/10.1016/j.lfs.2014.11.018

OECD (2022) Test no. 425: Acute oral toxicity: up-and-down procedure, OECD guidelines for the testing of chemicals, Sect. 4. Paris: OECD publishing. https://doi.org/10.1787/9789264071049-en

Okesola MA, Ajiboye BO, Oyinloye BE, Ojo OA (2019) Effect of Zingiber officinale on some biochemical parameters and cytogenic analysis in lead-induced toxicity in experimental rats. Toxicol Mech Methods 29:255–262. https://doi.org/10.1080/15376516.2018.1558321

Orhan IE, Senol FS (2013) Alkaloids and inhibitory effects against enzymes linked to neurodegenerative diseases (physostigmine, galantamine, huperzine, etc). Nat Prod 505:1525–1539. https://doi.org/10.1007/978-3-642-22144-6_23

Pawar N, Pai S, Nimbalkar M, Dixit G (2011) RP-HPLC analysis of phenolic antioxidant compound 6-gingerol from different ginger cultivars. Food Chem 126:1330–1336. https://doi.org/10.1016/j.foodchem.2010.11.090

Phachonpai W, Tongun T (2021) Cognition enhancing effects of Clausena lansium (lour.) Peel extract attenuate chronic restraint stress-induced memory deficit in rats. Heliyon 7:1–7. https://doi.org/10.1016/j.heliyon.2021.e07003

Pisar MM, Chee BJ, Long I, Osman A (2023) Protective effects of Centella asiatica extract on spatial memory and learning deficits in animal model of systemic inflammation induced by lipopolysaccharide. Ann Med 55:1–16. https://doi.org/10.1080/07853890.2023.2224970

Promdam N, Panichayupakaranant P (2022) [6]-Gingerol: a narrative review of its beneficial effect on human health. Food Chem Adv 1:100043. https://doi.org/10.1016/j.focha.2022.100043

Rabiei Z, Rafieian-kopaei M, Heidarian E, Saghaei E, Mokhtari S (2014) Effects of Zizyphus jujube extract on memory and learning impairment induced by bilateral electric lesions of the nucleus basalis of meynert in rat. Neurochem Res 39:353–360. https://doi.org/10.1007/s11064-013-1232-8

Rao YL, Ganaraja B, Marathe A, Manjrekar PA, Joy T, Ullal S, Pai MM, Murlimanju BV (2021) Comparison of malondialdehyde levels and superoxide dismutase activity in resveratrol and resveratrol/donepezil combination treatment groups in Alzheimer's disease induced rat model. 3 Biotech 11:329. https://doi.org/10.1007/s13205-021-02879-5

Roy RG, Mandal PK, Maroon JC (2023) Oxidative stress occurs prior to amyloid Aβ plaque formation and tau phosphorylation in Alzheimer's disease: role of glutathione and metal ions. ACS Chem Neurosci 14:2944–2954. https://doi.org/10.1021/acschemneuro.3c00486

Sartori AC, Vance DF, Slater LZ, Crowe M (2012) The impact of inflammation on cognitive function in older adults: implications for healthcare practice and research. J Neurosci Nurs 44:206–217. https://doi.org/10.1097/JNN.0b013e3182527690

Seeliger D, de Groot B (2010) Ligand docking and binding site analysis with PyMOL and Autodock/Vina. J Comput Aided Mol Des 24:417–422. https://doi.org/10.1007/s10822-010-9352-6

Sener G, Karakadıoglu G, Ozbeyli D, Ede S, Yanardag R, Sacan Q, Aykac A (2022) Petroselinum crispum extract ameliorates scopolamine-induced cognitive dysfunction: role on apoptosis, inflammation and oxidative stress. Food Sci Hum Wellness 11:1290–1298. https://doi.org/10.1016/j.fshw.2022.04.009

Shelar M, Nanaware S, Arulmozhi S, Lohidasan S, Mahadik K (2018) Validation of ethnopharmacology of ayurvedic sarasvata ghrita and comparative evaluation of its neuroprotective effect with modern alcoholic and lipid based extracts in β-amyloid induced memory impairment. J Ethnopharmacol 219:182–194. https://doi.org/10.1016/j.jep.2018.02.032

Simunkova M, Alwasel SH, Alhazza IM, Jomova K, Kollar V, Rusko M, Valko M (2019) Management of oxidative stress and other pathologies in Alzheimer's disease. Arch Toxicol 93:2491–2513. https://doi.org/10.1007/s00204-019-02538-y

Talebi M, Ilgun S, Ebrahimi V, Talebi M, Farkhondeh T, Ebrahimi H, Samarghandian S (2021) Zingiber officinale ameliorates Alzheimer's disease and cognitive impairments: lessons from preclinical studies. Biomed Pharmacother 133:1–13. https://doi.org/10.1016/j.biopha.2020.111088

Tripathi S, Maier KG, Bruch D, Kittur DS (2007) Effect of 6-gingerol on pro-inflammatory cytokine production and costimulatory molecule expression in murine peritoneal macrophages. J Surg Res 138:209–213. https://doi.org/10.1016/j.jss.2006.07.051

Wang Z, Lian W, He J, He X, Wang Y, Pan C, Li M, Zhang W, Liu L, Xu J (2022) Cornuside ameliorates cognitive impairments in scopolamine induced AD mice: involvement of neurotransmitter and oxidative stress. J Ethnopharmacol 293:1–10. https://doi.org/10.1016/j.jep.2022.115252

Youssef P, Chami B, Lim J, Middleton T, Sutherland GT, Witting P (2018) Evidence supporting oxidative stress in a moderately affected area of the brain in Alzheimer's disease. Sci Rep 8:11553. https://doi.org/10.1038/s41598-018-29770-3

Zeng G, Zong S, Zhang Z, Fu S, Li K, Fang Y, Lu L, Xiao D (2015) The role of 6-gingerol on inhibiting amyloid β protein-induced apoptosis in PC12 cells. Rejuvenation Res 18:413–421. https://doi.org/10.1089/2Frej.2014.1657

Zeng Z, Chen C, Situ Y, Shen Z, Chen Y, Zhang Z, Tang C, Jiang T (2022) Anoectochilus roxburghii flavonoids extract ameliorated the memory decline and reduced neuron apoptosis via modulating SIRT1 signaling pathway in senescent mice. J Ethnopharmacol 296:115361. https://doi.org/10.1016/j.jep.2022.115361

# Suparna Ghosh_Thesis

ORIGINALITY REPORT

7%
SIMILARITY INDEX

PRIMARY SOURCES

| | | |
|---|---|---|
| 1 | www.mdpi.com<br>Internet | 274 words — 1% |
| 2 | louisdl.louislibraries.org<br>Internet | 256 words — 1% |
| 3 | link.springer.com<br>Internet | 114 words — < 1% |
| 4 | www.frontiersin.org<br>Internet | 109 words — < 1% |
| 5 | baadalsg.inflibnet.ac.in<br>Internet | 56 words — < 1% |
| 6 | Luo, J.. "Preparative separation of phenylpropenoid glycerides from the bulbs of Lilium lancifolium by high-speed counter-current chromatography and evaluation of their antioxidant activities", Food Chemistry, 20120401<br>Crossref | 47 words — < 1% |
| 7 | www2.mdpi.com<br>Internet | 47 words — < 1% |
| 8 | cytojournal.com<br>Internet | 44 words — < 1% |